Fluoromethyl Ketone Prodrugs: Potential New Insecticides Towards *Anopheles gambiae*

Eugene Camerino

Dissertation submitted to the faculty of the Virginia Polytechnic Institute and State University in partial fulfillment of the requirements for the degree of

Doctor of Philosophy

In

Chemistry

Paul R. Carlier, Chair

Felicia A. Etzkorn

David G. I. Kingston

Webster L. Santos

May 5th, 2015

Blacksburg, VA

Keywords: Acetylcholinesterase, trifluoromethyl ketones, difluoromethyl ketones, fluoromethyl ketones, Anopheles gambiae, insecticide treated nets, malaria, pyrazoles, propoxur, insecticide resistance, oxime, oxime ether

Fluoromethylketone Prodrugs: Potential New Insecticides Towards *Anopheles gambiae*

Eugene Camerino

Abstract

Malaria continues to cause significant mortality in sub-Saharan Africa and elsewhere, and existing vector control measures are being threatened by growing resistance to pyrethroid insecticides. With the goal of developing new human-safe, resistance-breaking insecticides we have explored several classes of acetylcholinesterase inhibitors. In vitro assay studies demonstrate that tri- and difluoromethyl ketones can potentially inhibit *An. gambiae* AChE (*Ag*AChE). These compounds inhibit the enzyme by making a covalent adduct with the catalytic serine of AChE. Trifluoromethyl ketones however are poor inhibitors of the G119S resistant mutant of *Ag*AChE. However difluoromethyl ketones can inhibit G119S *Ag*AChE and compound **3-10g** showed an IC_{50} value of 25.1 nM after 23h incubation time. Despite this potent inhibition of *Ag*AChE, the tri-, di-, and (mono)fluoroketones showed very low toxicity to *An. gambiae*, perhaps due to hydration and rapid clearance.

In an attempt to improve *An. gambiae* toxicity, oximes and oxime ethers of these compounds were prepared as potential prodrugs. These structures identified trifluoromethyl ketone oxime **3-2d** as a potent toxin against both wild-type (G3-strain) and a multiply resistant (Akron) strain of *An. gambiae*. This compound is within 3-fold of the toxicity of propoxur to wild type *An. gambiae* (LC_{50} values of 106 and 39 µg/mL, respectively). Most significantly, **3-2d** was much more toxic than propoxur to multiply-resistant (Akron) strain *An. gambiae* (LC_{50} = 112 and >5,000 µg/mL, respectively). However, thus far we have not been able to link the toxicity of these

compounds to a cholinergic mechanism. Pre-incubation studies suggest that significant hydrolysis of these compounds to TFKs does not occur over 22 h at pH 7.7 or 5.5.

The mechanism of action of **3-2d** remains unknown. Our enzyme inhibition studies have demonstrated that **3-2d** does not hydrolyze to the trifluoromethyl ketone **2-9d** at pH 7.7. The high Akron toxicity of **3-2d** and poor inhibition of G119S *Ag*AChE by **2-9d** argue against enzyme mediated conversion of **3-2d** to **2-9d** within the mosquito. Thus, we can rule out an AChE inhibition mechanism for toxicity. Additional experiments by our collaborator (Dr. Jeffrey Bloomquist, University of Florida) also rule out inhibition of mitochondrial respiration or agonism of the muscarinic acetylcholine receptor. Future work will address other potential insecticidal modes of action.

Acknowledgements

This degree would not be possible without my adviser, Dr. Paul R. Carlier, to whom I owe my utmost gratitude. I haven't been the best graduate student, but he was patient with me throughout this whole journey, which I am grateful for. There were times that seemed difficult and sometimes impossible but his perseverance never wavered. His knowledge about science is something of which I admired and wish to mimic. Without his guidance, I do not think that I would be the person that I am now. I would also like to thank the members of my advisory committee, Dr. Etzkorn, Dr. Kingston, and Dr. Santos and for the knowledge and experiences that they imparted to me during this journey.

I would like to thank my colleagues in the Carlier group, both past and current: Dr. Dawn Wong, Mr. Gary Richoux, Ms. Maryam Ghavami, Mr. Joseph Clements, Dr. Astha Verma, Dr. Neeraj Patwardhan, Dr. Zhong-ke Yao, Dr. Dinesh Nath, Dr. Josh Hartsel, Dr. Qiao Hong Chen, Dr. Ming Gao, Dr. Ming Ma, Dr. Derek Craft, Ms. Stephanie Antolak, Mr. Michael Black and Ms. Rachel Davis, for all the help that they offered to me these past 5 years. I would like to personally thank Dr. Dawn Wong for the essential data that she gave to me from the assay studies that she performed, which proved to be pivotal in understanding aspects of the project. Also, many thanks for the discussions with Dr. Verma about synthesis and an understanding of the medicinal chemistry aspects of my project.

I would also like to thank my parents, Arturo and Carmina Mateo, for raising me with the passion to be successful in life. Without the lessons that they taught me, I know that I would not the person that I am today. The friends that I have made here kept me sane throughout these past few years, and for that I thank them. I would lastly like to thank my fiancé Ms. Emily Morris.

She is one of the key reasons for my staying and continuing to pursue my degree. She is the best thing in my life and I cannot wait for many more years to come with this beautiful woman.

Dedication

To my parents Arturo and Carmina Mateo for always being there with me through the ups and downs of life and grandparents Cesar and Leonisa Camerino for always wanting the best for me.

Table of contents

List of Figures

List of Schemes

List of Tables

List of Abbreviations

ACh: Acetylcholine

AChE: Acetylcholinesterase

AChEIs: Acetylcholinesterase inhibitors

ATCh: Acetylthiocholine

AD: Alzheimer's disease

An. gambiae: Anopheles gambiae

ACT: Artemisinin-based combination therapy

ASM: American Society for Microbiology

BBB: Blood-brain barrier

CAS: Catalytic active site

CNS: Central nervous system

CPA1: carboxypeptidase A

DDT: Dichlorodiphenyltrichloroethane

DEET: N, N-diethyl-3-methylbenzamide

DFK: Difluoromethyl ketone

Electrophorus electricus: Electric eel

HLE: Human Leukocyte elastase

IRS: Indoor-residual spraying

LLITNs: Long lasting insecticide-treated nets

ITNs: Insecticide-treated nets

JHE: Juvenile-hormone esterase

Kdr: Knockdown resistance

MFK: Monofluoromethyl ketone

OPs: Organophosphates

OPIDN: Organophosphate induced delayed neuropathy

TFK: Trifluoromethyl ketone

TLC: Thin-layer chromatography

Tc: Torpedo californica

WHO: World Health Organization

WHOPES: World Health Organization Pesticide Evaluation Scheme

Chapter 1: Malaria and the introduction of Acetylcholinesterase as an insecticidal target

1.1 Introduction

While the number of deaths attributed to malaria has decreased globally by 47% since 2000, it continues to persist as a devastating disease.[1] Malarial symptoms include fever, nausea, and muscle pain, and the disease can eventually lead to death: it was responsible for 584,000 deaths in 2013.[2-3] The regions most affected by malaria are sub-Saharan regions in Africa, where impoverished conditions and refugee movement allow the disease to run rampant.[4]

1.2 Malaria

Malarial symptoms can be traced back to 2700 BC in ancient Chinese medical writings.[5] Symptoms were treated by the Qinghao plant, originating in China during the second century BC. Artemisinin, the active ingredient in the Qinghao plant, is still used today as a potent and effective antimalarial drug.[5] Elsewhere, symptoms began to become widely recognized in Greece during the 4th century. Scholars during that time were aware that characteristics such as poor health, malarial fevers, and enlarged spleens were observed in people residing in marshy environments; for this reason it was believed that malarial fevers were caused by miasmas rising from swamps. It is commonly believed that malaria derives from the Italian word mal'aria meaning spoiled air. In 1880, a surgeon in the French army named Charles Louis Alphonse Laveran was the first to discover the parasite in the blood of a patient suffering from malaria. He was later awarded the Nobel Prize in 1907 for this discovery.[5]

Figure 1-1: Associated with malaria, the *Anopheles gambiae* mosquito is responsible for transmission of the disease in sub-Saharan Africa. Credit for picture goes to James Gathany.

Malaria is an example of a vector-borne disease; Ronald Ross, a British officer in the Indian Medical Service, was the first to establish the connection that mosquitoes were responsible for the spread of the parasite in 1897.[6] Malaria is caused by parasites of the *Plasmodium* genus[4], and there are five species known to cause to malarial harm to humans: *P. falciparum, P. vivax, P. ovale, P. malariae, and P. knowlesi*.[7] *P. falciparum* remains the most predominant species in endemic countries and is responsible for most malaria cases.[7] *P. vivax* is the next most common species, but more prevalent in Asia and South America.[8] Malaria caused by *P. vivax* proves problematic to control due to the dormancy of the hypnozoite stage of the parasite, causing relapses.[8] *P. malariae* may persist in the body for years without exhibiting any outward symptoms, and is less common than *P. vivax* or *P. falciparum*. *P. ovale* is only known to be located in Africa, and *P. knowlesi* has presented cases of infection in countries such as Malaysia.[9]

The life cycle of the parasite involves both intra-human and intra-mosquito stages and is described in Figure 1-2.[10]

Stage 1: The parasite enters the bloodstream as sporozoites during a blood meal by the mosquito. Upon entry, they migrate to the liver to multiply by invading hepatocytes, initiating asexual multiplication lasting between 5-10 days.[4, 7, 11]

Stage 2: Merozoites exit the liver and attack red blood cells initiating a multiplication cycle. Upon multiplication, some merozoites that exit the red blood cells come out as gametocytes, the transmissible parasite form. At this point, patients can exhibit malarial symptoms.[7, 11] Gametocytes that are formed spread throughout the bloodstream. During another blood feed, the parasite travels into the gut of the mosquito.[7, 11]

Stage 3: During this time, the parasite undergoes a reproductive cycle within the mosquito to produce sporozoites which move from the gut to the salivary glands, repeating the cycle once again.[7]

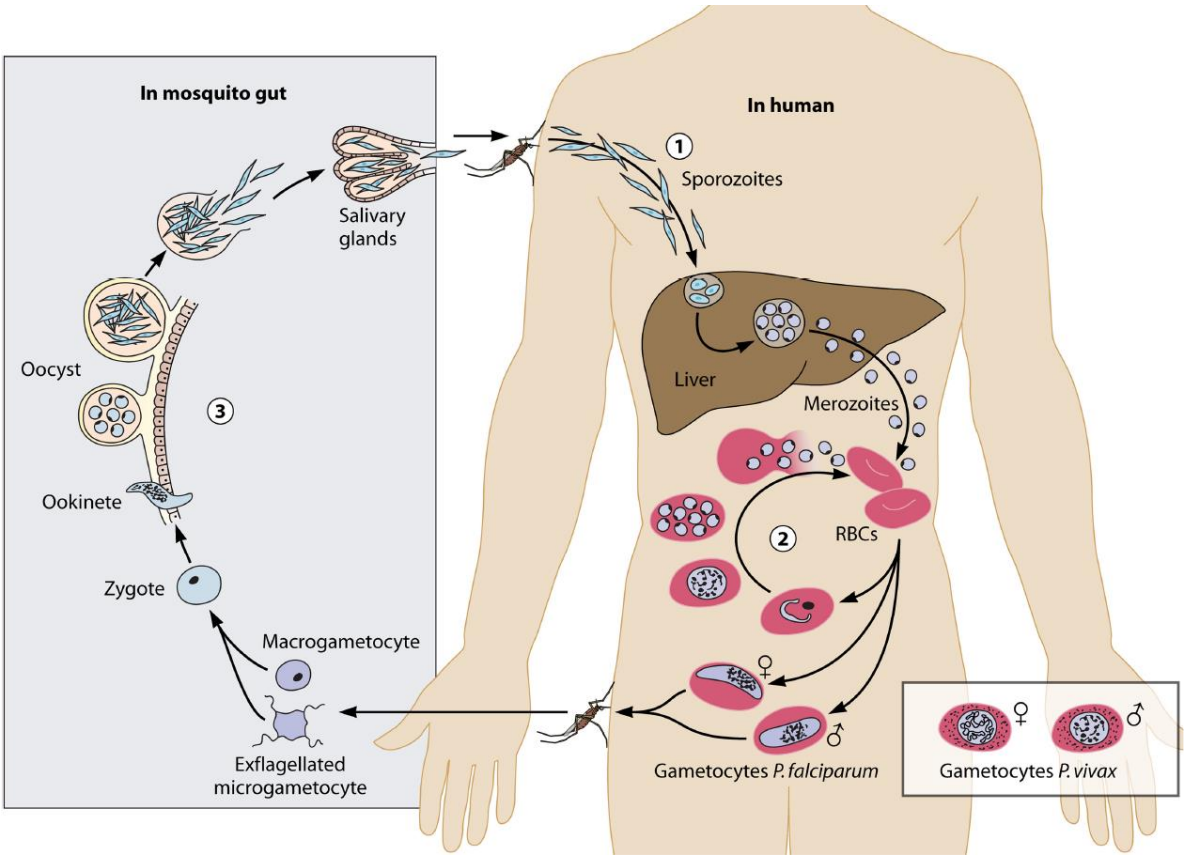

Figure 1-2: The life cycle of the *Plasmodium* parasite.[11] Reprinted with permission from the American Society for Microbiology (ASM).

1.3 Malaria Control

The types of approaches to control malaria will be discussed in detail below next.

1.3.1 Malaria Vaccines

To date, there is no currently approved vaccine for malaria. The most successful vaccine in development is RTS,S/AS01, developed by a joint effort between GlaxoSmithKline and the Malaria Vaccine Initiative at PATH with funding from the Bill and Melinda Gates Foundation.[12] RTS,S/AS01, a pre-erythrocytic vaccine, was inspired by a proof of concept study eliciting sterile immunity performed by Clyde and associates.[13] Currently the vaccine is undergoing

Phase III clinical trials.[12] The mechanism of action of the vaccine is currently unknown; one hypothesis is that RTS,S induces protection of the host by reducing the number of merozoites coming out of the liver.[12, 14] The increased number of asexual parasites that are produced may allow an immunity to be developed over time in the host.[14] First testing of the vaccine demonstrated reduced cases of severe malaria by 50% in children 5-17 months old and 37% in infants 6-12 weeks old.[15] The global malaria vaccine development road map dictates case reduction goals of 50% and 80% respectively, so it is unclear whether RTS,S will meet the standards set forth.[16] Until a vaccine is approved for malaria, eradicating malaria must be approached from a complementary angle.

1.3.2 Antimalarial drugs

Elimination of the parasite can prove to be a successful method to eliminate malaria.[17-18] Factors such as drug resistance, low efficacy, and the use of counterfeit drugs due to rising costs poses challenges however.[19] While chloroquine (**1-1**) and sulfadoxine-pyrimethamine (**1-2**,**1-3**) were primarily used as the initial lines of defense, these drugs are becoming less effective due to an increase of drug resistant *P. falciparum* parasites (Figure 1-3).[17, 20] The emergence of drug resistant parasites directly correlates to hospital admissions and malaria mortality across various parts of Africa.[17]

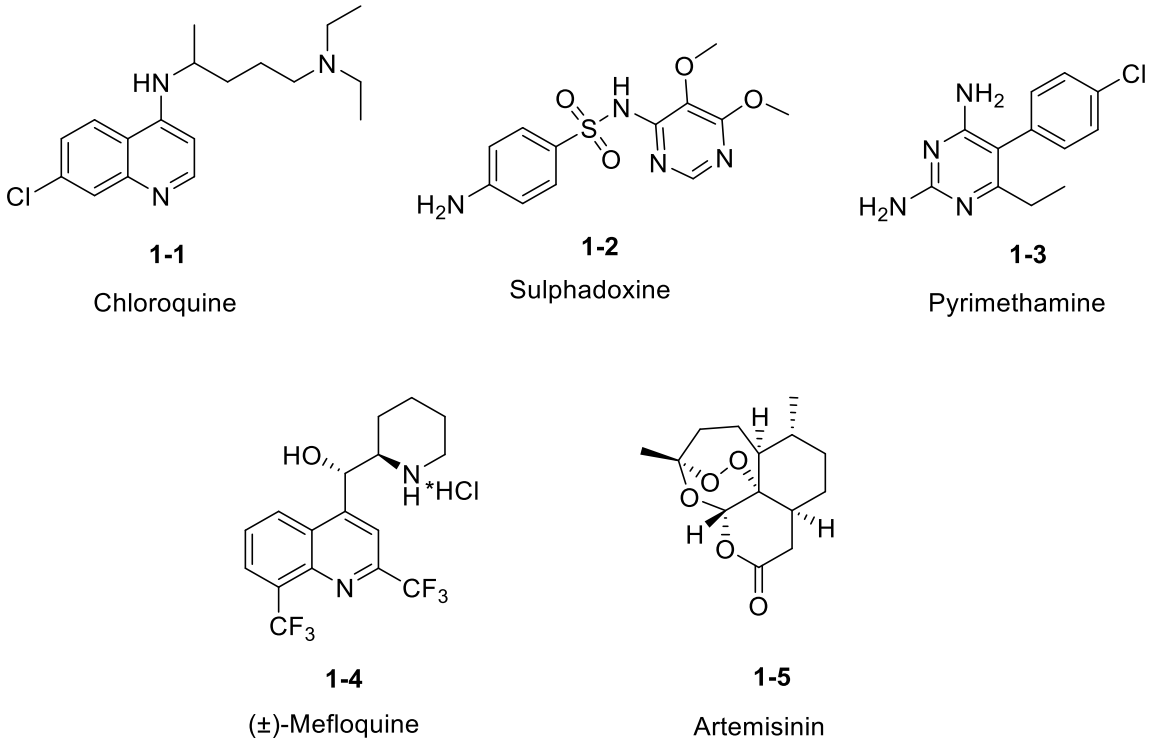

Figure 1-3: Antimalarial drugs chloroquine (**1-1**), sulphadoxine (**1-2**), pyrimethanime (**1-3**), (±)-mefloquine (**1-4**), and Artemisinin (**1-5**).

An increased risk of drug resistance can result from over administration of drugs.[21] New drugs have been developed in response to chloroquine-resistant parasites such as mefloquine (**1-4**) and artemisinin (**1-5**). As of 2013, mefloquine (**1-4**) is the only registered drug that is effective in a single dose. Artemisinin (**1-5**) can be effective as well in a single dose through artemisinin-based combination therapies (ACTs). ACTs comprise of a mixture of artemisinin or a derivative with a slow clearing drug such as lumefantrine or piperaquine and is the current method of choice for malarial cases.[21] As compared with other single drug treatments, combining drugs decreases the chance for drug resistance.[17, 21] However, the increased cost of using ACTs

prevents its use in poorer regions. Because targeting the parasite is not always practical, targeting the vector proves complementary in combating malaria.

1.3.3 Vector control

Vector control may prove to be the best method to eradicate malaria. Malaria relies on the vector to reproduce and transmit the parasite. Controlling the vector minimizes human-parasite interaction, which eliminates parasite dormancy and resistance issues, potentially eradicating the disease. Current method to control the vector include indoor residual spraying (IRS) and insecticide treated nets (ITNs). Using IRS and ITNs in conjunction has proven successful in reducing the number of malaria cases.[22]

IRS is a method in which dilute concentrations of insecticides are applied on the surfaces of the home. Landing on the surface promotes permeation of the insecticide into the mosquito, killing it and reducing the spread of malaria.[23-24] The push for using IRS started after World War II and remains an integral component in malaria control in 25 out of 42 malaria endemic regions. The effectiveness of IRS depends on factors such as: compound stability, timing of spraying, and susceptibility of the target vector. The WHO has approved 4 classes (organochlorines, pyrethroids, carbamates, and organophosphates) totaling 12 compounds for use in IRS, which target the only two sites exploited for insecticidal use: the voltage-gated sodium ion channel and the acetylcholinesterase enzyme.[25-27]

Initially, the use of nets as a physical barrier worked well in the past to separate mosquitoes from humans, thus reducing malarial cases. Due to the damage of nets over their lifetime, an innovation in the form of insecticide-treated nets were invented that works in two ways (Figure 1-4). First, the net serves as a barrier to separate vector from human, and secondly

reduces the vector population by killing them with the insecticides that are applied on the nets.[28-29] Without the use of ITNs, 75% of both types of mosquitoes (resistant and susceptible strains of *Anopheles gambiae*) were able to pass through holes and 63% of both types were able to blood feed; with permethrin treated ITNs, 3.9% of susceptible and 3.5% of resistant mosquitoes went through the holes and blood-fed successfully.[28] One drawback to ITNs initially was the short duration of toxicity. To protect younger children (5 years or less), the Global Malaria Action Plan suggested the use of long-lasting insecticide-treated nets (LLITNs). The use of LLITNs is now normal and will be referred to as ITNs henceforth.

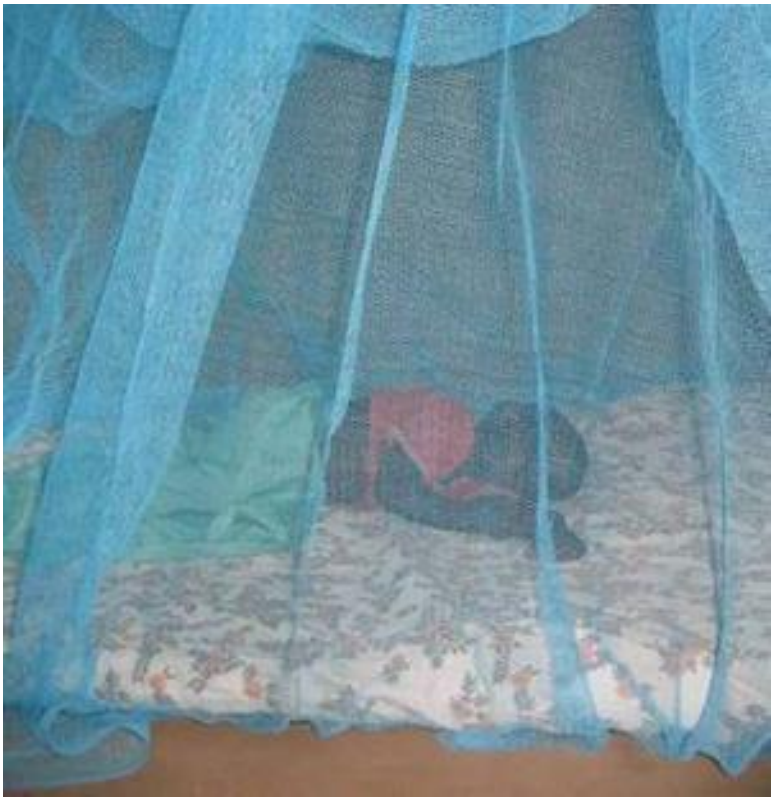

Figure 1-4: ITNs provide a barrier of defense against the malaria vector. Taken from CDC website. http://www.cdc.gov/malaria/how_can_i_help.html

Despite the initial success that IRS and ITNs have shown, emerging mosquitoes display resistance to the insecticides currently deployed, thus threatening to destroy the programs that have been implemented by WHO to protect the population against malaria. The classes of compounds, their mechanism of action, and resistance mechanisms to these compounds will be discussed in detail below next.

1.3.3.1 Repellents

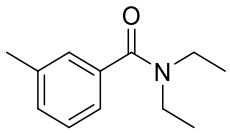

1-6

DEET

Figure 1-5: DEET is used as a repellent for vector control.

While many compounds are designed to kill the vector, simply deterring them from humans proves to be a viable strategy. Repellents control the vector by not killing them but rather by avoidance behavior preventing the vector from blood feeding. DEET (*N*, *N*-diethyl-3-methylbenzamide) (**1-6**, Figure 1-5) is one such example.[30-31] The mechanism for repellency is unclear and scientists have proposed different hypotheses for its actions.[32] The initial hypothesis was that DEET interfered with the mosquito's ability to detect lactic acid.[32] Syed and associates challenged this idea and suggested that mosquitoes directly avoid the DEET chemical.[32]

1.3.3.2 Voltage-gated sodium ion channel blockers

Organochlorines and pyrethroids are classes of neurotoxic compounds that target the voltage-gated sodium ion channel (Figure 1-6).[28, 33] The compounds slow the activation and inactivation of the sodium ion channel causing a prolonged opening, allowing sodium ions to cross the membrane. The efflux of sodium ions depolarizes the membrane causing synaptic disturbances and hypersensitivity. This is observed as paralysis in insects, leading to death.[33-34] It is of interest to note that DDT affects the peripheral nervous system while pyrethroids affect both the peripheral and central nervous systems.

1.3.3.3 Organochlorines

4,4'-(2,2,2-trichloroethane-1,1-diyl)bis(chlorobenzene) (DDT), an organochlorine insecticide (**1-7**, Figure 1-6), was discovered to be insecticidal by a Swiss chemist named Paul Müller.[35] It was first used on a full scale during World War II and proved to be successful. The success spread worldwide and by 1975, Europe was declared free of malaria. DDT's popularity arose from being cheap to make, its demonstrated low human toxicity, and its prolonged stability. The long stability proved to be a double edged sword; the WHO restricted the use of DDT due to environmental concerns, particularly its presence in high concentrations in non-target organisms due to solubility in the fatty tissues.[34-35] The WHO reinstated the use of DDT for indoor residual spraying as of 2006 in response to areas with constant and high malaria transmission.[36]

1.3.3.4 Pyrethroids

Pyrethroids are insecticidal esters of chrysanthemic acid and pyrethic acid, which are found in the flowers of *Chrysanthemum cinerafolis*.[37] Their use dates back to the 1970s to

control insects for agriculture and public health.[37] The first pyrethroid synthesized was permethrin (**1-9**, Figure 1-6) followed by cypermethrin (**1-8**, Figure 1-6), and deltamethrin (**1-10**, Figure 1-6). Deltamethrin (**1-10**) is still the most active pyrethroid to date.[35]

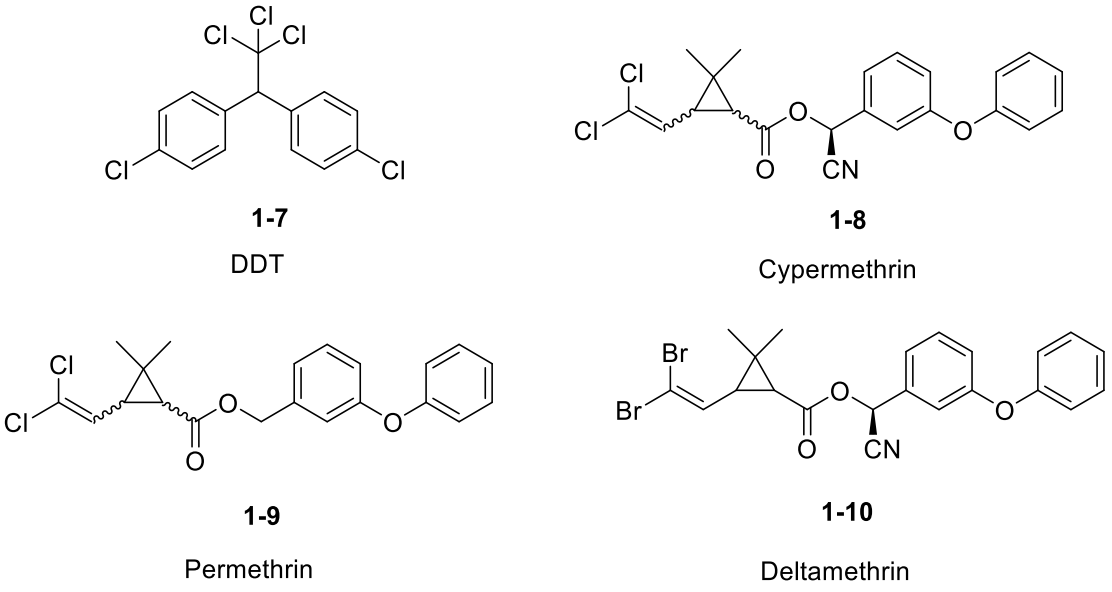

Figure 1-6: Organochlorines and pyrethroids are insecticides that act on the voltage-gated sodium ion channel. Examples include DDT (**1-7**), cypermethrin (**1-8**), permethrin (**1-9**), and deltamethrin (**1-10**).

All of the compounds (6 in total) that are approved for use on ITNs all belong to the pyrethroid class. Their popularity is attributed to their potency and low mammalian toxicity. However, the increased use of pyrethroids on ITNs led to an overuse and resulted in an emergence of mosquitoes exhibiting knockdown resistance (*kdr*) to these compounds.[23, 34] The knockdown resistance studied in houseflies derived from 2 amino acid mutations, specifically

L1014F (*kdr*) where a leucine residue is replaced with a phenylalanine and M918T (in the case of super-*kdr*) where a methionine residue is replaced with a threonine.[35]

A second mechanism for resistance is metabolic.[35] The resistance may be credited to an overproduction of Cyp450.[38] The resulting increase in enzyme activity reduces the amount of insecticide due to oxidation and subsequent excretion.[39] The prevalence of pyrethroid use on ITNs caused an emergence of pyrethroid-resistant strains of *An. gambiae*, thus driving a need to develop new insecticides that might be safe and effective on ITNs.[39] Another biologically-exploited target against the vector is the enzyme acetylcholinesterase (AChE). AChE inhibitors (AChEIs) have shown success against pyrethroid-resistant strain mosquitoes.[40] The use of two-in-one nets, ITNs treated with both pyrethroid and non-pyrethroid insecticides (e.g. carbamates), proved overall more effective in eliminating *Anopheles gambiae*.[40] The emergence of a strain of mosquitoes that is resistant to both currently approved pyrethroids and acetylcholinesterase inhibitor insecticides (Akron mosquitoes) has prompted a reinvestigation into AChEIs that could be efficacious against them. An introduction to acetylcholinesterase inhibitors will be provided below.

1.4 Acetylcholinesterase as an insecticidal target

As stated previously, AChE is the only other successfully exploited insecticidal target for adult mosquitoes other than the voltage-gated sodium channel.[26] The emergence of Akron mosquitoes drives a need for new effective insecticides. The Carlier group has previously reinvestigated another known chemotype (carbamates, discussed in section 1.6.2) and developed AChEIs that show selectivity, activity, and toxicity against Akron mosquitoes.[27, 41-42]

1.4.1 Acetylcholine

Acetylcholine (ACh, **1-11**, Scheme 1-1) is a neurotransmitter that is located throughout the nervous system and is believed to modulate critical functions such as cerebral blood flow, cortical activity, and the sleep-wake cycle.[43-45]

1.4.2 Acetylcholinesterase

AChE is an enzyme whose primary function is to cleave ACh after it is released into the synaptic cleft, thus ending cholinergic transmission.[46] It accomplishes this task by hydrolyzing ACh (**1-11**) into choline (**1-12**); the acylated enzyme this formed rapidly hydrolyzes to regenerate the enzyme (Scheme 1-1).[47] AChE accomplishes this task with great efficiency, with a turnover of 10^3-10^4 per second, a process which is only limited by the rate of the substrate entering the active site, known as diffusion controlled. AChE is present in both humans and mosquitoes. The first X-ray crystal structure was derived from *Torpedo californica* AChE and provided much information about the enzyme.[48]

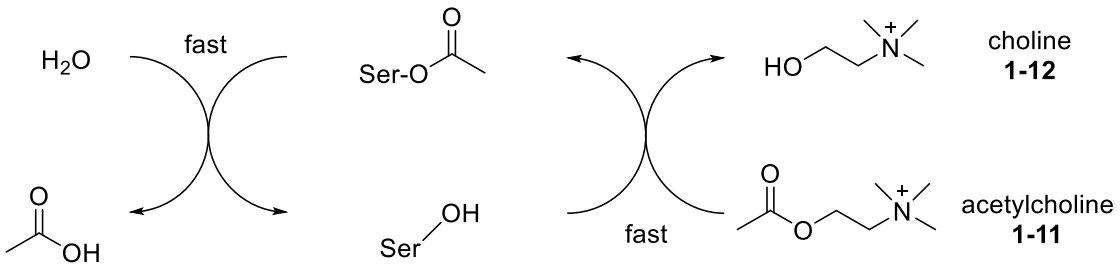

Scheme 1-1: The serine hydroxyl attacks the carbonyl and the short lived intermediate ejects choline (**1-12**) forming an acylated enzyme. The acylated enzyme rapidly hydrolyzes to give back the free enzyme and acetic acid.

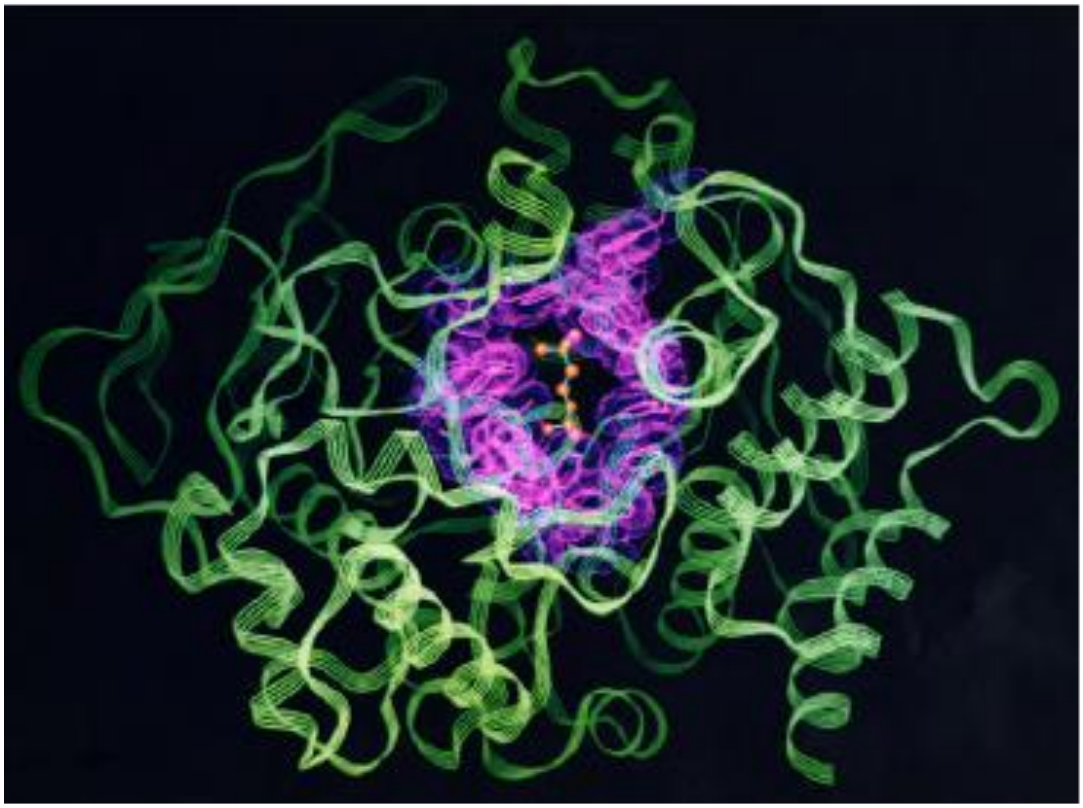

Figure 1-7: 3D structure of Tc-AChE as a ribbon diagram. The 14 conserved aromatic residues are shown as pink sticks on a dot surface. ACh is also shown at the bottom of the active site gorge as a ball and stick model. Reprinted with permission from Elsevier.[49]

AChE contains 12 beta-strands in the interior and 14 alpha helixes on the outside (Figure 1-7).[50] The enzyme contains a deep narrow gorge, lined with 14 conserved aromatic residues, 15 Å in length of which the substrate can enter leading into the active site.[49] ACh interacts with the aromatic residues lining the gorge and can diffuse down to the active site though a phenomenon called aromatic guidance.[49] Afterwards, ACh enters the active site; X-ray crystal structures show that the active site is at the bottom of 20 Å deep gorge.[49]

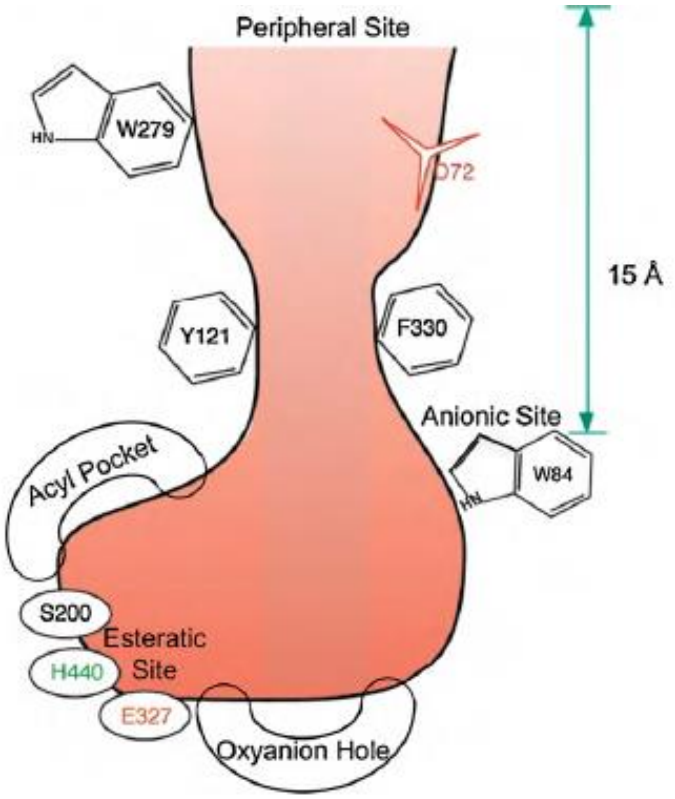

Figure 1-8: Representation of the active gorge of *Tc*-AChE.[49] Reprinted with copyright permission from Elsevier.

Four distinct regions in the enzyme define the active site where ACh is cleaved: the oxyanion hole, acyl pocket, anionic site, and the esteratic site (Figure 1-8).[46] Each region provides an interaction to help AChE to cleave ACh with great efficiency. The anionic site helps to dock ACh in place via a cation-pi interaction between W84 and the quaternary ammonium species in ACh.[51] The acyl pocket acts in a similar manner like the choline binding site; the acetate methyl of ACh interacts with hydrophobic residues in the acyl pocket. With ACh docked in place, the hydroxyl of the serine residue is able to attack the carbonyl of ACh through a charge relay mechanism of the catalytic triad (E325, H439, and S199) (Figure 1-9). Upon attack by S199, the oxyanion hole is able to stabilize the tetrahedral intermediate via hydrogen bonding

with residues A200, G119, and G118. The tetrahedral intermediate is short-lived and upon collapse, gives choline and an acylated serine residue. This acylated species is also short-lived and is then hydrolyzed to give back the enzyme and acetic acid (Scheme 1-1).

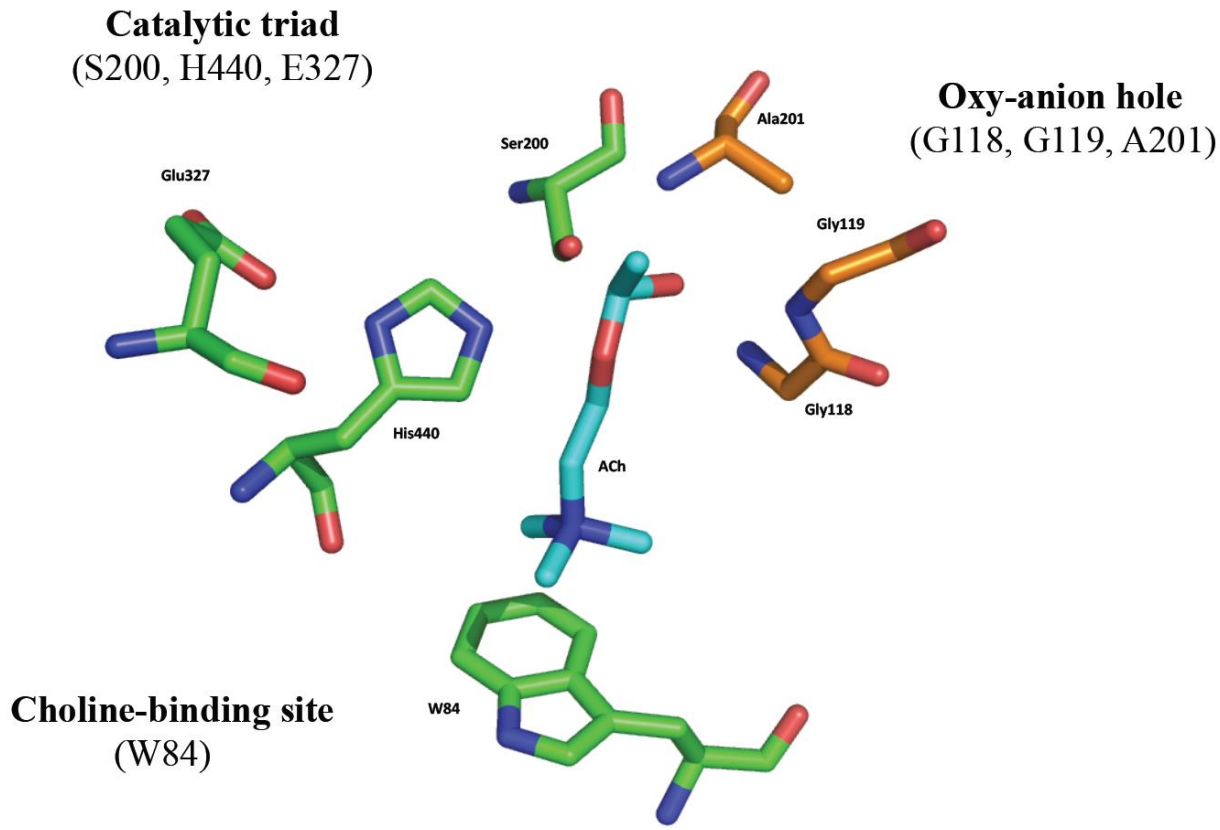

Figure 1-9: AChE is able to hydrolyze ACh with great efficiency due to four areas of interest: the esteratic site (also known as the catalytic triad), oxyanion hole, acyl pocket (not pictured) and anionic site (also known as the choline binding site). This graphic courtesy of Dr. Dawn Wong of the Carlier group.

1.5 Inhibitors of AChE

1.5.1 AChEI applications

AChE has been targeted for various purposes. Drugs have been synthesized to inhibit AChE in Alzheimer's patients, thereby improving cognition.[52] The cholinergic hypothesis states that symptoms of Alzheimer's disease are due to decreased levels of ACh in the brain; careful dosing of an AChEI works to increase ACh levels back to normal, providing symptomatic relief.[53-54] AChEIs can achieve this by binding to the enzyme through reversible, pseudo-irreversible, or irreversible means. [41, 55-57]

Unfortunately, AChEIs are also used as chemical warfare agents. Complete inhibition of AChE floods the host with an excess of ACh in the synapse, which will lead to paralysis and eventually death.[45, 50] The Tokyo Subway attack of 1995 was an instance in which an AChEI (sarin, an organophosphate) was used in an anti-government terror attack attacking humans. While used to harm humans, AChEIs also can be applied towards killing insects. Carbamates and organophosphates are the only approved classes of pesticides that target AChE. These compounds will be discussed in detail in the following sections due to their role in controlling malaria.

1.5.2 Carbamates

Carbamates, substrate analogs of ACh, are a class of pseudo-irreversible AChEIs. The serine hydroxyl of AChE attacks the electrophilic carbonyl in a manner similar to that of ACh.[58] Upon collapse of the tetrahedral intermediate, a phenol (ArOH), and a carbamoylated serine are formed. This species is slower to hydrolyze due to the reduced electrophilicity of the

carbamoylated serine compared to the acylated serine (Scheme 1-2). This resulting increase in synaptic ACh produces an insecticidal effect in the vector.

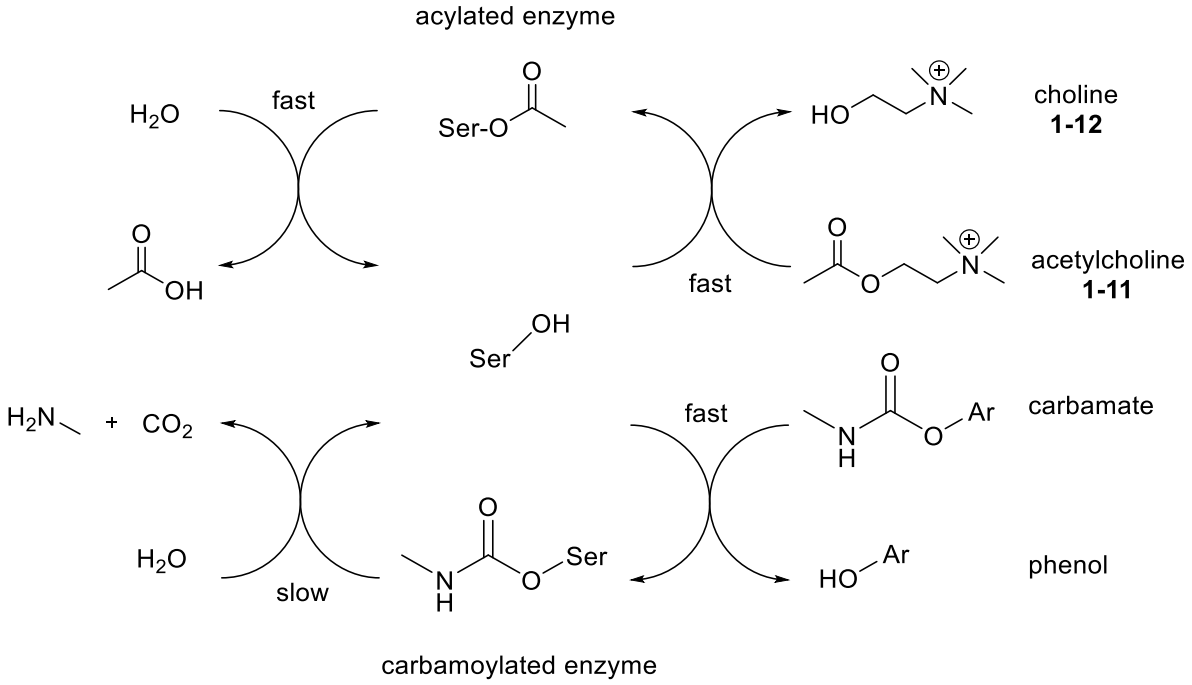

Scheme 1-2: Upon addition of a carbamate, the serine residue will bind to the carbamate, ejecting a phenol group and forming a carbamoylated serine. The resulting species is slower to hydrolyze than the acylated serine and thus is longer lived.

If applied to insecticide treated nets, potential mammalian toxicity is a concern. Research in the Carlier group has successfully synthesized carbamates as AChEIs that show 530:1 selectivity of *Anopheles gambiae* AChE (*Ag*AChE) to human AChE (*h*AChE) (Figure 1-10, **1-13**).[59] Carbamates have additionally been developed in the Carlier group that show toxicity towards carbamate-resistant *An. gambiae*. The key insight here was that reducing the size of the aromatic core of the carbamates made (**1-14**, **1-15**) allowed for a better fit in the resistant G119S active site, thus giving improved inhibition.[41-42] Some examples of commercial carbamates

applied as insecticides in agriculture and horticulture include aldicarb (**1-16**), propoxur (**1-17**), carbaryl (**1-18**), and pirimicarb (**1-19**) (Figure 1-11). With the exception of aldicarb, all commercial carbamates are ineffective at killing carbamate-resistant *An. gambiae*.

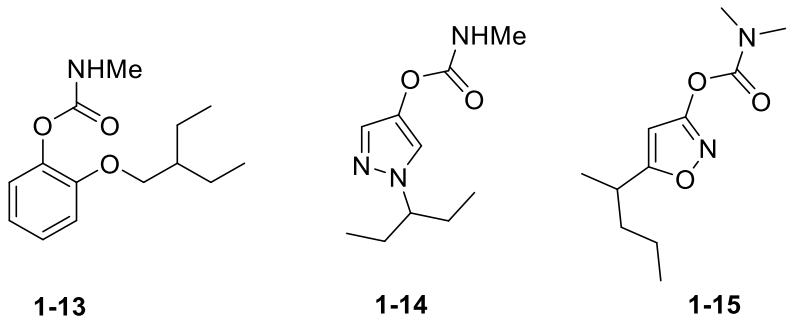

Figure 1-10: Carbamates have been developed in the Carlier group that show excellent selectivity towards *An. gambiae* AChE (**1-13**) and activity against G119S AgAChE (**1-14**, **1-15**).

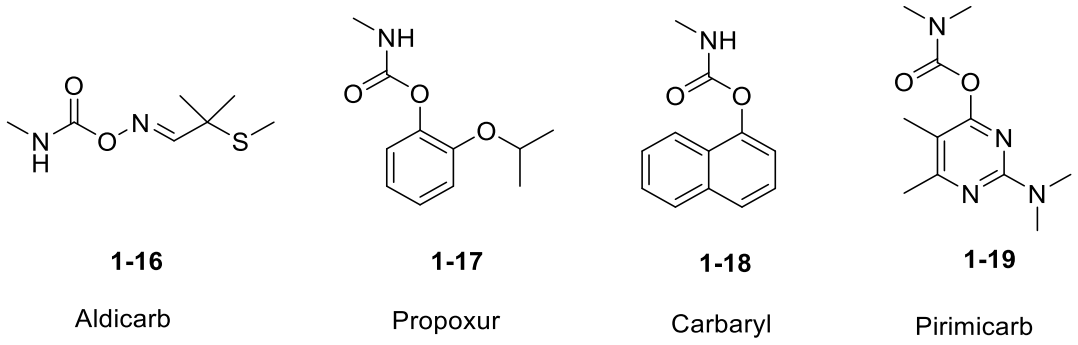

Figure 1-11: Carbamates, one class of AChEI, have been used as insecticides against *Anopheles gambiae*. Such examples include aldicarb (**1-16**), propoxur (**1-17**), carbaryl (**1-18**), and pirimicarb (**1-19**).

1.5.3 Organophosphates

Organophosphates (OPs) are well known AChEIs and inhibit AChE in a similar fashion to that of carbamates.[60-62] The phosphorus of the OP is attacked by the serine hydroxyl and after

collapse, a phosphorylated serine is formed (Scheme 1-3). The phosphorylated serine is even slower to hydrolyze compared with the carbamylated serine. This quality makes OPs ideal candidates for use as these insecticides; some commercial OPs, such as parathion (**1-20**), malathion (**1-21**, and chlorpyrifos (**1-22**), are used in IRS (Figure 1-12). Unfortunately, human toxicity concerns are associated with the use of insecticides; poisoning cases in human associated with exposure to OPs may result in death.[55, 60, 63] OPs, unlike carbamates, can undergo a process called aging in which phosphorylated serine residue can lose an alkyl group, resulting in permanent inactivation of the enzyme (Scheme 1-3).[55, 63]

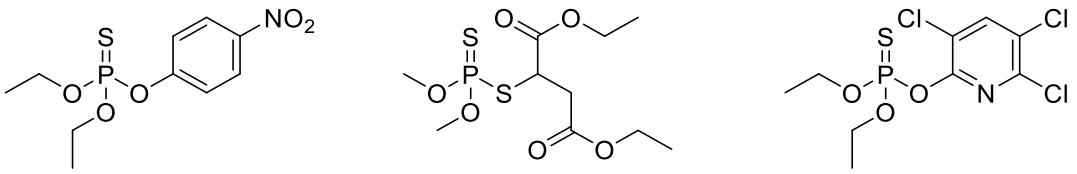

1-20

Parathion

1-21

Malathion

1-22

Chlorpyrifos

Figure 1-12: Organophosphates, a type of AChEIs, have been used as insecticides against *Anopheles gambiae*. Such examples include parathion (**1-20**), malathion (**1-21**), and chlorpyrifos (**1-22**).

Furthermore, organophosphate induced delayed neuropathy (OPIDN) can occur upon exposure to OPs. OPIDN is a neurodegenerative disorder with symptoms ranging from loss of motor and sensory function, to ataxia.[64] The drawbacks mentioned above have caused a decrease in the exploration of OPs as insecticidal candidates, and perhaps for this reason they have not been approved for use in ITNs.

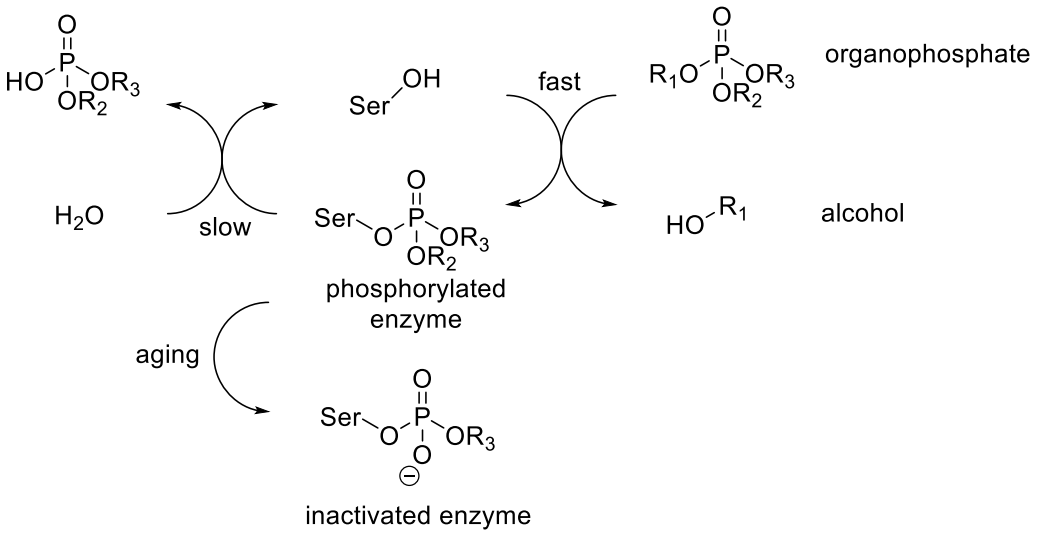

Scheme 1-3: Organophosphates inhibit AChE in a similar fashion to carbamates. It can correspondingly undergo a process of aging which inactivates the enzyme.

1.5.4 Trifluoromethylketones (TFKs)

Emerging pesticide-resistant mosquitoes drive a need for developing new insecticides. A known AChEI chemotype that has received little attention for insecticide development is the trifluoromethylketone.[56, 65] These compounds are regarded as reaction coordinate analogues, since they mimic the intermediate formed when ACh is attacked by the serine hydroxyl of AChE.[55, 66] Mirroring the intermediate allows for tighter binding between the enzyme and substrate (Figure 1-13). The tight binding is made possible by an inductive effect produced by the trifluoromethyl group, which stabilizes the negatively charged oxygen in the oxyanion hole.[67] The high electrophilicity that TFKs possess causes them to be extensively hydrated in water; the geminal diol cannot react with the catalytic serine. Thus hydration reduces the amount of active inhibitor present at equilibrium. The resulting geminal diol that is formed has been shown to be a poor AChE inhibitor (Scheme 1-4).[68] Yet TFKs can have excellent potency for inhibiting

AChE; Nair and associates showed that TFK **1-23** (Figure 1-14) had K_i values of 1.3 and 15 fM for *E. electricus* and *T. californica* AChE respectively.[56]

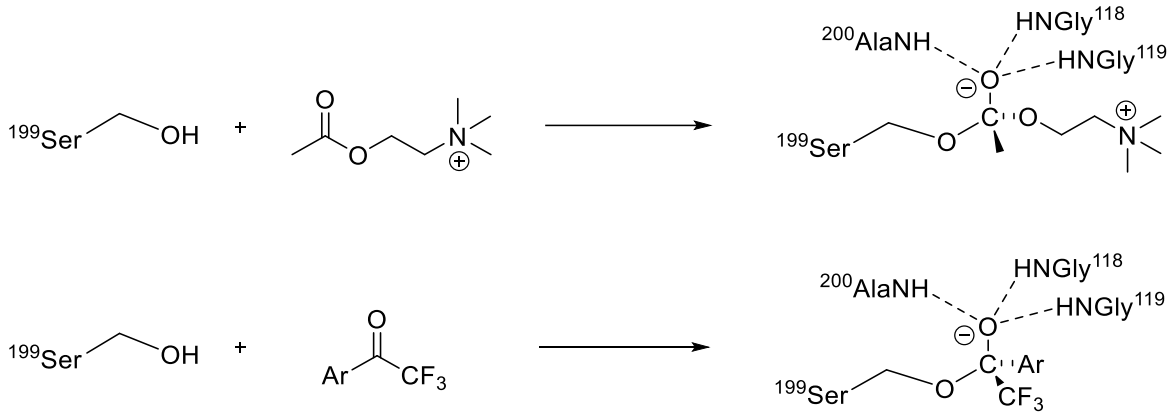

Figure 1-13: TFKs are known as reaction coordinate analogs. TFKs mimic the AChE-ACh intermediate along with an inductive effect produced by the trifluoromethyl group provides for greater stabilization.

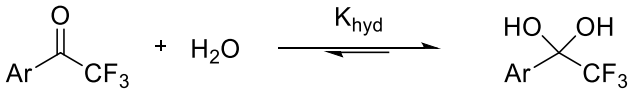

Scheme 1-4: The TFK is in equilibrium with the diol *in vivo*. Because equilibrium lies towards the diol, considerations must be made to shift it towards the ketone.

However, the extent of hydration that TFKs exhibit may also present a pharmacokinetic challenge.[69] As discussed previously, when the TFK is attacked by H_2O, the diol formed is a poor inhibitor of AChE. Hypothetically in the diol form, glucuronidation could occur with the addition of UDP-glucuronic acid, potentially making it more water soluble and allowing for

faster excretion of the compound.[70] The diol may also not have optimum lipophilicity to travel through barriers such as the mosquito cuticle or the blood brain barrier.[71]

1.5.4.1 Trifluoromethyl ketone design strategies

For TFKs to be successfully applied as insecticides, considerations must be made to improve delivery while retaining potency. A known crystal structure of **1-23** complexed with *Torpedo californica* (*Tc*) AChE (RCSB ID: 1HBJ) and mouse AChE (PDB ID: 2H9Y) provides insight as to the interactions that need to be maintained (Figure 1-14).[56-57, 67]

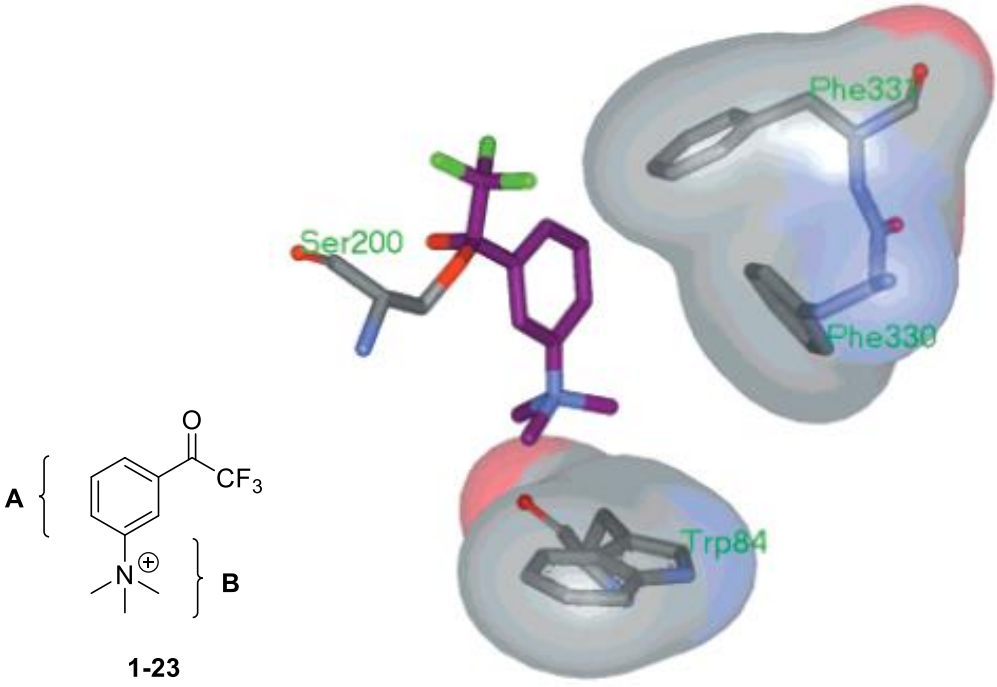

Figure 1-14: Representation of the *Tc*AChE/**1-23** complex (RCSB ID: 1HBJ). Key interactions include an electrostatic interaction of the quaternary ammonium of **1-23** with the indole ring of W84 and π-π interaction with the benzene rings of **1-23** and F330.[72-73] Reprinted with permission from Doucet-Personeni, C. *et al*. *J. Med. Chem.* **2001**, *44* , 3203-3215.

The benzene ring in **1-23** provides rigidity in positioning the carbonyl to be attacked (Figure 1-14). The trimethylammonium group docks the molecule in the active site through a cation-pi interaction between the charged ammonium group and the indole ring of the W84 residue.

Given that **1-23** is a potent inhibitor of *Ee*-AChE, *Tc*-AChE and mouse AChE, the starting point involved modifying **1-23** to cater our needs.[56, 74] Two areas of modification involve the ring and the trimethylammonium substituent (area A and B, Figure 1-14). The benzene ring in **1-23** may make the compound too large to fit into the active site of G119S *Ag*AChE. The proposed modification involves a reduction of ring size from a benzene ring to a pyrazole ring. The Carlier group has shown success with pyrazole and isoxazole rings by preparing carbamates displaying toxicity towards Akron mosquitoes (Figure 1-10).[41] While the charged ammonium group provides affinity and proper positioning, its permanent charge will impede permeation of the BBB and cuticle of the mosquito. One change involves a replacement from a charged nitrogen to a neutral carbon or silicon, thereby improving lipophilicity.[54, 69, 75-76]

1.5.4.2 Fluorinated methyl ketones as inhibitors of other enzymes

While TFKs are well-known for AChE inhibition, di-, and fluoromethyl ketones have also been shown to be inhibitors of various hydrolases and proteases, as discussed below. Difluoroketone **1-24** (Figure 1-15), based on the structure of ACh, was synthesized by Abeles and associates to investigate fluorinated methyl ketone activity against *Electric eel* (*Ee*) AChE.[68] It was found that compound **1-24** exhibited the best activity with a K_i of 1.6 nM, more potent than a TFK (**1-25**) also discussed in the paper with a K_i of 16 nM.[68] Szekacs and associates also described an inhibitor of AChE containing a TFK moiety (**1-26**) and exhibiting an IC_{50} of 627 nM.[77]

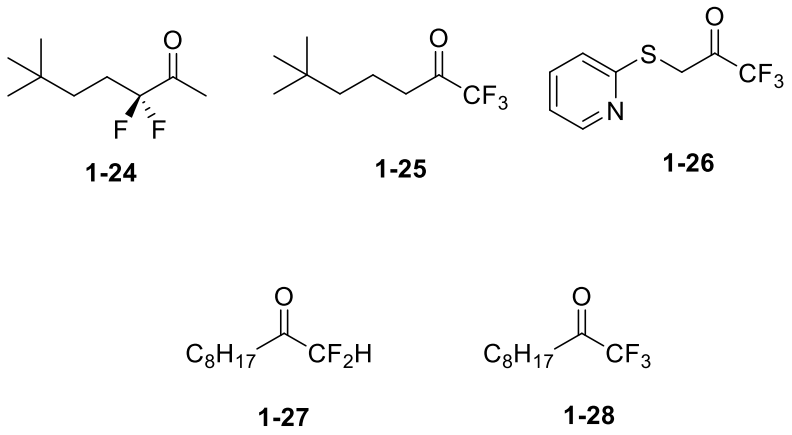

Figure 1-15: Tri- and difluoromethyl ketone inhibitors of AChE (**1-24**, **1-25**, and **1-26**) and JHE (**1-26**, **1-27**, and **1-28**), both serine hydrolases.

Fluorinated methyl ketones have also shown activity towards other serine hydrolases. Compound **1-26**, which was shown to be a good inhibitor of AChE, was also tested against juvenile-hormone esterase (JHE) and displayed an IC_{50} value of 97.8 nM.[77] Difluoroketones show reduced inhibition of JHE; **1-27** was show to have a 3 μM IC_{50} value.[74] Increasing the electrophilicity via the addition of one more fluorine (**1-28**) proved beneficial, decreasing the IC_{50} value to 100 nM.

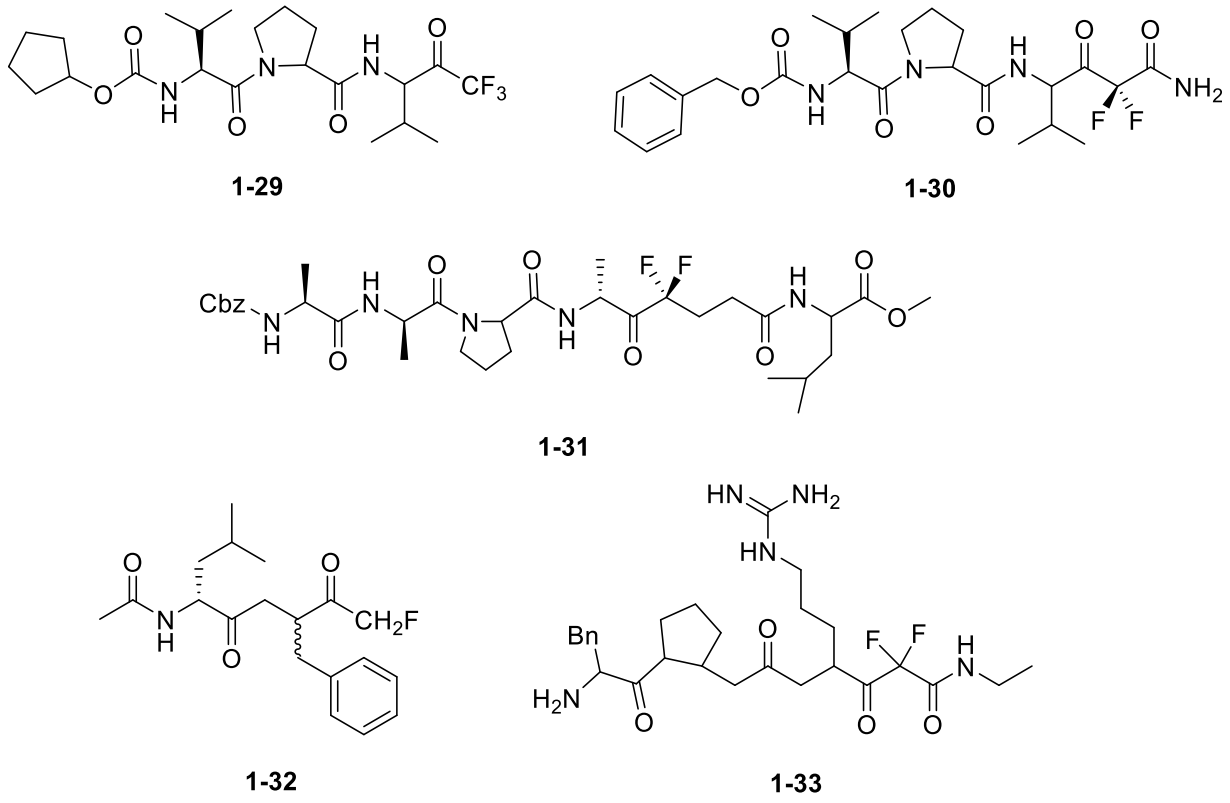

Figure 1-16: Fluorinated methyl ketones have been shown to be excellent inhibitors of serine proteases such as HLE (**1-29**, **1-30**, and **1-31**), α-chymotrypsin (**1-32**), thrombin (**1-33**) and α-lyticprotease. Where stereochemical configuration is not specified, the compounds exist as a mixture of stereoisomers.

Fluorinated methyl ketones have also been incorporated into peptides as inhibitors of the serine protease human leukocyte elastase (HLE). Inhibitors of this enzyme could be useful to treat pulmonary emphysema and acute respiratory distress syndrome.[78-79] During one investigation, a peptidyl TFK (**1-29)** was synthesized that exhibited a K_i of 1.9 nM against HLE (Figure 1-16). Peptidyl DFKs (**1-30** and **1-31**) also showed activity towards HLE; in one case lowering the K_i value to 0.38 nM (**1-30**). Compound **1-31** displays potency towards other serine proteases such as α-lyticprotease, with a K_i of 40 nM.[80] Imperiali and associates investigated the

use of fluorinated methyl ketones and their activity towards the serine protease α-chymotrypsin and found that **1-32** showed only low potency towards the enzyme (K_i = 200 μM). Compound **1-32** displayed characteristics of both reversible competitive inhibition and irreversible inhibition. They attributed the irreversible inhibition of **1-32** to ejection of the fluorine deactivating the enzyme. Incorporation of additional fluorines saw the expected decrease in K_i due to increased electrophilicity.[81] Thrombin is a serine protease involved in the coagulation cascade to promote blood loss. Fluorinated methyl ketone inhibitors were made to inhibit thrombin as potential therapeutic agents. The results showed that these compounds were very successful in inhibiting the enzyme with IC_{50} values as low as 7 nM (compound **1-33**, Figure 1-17).[82]

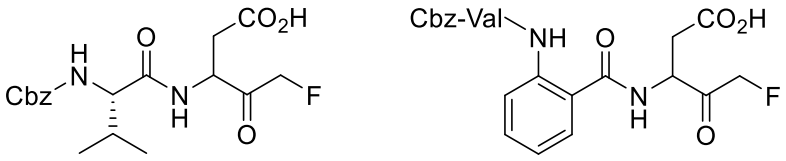

1-34 **1-35**

Figure 1-17: Fluorinated methyl ketones have been shown to be excellent inhibitors of cysteine proteases such as caspase (**1-34** and **1-35**). Where stereochemical configuration is not specified, the compounds exist as a mixture of stereoisomers.

Inhibitors of cysteine proteases that contain fluorinated methyl ketones have also been developed.[83-84] Wang and associates developed peptidyl inhibitors of caspase containing a monofluoroketone (Figure 1-17). In 2004, **1-34** was developed that exhibited excellent activity towards various caspases (caspase 1,3,6,7,8, and 9) with an IC_{50} as low as 5 nM.[84] A later attempt to improve upon the original design with the incorporation of 2-aminoaryl acids (**1-35**) did not prove as beneficial.[83]

It should be noted that fluorinated methyl ketones have also been employed as transition state isostere inhibitors for aspartic proteases. Unlike serine and cysteine proteases, aspartic proteases do not use an amino acid side chain to nucleophilically attack the carbonyl carbon of the scissile amide bond. Instead, two aspartic residues activate a water molecule to attack the same carbonyl. Consequently stable geminal diols can serve as transition state isosteres (Figure 1-18).

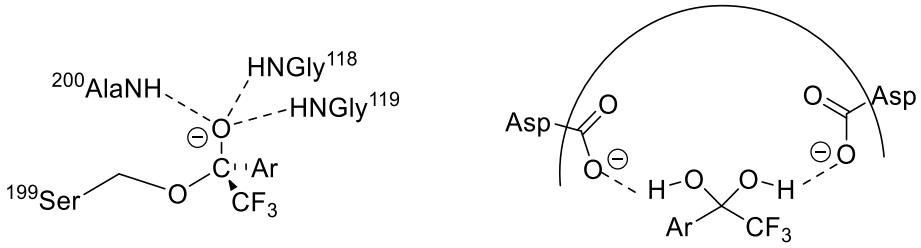

Figure 1-18: Serine/Cysteine protease inhibitors work through a covalent means. Aspartic protease inhibitors work through non-covalent means.

Difluoroketone **1-36** showed excellent activity against pepsin, an aspartyl protease responsible for digestion in the stomach, with K_i = 0.06 μM (Figure 1-19).[68]

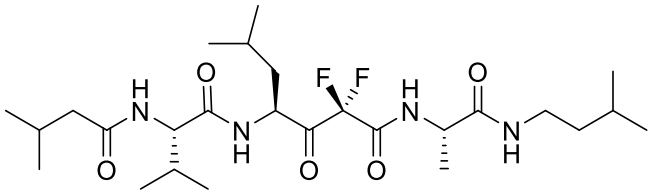

1-36

Figure 1-19: Difluoroketone **1-36** is an excellent inhibitor towards pepsin, an aspartic protease. Where stereochemical configuration is not specified, the compounds exist as a mixture of stereoisomers.

The same strategy can be used also for metalloproteases which also activate water to attach the scissile amide carbon. Gelb and associates investigated TFKs as inhibitors of carboxypeptidase A (CPA1), a zinc metalloprotease, crucial to processes such as digestion, blood clotting, and reproduction.[68] Compound **1-37** was found to be a potent inhibitor of CPA1 with a K_i = 0.2 μM (Figure 1-20). Incorporation of an aldehyde (**1-38**) in the place of the TFK decreased binding 2-fold, suggesting that the TFK allows for stronger binding to the enzyme. Another zinc metalloprotease, angiotensin converting enzyme, was also investigated for inhibition. Compound **1-39**, with the incorporation of the TFK group, showed excellent activity against the enzyme (K_i=0.012 μM).[68]

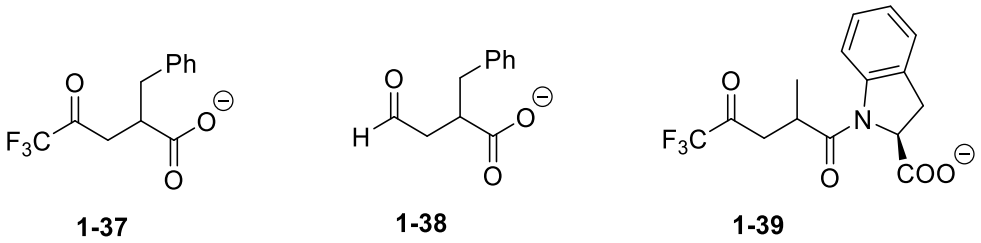

Figure 1-20: Trifluoroketone **1-37** is a potent inhibitor of carboxypeptidase A, a zinc metalloproteases and trifluoroketone **1-39** displays activity towards aspartic proteases such as angiotensin converting enzyme.

The next chapter will discuss the synthesis, *in vitro* activity, and toxicity results of the proposed fluorinated methyl ketones from a manuscript in progress.

1.6 References:

1. 10 facts on malaria, available at http://www.who.int/features/factfiles/malaria/en/. (accessed 01/15/15).

2. NIH website, available at http://www.ncbi.nlm.nih.gov/pubmedhealth/PMH0001646/. (accessed 12/10/15).

3. World Malaria Report 2014, The World Health Organization, available at http://apps.who.int/iris/bitstream/10665/144852/2/9789241564830_eng.pdf, last accessed 12/17/14.

4. Mueller, A. K.; Kohlhepp, F.; Hammerschmidt, C.; Michel, K., Invasion of mosquito salivary glands by malaria parasites: prerequisites and defense strategies. *Int. J. Parasit.* **2010,** *40*, 1229-1235.

5. The History of Malaria, an Ancient Disease, available at http://www.cdc.gov/malaria/about/history/.

6. Cox, F. E. G., History of the discovery of the malaria parasites and their vectors. *Parasites and Vectors* **2010,** *3*, 1-9.

7. Crawley, J.; Chu, C.; Mtove, G.; Nosten, F., Malaria in children. *Lancet* **2010,** *375*, 1468-1481.

8. Markus, M. B., Malaria: origin of the term "hypnozoite". *J. Hist. Biol.* **2011,** *44*, 781-786.

9. Cox-Singh, J.; Davis, T. M. E.; Lee, K. S.; Shamsul, S. S. G.; Matusop, A.; Ratnam, S.; Rahman, H. A.; Conway, D. J.; Singh, B., *Plasmodium knowlesi* malaria in humans is widely distributed and potentially life threatening. *Clin. Infect. Dis.* **2008,** *46*, 165-171.

10. Gerald, N. G. N.; Mahajan, B.; Kumar, S., Mitosis in the human malaria parasite *Plasmodium falciparum*. *Eukaryot. Cell* **2011,** *10*, 474-482.

11. Bousema, T. B. T.; Drakeley, C., Epidemiology and infectivity of *Plasmodium falciparum* and *Plasmodium vivax* gametocytes in relation to malaria control and elimination. *Clin. Microbiol. Rev.* **2011,** *24*, 377.

12. Heppner, D. G., The malaria vaccine - status quo 2013. *Travel Med. Infect. Dis.* **2013,** *11*, 2-7.

13. Clyde, D. F.; Most, H.; McCarthy, V. C.; Vanderberg, J. P., Immunization of man against sporozoite induced *falciparum* malaria. *Am. J. Med. Sci.* **1973,** *266*, 169-177.

14. Crompton, P. D.; Pierce, S. K.; Miller, L. H., Advances and challenges in malaria vaccine development. *J. Clin. Invest.* **2010,** *120*, 4168-4178.

15. Mwangoka, G.; Ogutu, B.; Msambichaka, B.; Mzee, T.; Salim, N.; Kafuruki, S.; Mpina, M.; Shekalaghe, S.; Tanner, M.; Abdulla, S., Experience and challenges from clinical trials with malaria vaccines in Africa. *Malaria J.* **2013,** *12*.

16. Casares, S.; Brumeanu, T. D.; Richie, T. L., The RTS,S malaria vaccine. *Vaccine* **2010,** *28*, 4880-4894.

17. Barnes, K. I.; White, N. J., Population biology and antimalarial resistance: the transmission of antimalarial drug resistance in *Plasmodium falciparum*. *Acta Trop.* **2005,** *94*, 230-240.

18. Lochner, M.; Thompson, A. J., The antimalarial drug proguanil Is an antagonist at 5-HT3 receptors. *J. Pharmacol. Exp. Ther.* **2014,** *351*, 674-684.

19. Koesdjojo, M. T.; Wu, Y. Y.; Boonloed, A.; Dunfield, E. M.; Remcho, V. T., Low-cost, high-speed identification of counterfeit antimalarial drugs on paper. *Talanta* **2014,** *130*, 122-127.

20. Petersen, I.; Eastman, R.; Lanzer, M., Drug-resistant malaria: Molecular mechanisms and implications for public health. *FEBS Lett.* **2011,** *585*, 1551-1562.

21. Biamonte, M. A.; Wanner, J.; Le Roch, K. G., Recent advances in malaria drug discovery. *Bioorg. Med. Chem. Lett.* **2013,** *23*, 2829-2843.

22. Okumu, F. O.; Moore, S. J., Combining indoor residual spraying and insecticide-treated nets for malaria control in Africa: a review of possible outcomes and an outline of suggestions for the future. *Malar. J.* **2011,** *10*.

23. Raghavendra, K.; Barik, T. K.; Reddy, B. P. N.; Sharma, P.; Dash, A. P., Malaria vector control: from past to future. *Parasitol. Res.* **2011,** *108*, 757-779.

24. Perveen, F., *Insecticides - advances in integrated pest management*. InTech: 2012.

25. WHO recommended insecticides for indoor residual spraying against malaria vectors, available at: http://www.who.int/whopes/Insecticides_IRS_Malaria_25_Oct_2013.pdf. 2007.

26. Nauen, R., Insecticide resistance in disease vectors of public health importance. *Pest Manag. Sci.* **2007,** *63*, 628-633.

27. Wong, D. M. L., J.; Lam, P. C. H.; Hartsel, J. A.; Mutunga J. M.; Totrov, M.; Bloomquist, J. R.; Carlier, P. R. , Aryl methylcarbamates: potency and selectivity towards wild-type and carbamate-insensitive (G119S) *Anopheles gambiae* acetylcholinesterase, and toxicity to G3 Strain *An. gambiae*. *Chem.-Biol. Interact.* **2012,** *203*, 314-318.

28. Enayati, A. A.; Hemingway, J., Pyrethroid insecticide resistance and treated bednets efficacy in malaria control. *Pestic. Biochem. Physiol.* **2006,** *84*, 116-126.

29. Insecticide-Treated Bed Nets, available at. http://www.cdc.gov/malaria/malaria_worldwide/reduction/itn.html.

30. Pickett, J. A.; Birkett, M. A.; Logan, J. G., DEET repels ORNery mosquitoes. *Proc. Natl. Acad. Sci. U. S. A.* **2008,** *105*, 13195-13196.

31. Pellegrino, M., A natural polymorphism alters odour and DEET sensitivity in an insect odorant receptor. *Nature* **2011**, 511-516.

32. Syed, Z.; Leal, W. S., Mosquitoes smell and avoid the insect repellent DEET. *Proc. Natl. Acad. Sci. U. S. A.* **2008,** *105*, 13598-13603.

33. Corbel, V.; Stankiewicz, M.; Pennetier, C.; Fournier, D.; Stojan, J.; Girard, E.; Dimitrov, M.; Molgó, J.; Hougard, J.-M.; Lapied, B., Evidence for inhibition of cholinesterases in insect and mammalian nervous systems by the insect repellent deet. *BMC Biol.* **2009,** *7*, 47.

34. Jamali, S. J. S., Role of pyrethroids in control of malaria amongst refugee population. *J. Pak. Med. Assoc.* **2011,** *61*, 486-490.

35. Walker, K., Cost-comparison of DDT and alternative insecticides for malaria control. *Med. Vet. Entomol.* **2000,** *14*, 345-354.

36. Davies, T. G. E.; Field, L. M.; Usherwood, P. N. R.; Williamson, M. S., DDT, pyrethrins, pyrethroids and insect sodium channels. *IUBMB Life* **2007,** *59*, 151-162.

37. WHO gives indoor use of DDT a clean bill of health for controlling malaria, available at. http://www.who.int/mediacentre/news/releases/2006/pr50/en/.

38. Soderlund, D. M.; Clark, J. M.; Sheets, L. P.; Mullin, L. S.; Piccirillo, V. J.; Sargent, D.; Stevens, J. T.; Weiner, M. L., Mechanisms of pyrethroid neurotoxicity: implications for cumulative risk assessment. *Toxicology* **2002,** *171*, 3-59.

39. Mulamba, C.; Riveron, J. M.; Ibrahim, S. S.; Irving, H.; Barnes, K. G.; Mukwaya, L. G.; Birungi, J.; Wondji, C. S., Widespread pyrethroid and DDT resistance in the major malaria vector *Anopheles funestus* in east Africa is driven by metabolic resistance mechanisms. *PLoS One* **2014,** *9*, 10.

40. Ochomo, E.; Bayoh, M. N.; Brogdon, W. G.; Gimnig, J. E.; Ouma, C.; Vulule, J. M.; Walker, E. D., Pyrethroid resistance in *Anopheles gambiae* s.s. and *Anopheles arabiensis* in western Kenya: phenotypic, metabolic and target site characterizations of three populations. *Med. Vet. Entomol.* **2013,** *27*, 156-164.

41. Guillet, P.; N'Guessan, R.; Darriet, F.; Traore-Lamizana, M.; Chandre, F.; Carnevale, P., Combined pyrethroid and carbamate 'two-in-one' treated mosquito nets: field efficacy against pyrethroid-resistant Anopheles gambiae and Culex quinquefasciatus. *Med. Vet. Entomol.* **2001,** *15*, 105-112.

42. Wong, D. M.; Li, J.; Chen, Q.-H.; Han, Q.; Mutunga, J. M.; Wysinski, A.; Anderson, T. D.; Ding, H.; Carpenetti, T. L.; Verma, A.; Islam, R.; Paulson, S. L.; Lam, P. C. H.; Totrov, M.; Bloomquist, J. R.; Carlier, P. R., Select small core structure carbamates exhibit high contact toxicity to "carbamate-resistant" strain malaria mosquitoes, *Anopheles gambiae* (Akron). *PLoS One* **2012,** *7*, e46712.

43. Verma, A. W., Dawn M.; Islam, Rafique; Tong, Fan; Ghavami, Maryam; Mutunga, James M.; Slebodnick, Carla; Li, Jianyong; Viayna, Elisabet; Lam, Polo C.-H.; Totrov, Maxim M.; Bloomquist, Jeffrey R.; Carlier, Paul R., 3-Oxoisoxazole-2(3*H*)-carboxamides and isoxazol-3-yl carbamates: Resistance-breaking acetylcholinesterase inhibitors targeting the malaria mosquito, *Anopheles gambiae*. *Bioorg. Med. Chem.* **2015,** *23*, 1321-1340.

44. Schliebs, R.; Arendt, T., The cholinergic system in aging and neuronal degeneration. *Behav. Brain Res.* **2011,** *221*, 555-563.

45. Hicks, D.; John, D.; Makova, N. Z.; Henderson, Z.; Nalivaeva, N. N.; Turner, A. J., Membrane targeting, shedding and protein interactions of brain acetylcholinesterase. *J. Neurochem.* **2011,** *116*, 742-746.

46. Van Beek, A.; Claassen, J., The cerebrovascular role of the cholinergic neural system in Alzheimer's disease. *Behav. Brain Res.* **2011,** *221*, 537-542.

47. Park, S. Y., Potential therapeutic agents against Alzheimer's disease from natural sources. *Arch. Pharm. Res.* **2010,** *33*, 1589-1609.

48. Nordberg, A.; Svensson, A. L., Cholinesterase inhibitors in the treatment of Alzheimer's disease - a comparison of tolerability and pharmacology. *Drug Saf.* **1998,** *19*, 465-480.

49. Li, W. M.; Kan, K. K. W.; Carlier, P. R.; Pang, Y. P.; Han, Y. F., East meets west in the search for Alzheimer's therapeutics - novel dimeric inhibitors from Tacrine and Huperzine A. *Curr. Alzheimer Res.* **2007,** *4*, 386-396.

50. Carlier, P. R.; Anderson, T. D.; Wong, D. M.; Hsu, D. C.; Hartsel, J.; Ma, M.; Wong, E. A.; Choudhury, R.; Lam, P. C. H.; Totrov, M. M.; Bloomquist, J. R., Towards a species-selective acetylcholinesterase inhibitor to control the mosquito vector of malaria, *Anopheles gambiae*. *Chem.-Biol. Interact.* **2008,** *175*, 368-375.

51. Colletier, J. P.; Fournier, D.; Greenblatt, H. M.; Stojan, J.; Sussman, J. L.; Zaccai, G.; Silman, I.; Weik, M., Structural insights into substrate traffic and inhibition in acetylcholinesterase. *EMBO J.* **2006,** *25*, 2746-2756.

52. Sussman, J. L.; Harel, M.; Frolow, F.; Oefner, C.; Goldman, A.; Toker, L.; Silman, I., Atomic-structure of acetylcholinesterase from *Torpedo californica* - A protoypic acetylcholine-binding protein. *Science* **1991,** *253*, 872-879.

53. Dvir, H.; Silman, I.; Harel, M.; Rosenberry, T. L.; Sussman, J. L., Acetylcholinesterase: From 3D structure to function. *Chem.-Biol. Interact.* **2010,** *187*, 10-22.

54. Ma, J. C.; Dougherty, D. A., The cation-pi interaction. *Chem. Rev.* **1997,** *97*, 1303-1324.

55. Braida, D.; Sala, M., Eptastigmine: Ten years of pharmacology, toxicology, pharmacokinetic, and clinical studies. *CNS Drug Rev.***2001,** *7*, 369-386.

56. Scarpini, E.; Scheltens, P.; Feldman, H., Treatment of Alzheimer's disease: current status and new perspectives. *Lancet Neurol.* **2003,** *2*, 539-547.

57. Cutler, N. R.; Seifert, R. D.; Schleman, M. M.; Sramek, J. J.; Szylleyko, O. J.; Howard, D. R.; Barchowsky, A.; Wardle, T. S.; Brass, E. P., Acetylcholinesterase inhibition by zifrosilone - pharmacokinetics and pharmacodynamics. *Clin. Pharmacol. Ther.* **1995,** *58*, 54-61.

58. Gupta, *Toxicology of Organophosphate and Carbamate Compounds*. Elsevier: London, 2006; Vol. 1, p 763.

59. Nair, H. K.; Lee, K.; Quinn, D. M., *m*-(N,N,N-Trimethylammonio)trifluoroacetophenone - a femtomolar inhibitor of acetylcholinesterase. *J. Am. Chem. Soc.* **1993,** *115*, 9939-9941.

60. Harel, M.; Quinn, D. M.; Nair, H. K.; Silman, I.; Sussman, J. L., The X-ray structure of a transition state analog complex reveals the molecular origins of the catalytic power and substrate specificity of acetylcholinesterase. *J. Am. Chem. Soc.* **1996,** *118*, 2340-2346.

61. Rosman, Y.; Makarovsky, I.; Bentur, Y.; Shrot, S.; Dushnistky, T.; Krivoy, A., Carbamate poisoning: treatment recommendations in the setting of a mass casualties event. *Am. J. Emerg. Med.* **2009,** *27*, 1117-1124.

62. Hartsel, J. A.; Wong, D. M.; Mutunga, J. M.; Ma, M.; Anderson, T. D.; Wysinski, A.; Islam, R.; Wong, E. A.; Paulson, S. L.; Li, J. Y.; Lam, P. C. H.; Totrov, M. M.; Bloomquist, J. R.; Carlier, P. R., Re-engineering aryl methylcarbamates to confer high selectivity for inhibition of *Anopheles gambiae* versus human acetylcholinesterase. *Bioorg. Med. Chem. Lett.* **2012,** *22*, 4593-4598.

63. Eyer, P.; Worek, F.; Thiermann, H.; Eddleston, M., Paradox findings may challenge orthodox reasoning in acute organophosphate poisoning. *Chem.-Biol. Interact.* **2010,** *187*, 270-278.

64. Lorke, D. E.; Hasan, M. Y.; Nurulain, S. M.; Shafiullah, M.; Kuca, K.; Petroianu, G. A., Pretreatment for acute exposure to diisopropylfluorophosphate: in vivo efficacy of various acetylcholinesterase inhibitors. *J. Appl. Toxicol.* **2011,** *31*, 515-523.

65. Fukuto, Mechanism of action of organophosphorus and carbamate insecticides. *Environ. Health Perspect.* **1990,** *87*, 245-254.

66. Karami-Mohajeri, S.; Abdollahi, M., Toxic influence of organophosphate, carbamate, and organochlorine pesticides on cellular metabolism of lipids, proteins, and carbohydrates: a systematic review. *Hum. Exp. Toxicol.* **2011,** *30*, 1119-1140.

67. Jokanovic, M.; Kosanovic, M.; Brkic, D.; Vukomanovic, P., Organophosphate induced delayed polyneuropathy in man: an overview. *Clin. Neurol. Neurosurg.* **2011,** *113*, 7-10.

68. Nair, H. K.; Quinn, D. M., *m*-Alkyl α,α,α-trifluoroacetophenones - a new class of potent transition-state analog inhibitors of acetylcholinesterase. *Bioorg. Med. Chem. Lett.* **1993,** *3*, 2619-2622.

69. Rayo, J.; Muñoz, L.; Rosell, G.; Hammock, B. D.; Guerrero, A.; Luque, F. J.; Pouplana, R., Reactivity versus steric effects in fluorinated methyl ketones as esterase inhibitors: a quantum mechanical and molecular dynamics study. *J. Mol. Model.* **2010,** *16*, 1753-1764.

70. Bourne, Y.; Radic, Z.; Sulzenbacher, G.; Kim, E.; Taylor, P.; Marchot, P., Substrate and product trafficking through the active center gorge of acetylcholinesterase analyzed by crystallography and equilibrium binding. *J. Biol. Chem.* **2006,** *281*, 29256-29267.

71. Gelb, M. H.; Svaren, J. P.; Abeles, R. H., Fluoro ketone inhibitors of hydrolytic enzymes. *Biochemistry* **1985,** *24*, 1813-1817.

72. Cannon, J., *Pharmacology for Chemists*. 2nd ed.; Oxford University Press: New York, 1999; p 272.

73. Rais, R.; Thomas, A. G.; Wozniak, K.; Wu, Y.; Jaaro-Peled, H.; Sawa, A.; Strick, C. A.; Engle, S. J.; Brandon, N. J.; Rojas, C.; Slusher, B. S.; Tsukamoto, T., Pharmacokinetics of oral D-serine in D-amino acid oxidase knockout mice. *Drug Metab. Dispos.* **2012,** *40*, 2067-2073.

74. Doan, K. M. M.; Humphreys, J. E.; Webster, L. O.; Wring, S. A.; Shampine, L. J.; Serabjit-Singh, C. J.; Adkison, K. K.; Polli, J. W., Passive permeability and P-glycoprotein-mediated efflux differentiate central nervous system (CNS) and non-CNS marketed drugs. *J. Pharmacol. Exp. Ther.* **2002,** *303*, 1029-1037.

75. Nair, H. K.; Seravalli, J.; Arbuckle, T.; Quinn, D. M., Molecular recognition in acetylcholinesterase catalysis - free-energy correlations for substrate turnover and inhibition by trifluoro ketone transtion-state analogs. *Biochemistry* **1994,** *33*, 8566-8576.

76. Doucet-Personeni, C.; Bentley, P. D.; Fletcher, R. J.; Kinkaid, A.; Kryger, G.; Pirard, B.; Taylor, A.; Taylor, R.; Taylor, J.; Viner, R.; Silman, I.; Sussman, J. L.; Greenblatt, H. M.; Lewis, T., A structure-based design approach to the development of novel, reversible AChE inhibitors. *J. Med. Chem.* **2001,** *44*, 3203-3215.

77. Hammock, B. D.; Wing, K. D.; McLaughlin, J.; Lovell, V. M.; Sparks, T. C., Trifluoromethylketones as possible transition state analog inhibitors of juvenile hormone esterase. *Pestic. Biochem. Physiol.* **1982,** *17*, 76-88.

78. Aberman, A.; Segal, D.; Shalitin, Y.; Gutman, A. L., Silicon-compounds as substrates and inhibitors of acetylcholinesterase. *Biochim. Biophys. Acta* **1984,** *791*, 278-280.

79. Sieburth, S. M.; Lin, S. Y.; Cullen, T. G., New insecticides by replacement of carbon by other group-IV elements. *Pestic. Sci.* **1990,** *29*, 215-225.

80. Szekacs, A.; Halarnkar, P. P.; Olmstead, M. M.; Prag, K. A.; Hammock, B. D., Heterocyclic-derivatives of 3-substituted-1,1,1-trifluoro-2-propanones as inhibitors of esterolytic enzymes. *Chem. Res. Toxicol.* **1990,** *3*, 325-332.

81. Veale, C. A.; Bernstein, P. R.; Bohnert, C. M.; Brown, F. J.; Bryant, C.; Damewood, J. R., Jr.; Earley, R.; Feeney, S. W.; Edwards, P. D.; Gomes, B.; Hulsizer, J. M.; Kosmider, B. J.; Krell, R. D.; Moore, G.; Salcedo, T. W.; Shaw, A.; Silberstein, D. S.; Steelman, G. B.; Stein, M.; Strimpler, A.; Thomas, R. M.; Vacek, E. P.; Williams, J. C.; Wolanin, D. J.; Woolson, S., Orally active trifluoromethyl ketone inhibitors of human leukocyte elastase. *J. Med. Chem.* **1997,** *40*, 3173-3181.

82. Veale, C. A.; Damewood, J. R., Jr.; Steelman, G. B.; Bryant, C.; Gomes, B.; Williams, J., Non-peptidic inhibitors of human leukocyte elastase. 4. Design, synthesis, and in vitro and in vivo activity of a series of β-carbolinone-containing trifluoromethyl ketones. *J. Med. Chem.* **1995,** *38*, 86-97.

83. Govardhan, C. P.; Abeles, R. H., Structure activity studies of fluoroketone inhibitors of α-lytic protease and human-leukocyte elastase. *Arch. Biochem. Biophys.* **1990,** *280*, 137-146.

84. Imperiali, B.; Abeles, R. H., Inhibition of serine proteases by peptidyl fluoromethyl ketones. *Biochemistry* **1986,** *25*, 3760-7.

85. Jones, D. M.; Atrash, B.; TegerNilsson, A. C.; Gyzander, E.; Deinum, J.; Szelke, M., Design and synthesis of thrombin inhibitors. *Lett. Pept. Sci.* **1995,** *2*, 147-154.

86. Wang, Y.; Jia, S. J.; Tseng, B.; Drewe, J.; Cai, S. X., Dipeptidyl aspartyl fluoromethylketones as potent caspase inhibitors: Peptidomimetic replacement of the P-2 amino

acid by 2-aminoaryl acids and other non-natural amino acids. *Bioorg. Med. Chem. Lett.* **2007,** *17*, 6178-6182.

87. Wang, Y.; Huang, J. C.; Zhou, Z. L.; Yang, W.; Guastella, J.; Drewe, J.; Cai, S. X., Dipeptidyl aspartyl fluoromethylketones as potent caspase-3 inhibitors: SAR of the P-2 amino acid. *Bioorg. Med. Chem. Lett.* **2004,** *14*, 1269-1272.

Chapter 2: Fluorinated methyl ketones and their activity against AChE and toxicity against *Anopheles gambiae*

2.1 Contributions:

The work described in this chapter was conducted in collaboration with Dr. Jeffrey Bloomquist and his group members at the University of Florida and Dr. Jianyong Li and his group members from Virginia Tech. The author is responsible for the synthesis of the ketone inhibitors, while the enzyme activity assays were performed by Dr. Dawn Wong of the Carlier group. Mosquito toxicity testing was performed by Dr. Rafique Islam and Dr. Fan Tong of the Bloomquist group. The Li group was responsible for providing the enzyme sources for testing. Computer modeling of inhibitors bound to G119s AgAChE was performed by our collaborator Dr. Max Totrov of Molsoft LLC (San, Diego, CA). This chapter is based on a manuscript in preparation for submission

Camerino, E. W., Dawn M.; Körber, Florian; Tong, Fan; Islam, Rafique; Viayna, Elisabet; Totrov, Maxim M.; Li, Jianyong; Bloomquist, Jeffrey R.; Carlier, Paul R., Difluoromethylketones: potent inhibitors of WT and carbamate-insensitive G119S mutant *Anopheles gambiae* acetylcholinesterase.

2.2 Abstract

As discussed in sections 1.2 and 1.3, malaria is a devastating disease in sub-Saharan Africa, and current vector control measures are threatened by emerging resistance mechanisms. With the goal of developing new human-safe, resistance-breaking insecticides we have explored trifluoro-, difluoro-, and fluoromethyl ketones as reversible covalent inhibitors of *Anopheles gambiae* acetylcholinesterase (*Ag*AChE). Trifluoromethylketones **2-9c**, **e, f, g, h** exhibit potent (1-100 nM) inhibition of WT *Ag*AChE, approaching steady-state within one hour. However these compounds are poor inhibitors of G119S mutant *Ag*AChE found in carbamate-resistant *An. gambiae*. Fluoromethyl ketones **2-11c-j** exhibit submicromolar to micromolar inhibition of WT *Ag*AChE, but again only weakly inhibit G119S *Ag*AChE. Interestingly, difluoromethyl ketone inhibitors **2-10c**, **g** exhibit single digit nanomolar inhibition of WT *Ag*AChE and **2-10g** has excellent potency against G119S *Ag*AChE. Approach to steady-state inhibition requires more than 3 h, and after 23 h incubation an IC_{50} value of 25.1 ± 1.2 nM is measured. We attribute the slow, tight-binding G119S *Ag*AChE inhibition of this compound to the right balance of steric size and electrophilicity. However, tarsal contact toxicity of these tri-, di-, and (mono) fluoromethyl ketones to adult *An. gambiae* is low; possible reasons are discussed.

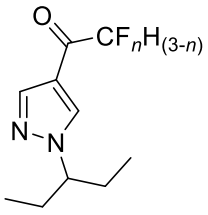

1 h incubation

	n	WT *Ag*AChE IC_{50} (nM)	G119s AgAChE IC_{50} (nM)	
2-9g	3	0.68 ± 0.01	1,730 ± 140	⟹ **25 ± 1 nM** (23 h)
2-10g	2	1.22 ± 0.03	125 ± 6	
2-11g	1	612 ± 12	5,030 ± 130	

2.3 Bioassays

2.3.1 Tarsal contact toxicity assay

The measurements of mosquito toxicity of all AChE inhibitors were performed by members of the Bloomquist group (Department of Entomology, University of Florida). The tarsal contact toxicity of the synthesized compounds was determined by using the standard WHO filter paper assay towards *An. gambiae* (G3 strain, susceptible), and *An. gambiae* resistant (Akron strain, carbamate resistant) mosquitoes.[1] The test compound (2 mg) was dissolved in 2 mL of ethanol and impregnated on the filter paper (Whatman No. 1) measuring 12 x 15 cm. To prevent loss of insecticide solution during transfer onto the filter paper, the paper is supported on several pins attached to a cardboard sheet. An insecticide solution (1 mg/mL) is then applied uniformly on the paper. After drying for 24 hours, it is put into an exposure tube (Figure 2-1). The WHO protocol dictates that the treated paper can only be reused five times.

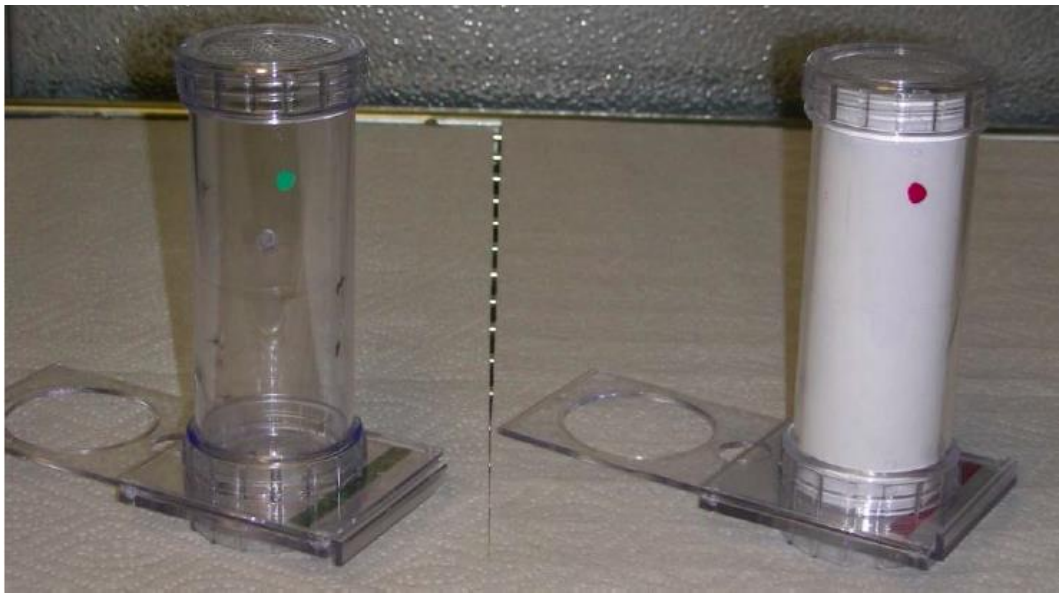

Figure 2-1: WHO filter paper assay tubes. The left tube (designated with a green dot) is the holding chamber. The right tube (designated with a red dot) is the exposure chamber, and the treated paper is clearly visible.

Each experiment was performed in duplicate at the given concentration. A batch of 25 non-blood fed, 2-5 day old female *An. gambiae* mosquitoes was used. Mosquitoes were anaesthetized by keeping them on ice for several minutes, followed by transferring to the holding tube. After acclimating in the tube for an hour, they were gently blown into the exposure tube, where they were exposed to the treated filter paper for an hour. After an hour, they were blown back into the holding tube and mortality was recorded after an hour. The holding tubes were left in a dark room at 25 ˚C ± 1 ˚C with a relative humidity of 80% ± 10%. Mosquitoes were provided with sugar water on a cotton wool during the post exposure period. After 24 hours, mortality was recorded.

2.3.2 Enzyme inhibition

Inhibition of AChE by the various fluorinated methyl ketones was determined by using an Ellman assay[2], and was performed by Dr. Dawn Wong of the Carlier group: inhibition is expressed by IC_{50} values. The Ellman assay has been used for decades to measure cholinesterase activity [2] using acetylthiocholine (ATCh, **2-1**) in place of ACh.[3] The thiocholine (TCh, **2-2**) produced by AChE-catalyzed hydrolysis of ATCh then reacts quickly with 5-dithiobis-2-nitrobenzoate (DTNB, **2-3**) to produce 2-nitrosulfidobenzoate (**2-5**), an intensely colored anion that can be detected at 405 nm (Scheme 2-1). The assay is performed at various concentrations of inhibitor, and enzyme activity measured in order to produce a concentration-response curve (Figure 2-2). Inhibition potency is measured by calculating the IC_{50} value, the concentration of inhibitor needed to reduce the activity of the enzyme to 50% of the inhibitor-free control.

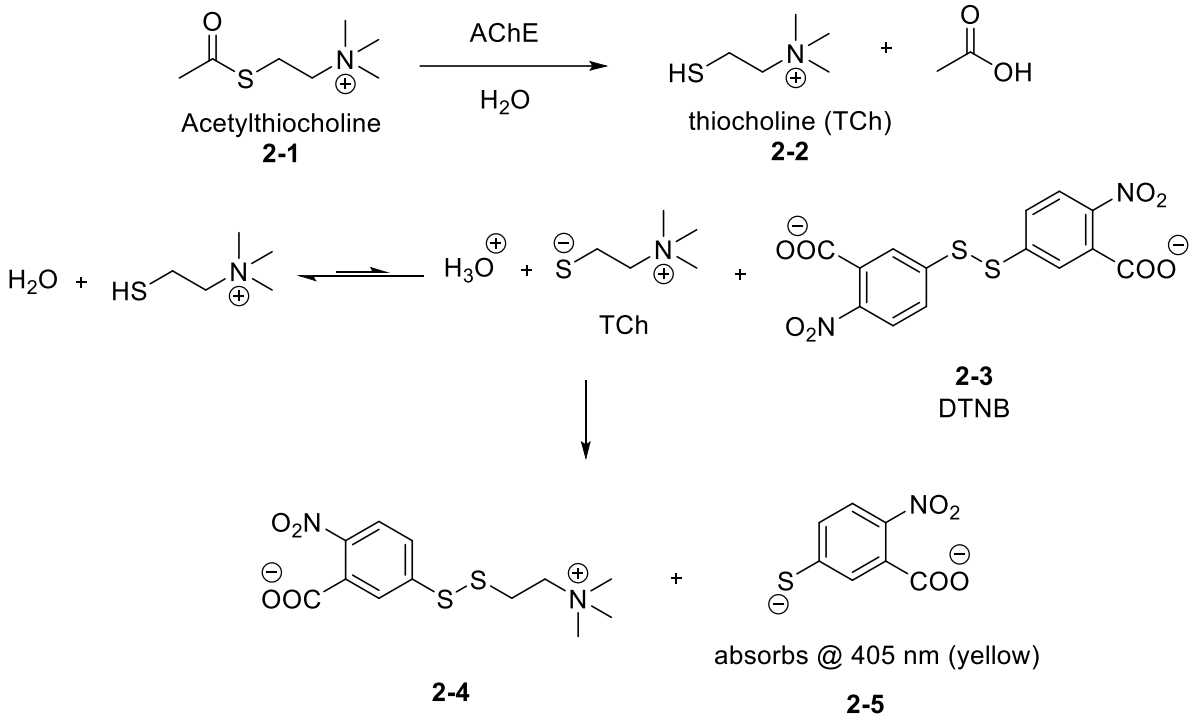

Scheme 2-1: The Ellman assay test used to determine AChE activity using ATCh and DTNB. Activity is measured by absorbance of the leaving group (**2-5**) formed by the reaction of TCh and DTNB.

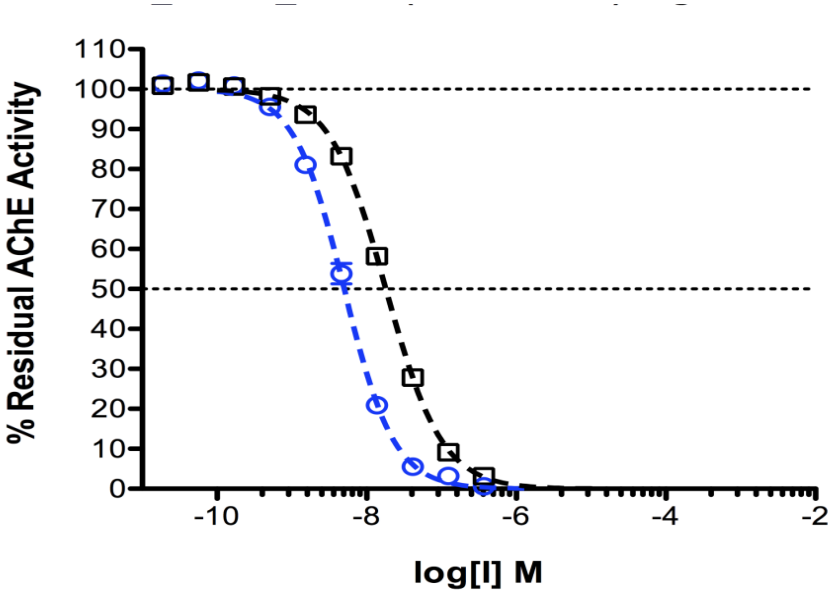

Figure 2-2: Inhibition response curve of **2-9c** with *h*AChE (in blue) and WT AChE (in black). Note that activity was taken at 10 different concentrations to obtain an IC_{50} value.

Three types of enzyme sources are used for the Ellman assays: human AChE (*h*AChE) that was purchased from Sigma-Aldrich, recombinant wild type *An. gambiae* AChE (*Ag*AChE-WT), and G119S *Ag*AChE, both prepared by Dr. Jianyong Li group, a collaborator with the Carlier group at Virginia Tech Department of Biochemistry. The enzymes (*Ag*AChE-WT, r*h*AChE, and G119S AgAChE) were diluted in buffer A, which is comprised of 0.01 M sodium phosphate containing 0.3% sodium azide (w/v), 1 mg/mL bovine serum albumin (BSA), and 0.3% Triton X-100 (v/v). The inhibitor was diluted in buffer B containing 0.01 M sodium phosphate with 0.3% sodium azide (w/v). Because time-dependent inhibition of AChE by trifluoromethylketones is well-documented,[4-6] enzyme velocities (v/v_0) were measured as a function of inhibitor concentrations [I] at incubation times of 10 min and 60 min. The assay was performed at pH 7.7 and 23 ˚C for maximum activity. The enzymes were pre-incubated for 10 or 60 minutes with five different concentrations of inhibitor; the longer incubation time (e.g. 60 min) was examined to determine if

inhibitors were exhibiting slow, tight-binding characteristics. Each inhibitor concentration was present in duplicate in a 96-well microplate and each experiment was repeated. When the desired incubation time was reached, a fresh solution of the substrate (ATCh) and indicator (DTNB), 4 and 3 mM in buffer B, respectively were added. During the course of the enzymatic reaction, 2-nitro-5-sulfidobenzoate (**2-5**,Scheme 2-1) is produced giving off a yellow color. Enzyme activity was monitored at 405 nm at room temperature using a microplate reader. Sigmoidal plots of enzyme velocity (v/v_0) *vs*. [I] were then constructed, from which the IC_{50} values were obtained (Table 2-1, Table 2-2, and Table 2-4).

2.4 Synthesis of fluorinated methyl ketones

The Carlier group has shown previous success with designing carbamate inhibitors that display activity against G119S AgAChE. The hypothesis was that carbamates containing smaller rings would allow for a better fit in the constricted active site. This hypothesis proved successful since compounds synthesized by the Carlier group allowed a better fit in the enzyme pocket as previously discussed in section 1.1.5 (Figure 1-10).[7-8] Following a similar strategy, we synthesized a series of tri-, di-, and (mono)fluoromethyl ketones bearing substituted benzene and pyrazol-4-yl substituents (Scheme 2-3, Scheme 2-4, and Scheme 2-6).

The *N*-alkyl-4-bromopyrazole starting materials **2-9d-k** required for the pyrazole ketones were prepared in two steps from pyrazole.[9-10] Pyrazole was brominated using *N*-bromosuccinimide in H_2O followed by alkylation with sodium hydride in DMF to furnish the 4-bromo-*N*-alkylpyrazoles (**2-7d-j**) in yields ranging from 60-88%; select intermediates (**2-7d-f** and **h**) were previously synthesized and characterized in my M.S. thesis.[11]

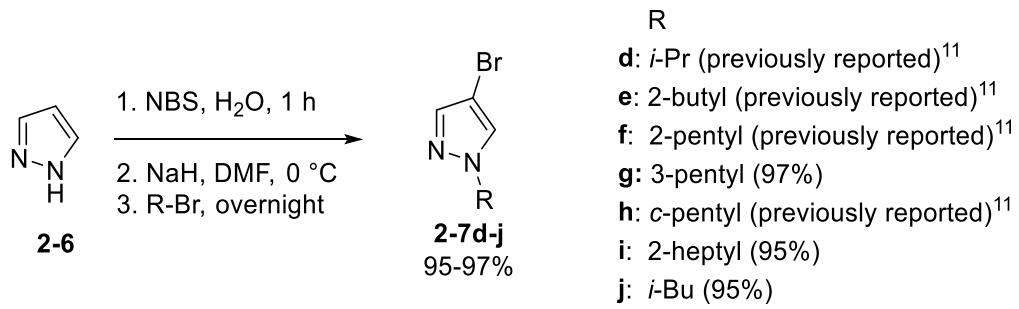

Scheme 2-2: Synthesis of 4-bromo-N-alkylpyrazoles **2-7d-j**.

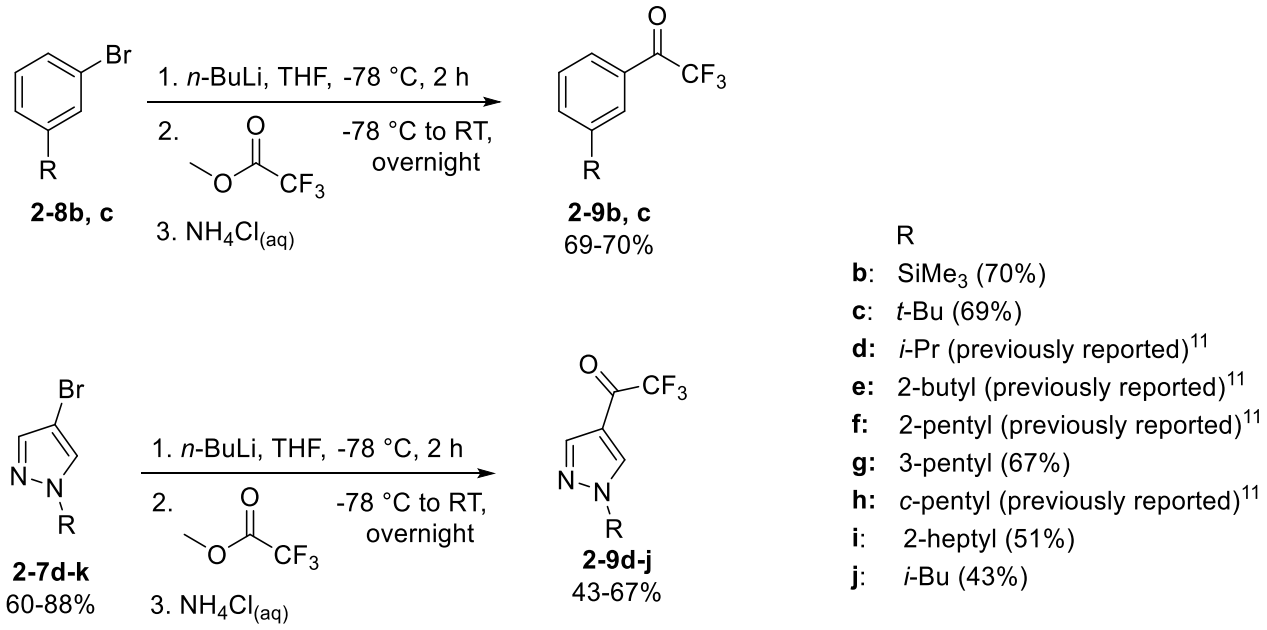

Scheme 2-3: Synthesis of trifluoromethylketones **2-9b-j**.

Trifluoromethylketones **2-9b-j** were prepared by the literature route for **2-9c** involving a metal-halogen exchange of the appropriate aryl or heteroaromatic bromide and trapping with methyl trifluoroacetate (Scheme 2-3).[12] Pyrazol-4-yl TFKs containing *i*-Pr, *sec*-butyl, 2-pentyl, and *c*-C_5H_9 substituents (**2-9d**, **2-9e**, **2-9f**, and **2-9h**) were previously synthesized.[11] New alkyl substituents such as 3-pentyl (**2-9g**), heptyl (**2-9i**), and isobutyl (**2-9j**) were incorporated on the

pyrazole ring in good to moderate yields; yields of the trifluoromethylketones **2-9b-j** ranged from 43-70%. Further optimization of these moderate yields was thwarted due to compound volatility (attributed to decreased van der Waal interactions attributed to the $-CF_3$ group), and possible side reactions (discussed in the next paragraph). Previous work in the Carlier group has explored various roles of alkyl groups in the choline binding site; the preponderance of α-branched alkyl groups we selected reflects the observation that select substituents increase *Ag*AChE inhibition potency of pyrazol-4-yl[8] and isoxazol-3-yl methylcarbamates and carboxamides.[7]

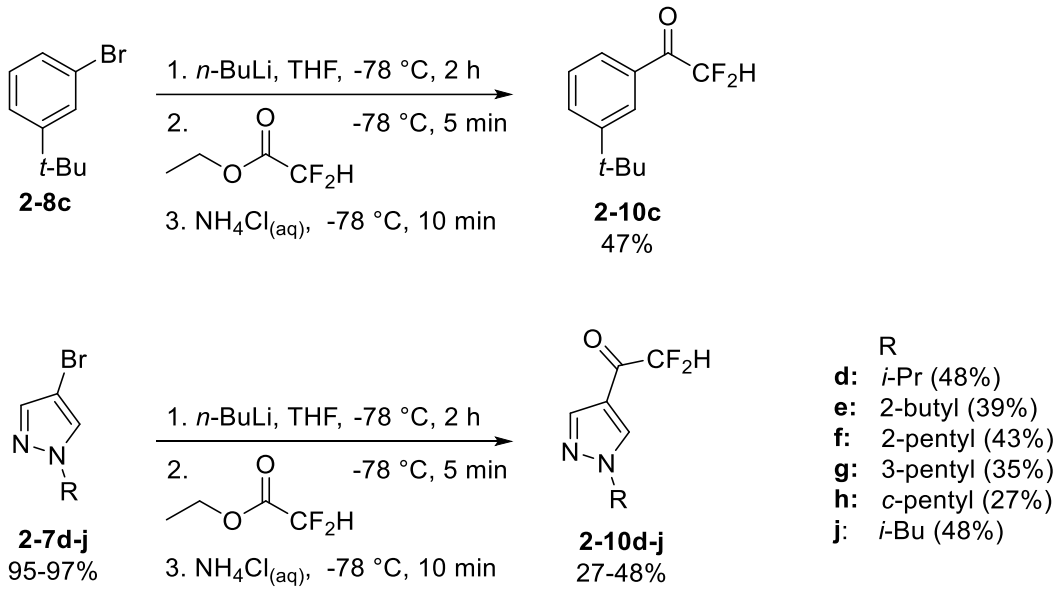

Scheme 2-4: Synthesis of difluoromethylketones **2-10d-j**.

Difluoromethylketones **2-10d-j** were prepared by using ethyl difluoroacetate as the electrophilic trapping reagent (Scheme 2-4). The inspiration for the use of ethyl difluoroacetate stemmed from trifluoroketone synthesis using ethyl trifluoroacetate discussed in the previous paragraph. Yields of the difluoromethylketones (**2-10d-j**) were 27-50%, slightly lower than that

of the trifluoromethyl ketones, which we attribute to the encroachment of competing side reactions (Scheme 2-5). Upon introduction of the electrophile to our lithiated species one of two reactions can happen, either an acid-base reaction with the α-hydrogen or attack of the carbonyl. While carbonyl attack is desired to form the tetrahedral intermediate, it is necessary that the intermediate stay intact until workup. If collapse occurred and ketone was present in the reaction mixtures prior to quench, **2-10** and **2-11** could react as an electrophile or Brønsted acid towards residual organolithiums via nucleophilic attack or an additional acid-base reaction.

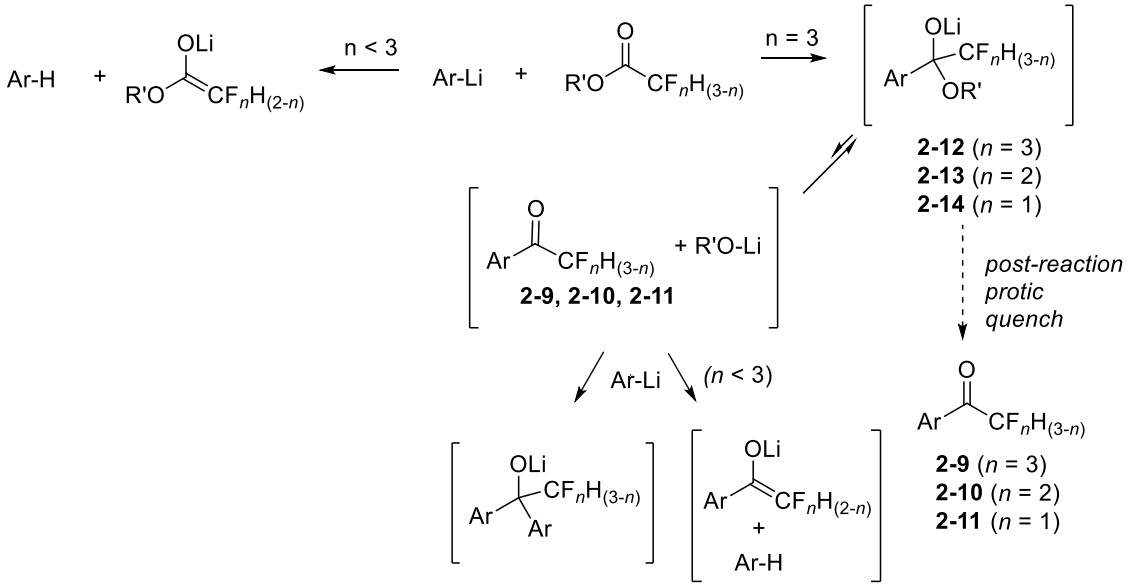

Scheme 2-5: Possible side reactions in the synthesis of fluorinated methylketones. An acid-base reaction may occur via two routes: between the lithiated species and fluorinated ester and between an alpha hydrogen of the fluorinated methyl ketone product and another equivalent of lithiated species. If the tetrahedral intermediate collapses, another equivalent of lithiated species may add.

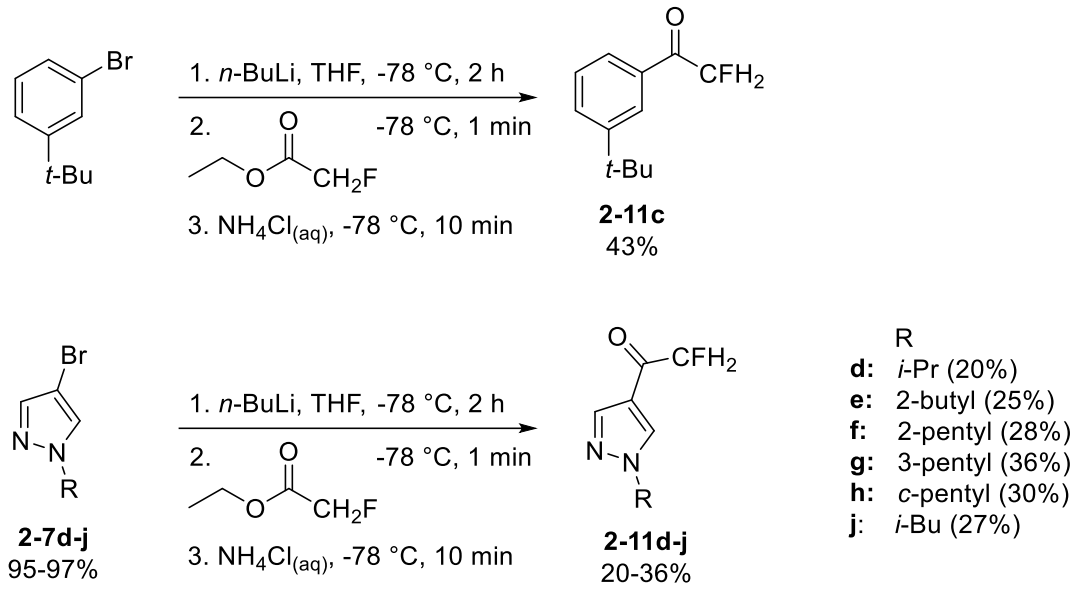

Scheme 2-6: Synthesis of fluoro methylketones **2-11c-j**.

In a similar fashion, fluoromethyl ketones **2-11d-j** were prepared by using ethyl fluoroacetate as the electrophilic trapping reagent (Scheme 2-6). Initially, MFK synthesis employed fluoroacetonitrile as the electrophile following literature precedent[13] and concern regarding toxicity of fluoroacetate. Switching to ethyl fluoroacetate increased the yields and decreased the number of side products formed seen via TLC. Nevertheless, yields of the fluoromethyl ketones **2-11d-j** were 13-36% respectively, lower than the yields of the DFKs and TFKs. We attribute the lower yields to two things: an acid-base reaction between the lithiated species and ethyl fluoroacetate or to the tendency of the tetrahedral adduct formed from the organolithium and fluorinated methyl ketone to collapse prior to protic quench (Scheme 2-5). If the ketone form is more present, which can be hypothesized due to a reduced inductive effect, then it is more prone to side reactions, such as an unwanted acid-base reaction or addition of a lithiated species previously discussed in Scheme 2-5.

2.5 Enzyme inhibition by fluorinated methyl ketones

In our enzyme inhibition studies, we also examined the commercial carbamate propoxur, since it has excellent contact activity against the susceptible (G3) strain of *An. gambiae*, but poor toxicity against carbamate-resistant (Akron) strain *An. gambiae*.[8, 14] Propoxur carbamoylates the active site serine of AChE (previously described in section 1.6.2) and its time-dependent inhibition of *h*AChE and WT *Ag*AChE is evident in Table 2-1. For example propoxur has an IC_{50} of 182 ± 3 nM at *Ag*AChE after a 10 minute incubation, but the IC_{50} drops more than 4-fold (to 43.6 ± 1.0 nM) after a 60 minute incubation. However this compound is not a very good inhibitor of G119S AgAChE at 10 or 60 min incubation time (IC_{50} > 10,000 nM), consistent with the carbamate resistance phenotype this mutation confers.

Table 2-1: Inhibition IC_{50} values for trifluoromethylketones **2-9b-j** against *h*AChE and *Ag*AChE (WT and G119S)

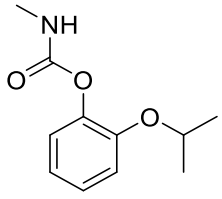

1-17

Propoxur

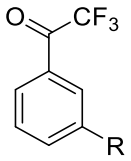

2-9b, c

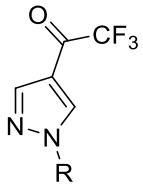

2-9d-j

Compound	R	Incubation time (min)	*h*AChE IC_{50} (nM)[a]	WT *Ag*AChE IC_{50} (nM)[a]	G119S *Ag*AChE IC_{50} (nM)[a]
propoxur	-	10	2,300 ± 50	182 ± 3	>10,000
		60	590 ± 19	43.6 ± 1.0	>10,000
2-9b		10	285 ± 15	848 ± 44	>10,000
		60	92.9 ± 5.8	257 ± 15	10,100 ± 500
2-9c		10	14.6 ± 0.2	53.4 ± 0.8	>10,000
		60	5.00 ± 0.16	18.1 ± 0.4	20,800 ± 1,900
2-9d		10	77.5 ± 2.2	142 ± 5	>10,000

		60	121 ± 3	285 ± 7	>10,000
2-9e	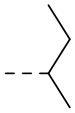	10	6.47 ± 0.15	2.47 ± 0.04	8,180 ± 450
		60	8.84 ± 0.28	2.29 ± 0.17	2,340 ± 90
2-9f	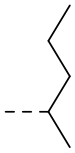	10	7.15 ± 0.11	3.74 ± 0.08	19,900 ± 2,400
		60	8.37 ± 0.16	2.06 ± 0.06	2,000 ± 140
2-9g	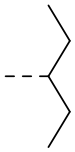	10	3.77 ± 0.06	2.75 ± 0.04	>10,000
		60	2.27 ± 0.04	0.68 ± 0.01	1,730 ± 140
2-9h	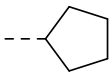	10	5.20 ± 0.15	2.87 ± 0.07	>10,000
		60	6.11 ± 0.18	1.54 ± 0.08	3,520 ± 140
2-9i	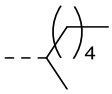	10	58.39 ± 1.32	223.6 ± 6.33	>10000
		60	89.18 ± 1.69	338.6 ± 15.0	>10000
2-9j	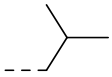	10	591 ± 11	950 ± 19	>10,000
		60	678 ± 15	1,040 ± 20	>10,000

[a]Measured at 23 ± 1°C, pH 7.7, 0.1% (v/v) DMSO; all enzymes are recombinant. Standard error (SE) of the IC_{50} values are calculated from the 95% confidence interval according to the standard error formula SE = (upper limit – lower limit)/(2x1.96).[15]

Trifluoromethylketones **2-9b-j** showed varying degrees of time-dependence to their inhibition of *h*AChE and WT *Ag*AChE; those bearing a phenyl group (**2-9b**, **c**) showed time-dependent inhibition of *h*AChE and WT *Ag*AChE. The IC_{50} values for **2-9b** decreased from 285 nM to 92.9 nM for *h*AChE, and 848 nM to 257 nM for *Ag*AChE-WT as incubation time was increased from 10 to 60 min. This TFK appears to slowly reach equilibrium with *h*AChE and *Ag*AChE-WT IC_{50} values decreased by a factor of 3 when incubation time was increased by a factor of 6. Increasing the incubation time further will likely decrease IC_{50} further, but the steady-state IC_{50} value is not yet known. Compound **2-9c** also showed time-dependent inhibition of

*h*AChE and *Ag*AChE-WT and displayed excellent activity against WT *Ag*AChE (IC_{50} = 18 nM at 60 min).

Turning to the pyrazole-4-yl TFKs, compound **2-9d** with an isopropyl substituent displayed moderate activity against the enzyme; after a 10 minute incubation, an IC_{50} value of 142 nM was observed. Curiously however, compound **2-9d** exhibits higher *h*AChE and WT *Ag*AChE IC_{50} value at 60 min than at 10 min; we attribute this phenomenon to evaporation of **2-9d** out of the well plate during the long incubation. Fluorinated compounds can be surprisingly volatile, and **2-9d** has the lowest molecular weight of all the trifluoromethylketones tested. Increasing the molecular weight by the addition of a $–CH_2-$ group proved beneficial. Modification to a *sec*-butyl branch (**2-9e**) conferred excellent activity against both *h*AChE and *Ag*AChE, giving single digit nanomolar IC_{50} values after a 60 min incubation (8.84 and 2.29 nM respectively). Further addition of a $–CH_2-$ unit giving a 2-pentyl substituent (**2-9f**) did not result in better potency compared to **2-9e**, but IC_{50} values remained at 8 and 2 nM (*h*AChE and *Ag*AChE-WT respectively). Modification of the pentyl chain connectivity proved fruitful. A modification from a 2-pentyl to a 3-pentyl substitution gave the best IC_{50} values at WT *Ag*AChE (IC_{50} = 0.68 nM at 60 min). Conformational restriction of the 3-pentyl group into a cyclopentyl group did not adversely affect activity; **2-9h** had an IC_{50} of 1.54 nM at *Ag*AChE-WT after 60 minute incubation time. While **2-9g** and **2-9h** are both quite potent, the slightly lower IC_{50} values for **2-9g** suggest that the flexible 3-pentyl provides the optimum fit in the binding sites of *Ag*AChE-WT and *h*AChE.

Single-digit nanomolar IC_{50} values were observed with both enzyme sources (*h*AChE and *Ag*AChE) for α-branched alkyl-substituted compounds **2-9d**, **2-9g**, and **2-9h**. Compound **2-9j**, which bears a β-branched isobutyl group, is considerably less potent at *h*AChE and WT *Ag*AChE than any of the pyrazol-4-yl compounds bearing α-branched substituents (**2-9c-h**). Although potent

inhibition of WT *Ag*AChE can be achieved with a pyrazol-4-yl trifluoromethylketone, this structure confers no inhibition selectivity against *h*AChE. In addition, none of these inhibitors offered potent inhibition of G119S *Ag*AChE, most likely due to crowding in the oxyanion hole caused by the glycine to serine mutation; a molecular model provided by Dr. Max Totrov demonstrates the crowding in the smaller active site and an unfavorable steric repulsion between the S119 hydroxyl group and one of the fluorine atoms of the CF_3 group of **2-9g** (Figure 2-3). Compound **2-9g** proved most potent at this enzyme, but its 1,730 nM IC_{50} value after 60 minutes incubation is roughly 2,500-fold greater than the 0.7 nM value observed for WT *Ag*AChE. Finally as will be discussed in later sections, the volatility of these compounds have implications for both inhibition assay protocol and mosquito toxicology.

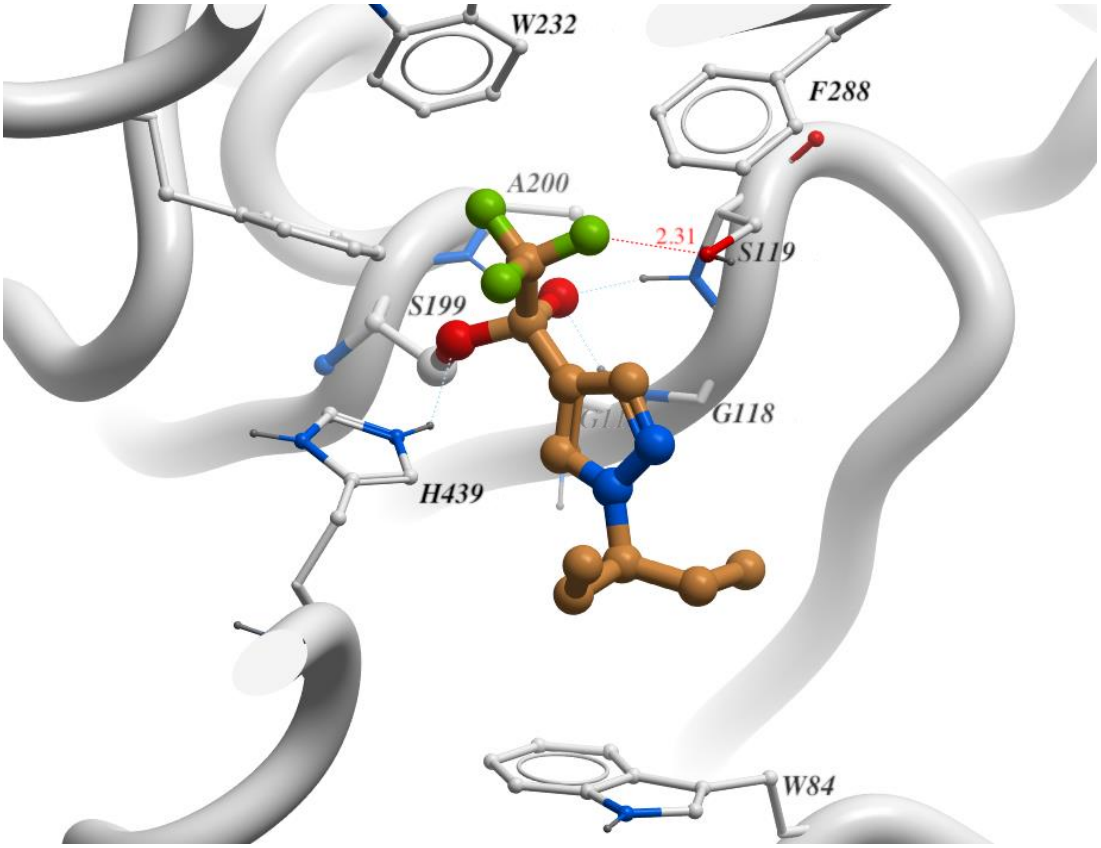

Figure 2-3: Molecular modeling of **2-9g** docked in G119S *Ag*AChE. Note the steric interaction between the fluorine and the S119. Graphic courtesy of Dr. Max Totrov.

The difluoromethylketones **2-10c-j** were then examined (Table 2-2). As expected, IC_{50} values for the difluoromethylketones with *h*AChE and WT *Ag*AChE were generally higher than the values for the corresponding trifluoromethylketones (for example, difluoromethyl ketone **2-10d** had 60 min IC_{50} values of 869 nM for *h*AChE and 430 nM for *Ag*AChE compared to 121 and 285 nM for the corresponding trifluoromethyl ketone **2-9d**. This decrease in potency is attributed to a less stable tetrahedral intermediate; the inductive effect produced by a $–CF_2H$ group is not as strong as that produced by a $–CF_3$ group. Interestingly, there are a few noteworthy exceptions in which the difluoromethylketone exhibited better activity than the trifluoromethylketone.

Table 2-2: Inhibition IC_{50} values for difluoromethylketones **2-10c**-**j** against *h*AChE and *Ag*AChE (WT and G119S)

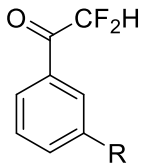

2-10c

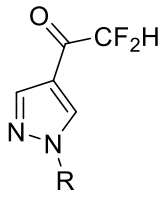

2-10d-j

Compound	R	Incubation time (min)	*h*AChE IC_{50} (nM)[a]	WT *Ag*AChE IC_{50} (nM)[a]	G119S *Ag*AChE IC_{50} (nM)[a]
2-10c		10	6.05 ± 0.11	9.12 ± 0.31	1,650 ± 100
		60	8.69 ± 0.18	9.79 ± 0.32	996 ± 39
2-10d		10	802 ± 30	354 ± 8	8,290 ± 400
		60	869 ± 20	430 ± 7	8,380 ± 420
2-10e	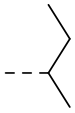	10	110 ± 2	26.3 ± 0.4	452 ± 12
		60	85.9 ± 1.6	25.2 ± 0.6	185 ± 7
2-10f	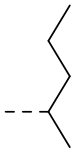	10	149 ± 2	23.4 ± 0.4	797 ± 20
		60	158 ± 3	29.1 ± 0.4	297 ± 6
2-10g	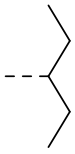	10	28.8 ± 0.7	1.01 ± 0.02	680 ± 43
		60	35.2 ± 0.8	1.22 ± 0.03	125 ± 6
		330	ND	ND	36.7 ± 1.7
		1380	ND	ND	25.1 ± 1.2
2-10h	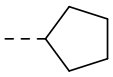	10	208 ± 5	106 ± 2	3,220 ± 150
		60	244 ± 5	134 ± 2	3,390 ± 110
2-10j	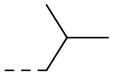	10	9,780 ± 470	3,000 ± 80	>10,000
		60	11,000 ± 400	3,950 ± 80	>10,000

[a]Measured at 23 ± 1°C, pH 7.7, 0.1% (v/v) DMSO; all enzymes are recombinant. Standard error (SE) of the IC_{50} values are calculated from the 95% confidence interval according to the standard error formula SE = (upper limit – lower limit)/(2x1.96).[15]

Difluoromethylketone **2-10c** was more potent than trifluoromethylketone analog **2-9c** at both *h*AChE and WT *Ag*AChE, and difluoromethylketone **2-10g** was similar in potency to trifluoromethylketone analog **2-9g** at WT *Ag*AChE (~1 nM). Both compounds have rather large alkyl substituents (*t*-Bu and 3-pentyl respectively). This suggests that, in some cases, the smaller size of the $-CF_2H$ group compared to $-CF_3$ can compensate for its lower electron-withdrawing ability. This effect also appears to be operative in the inhibition of G119S *Ag*AChE, which has a more crowded oxyanion hole than WT *Ag*AChE (Figure 2-3).

Against G119S *Ag*AChE, IC_{50} values of difluoromethylketones **2-10c**-**j** were uniformly lower than that of their corresponding trifluoromethylketones. Compound **2-10g** demonstrated the best activity against G119S *Ag*AChE. In addition, time-dependent inhibition is seen for the G119S enzyme: after a 60 min incubation the G119S *Ag*AChE IC_{50} value of **2-10g** is 125 nM, 13-fold lower than that of trifluoromethylketone **2-9g**. It was of interest to investigate how long this DFK in particular required to achieve equilibrium with the enzyme; it was noticed that the inhibition decreased by nearly a factor of 6 when incubation time was increased by a factor of 6 suggesting that increasing the incubation time would significantly increase inhibition of the enzyme (Table 2-2). Steady-state inhibition of G119S *Ag*AChE by **2-10g** appears to be attained with after 1380 min (23 h) incubation, giving an IC_{50} value of 25 nM (Table 2-3, Figure 2-4).

Table 2-3: Inhibition of **2-10g** at G119S *Ag*AChE with respect to time.

Incubation time (min)	IC_{50} (nM)	Incubation time (min)	IC_{50} (nM)
10	622 ± 36.4	225	43.9 ± 2.5
60	126 ± 5	240	45.4 ± 2.2
120	66.9 ± 4.3	300	37.5 ± 2.2
180	56.3 ± 3.0	330	36.7 ± 1.7
210	48.4 ± 2.3	1380	25.1 ± 1.2

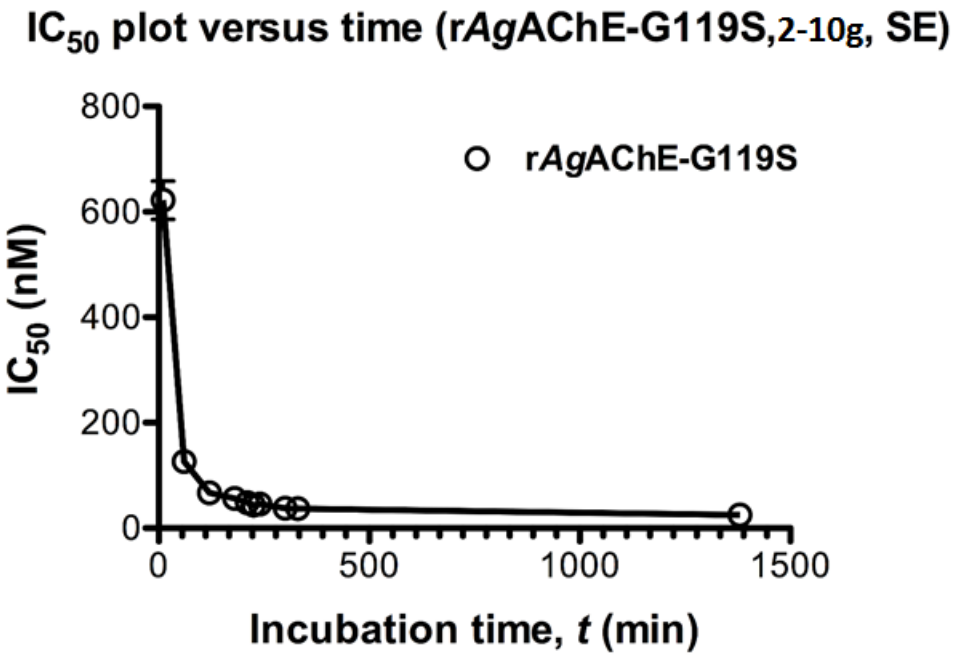

Figure 2-4: Progressive inhibition of **2-10g** at G119S *Ag*AChE.

Thus in the case of **2-10g**, the smaller size of the -CF_2H group appears to effectively compensate for its lower electron-withdrawing power, creating a slow, tight-binding inhibitor of G119S *Ag*AChE. This proposal is supported by a computed structure of **2-10g** bound to G119S *Ag*AChE (Dr. Max Totrov, Figure 2-5); note that the distance from the -CH_2F carbon to the S119 oxygen may potentially reduce steric interactions. As can be seen in Table 2-2, when observing *h*AChE and WT *Ag*AChE, increasing the incubation time did not show time-dependent inhibition. It thus can be inferred that DFKs are rapidly reversible inhibitors with *h*AChE and WT*Ag*AChE.

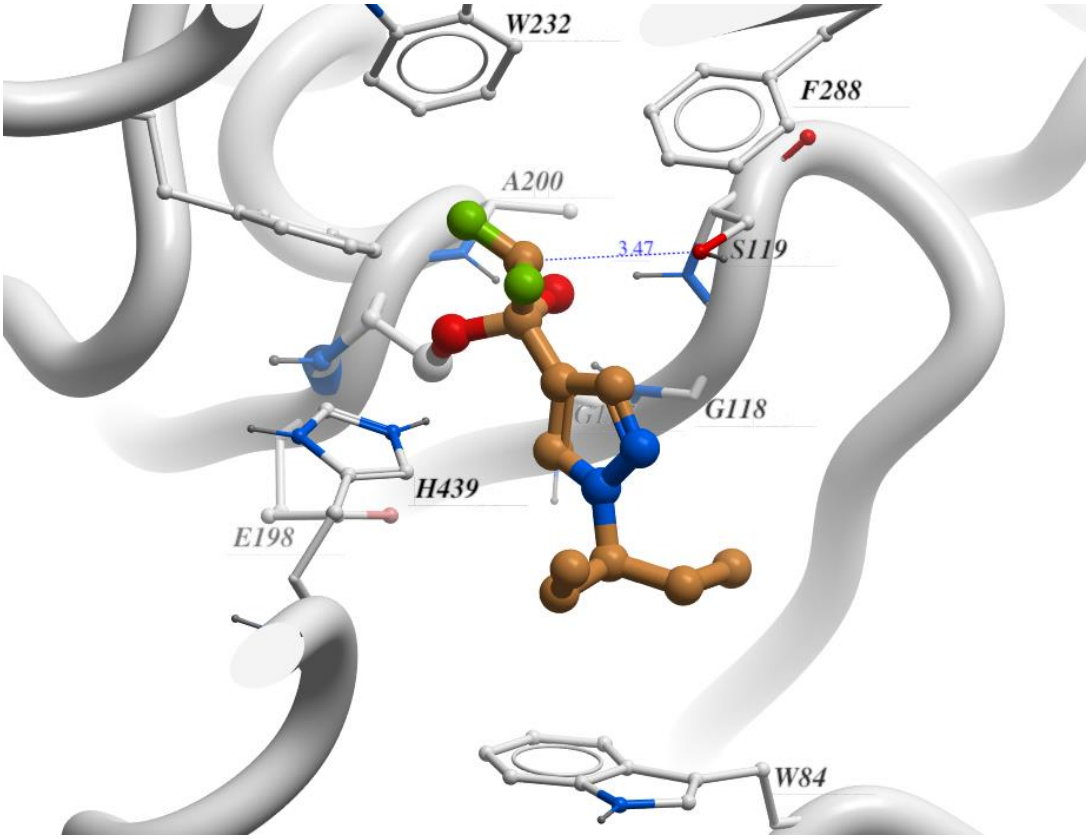

Figure 2-5: Molecular modeling of **2-10g** docked in G119S *Ag*AChE. Increased potency of inhibition of **2-10g** may be attributed by the smaller $–CF_2H$ group of **2-10g**.

Turning to the fluoro methylketones **2-11c-j**, much weaker inhibition of *h*AChE and WT *Ag*AChE was seen compared to that of difluoromethylketones **2-10c-j** and trifluoromethylketones **2-9b-j**. (Table 2-4).

Table 2-4: Inhibition IC_{50} values for fluoro methylketones **2-11c**-**j** against *h*AChE and *Ag*AChE (WT and G119S)

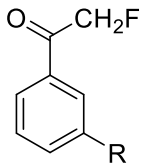

2-11c

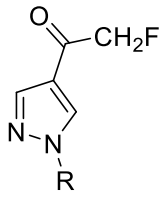

2-11d-j

Compound	R	Incubation time (min)	*h*AChE IC_{50} (nM)[a]	WT *Ag*AChE IC_{50} (nM)[a]	G119S *Ag*AChE IC_{50} (nM)[a]
2-11c		10	578 ± 12	726 ± 12	>10,000
		60	715 ± 15	953 ± 18	>10,000
2-11d		10	>10,000	>10,000	>10,000
		60	>10,000	>10,000	>10,000
2-11e	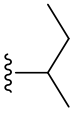	10	>10,000	2,750 ± 50	>10,000
		60	>10,000	2,860 ± 60	>10,000
2-11f	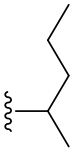	10	24,200 ± 2,700	3,520 ± 70	>10,000
		60	17,600 ± 1,800	3,290 ± 80	>10,000
2-11g	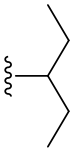	10	5,290 ± 250	355 ± 11	2,990 ± 160
		60	5,190 ± 270	337 ± 11	3,000 ± 160
2-11h	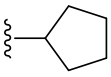	10	2,500 ± 80	5,860 ± 160	>10,000
		60	1,310 ± 30	1,540 ± 40	>10,000
2-11j	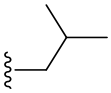	10	>10,000	>10,000	>10,000
		60	>10,000	>10,000	>10,000

[a]Measured at 23 ± 1°C, pH 7.7, 0.1% (v/v) DMSO; all enzymes are recombinant. Standard error (SE) of the IC_{50} values are calculated from the 95% confidence interval according to the standard error formula SE = (upper limit – lower limit)/(2x1.96).[15]

This outcome is understandable in view of the low electrophilicity of the fluoro methylketones. Two results stand out, however. Firstly, fluoro methylketone **2-11g** is a sub-

micromolar inhibitor of WT *Ag*AChE (337 ± 11 nM at 60 min). At a 10 minute incubation time, its IC_{50} value is roughly 3-fold that of propoxur (Table 2-4). Secondly, compound **2-11g** also showed micromolar inhibition of G119S *Ag*AChE (3 μM ± 0.1 μM at 60 min).

At several points in the preceding discussion, I have referred to the high volatility of some of the fluorinated methyl ketones. In fact, signs of inhibitor volatility were detected early in old enzyme studies, and these observations caused Dr. Dawn Wong to further optimize her microtiter plate format. To convincingly demonstrate which inhibitors were and were not volatile, the following spreading experiment was performed by Dr. Dawn Wong (Figure 2-6). In this experiment, inhibitor was placed in the middle two wells (cells D6 and D7) in the 96 well plate while the rest were inhibitor free. After a 10 minute incubation time, enzyme activity was tested on every well plate and designated a color; enzyme activity (v/ v_o) ≤ 10% representing low activity is designated by dark orange, moderate activity ((v/ v_o) ≤ 75%) is designated by a yellow color and excellent activity ((v/ v_o) > 93%) is represented by a green color. Four inhibitors were chosen for investigation: a matched set of fluorinated methyl pyrazole-4-yl ketones all bearing a 3-pentyl group (**2-9g**, **2-10g**, **2-11g**), and propoxur as a non-volatile control. In the case of the TFK **2-9g**, whereas greatest inhibition is seen in wells D6 and D7, other wells also exhibit inhibition of the enzyme suggesting that the TFK is volatile and spreads to other wells. Spreading also occurs in the case of the DFK **2-10g**, but not to the extent of TFK **2-9g**. The MFK **2-11g** is not volatile as evidenced by the lack of inhibition in adjacent wells. Finally as expected, no spreading was seen for the negative control propoxur.

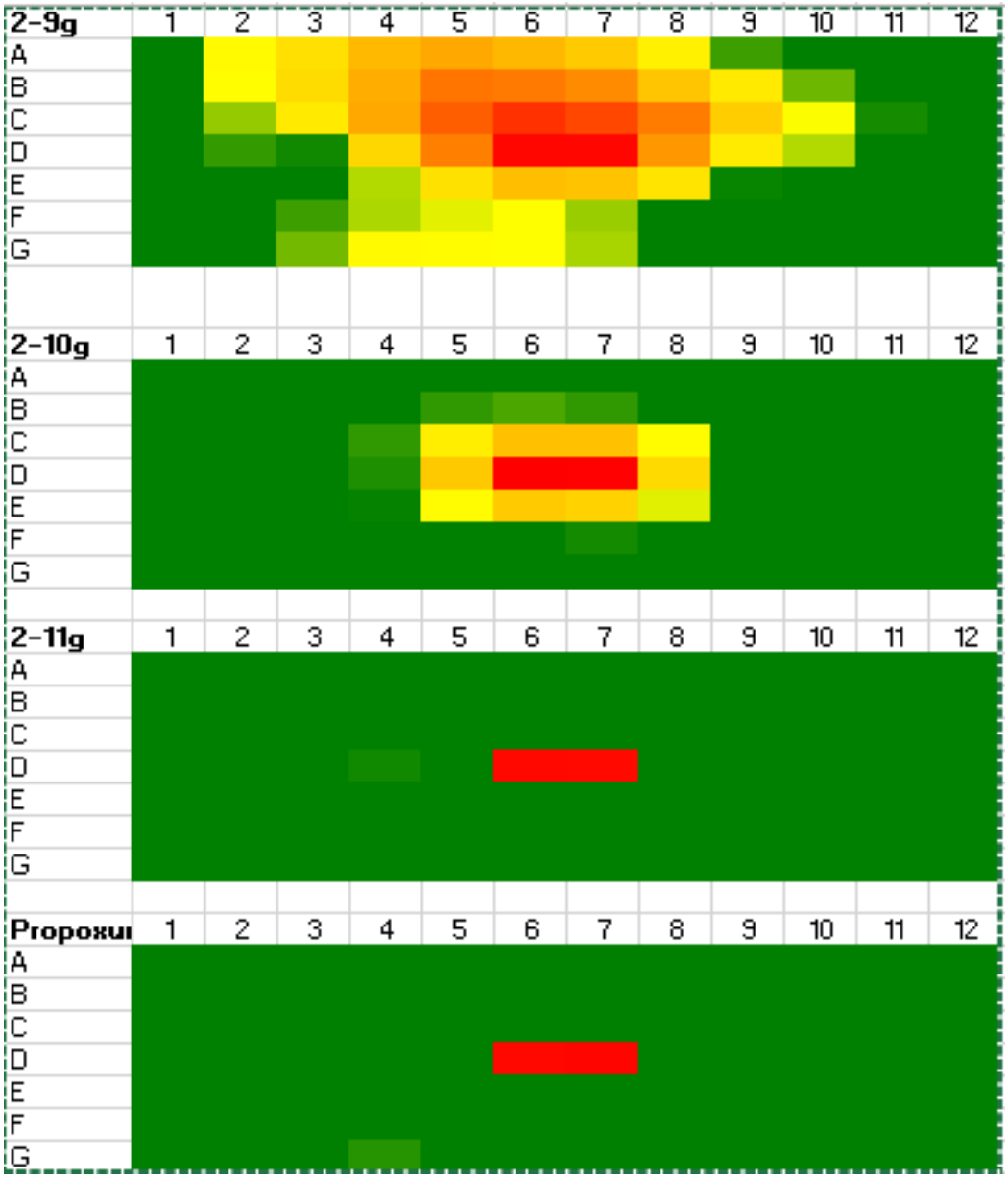

Figure 2-6: Microtiter plate heat maps of WT AgAChE residual velocity in which only wells D6-D7 of the microtiter plates were charged with 10,000 nM of inhibitor (10 min incubation at 23 ± 1°C, unsealed). Data for Row H (enzyme-free background wells) are not shown. Vapor phase diffusion of **2-9g** and **2-10g** is evident.

2.6 Tarsal contact toxicity of fluorinated methyl ketones

Several of the inhibitors examined demonstrated good inhibition of WT *Ag*AChE, and **2-9m** evidenced good inhibition of G119S *Ag*AChE. We thus examined the tarsal contact toxicity of select compounds that were found to inhibit WT *Ag*AChE well towards adult susceptible (G3) strain, using the WHO treated paper protocol[1] (Table 2-5).

Table 2-5: Tarsal contact toxicity of select fluorinated methyl ketones to susceptible (G3) strain adult *An. gambiae*.[a]

Compound	G3 Strain LC_{50} or % mortality at 1 mg/mL	Compound	G3 Strain LC_{50} or % mortality at 1 mg/mL
propoxur	39 µg/mL (32-45)[b]	**2-10e**	50%
2-9b	10%	**2-10f**	0%
2-9c	8%	**2-10g**	0%
2-9d	20%	**2-10h**	0%
2-9e	30%	**2-11c**	50%
2-9f	0%	**2-11d**	85%
2-9g	40%	**2-11e**	65%
2-9h	40%	**2-11f**	20%
2-9i	47%	**2-11g**	85%
2-10c	20%	**2-11h**	0%
2-10d	50%	**2-11j**	20%

[a]Mosquitoes were exposed (1 h) to dried filter papers previously treated with ethanolic solutions of fluorinated methyl ketones; mortality was recorded after 24 h. LC_{50} values are derived from the concentrations of inhibitor used to treat the paper; 95% confidence limits are given in parenthesis. [b]Data for propoxur were reported previously.[14]

Trifluoromethylketones containing a phenyl core exhibited low toxicity at 1mg/mL; **2-9b** had 10% mortality and **2-9c** had 8% mortality. Pyrazole core TFKs displayed higher toxicity than their phenyl core counterparts but there was no observed trend with increasing chain length.

Compound **2-9d,** with an isopropyl branch, had 20% mortality at 1 mg/mL. Increasing the chain length to a *sec*-butyl chain (**2-9e**) displayed 30% toxicity and a 3-pentyl chain (**2-9g**) gave 40% mortality. Modifying the connectivity of the pentyl chain had appeared to affect toxicity. While 3-pentyl analog **2-9g** displayed 40% mortality, 2-pentyl analog **2-9f** inexplicably exhibited 0% mortality. Modification to the cyclopentyl analogy **2-9h** increased mortality back to 40%. Compared to the trifluoromethyl ketone, difluoromethylketones had similar toxicities and again no consistent trends were noted; compounds **2-10d** and **2-10e** both showed 50% mortality while **2-10c** displayed 20% mortality. MFKs appeared to cause greater mortality than the DFKs or TFKs. Compound **2-11c** had 50% mortality while **2-11d**, **2-11e**, and **2-11g** had mortality values of 85%, 65%, and 85% respectively. There is also no observable trend with alkyl length or number of fluorines towards the toxicity of *Anopheles gambiae*. While many fluorinated methyl ketones proved to be active against *Ag*AChE, the toxicity results presented above did not correlate with the observed enzyme inhibition potencies. How can we account for this poor correlation? We believe that compound volatility (demonstrated in the spreading experiments (Figure 2-6)) is largely responsible. Since solutions of the inhibitor are applied to paper, and the solvent (EtOH) is allowed to evaporate before the paper is used for mosquito toxicity determination, it is quite likely that substantial evaporation of the test compounds occurs as well. According to the WHO protocol these papers should be allowed to dry for 24 h; we have recently learned that the Bloomquist group did not rigorously follow this recommendation. Thus it is possible the poor correlation between enzyme inhibition and mosquito toxicity reflects variations in compound volatility and paper drying times. Because a volatile insecticide would have very little practical use on nets, we did not explore any other measures of mosquito toxicity.

2.7 Conclusion

Fluorinated methylketones have the potential to be toxic towards *Anopheles gambiae*. Yet as we have shown in this chapter, excellent inhibition of AgAChE does not translate to significant *An. gambiae* contact toxicity. Consideration must be made in order to address problems such as permeation, volatility, and metabolism.[16] The next chapter will discuss our potential solution to this problem in the form of oximes and oxime ether prodrugs.

2.8 References:

1. Guidelines for testing mosquito adulticides for indoor residual spraying and treatment of mosquito nets. WHO/CDS/NTD/WHOPES/GCDPP/2006.3 World Health Organization, Geneva. **2006**. (accessed Jan 15).

2. Ellman, G., A new and rapid colorimetric determination of acetylcholinesterase activity. *Biochem. Pharmacol.* **1961,** *7*, 88-95.

3. Colletier, J. P.; Fournier, D.; Greenblatt, H. M.; Stojan, J.; Sussman, J. L.; Zaccai, G.; Silman, I.; Weik, M., Structural insights into substrate traffic and inhibition in acetylcholinesterase. *EMBO J.* **2006,** *25*, 2746-2756.

4. Brodbeck, U.; Schweikert, K.; Gentinetta, R.; Rottenberg, M., Fluorinated aldehydes and ketones acting as quasi-substrate inhibitors of acetylcholinesterase. *Biochim. Biophys. Acta* **1979,** *567*, 357-369.

5. Nair, H. K.; Lee, K.; Quinn, D. M., *m*-(*N*,*N*,*N*-Trimethylammonio)trifluoroacetophenone: A femtomolar inhibitor of acetylcholinesterase. *J. Am. Chem. Soc.* **1993,** *115*, 9939-9941.

6. Nair, H. K.; Seravalli, J.; Arbuckle, T.; Quinn, D. M., Molecular recognition in acetylcholinesterase catalysis: free-energy correlations for substrate turnover and inhibition by trifluoro ketone transition-state analogs. *Biochemistry* **1994,** *33*, 8566-8576.

7. Verma, A. W., Dawn M.; Islam, Rafique; Tong, Fan; Ghavami, Maryam; Mutunga, James M.; Slebodnick, Carla; Li, Jianyong; Viayna, Elisabet; Lam, Polo C.-H.; Totrov, Maxim M.; Bloomquist, Jeffrey R.; Carlier, Paul R., 3-Oxoisoxazole-2(3*H*)-carboxamides and isoxazol-3-yl carbamates: Resistance-breaking acetylcholinesterase inhibitors targeting the malaria mosquito, *Anopheles gambiae*. *Bioorg. Med. Chem. Lett.* **2015,** *23*, 1321-1340.

8. Wong, D. M.; Li, J.; Chen, Q.-H.; Han, Q.; Mutunga, J. M.; Wysinski, A.; Anderson, T. D.; Ding, H.; Carpenetti, T. L.; Verma, A.; Islam, R.; Paulson, S. L.; Lam, P. C. H.; Totrov, M.; Bloomquist, J. R.; Carlier, P. R., Select small core structure carbamates exhibit high contact toxicity to "carbamate-resistant" strain malaria mosquitoes, *Anopheles gambiae* (Akron). *PLoS One* **2012,** *7*, e46712.

9. Moslin, R. M. W., David S.; Wrobleski, Stephen T.; Tokarski, John, S; Kuman, Amit Amide substituted heterocyclic compounds useful as modulators of IL-12-23 and/or IFN alpha responses WO 2014074661 A1, May 15, 2014;.

10. Chen, L. D., M. P.; Feng, L.-C.; Hawley, R. C.;Yang, M.-M. Pyrazole-substituted arylamide derivatives and their use as P2X3 and/or P2X23 purinergic receptor antagonists and their preparation and use in the treatment of disease. WO 2009077367 A1, June 25, **2009**.

11. Camerino, E. (2012) *Trifluoromethyl ketones: Potential insecticides towards Anopheles gambiae* (Master's thesis). Retrieved from www.lib.vt.edu

12. Nair, H. K.; Quinn, D. M., *m*-Alkyl α,α,α-Trifluoroacetophenones: A new class of potent transition state analog inhibitors of acetylcholinesterase. *Bioorg. Med. Chem. Lett.* **1993,** *3*, 2619-2622.

13. Kim, D. W.; Ko, Y. K.; Kim, S. H., A new and facile synthesis of sulfonyl chlorides. *Synthesis.* **1992**, 1203-1204.

14. Wong, D. M.; Li, J.; Lam, P. C. H.; Hartsel, J. A.; Mutunga, J. M.; Totrov, M.; Bloomquist, J. R.; Carlier, P. R., Aryl methylcarbamates: Potency and selectivity towards wild-type and carbamate-insensitive (G119S) *Anopheles gambiae* acetylcholinesterase, and toxicity to G3 strain *An. gambiae*. *Chem.-Bio. Interact.* **2013,** *203*, 314-318.

15. Altman, D. G.; Bland, J. M., How to obtain the P value from a confidence interval. *BMJ* **2011,** *343*, d2304.

16. Rais, R.; Thomas, A. G.; Wozniak, K.; Wu, Y.; Jaaro-Peled, H.; Sawa, A.; Strick, C. A.; Engle, S. J.; Brandon, N. J.; Rojas, C.; Slusher, B. S.; Tsukamoto, T., Pharmacokinetics of oral D-serine in D-amino acid oxidase knockout mice. *Drug Metab. Dispos.* **2012,** *40*, 2067-2073.

Chapter 3: Fluorinated methyl ketone oxime and oxime ether prodrugs: Potential new insecticides against *Anopheles gambiae*

3.1 Contributions

The work described in this chapter was conducted in collaboration with the Bloomquist group at the University of Florida and the Li group from Virginia Tech. The author is responsible for the majority of the synthesis of the insecticidal fluorinated methyl ketone derivatives, while the DFK oxime and some methyl oxime ethers were synthesized by Mr. Florian Körber, a visiting researcher who I supervised. The enzyme activity assays were performed by Dr. Dawn Wong of the Carlier group. Mosquito toxicity testing was performed by Dr. Rafique Islam and Dr. Fan Tong of the Bloomquist group. The Li group was responsible for providing the enzyme sources for testing. X-ray crystal structures of oximes were provided by Dr. Carla Slebodnick. This chapter is based on a manuscript in preparation for submission.

Camerino, E. W., Dawn M.; Körber, Florian; Islam, Rafique; Li, Jianyong; Slebodnick, Carla; Bloomquist, Jeffrey R.; Carlier, Paul R., Fluorinated methyl ketone oxime and oxime ether prodrugs: Potential new insecticides against *Anopheles gambiae*

3.2 Abstract

As previously discussed in Chapter 2, while fluorinated methyl ketones displayed excellent activity towards *Ag*AChE, poor toxicity was observed against *Anopheles gambiae*. Prodrugs in the form of oxime and oxime ethers were synthesized to improve toxicity. While many derivatives were prepared, a TFK oxime (**3-2d**), displayed contact toxicity towards *An. gambiae* within 4-fold of propoxur. Interestingly, oxime **3-2d** proved quite resistant to hydrolysis. Thus the toxicity of this compound cannot be ascribed to a AChE inhibition mechanism. A survey of the literature revealed pyrazole oxime ethers that interact with other targets. However, preliminary testing has shown that **3-2d** does not kill through inhibition of mitochondrial respiration, or agonism of the muscarinic receptor. Future work will be directed towards determinating the mechanism of action.

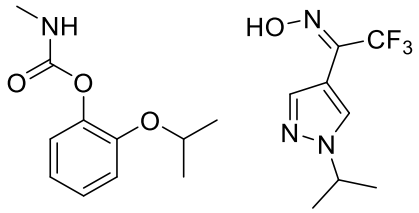

	Propoxur	**3-2d**
Anopheles gambiae Contact Toxicity LC_{50} (µg/mL)	35	83

3.3 Introduction

In the previous chapter, tri-, di-, and (mono)fluoromethyl ketones were explored as potential insecticides towards *Anopheles gambiae*. These reaction coordinate analogs covalently bind to the catalytic serine of AChE and thus mimic the ACh-AChE intermediate.[1-2] TFKs were developed with pyrazole cores that exhibited significant activity towards *h*AChE and *Ag*AChE (section 2.5). 3-Pentyl-substituted pyrazol-4-yl TFK (**2-9g**) displayed the best inhibition, with a sub-nanomolar IC_{50} value after a 60 min incubation time (Table 2-2). Di- and (mono)fluoromethyl ketones (DFKs and MFKs) were also synthesized as inhibitors of *h*AChE and *Ag*AChE. Interestingly, while MFKs did not inhibit *h*AChE and *Ag*AChE as well as TFKs, some DFKs were found to inhibit *h*AChE and *Ag*AChE as well as TFKs. DFKs were found to inhibit G119S AgAChE better than TFKs, and 3-pentyl substituted DFK (**2-10g**) remarkably displayed an IC_{50} value of 25.1 nM after 23 h incubation. While fluorinated methyl ketones exhibited good inhibition potencies towards *Ag*AChE, none displayed 100% toxicity to *An. gambiae* at the highest dosage tested (1 mg/mL). Hydration, volatility, and metabolism issues may all limit toxicity by preventing sufficient quantities of the test compounds from reaching the mosquito central nervous system (CNS). One way to improve delivery may be through a prodrug approach, namely to use oxime and oxime ethers (Scheme 3-1).

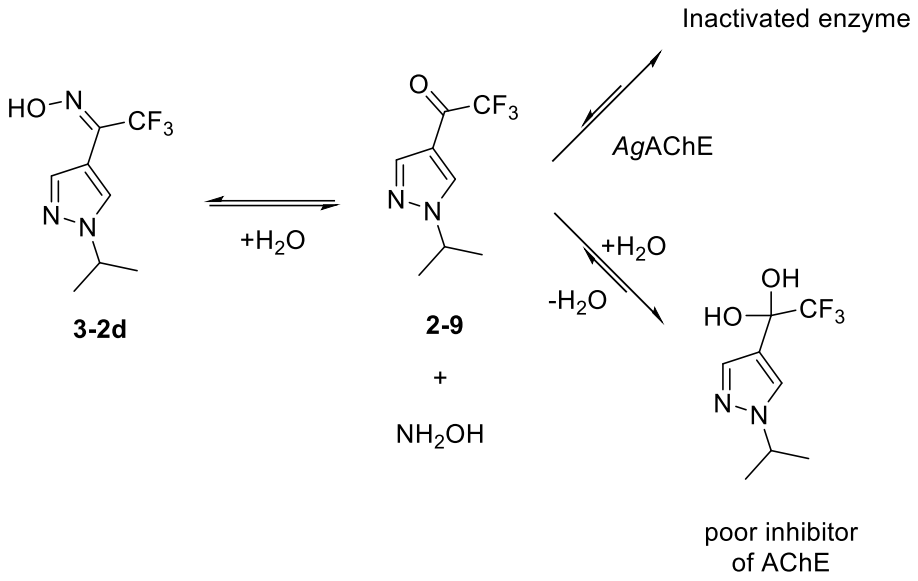

Scheme 3-1: Initial proposed mechanism of trifluoromethyl ketone prodrugs. The oxime is expected to hydrolyze *in vivo* to the ketone.

3.4 Oximes and oxime ethers as prodrugs

Oximes are proposed as prodrug candidates to improve toxicity against *Anopheles gambiae*. They have been used to mask the C=O functional group of ketones and the C=N functional group of an imine to address issues such as permeability or metabolism.[3-5]

Ketone-containing non-steroidal anti-inflammatory drugs Ketoprofen and Nabumetone have been evaluated as their oxime prodrugs **3-1a** and **3-1b** (Figure 3-1).[4]

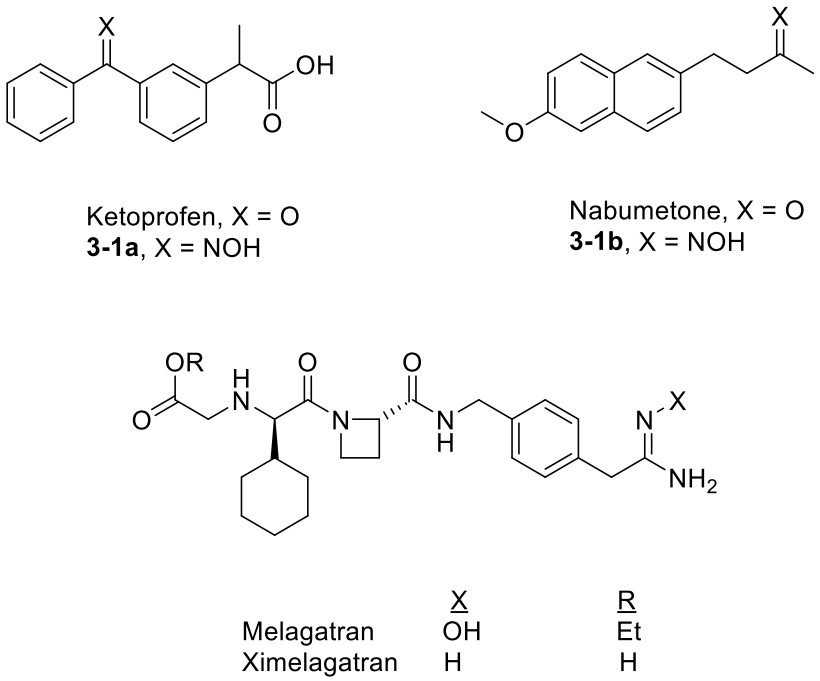

Figure 3-1: Ketoprofen, Nabumetone, Melagatran and their oxime prodrugs (**3-1a**, **3-1b**, and Ximelagatran)

Although these compounds undergo hydrolysis to the ketones at acidic pH, conversion to the ketone is greatly accelerated by Cyp450 oxidation (**Scheme 3-2**).[4,6] This mechanism generates NO, which may also have some favorable physiological effects. The amidine-containing anticoagulant drug Melagatran has also been successfully delivered as the *N*-hydroxy amidine prodrug Ximelagatran (Figure 3-1).[5]

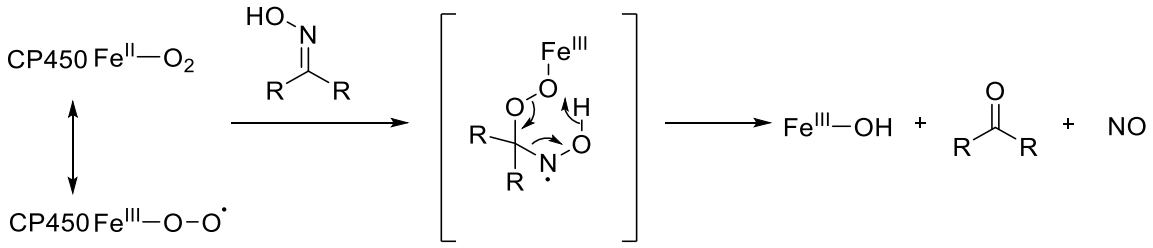

Scheme 3-2: Proposed Cyp450-assisted hydrolysis of oximes into ketones.[6]

Although **3-1e** does not contain a C=O functional group, it can be synthesized in vivo by Cyp450-mediated oxidation of ketone **3-1d**. Compound **3-1d** in turn can be generated from the oxime derivative **3-1c**, by Cyp450-mediated hydrolysis. Cascade prodrugs incorporating oximes have also been developed to increase the oral bioavailibity of the anti-Parkinson's drug, **3-1e** (Scheme 3-3).[3]

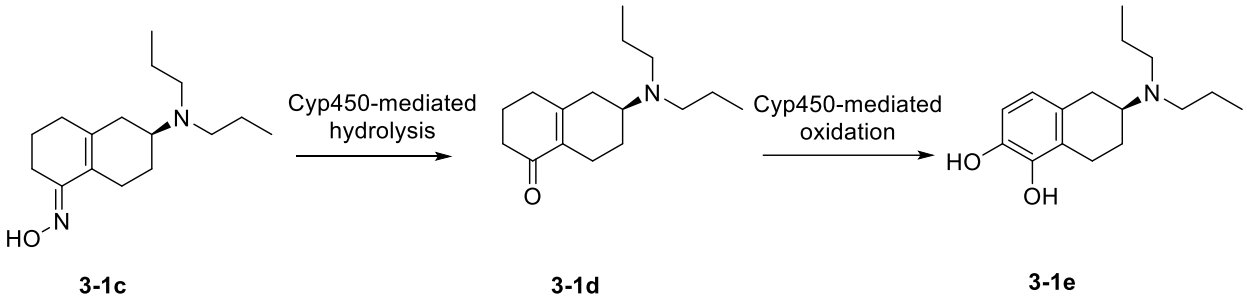

Scheme 3-3: An anti-Parkinson's prodrug incorportating an oxime functional group.

3.5 Synthesis of oxime and oxime ethers

We have synthesized oxime and oxime ethers of fluorinated methyl ketones bearing substituted benzene and pyrazol-4-yl substituents (Scheme 3-4 to Scheme 3-15).[7] The synthesis of the fluorinated methyl ketones was discussed in section 2.4.

The oximes were made by refluxing the corresponding ketone with hydroxylamine hydrochloride and sodium acetate (or hydroxide). Initially, TFK oxime synthesis was achieved by refluxing sodium hydroxide and hydroxylamine hydrochloride with the TFK in ethanol (Scheme 3-4 and Scheme 3-5, method i).[7] However better yields (18-80%) were obtained by heating sodium acetate and hydroxylamine hydrochloride with the TFK in a 1 to 1 mixture of ethanol and water

(Scheme 3-5, method ii).[8] In this solvent mixture, we found the product would often precipitate out, thus facilitating purification.

It is of interest to note that for some trifluoromethyl ketone oximes, *E* and *Z* isomers were formed. This observation was confirmed via NMR spectroscopy; the doubling of various peaks in ^{1}H and ^{13}C NMR spectra and two distinct peaks in ^{19}F NMR spectra appearing between -64 and -69 ppm suggests two distinct isomers. In cases where there were isomers, ^{19}F resonances for the isomers differed by ~3 ppm and were not mistaken for the starting material ^{19}F peak between -74 to -77 ppm. In most cases, ^{19}F NMR spectra were recorded with C_6F_6 an internal ^{19}F reference. However, periodically C_6F_6 in acetone was used as an external reference in the form of a separate sample. In each case, the measured ^{19}F NMR chemical shift for C_6F_6 was within 0.1 ppm of the literature value of -164.9 ppm. Therefore we consider our measured ^{19}F chemical shifts to be reliable to within 0.1 ppm. All of the TFK oximes were solids, and most adopted a single isomeric form. Only in the case of **3-2b**, **3-2c**, **3-2k**, **3-2m**, and **3-2n** did ^{1}H and ^{19}F NMR spectra indicate the presence of *(E)*- and *(Z)*- isomers.

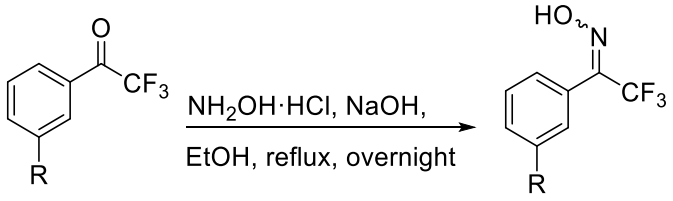

2-9b,c **3-2b,c**

Scheme 3-4: Synthesis of trifluoroketone oximes (**3-2b, c**) bearing a phenyl core.

Table 3-1: Isolated yields of phenyl trifluoroketone oximes (**3-2b, c**).

Compound	R	Yield	*E* : *Z* ratio	^{19}F Chemical Shift (ppm)
3-2b		56%	7 : 10	-69.9 *(E)*, -66.5 *(Z)*
3-2c		65%	9 : 10	-69.2 *(E)*, -66.7 *(Z)*

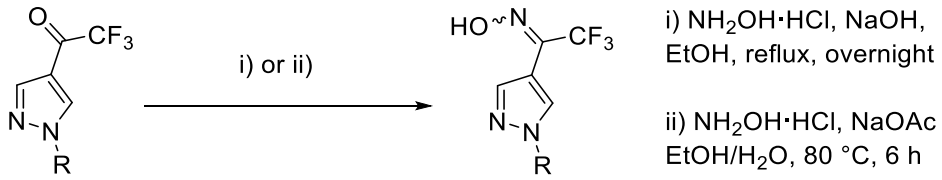

2-9c-r **3-2d-r**

Scheme 3-5: Synthesis of pyrazole trifluoroketone oximes (**3-2d-r**) bearing a pyrazole core.

Table 3-2: Isolated yields of pyrazole trifluoroketone oximes (**3-2d-r**).

Compound	R	Method	Yield	*E* : *Z* ratio	^{19}F Chemical Shift (ppm)
3-2d		i)	43%	100 : 0	-66.8 *(E)*
3-2e	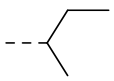	i)	46%	100 : 0	-66.6 *(E)*

3-2f	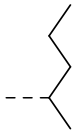	i)	45%	100 : 0	-69.3 *(E)*
3-2g	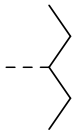	ii)	18%	100 : 0	-66.6 *(E)*
3-2h	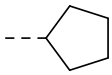	ii)	24%	100 : 0	-66.6 *(E)*
3-2i	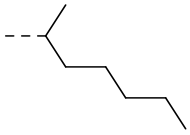	ii)	32%	100 : 0	-66.6 *(E)*
3-2j	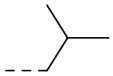	ii)	74%	100 : 0	-66.6 *(E)*
3-2k	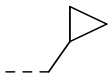	ii)	38%	3 : 1	-66.6 *(E)*, -64.7 *(Z)*
3-2l	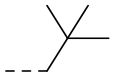	ii)	44%	100 : 0	-66.6 *(E)*
3-2m		ii)	80%	3 : 1	-66.5 *(E)*, -64.7 *(Z)*
3-2n	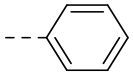	ii)	29%	5 : 1	-66.6 *(E)*, -64.7 *(Z)*
3-2o		ii)	38%	100 : 0	-66.7 *(E)*
3-3p		ii)	19%	100 : 0	-66.6 *(E)*
3-2q	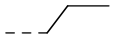	ii)	21%	100 : 0	-66.6 *(E)*
3-2r	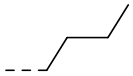	ii)	71%	100 : 0	-66.6 *(E)*

An X-ray crystal structure of **3-2d** was obtained, and demonstrated *(E)*-stereochemistry (Figure 3-2).

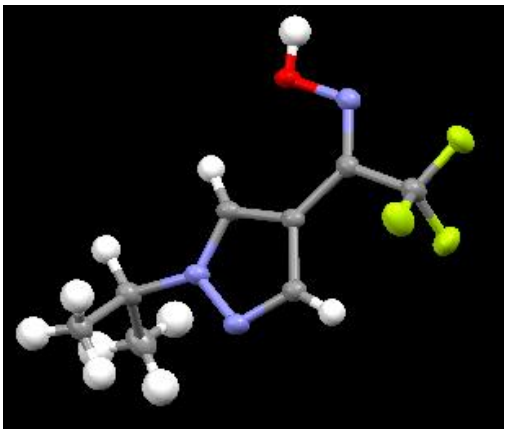

Figure 3-2: X-ray crystal structure of **3-2d** shown in an *(E)*- conformation.

Since the ^{19}F NMR chemical shift of **3-2d** was -66.8 ppm and the other single isomer oximes had ^{19}F chemical shifts ranging between -66.5 and -66.8 ppm, we presume that they are also *(E)*-configured. In the case of **3-2k**, **3-2m**, and **3-2n**, the major isomer displayed ^{19}F NMR resonances between -66.5 and -66.6 ppm, consistent with *(E)*-stereochemistry. The minor ^{19}F resonances for these compounds appeared approximately 2 ppm downfield at -64.7 ppm. We deduce that these minor compounds are *(Z)*-configured.

Using the EtOH/H_2O solvent system for synthesis of the DFK oximes did not prove as successful as in the case of TFK oximes. Instead, refluxing in only ethanol was found to give the best yields (50-90%, Scheme 3-6, Table 3-3).

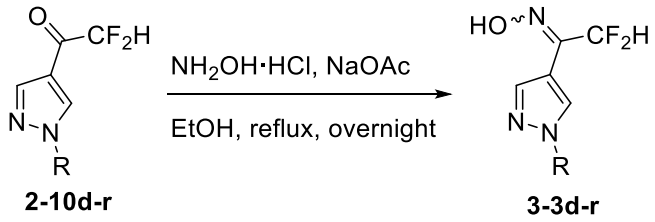

Scheme 3-6: Synthesis of pyrazole difluoroketone oximes (**3-3d-r**).

Table 3-3: Isolated yields of pyrazole difluoroketone oximes (**3-3d-r**).

Compound	R	Yield	*E* : *Z* ratio	^{19}F Chemical Shift (ppm)
3-3d		90%	100 : 0	-116.1 *(E)*
3-3e	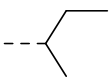	64%	100 : 0	-116.2 *(E)*
3-3f	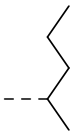	70%	100 : 0	-116.3 *(E)*
3-3g	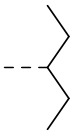	73%	100 : 0	-116.2 *(E)*
3-3h	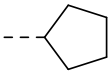	56%	100 : 0	-116.2 *(E)*
3-3j	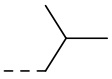	75%	100 : 0	-116.2 *(E)*
3-3r	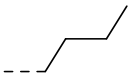	64%	100 : 0	-115.4 *(E)*

Again, the issue of *E/Z* isomerism must be addressed. In all cases examined, only a single isomer was evident by ^{1}H and ^{19}F NMR spectroscopy. Again, we were successful in obtaining an X-ray crystal structure of one of the DFK oximes. As shown in Figure 3-3, **3-3d** adopts the (*E*)-configuration.

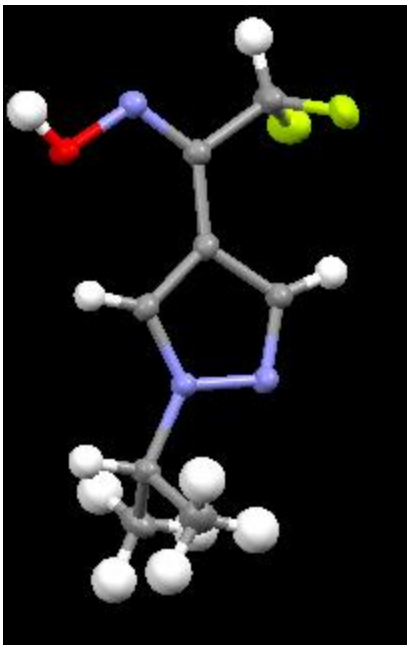

Figure 3-3: X-ray crystal structure of **3-3d** shown in an *(E)*- conformation.

Since its ^{19}F NMR chemical shift was -116.1 ppm, and the ^{19}F NMR chemical shifts of all the others ranged between -116.1 and -116.4 ppm, we conclude that all the DFK oximes are *(E)*-configured (Scheme 3-6, Table 3-3).

For the synthesis of MFK oximes, refluxing in pure ethanol proved the most effective procedure, as it was for DFK oximes (19-81%, Scheme 3-7). Because an X-ray crystal structure of an MFK oxime has not yet been attained, the assignment of *E*/*Z* stereochemistry is speculative. As previously discussed, the more upfield isomer for TFK oximes and DFK oximes corresponded to the *(E)* isomer, a trend we assume will apply to the MFK oximes. In one case (**3-4g**) there was an apparent 1:24 mixture of isomers with ^{19}F resonances at -231.5 and -215.2 ppm We assigned the minor upfield resonance to the (*E*)-isomer, and the major downfield resonance (-215.2 ppm) to the *(Z)*-isomer. In all of the other cases a single isomer with a ^{19}F

resonance between -215.2 and -215.7 ppm was observed, which we assign as *(Z)*-configured. We believe that the *(Z)*-conformation of the MFK oxime offers a favorable hydrogen-bonding interaction that may be stronger than that of the DFK and TFK oxime analogs (Figure 3-4). Although the proposal of hydrogen-bonding to organic fluorine is somewhat controversial, a recent study concluded that hydrogen-bond acceptor ability decreased in the series (e.g. $-CH_2F$ > $-CF_2H$ > $-CF_3$).[9] It is also posible that the steric interaction between the oxime O and H-3 in the *(E)*-configuration is more severe than that between the oxime O and CH_2F group in the *(Z)*-configuration.

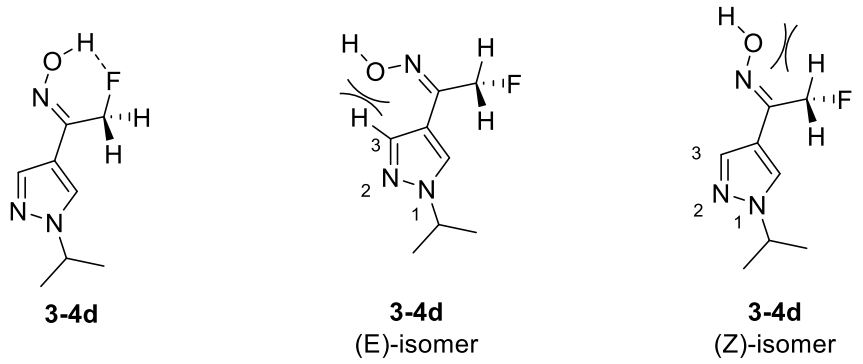

Figure 3-4: For MFK oximes, it is proposed that the *(Z)*-configuration may be favored by an H-F hydrogen-bonding interaction (shown by the dashed bond). Steric effects may also favor the *(Z)*-isomer

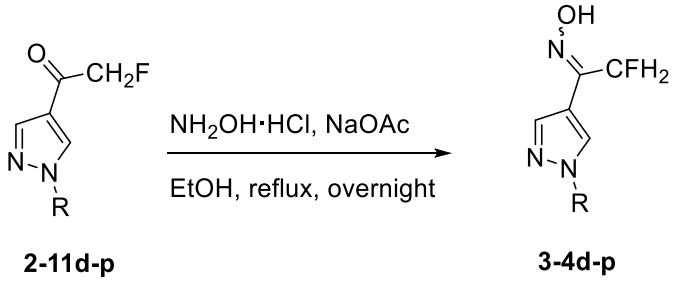

Scheme 3-7: Synthesis of pyrazole monofluoroketone oximes (**3-4d-p**).

Table 3-4: Isolated yields of pyrazole monofluoroketone oximes (**3-4d-p**).

Compound	R	Yield	*E* : *Z* ratio	^{19}F Chemical Shift (ppm)
3-4d		16%	0 : 100	-215.4 *(Z)*
3-4e	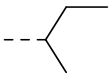	15%*	0 : 100	-215.3 *(Z)*
3-4f	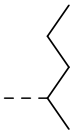	11%*	0 : 100	-215.2 *(Z)*
3-4g	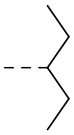	82%	1 : 24	-231.5 *(E)*, -215.2 *(Z)*
3-4h	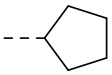	19%	0 : 100	-215.3 *(Z)*
3-4j	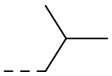	81%	0 : 100	-215.4 *(Z)*
3-4m		34%	0 : 100	-215.3 *(Z)*
3-4n	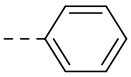	47%	0 : 100	-215.7 *(Z)*
3-4p		70%	0 : 100	-215.4 *(Z)*

*After two reactions.

In order to synthesize the oxime ethers bearing a methyl or benzyl group, the synthetic procedure was trivially modified by using the appropiate oxime ether hydrochloride salt (Scheme 3-8 to Scheme 3-15). In several cases, inseparable mixtures of the *(E)*- and *(Z)*- isomers were obtained. The ^{19}F NMR resonances of the trifluoromethylketone oxime methyl ether stereoisomers appeared at -69.3 and -65.4 ppm for **3-5c**, and at -69.0 and -61.1 ppm for **3-5d**. In the four other cases, a single stereoisomer with a ^{19}F resonance at -68.9 to -69.0 ppm was observed. We noted that in the case of the TFK oximes the more negative chemical shift resonance (i.e. more upfield) were attributed to the *(E)*-isomer. Thus we conclude that the *(E)*-

isomer of the oxime methyl ether gives rise to the peak near -69.0 ppm, and is thus the major or exclusive isomer in every case.

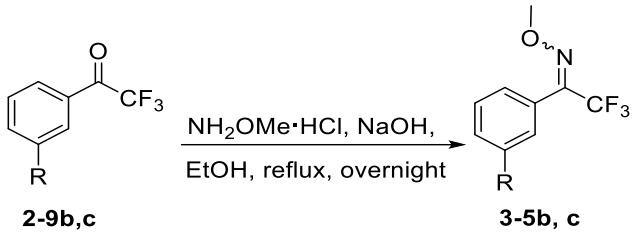

2-9b,c **3-5b, c**

Scheme 3-8: Synthesis of trifluoroketone methyl oxime ethers (**3-5b, c**) bearing a phenyl core.

Table 3-5: Isolated yields of phenyl trifluoroketone methyl oxime ethers (**3-5b, c**).

Compound	R	Yield	*E* : *Z* ratio	^{19}F Chemical Shift (ppm)
3-5b		70%	100 : 0	-69.1 *(E)*
3-5c		83%	5 : 4	-69.3 *(E)*, -65.4 *(Z)*

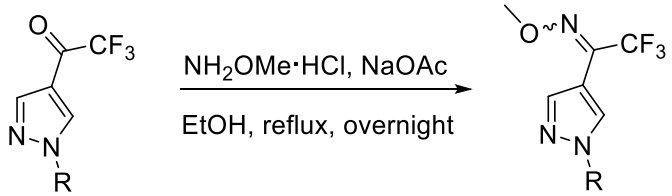

2-9d-h **3-5d-h**

Scheme 3-9: Synthesis of pyrazole trifluoroketone methyl oxime ethers (**3-5d-h**).

Table 3-6: Isolated yields of pyrazole trifluoroketone methyl oxime ethers (**3-5d-h**).

Compound	R	Yield	*E* : *Z* ratio	^{19}F Chemical Shift (ppm)
3-5d		72%	5 : 1	-69.0 *(E)*, -67.1 *(Z)*
3-5e	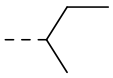	83%	100 : 0	-69.0 *(E)*
3-5f	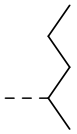	59%	100 : 0	-68.9 *(E)*
3-5h	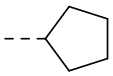	85%	100 : 0	-69.0 *(E)*

The syntheses of the DFK methyl oxime ethers were achieved in a similar fashion to that of the TFK methyl oxime ether and gave comparable yields (49-77%, Table 3-7). The ^{19}F resonances of these DFK oxime ethers indicate that in most cases a single isomer results around -115.1 ppm. In cases where *E/Z* isomerism appears, the major peak is the more downfield peak which we propose is the *(Z)*-isomer; in the case of **3-6g**, a 2:7 ratio of *E*/*Z* appears. It is not clear why the (*Z*)-isomer would be favored for the DFK methyl oxime ethers when the (*E*)-isomer was favored for the DFK oximes.

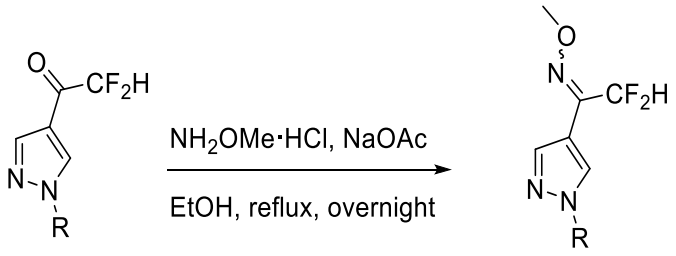

2-10d-j **3-6d-j**

Scheme 3-10: Synthesis of pyrazole difluoroketone methyl oxime ethers (**3-6d-j**).

Table 3-7: Isolated yields of pyrazole difluoroketone methyl oxime ethers (**3-6d-j**).

Compound	R	Yield	E : Z ratio	^{19}F Chemical Shift (ppm)
3-6d		75%	0 : 100	-115.0 *(Z)*
3-6e	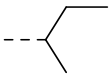	73%	0 : 100	-115.0 *(Z)*
3-6f	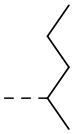	77%	0 : 100	-115.0 *(Z)*
3-6g	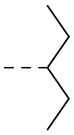	49%	2 : 7	-124.1 *(E)*, -115.1 *(Z)*
3-6h	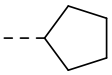	63%	0 : 100	-115.1 *(Z)*
3-6j	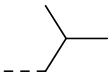	51%	2 : 5	-124.2 *(E)* , -115.2 *(Z)*

The synthesis of the MFK methyl oxime ethers proceeded in an analogous fashion to the synthesis of DFK and TFK methyl oxime ether synthesis; the yields of the reactions varied from 10%-90% (Scheme 3-11, Table 3-8). In all case, the major isomer corresponded to the more downfield peak (e.g. approximately -215.3 ppm) which we assign as (Z)-configured (Figure 3-4).

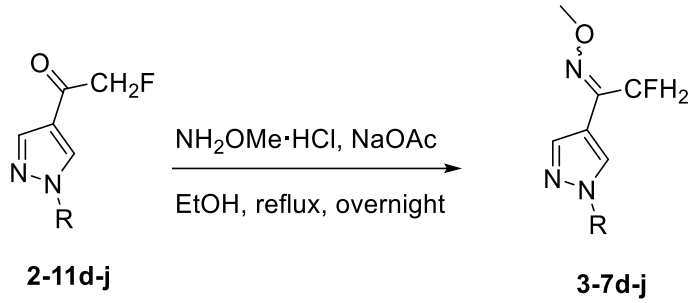

2-11d-j **3-7d-j**

Scheme 3-11: Synthesis of monofluoroketone methyl oxime ethers (**3-7d-j**).

Table 3-8: Isolated yields of monofluoroketone methyl oxime ethers (**3-7d-j**).

Compound	R	Yield	E : Z ratio	^{19}F Chemical Shift (ppm)
3-7d		15%*	0 : 100	-215.3 *(Z)*
3-7e	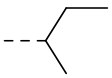	90%	0 : 100	-215.3 *(Z)*
3-7j	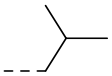	54%	2 : 3	-231.6 *(E)*, -215.3 *(Z)*
3-7p		10%*	0 : 100	-215.4 *(Z)*

*After two reactions.

The synthesis of the benzyl oxime ethers proceeded in an analogous fashion to that of the methyl oxime ethers. The ^{19}F shifts for the TFK benzyl oxime ethers were at -69.0 and -67.1 ppm for **3-8d**. In the case of single isomers, the phenyl core TFK benzyl oxime appeared between -69.1 to -69.4 ppm and between -68.7 to -69.0 ppm for the pyrazol-4-yl TFK benzyl oxime ether. Because the shifts were similar to those of the TFK methyl oxime ethers, it was reasonable to assign the *(E)*-isomer to the more upfield peak. As the number of fluorines decreased, we observed that a mixture of *(E)*- and *(Z)*- isomers was isolated. In the case of difluoromethyl ketone oxime benzyl ethers **3-9e** and **3-9g** (Scheme 3-14), nearly 1:1 mixtures of *(E)*- and *(Z)*- isomers were obtained. In the case of fluoromethyl ketone benzyl oxime ethers **3-**

10d, **3-10e**, and **3-10p** (Scheme 3-15), the *(Z)*-isomer is either the major isomer or is present in an equal amount to the *(E)*-isomer. Again, we believe that steric interaction caused by the pyrazole ring is greater than that caused by the -CFH_2 group (Figure 3-4).

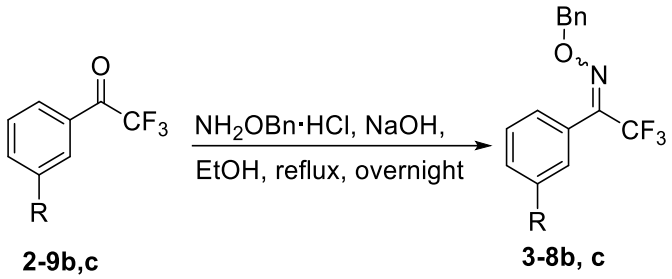

2-9b,c **3-8b, c**

Scheme 3-12: Synthesis of trifluoroketone benzyl oxime ethers (**3-8b, c**) bearing a phenyl core.

Table 3-9: Isolated yields of trifluoroketone benzyl oxime ethers (**3-8b, c**).

Compound	R	Yield	E : Z ratio	^{19}F Chemical Shift (ppm)
3-8b		73%	100 : 0	-69.4 *(E)*
3-8c		80%	100 : 0	-69.1 *(E)*

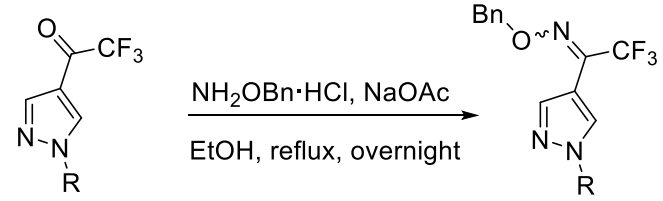

2-9d-h **3-8d-h**

Scheme 3-13: Synthesis of trifluoroketone benzyl oxime ethers (**3-8d-h**).

Table 3-10: Isolated yields of trifluoroketone benzyl oxime ethers (**3-8d-h**).

Compound	R	Yield	E : Z ratio	^{19}F Chemical Shift (ppm)
3-8d		78%	10 : 9	-68.9 *(E)*, -67.1 *(Z)*

3-8e	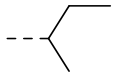	80%	100 : 0	-68.8 *(E)*
3-8f		70%	100 : 0	-68.7 *(E)*
3-8h	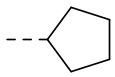	65%	100 : 0	-69.0 *(E)*

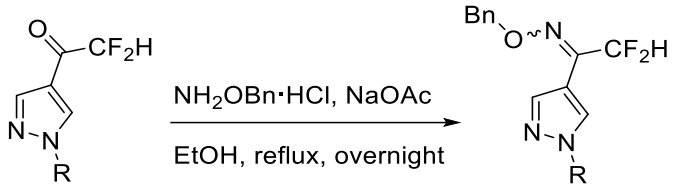

2-10e,g **3-9e,g**

Scheme 3-14: Synthesis of difluoroketone benzyl oxime ethers (**3-9e, g**).

Table 3-11: Isolated yields of difluoroketone benzyl oxime ethers (**3-9e, g**).

Compound	R	Yield	E : Z ratio	^{19}F Chemical Shift (ppm)
3-9e	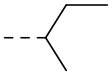	76%	2 : 3	-124.1 *(E)*, -115.1 *(Z)*
3-9g	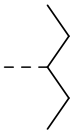	66%	3 : 2	-124.1 *(E)*, -115.1 *(Z)*

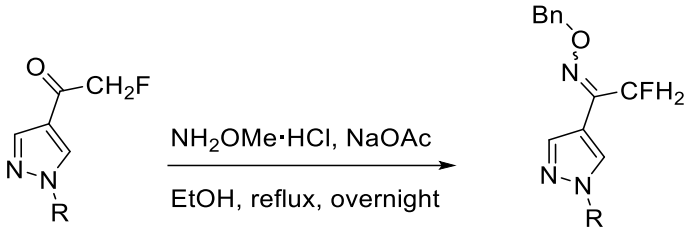

2-11d-p **3-10d-p**

Scheme 3-15: Synthesis of monofluoroketone benzyl oxime ethers (**3-10d-p**).

Table 3-12: Isolated yields of monofluoroketone benzyl oxime ethers (**3-10d-p**).

Compound	R	Yield	E : Z ratio	^{19}F Chemical Shift (ppm)
3-10d		10%*	0 : 100	-215.3 *(Z)*
3-10e	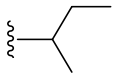	81%	1 : 1	-231.2 *(E)*, -215.3 *(Z)*
3-10p		8%*	0 : 100	-215.4 *(Z)*

*After two reactions.

3.6 Tarsal contact toxicity of oximes and oxime ethers of fluorinated methyl ketones

A critical characteristic of compounds intended for use on ITNs/IRS is good contact toxicity to *An. gambiae*. A practical way to test for compound lethality is the WHO regulated filter paper assay.[10] As previously discussed in Chapter 2 (Table 2-1, Table 2-2, and Table 2-4), fluorinated methyl ketones did not exhibit good contact toxicity against *Anopheles gambiae*. Our hypothesis that oxime and oxime ether derivatives would have greater contact toxicity proved correct (Table 3-13 to Table 3-16).

As seen in Table 3-13, benzene core trifluoroketoximes **3-2b** and **3-2c** did not exhibit significant toxicity, causing ≤30% mortality to *An. gambiae* at 1,000 µg/mL. However, trifluoroketoximes with a pyrazole core proved to be more toxic. Two of the pyrazole trifluoroketoximes (**3-2d** to **3-2r,** Table 3-13) tested showed compounds that possessed 100% mortality at the initial concentration of 1,000 µg/mL (e.g **3-2d** and **3-2e**) which prompted LC_{50} determinations. The most toxic oxime was **3-2d** having a LC_{50} value of 106 µg/mL, a value within a factor of three of the toxicity of propoxur. No observable trend was observed with increased chain length or branching at the alpha and beta positions. Exploration of oximes with varying numbers of fluorines did not lead to compounds with improved toxicity compared with

3-2d; the most toxic oxime that did not have a CF_3 group was fluoroketone oxime **3-4f** with an LC_{50} of 204 µg/mL (Table 3-14).

Table 3-13: Tarsal contact toxicity of propoxur and trifluoro methyl ketone oximes (**3-2b** to **3-2r**) to G3 strain of *An. gambiae*.[a]

Compound	*An. gambiae* G3 % mortality (1,000 µg/mL) or LC_{50} (µg/mL)	Compound	*An. gambiae* G3 % mortality (1,000 µg/mL) or LC_{50} (µg/mL)
propoxur	39 µg/mL (32-45)[b]	**3-2j**	0%
3-2b	0%	**3-2k**	35%
3-2c	30%	**3-2l**	36%
3-2d	106 µg/mL (81-152)	**3-2m**	10%
3-2e	531 µg/mL (410-670)	**3-2n**	10%
3-2f	50%	**3-2o**	40%
3-2g	18%	**3-2p**	80%
3-2h	70%	**3-2q**	0%
3-2i	70%	**3-2r**	6%

[a]Mosquitoes were exposed (1 h) to dried filter papers previously treated with ethanolic solutions of trifluoroketones oximes; mortality was recorded after 24 h. [b]LC_{50} values derive from the concentrations of inhibitor used to treat the paper; 95% confidence intervals are given in parenthesis.[11]

Table 3-14: Tarsal contact toxicity of di- and monofluoroketone oximes (**3-3d** to **3-4n**) to G3 strain of *An. gambiae*.[a]

Compound	*An. gambiae* G3 % mortality (1,000 µg/mL) or LC_{50} (µg/mL)	Compound	*An. gambiae* G3 % mortality (1,000 µg/mL) or LC_{50} (µg/mL)
3-3d	40%	**3-4e**	30%
3-3e	10%	**3-4f**	204 µg/mL (125-347)
3-3f	67%	**3-4g**	30%
3-3g	40%	**3-4p**	0%
3-3h	10%	**3-4h**	8%
3-3j	42%	**3-4j**	64%
3-3r	40%	**3-4m**	20%
3-4d	50%	**3-4n**	20%

[a]Mosquitoes were exposed (1 h) to dried filter papers previously treated with ethanolic solutions of triflluoroketone and oxime ethers; mortality was recorded after 24 h. LC_{50} values derive from the concentrations of inhibitor used to treat the paper; 95% confidence intervals are given in parenthesis. [11]

Oxime methyl ethers overall did not yield a compound that was as toxic as the best oxime **3-2d** (Table 3-15). Trifluoromethyl ketone oxime methyl ether **3-5b** had an LC_{50} value of 485 µg/mL and proved to be the most toxic methyl oxime ether. Compound **3-5d** gave moderate toxicity (90% mortality at 1,000 µg/mL) while **3-5f** and **3-5h** exhibited poor toxicity. **3-5c** and **3-5e** did not show any toxicity at the highest concentration tested (1,000 µg /mL). The difluoroketone oxime methyl ethers exhibited little to no toxicity (**3-6d-j**, Table 3-15) and the monofluoroketone oxime methyl ethers (**3-7d-p**, Table 3-15) fared better, but still not comparable to **3-5b**. Decreasing the number of fluorines appears to have a negative impact on the *Anopheles gambiae* contact toxicity.

Table 3-15: Tarsal contact toxicity of tri-, di-, and monofluoroketone methyl oxime ethers (**3-5b** to **3-8h**) to G3 strain of *An. gambiae.* [a]

Compound	*An. gambiae* G3 % mortality (1,000 µg/mL) or LC_{50} (µg/mL)	Compound	*An. gambiae* G3 % mortality (1,000 µg/mL) or LC_{50} (µg/mL)
3-5b	485 µg/mL (366-689)	**3-6f**	27%
3-5c	0%	**3-6g**	0%
3-5d	90%	**3-6h**	33%
3-5e	0%	**3-6j**	42%
3-5f	30%	**3-7d**	10%
3-5h	10%	**3-7e**	50%
3-6d	0%	**3-7p**	13%
3-6e	0%		

[a]Mosquitoes were exposed (1 h) to dried filter papers previously treated with ethanolic solutions of trifluoroketone and oxime ethers; mortality was recorded after 24 h. LC_{50} values derive from the concentrations of inhibitor used to treat the paper; 95% confidence intervals are given in parenthesis.[11]

The oxime benzyl ethers tested displayed varying contact toxicity properties (Table 3-16). Amongst the trifluoroketone benzyl oxime ethers explored, **3-8c** and **3-8g** didn't exhibit mortality @ 1,000 µg/mL. On the other hand at the same concentration, **3-8b**, **3-8d**, and **3-8f** displayed 100% mortality. At 100 µg/mL, their toxicity dropped sharply (Table 3-16) suggesting approximate LC_{50} values of 500 µg/mL. When transitioning to difluoroketone and monofluoroketone oxime benzyl ethers, the toxicity sharply drops suggesting that electrophilicity may play a part in toxicity (Table 3-16).

Table 3-16: Tarsal contact toxicity of tri-, di-, and monofluoroketone benzyl oxime ethers (**3-8b** to **3-10p**) to G3 strain of *An. gambiae*. [a]

Compound	*An. gambiae* G3 % mortality (1,000 µg/mL)	Compound	*An. gambiae* G3 % mortality (1,000 µg/mL)
3-8b	0%	**3-9d**	0%
3-8c	40%	**3-9g**	40%
3-8d	100%	**3-10d**	0%
	10% (100 µg/mL)		
3-8e	ND	**3-10e**	25%
3-8f	100%	**3-10p**	27%
	0% (100 µg/mL)		
3-8h	0%		

[a]Mosquitoes were exposed (1 h) to dried filter papers previously treated with ethanolic solutions of diflouroketone oximes and oxime ethers; mortality was recorded after 24 h. ND designates "not determined". LC_{50} values derive from the concentrations of inhibitor used to treat the paper; 95% confidence intervals are given in parenthesis.[11]

Since variation of the fluorine count and oxime derivative of the lead compound (**3-2d**) did not produce increased toxicity, we decided to explore potentially isosteric analogs of **3-2d** (Scheme 3-16). In particular, modification of the fluorinated methyl group to a methyl, cyclopropyl, and isopropyl group were investigated. Synthesis of the analogs proceeded in an analogous manner to the TFKs; metal-halogen exchange was performed on 4-bromo-1-isopropyl-1*H*-pyrazole (**2-9d**) and the corresponding electrophile was introduced to produce the desired ketone. The ketoxime could then be produced by refluxing a mixture of the ketone and hydroxylamine hydrochloride salt in ethanol (Scheme 3-16).

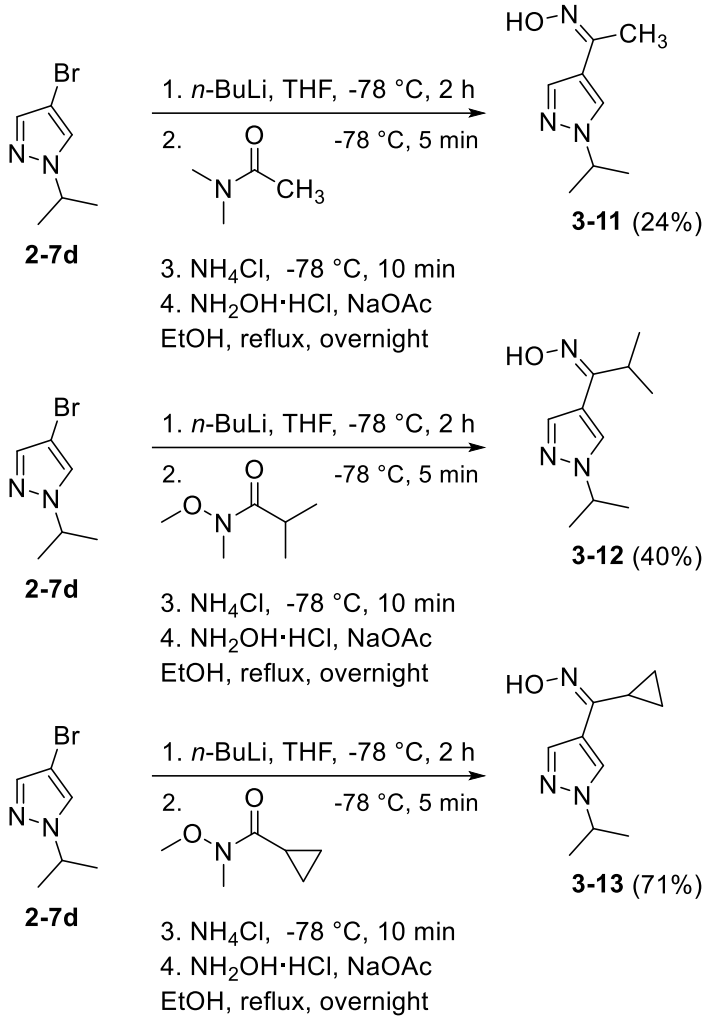

Scheme 3-16: Synthesis of analogs of **3-2d** (**3-11** to **3-13**). *(E)*-isomers shown arbitrarily. In each case, ^{1}H and ^{13}C NMR suggested a single isomer was produced, which we arbitrarily depict as *(E)*-configured.

Unfortunately, none of the analogs displayed a toxicity comparable to that of **3-2d**; **3-13** displayed the best toxicity with 70% mortality at 1,000 µg/mL (Table 3-17). However this series of compounds allows us to draw some conclusions about the role of the fluorines in the toxicity of **3-2d**. Difluoroketone oxime **3-3d** and fluoroketone oxime **3-4d** have approximate LC_{50}

values of 1,000 µg/mL, based on 40-50% mortality at this concentration. Thus they are ~ 10-fold less toxic that TFK oxime **3-2d**. Yet methyl ketone oxime **3-11** also has an approximate LC_{50} of 1,000 µg/mL, and it is isosteric to fluoromethyl ketone oxime **3-4d**. Perhaps the role of the fluorine atoms in *An. gambiae* toxicity has a significant steric component. The CF_3 group is much larger than a methyl group and is believed to approximate the size of an *i*-Pr group.[12] Interestingly *i*-Pr ketone oxime **3-12** is much less toxic that **3-2d**, giving only 20% mortality at 1,000 µg/mL. Yet a slight decrease in the size of the substituent from *i*-Pr to cyclopropyl led to a significant increase in toxicity. Compound **3-13** gave 70% at 1,000 µg/mL, indicating its IC_{50} is less than 1,000 µg/mL. Thus, its improved toxicity relative to the methyl and isopropyl ketone oxime **3-11** and **3-12** may suggest that cyclopropyl better approximates the size of CF_3 than does CH_3 or *i*-Pr.

Table 3-17: Tarsal contact toxicity of propoxur, fluorinated methyl ketones oximes (**3-2d** to **3-4d)** and isosteric analogs **3-11** to **3-13** to G3 strain of *An. gambiae*.

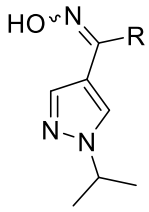

Compound	R	*An. gambiae* G3 % mortality (1,000 µg/mL)
propoxur	NA	39 µg/mL (32-45)[b]
3-2d	CF_3	106 µg/mL (81-152)[b]
3-3d	CF_2H	40%
3-4d	CFH_2	50%

3-11	CH_3	40%
3-12	*i*-Pr	20%
3-13	*c*-C_3H_5	70%

[a]Mosquitoes were exposed (1 h) to dried filter papers previously treated with ethanolic solutions of fluorinatedmethylketone oximes and ketoximes; mortality was recorded after 24 h. ND designates "not determined". [b]LC_{50} values derive from the concentrations of inhibitor used to treat the paper; 95% confidence intervals are given in parenthesis.[11]

Compound **3-2d** proved toxic to both G3 and Akron strain *An. gambiae* (Table 3-18) with LC_{50} values of 106 and 112 µg/mL respectively.

Table 3-18: Side by side comparison of toxicity values of **3-2d** and propoxur to *An. gambiae*.

Treatment (G3, Akron, and mice)	**3-2d**	Propoxur
G3 WHO paper LC_{50} (µg/mL)[a]	106 (81-152)	39 (32-45)
Akron WHO paper LC_{50} (µg/mL)[a]	112 (88-163)	>5000
G3 Topical application LD_{50} (ng/mg)[b]	12 (9-17)	3.2 (2.4-4.2)
Mouse oral LD_{50} (mg/kg)[c]	>2,000 (0 of 3 mice died)	100 (EXTOXNET)[13]

[a]WHO regulated filter paper assay[10]
[b]Topical application protocol of Pridgeon et. al.[14]
[c]Mouse oral protocol of Swale et. al.[15]

Compound **3-2d** also compares favorably in the topical application assay,[10] being about 1/4 as toxic as propoxur. It is of considerable interest to note that **3-2d** does not show toxicity towards mice with at an oral dose of >2,000 mg/kg as opposed to a reported LD_{50} of 100 mg/kg for propoxur. Thus **3-2d** has considerable promise as a public health mosquitocide. We will now address the question of how *An. gambiae* toxicity was achieved. As stated previously, we hypothesized that the oximes and oxime ethers could serve as prodrugs. The oxime/oxime ether

was selected to improve the possible problematic aspects of the ketone's properties such as permeation through the mosquito cuticle, blood brain barrier (BBB) penetration, and its high volatility. However, it has not yet been demonstrated that the oxime/ oxime ether hydrolyzes to a ketone *in vivo* and subsequently inhibits AChE. To test this hypothesis, an Ellman assay was performed on **3-2d** and **3-2f** (Table 3-19); if hydrolysis is occurring, low AChE activity should be seen due to formation of and inhibition by the TFK. In the case of **3-2d**, the corresponding ketone is **2-9d**, with a 60 min incubation IC_{50} value of 285 nM. Since **3-2d** gave an IC_{50} value of 45,400 nM after 60 min, we can conclude that no more than 0.6% of **3-2d** hydrolyzed to **2-9d**. For **3-2f**, the corresponding ketone would be **2-9f**, with a 60 min incubation IC_{50} value of 2.06 nM. Since **3-2f** gave an IC_{50} value of 6,760 nM after 60 min, we can conclude that no more than 0.03% of **3-2f** hydrolyzed to **2-9f**. This very low extent of hydrolysis of **3-2d** to **2-9d** and **3-2f** to **2-9f** would not be expected to have toxic consequences to *An. gambiae*.

Table 3-19: IC_{50} values for trifluoroketoximes (**3-2d, f**) for *h*AChE and *Ag*AChE (WT, G119S)

Compound	Hydrolysis time (min) (1×10^{-4} M [I])	*h*AChE IC_{50} (nM)	r*Ag*AChE-WT IC_{50}	G119S *Ag*AChE IC_{50} (nM)[a]
3-2d	10	28,900 ± 700	68,100 ± 3,600	>10,000
	60	22,900 ± 500	45,400 ± 1,700	>10,000
3-2f	10	37,500 ± 5,300	14,000 ± 600	>10,000
	60	35,000 ± 5,500	6,760 ± 230	>10,000

[a]Measured at 23 ± 1°C, pH 7.7, 0.1% (v/v) DMSO. Recombinant sources of *Ag*AChE are r*Ag*AChE-WT and r*Ag*AChE-G119S.

As can be seen in Table 3-19, **3-2d** and **3-2f** did not significantly hydrolyze to the corresponding TFKs over 60 minutes at pH 7.7. Exploration of more acidic pH and longer incubation time on a different oxime yielded the same results. When an oxime (**3-2e**) was in a pH 7.7 buffer when the Ellman assay was peformed, the IC_{50} value was 8,500 nM at rAgAChE (22 h incubation time, Table 3-20). Since the AgAChE IC_{50} of the corresponding ketone **3-9e** was 2.3 nM, we can estimate that no more than 0.03% of **3-2e** hydrolyzed to **2-9e**. These results were expected based on the results of **3-2d** and **3-2f**. Kalia *et. al*. showed that oxime hydrolysis occurred more rapidly under acidic conditions (e.g. pH 4).[16] We thus exposed **3-2e** into a pH 5.5 buffer solution to help facilitate hydrolysis. Yet the IC_{50} value of 14,900 nM at *Ag*AchE measured after 20 h hydrolysis time (Table 3-20), again suggesting that significant hydrolysis is not occuring.

Table 3-20: IC_{50} values of **3-2e** as a factor of pH and hydrolysis time.

Compound	pH	Hydrolysis time*	*Ag*AChE IC_{50} (nM)	*h*AChE IC_{50} (nM)
3-2e	7.7	10 min	7,500 ± 400	30,000 ± 3,000
		30 min	15,000 ± 6,000	20,000 ± 10,000
		68 min	4,700 ± 2,000	60,000 ± 40,000
		22 h	8,500 ± 300	20,000 ± 10,000
	5.5	10 min	17,000 ± 900	40,000 ± 9,000
		20 h	14,900 ± 900	20,000 ± 3,000

*Oxime kept at this pH and then added to the enzyme at pH 7.7

The data in Tables 3-19 and 3-20 show that oximes **3-2d**, **3-2e**, and **3-2f** do not hydrolyze to any appreciable extent over up to 20 h at pH 7.7 or pH 5.5. Therefore simple aqueous hydrolysis of **3-2d** to the TFK **2-9d** cannot account for the mosquito toxicity of **3-2d**. In

addition, ^{19}F NMR spectroscopy was used to monitor whether hydrolysis was occuring. In a mixture of DMSO and H_2O, ^{19}F NMR spectra were taken from 1 h to 24 h and the intregral ratios to added TFA were noted. In the DMSO:H_2O mixture, the ratio of peaks observed at -65 ppm and -74.5 ppm showed no change after 1 day (Figure 3-5). Had hydrolysis to the TFK (**2-9e**) occurred, a new peak at -78 ppm would have emerged. When H_2O was replaced 1N HCl, the pH effectively became between 0-1, which was expected to accelerate hydrolysis. However, no evidence of hydrolysis was observed up to 24 h (Figure 3-6). Could the transformation of **3-2d** to **2-9d** in vivo be promoted by an enzyme? We have described above in Scheme 3-2 how Cyp450 can oxidatively convert an oxime to the corresponding ketone. However, one critical observation suggests such a process is not occuring in *An. gambiae*. A filter paper assay of **3-2d** against Akron mosquitoes showed a LC_{50} of 114 µg/mL compared with 106 µg/mL for wild type mosquitoes. As is shown in Table 2-1, **2-9d** is a very poor inhibitor of G119S *Ag*AChE (IC_{50} = >10,000, Table 2-1) and it would be very difficult to achieve such high concentrations of **2-9d**. It is reasonable to conclude that **3-2d** is acting on another site, and is not toxic due to AChE inhibition.

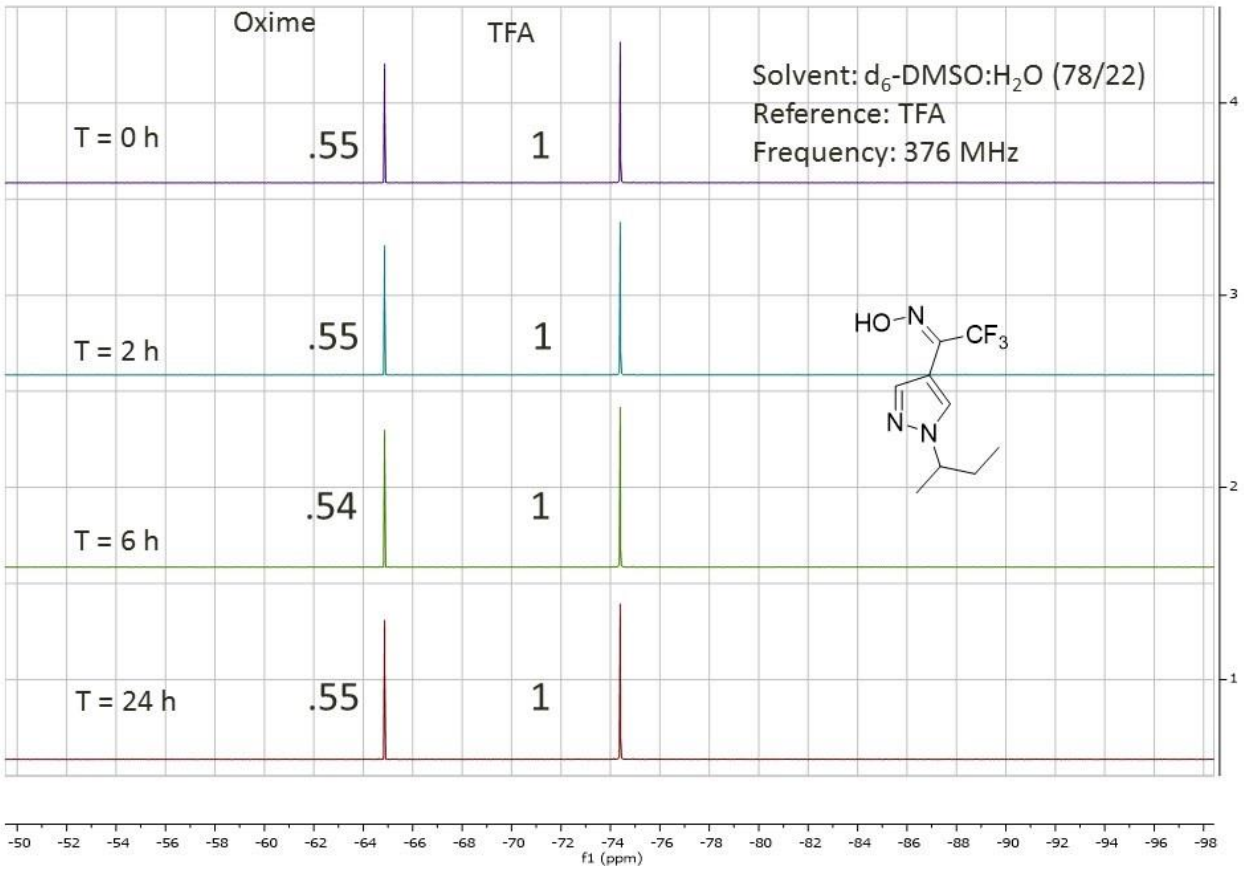

Figure 3-5: Oxime **3-2e** was monitored in d_6-DMSO:H_2O using ^{19}F NMR to determine if hydrolysis was occuring. TFA (1.8 equiv) was used as an internal reference.

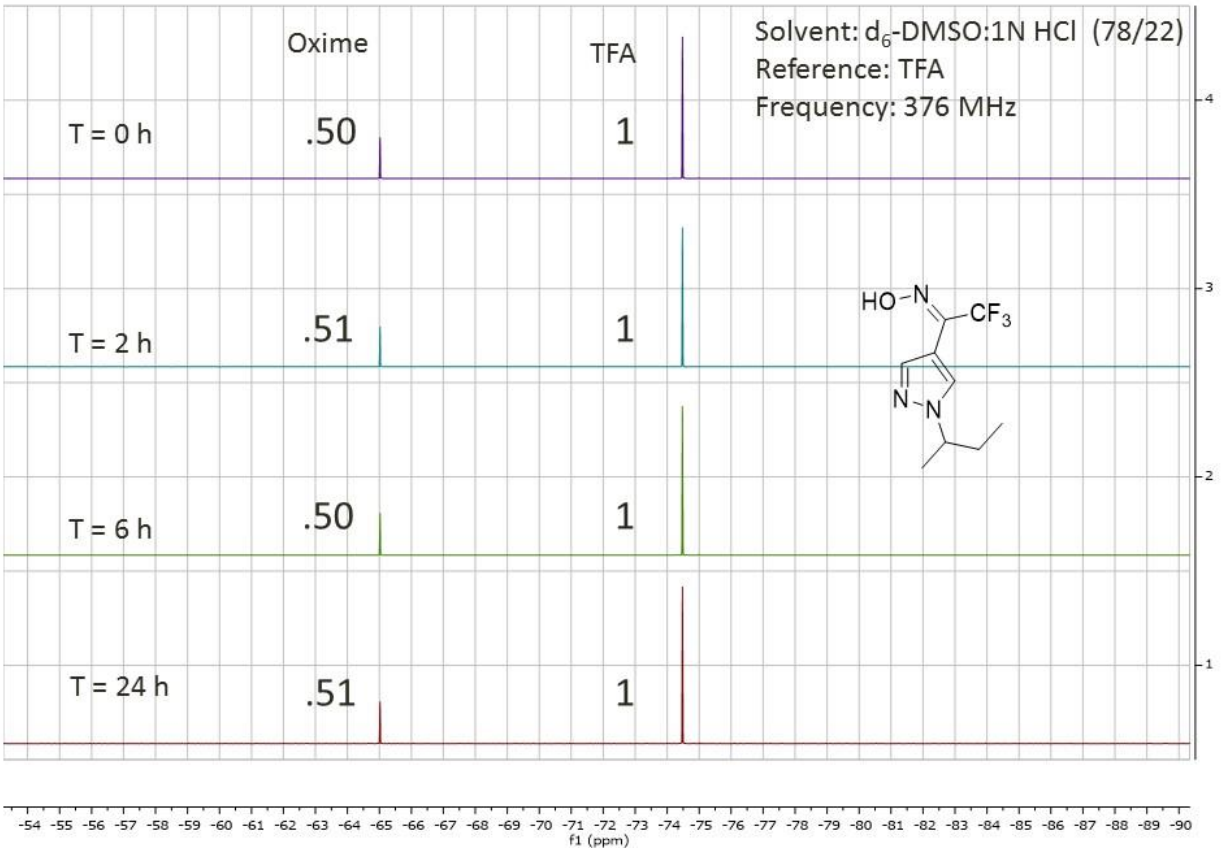

Figure 3-6: Oxime **3-2e** was monitored in d_6-DMSO:1N HCl using ^{19}F NMR to determine if hydrolysis was occuring. TFA (2.0 equiv) was used as an internal reference

3.7 Conclusion and future directions

As detailed in Chapter 2, trifluoromethyl ketones and difluoromethyl ketones provide very potent inhibition of *Ag*AChE. However, the toxicity of these compounds proved very low, which we attribute in part to high volatility and evaporation of the compounds from the treated papers before the mosquitoes had a chance to be exposed. In this chapter we prepared oximes, oxime methyl ethers, and oxime benzyl ethers of these fluorinated methyl ketones. This strategy was successful in generating more toxic compounds. Trifluoromethyl ketone oxime **3-2d** was

the most toxic to G3 strain *An. gambiae*. The LC_{50} of this compound was 106 (81-152) µg/mL, a value only 3-fold higher than that of propoxur. Other compounds showing significant toxicity were TFK oxime **3-2e** (LC_{50} = 531 (410-670) µg/mL), MFK oxime **3-4f** (LC_{50} = 204 (125-347) µg/mL), and TFK oxime methyl ether **3-5b** (LC_{50} = 485 (366-689) µg/mL). *In vitro* studies on **3-2d** and **3-2e** strongly suggest that they do not kill *Anopheles gambiae* through an AChE inhibition mechanism. Yet there are many other known mechanisms of insecticidal action. The Insecticide Resistance Action Committee has developed a listing to serve as an essential tool for the development of insecticide resistance management strategies; they are classified into one of many groups based on their mode of action (IRAC MoA) and on what physiological function they affect.[17] For example, AChE inhibitors such as carbamates and organophosphates are classified into group 1 which affect nerves and muscles. Other classes of insecticides that affect the nerve and muscle include: GABA-gated chloride channel antagonists (IRAC MoA 2), sodium channel modulators (IRAC MoA 3), and ryanodine receptor modulators (IRAC MoA 28). Other broad categories that need to be considered for toxicity to adult *Anopheles gambiae* are insecticides that affect respiration, such as uncouplers of oxidative phosphorylation (IRAC MoA 13).

An investigation into the literature was performed to to see if **3-2d** resembled any known insecticides. The pyrazole oxime portion of **3-2d** bears a strong resemblance to fenpyroximate (**3-14**), which is a pyrazole oxime ether (Figure 3-7). Fenpyroximate is a miticide[18] and it is believe to act by inhibition of mitochondrial complex I electron transport (IRAC MOA 21)[19]. Recently oxime-containing analogs of tebufenpyrad (e.g. **3-15**) were found to have larvicidal activity against the mosquito *Culex pipiens pallens*. The Bloomquist group thus tested **3-2d** in a mitochondrial respiration assay in *An. gambiae* Sua1B cells, using fenpyroximate and rotenone

as positive controls. The basis of this assay is to use a fluorescence probe to detect oxygen consumption by the cells. In the closed system of the assay, living cells cause the oxygen level to decrease (Mitoxpress Xtra-oxygen consumption assay kit, Luxel Biosciences). The decrease in O_2 concentration causes greater fluoresence of the probe molecule. As can be seen, the fluorescence values increase with respect to time for DMSO, the negative control. Fluorescence values for **3-2d** parallel that of DMSO suggesting normal mintochondrial respiration. In contrast, known mitochondrial respiration inhibitors rotenone and fenpyroximate stop any growth of the fluorescence signal. Thus we conclude **3-2d** does not kill *An. gambiae* by inhibiting mitochondrial respiration.

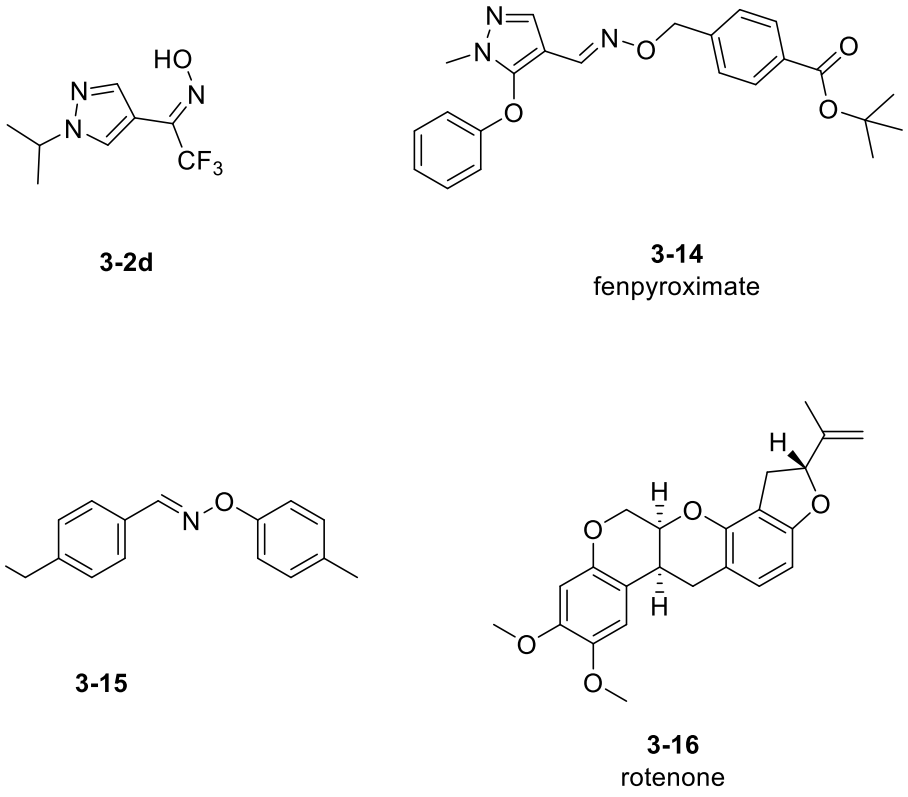

Figure 3-7: Compound **3-2d** resembles both fenpyroximate (**3-14**) and **3-15**, both known for inhibiting mitochondrial complex I electron transport. Rotenone (**3-16**) is also a commercial mitochondrial complex I electrontron transport inhibitor.

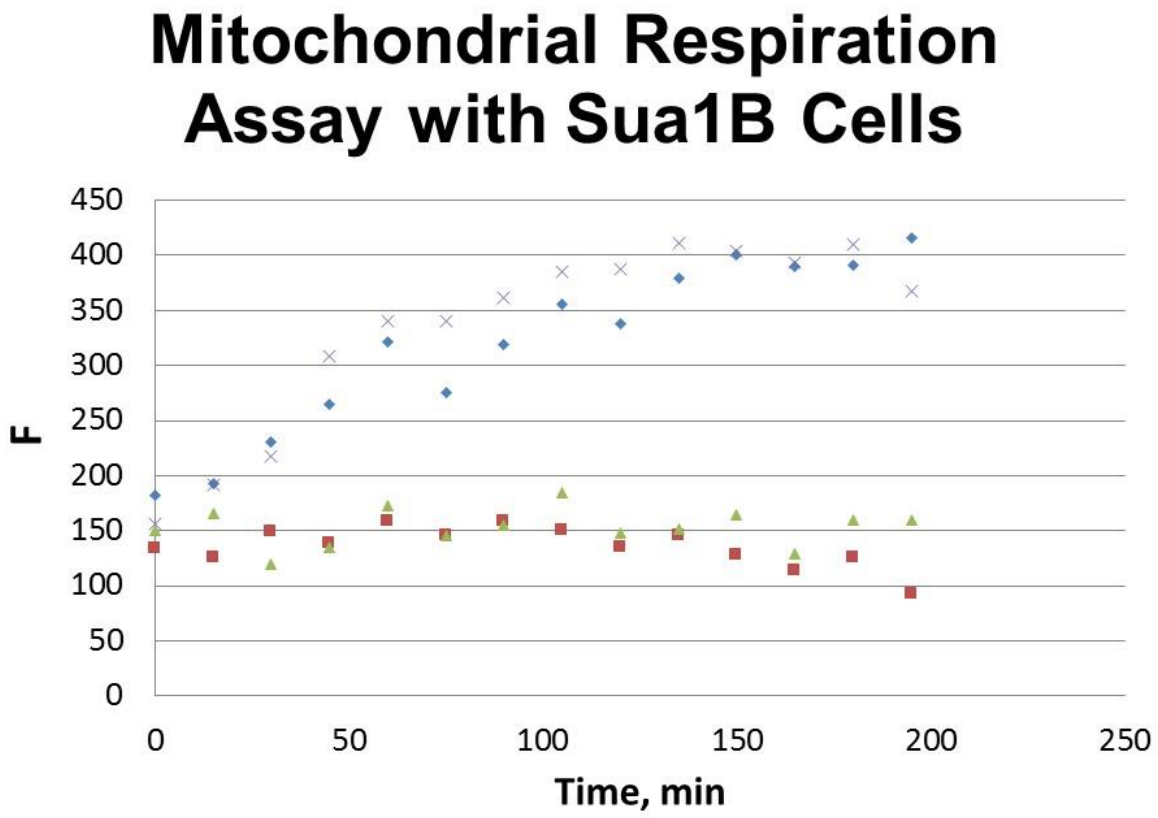

Figure 3-8: A mitochondrial respiration assay with *An. gambiae* Sua1B cells. DMSO is desginated in blue diamonds, rotenone is desinated in red squares, fenpyroximate is designated in green triangles, and **3-2d** is designated in purple x's. All compounds were tested at 100 µM.

The closest structural analogs for **3-2d** that we could find in the literature were the herbicide safeners fluoxfenim and oxabetrinil (Figure 3-9).[20] Herbicide safeners are used in agriculture to reduce the effect of the herbicide on crop plants to improve selectivity to target unwanted weeds. The literature suggests that fluxofenim acts by inducing glutathione-S-transferase in the plant, but it is unknown as to how this mechanism would prove toxic to

Anopheles gambiae. Another close analog was found in flucycloxuron[21], which is an insect growth regulator (inhibitor of chitin biosynthesis, type 0, IRAC MOA 15). A number of oxime ether and oxime ester analogs of flucycloxuron have been prepared and tested as larvicides. [22] Inhibition of chitin biosynthesis hinders formation of the insect exoskeleton and kills juveniles. But it is unclear as to how inhibition of chitin biosynthesis will prove to be toxic to adult mosquitoes, whose exoskeleton is already formed.

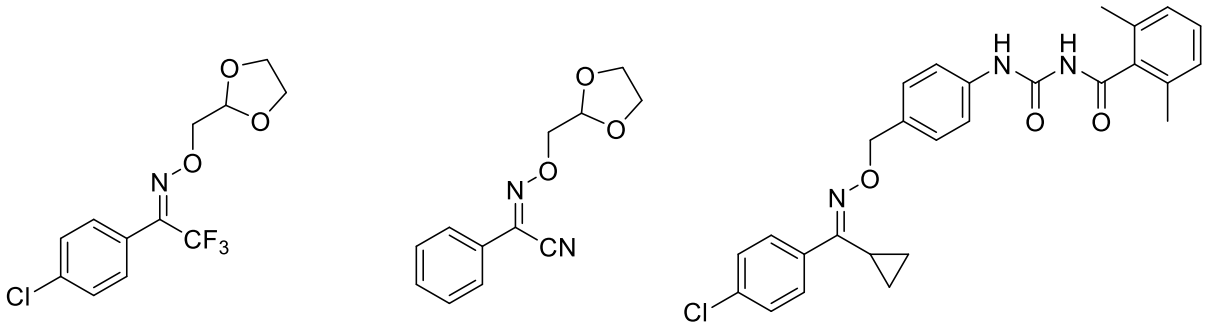

3-17
Fluxofenim

3-18
Oxabetrinil

3-19
Flucycloxuron

Figure 3-9: The mechanism of action of oximes towards *Anopheles gambiae* is unknown. It may act in a similar fashion as to fluxofenim (**3-17**) or oxabetrinil (**3-18**), both of which are herbicide safeners which work by inducing glutathione-S-transferase in the plant. An additional hypothesis is that it acts as an insect growth regulator (**3-19**).

Further searching in the literature led to the possibility that **3-2d** may act at the muscarinic acetylcholine receptor (*m*AChR). *m*AChR antagonists have been explored as insecticides previously[23], and several muscarinic agonists have oxime ether functional groups present in the molecule (**3-20** to **3-23**, Figure 3-10).[23-25] The very specific SAR we have observed with fluorinated methyl ketone oxime and oxime ethers is hard to rationalize in terms of receptor antagonism. However, the structural requirements for the receptor agonism can be exceedingly

specific. Is **3-2d** an agonist of the *m*AChR? This hypothesis was evaluated in the following way. A control experiment was run with pilocarpine, a known muscarinic agonist, and atropine, a known muscarinic antagonist; mortality was recorded following injection into *An. gambiae*. A 50 ng dose of the *m*AChR agonist pilocarpine caused 65% mortality and a 5 ng dose of the mAChR antagonist atropine caused 15% mortality (Figure 3-11). When both atropine and pilocarpine were injected together at these doses, the mortality dropped to 30%, consistent with the idea that atropine could antagonize the toxicity caused by a large dose of pilocarpine. When 50 ng of **3-2d** was injected, the mortality recorded was approximately 35%. However, when both **3-2d** and atropine were co-injected, the toxicity of **3-2d** was not reduced. The failure of atropine to reduce the toxicity of **3-2d** suggests that **3-2d** is not toxic due to agonism of the *m*AChR.

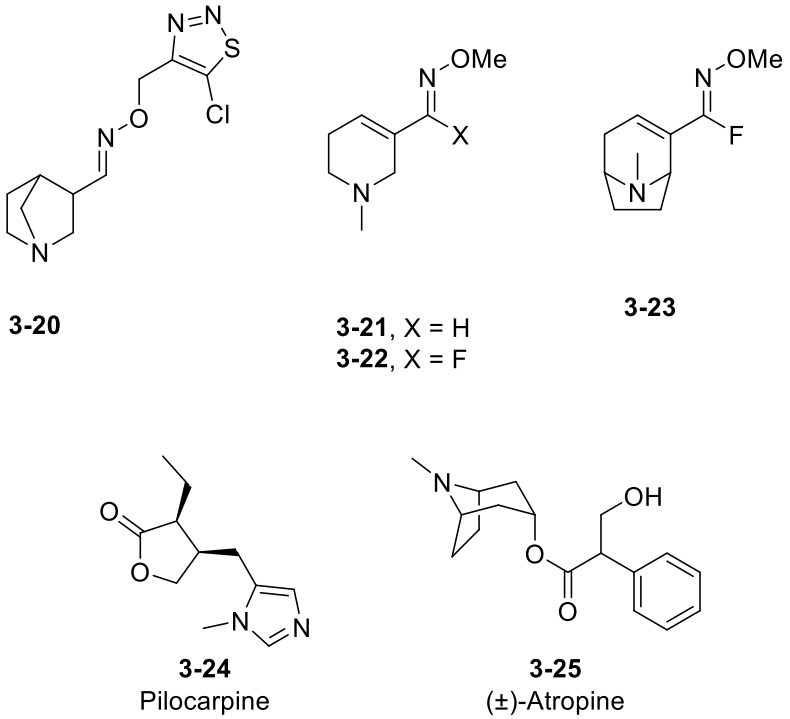

3-20

3-21, X = H
3-22, X = F

3-23

3-24
Pilocarpine

3-25
(±)-Atropine

Figure 3-10: Oxime ether-containg muscarinic agonist **3-20** to **3-23**, muscarinic agonist pilocarpine (**3-24**) and muscarinic antagonist atropine (**3-25**).

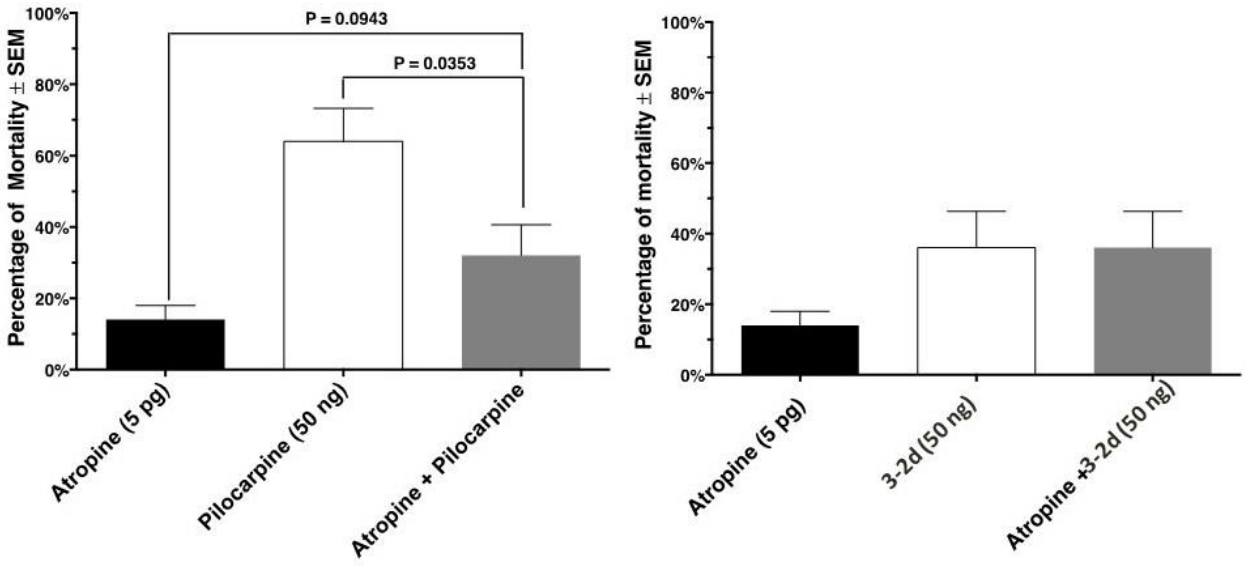

Figure 3-11: To test whether **3-2d** is a muscarinic agonist, a test was performed with a muscarinic antagonist and mortality was recorded.

In summary, incorporation of an oxime group into fluoromethyl ketones proved successful as toxicity increased significantly; the most toxic compound was **3-2d** with an LD_{50} of 106 μg/mL. Since that point, attempts to further increase toxicty of these ketones has not been successful. In addition, the mechanism of action is still unclear. While an initial literature searching led to several possible mechanism of actions (e.g. mitochondrial complex I electron transport inhibitor and *m*AChR agonist), experiments in the Bloomquist group ruled out these possibilites. Further efforts will be directed towards elucidation of a mechansim of action for **3-2d** in addition to continued efforts to increase toxicity by further derivatizing **3-2d**.

3.8 References

1. Nair, H. K.; Lee, K.; Quinn, D. M., *m*-(*N*,*N*,*N*-Trimethylammonio)trifluoroacetophenone - a femtomolar inhibitor of acetylcholinesterase. *J. Am. Chem. Soc.* **1993,** *115*, 9939-9941.

2. Harel, M.; Quinn, D. M.; Nair, H. K.; Silman, I.; Sussman, J. L., The X-ray structure of a transition state analog complex reveals the molecular origins of the catalytic power and substrate specificity of acetylcholinesterase. *J. Am. Chem. Soc.* **1996,** *118*, 2340-2346.

3. Venhuis, B. J.; Dijkstra, D.; Wustrow, D.; Meltzer, L. T.; Wise, L. D.; Johnson, S. J.; Wikstrom, H. V., Orally active oxime derivatives of the dopaminergic prodrug 6-(N,N-Di-*n*-propylamino)-3,4,5,6,7,8-hexahydro-2*H*-naphthalen-1-one. Synthesis and pharmacological activity. *J. Med. Chem.* **2003,** *46*, 4136-4140.

4. Kumpulainen, H.; Mahonen, N.; Laitinen, M. L.; Jaurakkajarvi, M.; Raunio, H.; Juvonen, R. O.; Vepsalainen, J.; Jarvinen, T.; Rautio, J., Evaluation of hydroxyimine as cytochrome P450-selective prodrug structure. *J. Med. Chem.* **2006,** *49*, 1207-1211.

5. Rautio, J.; Kumpulainen, H.; Heimbach, T.; Oliyai, R.; Oh, D.; Jarvinen, T.; Savolainen, J., Prodrugs: design and clinical applications. *Nat. Rev. Drug Discov.* **2008,** *7*, 255-270.

6. Jousserandot, A.; Boucher, J. L.; Henry, Y.; Niklaus, B.; Clement, B.; Mansuy, D., Microsomal cytochrome P450 dependent oxidation of N-hydroxyguanidines, amidoximes, and ketoximes: Mechanism of the oxidative cleavage of their C=N(OH) bond with formation of nitrogen oxides. *Biochemistry* **1998,** *37*, 17179-17191.

7. Savarin, C. G.; Grise, C.; Murry, J. A.; Reamer, R. A.; Hughes, D. L., Novel intramolecular reactivity of oximes: Synthesis of cyclic and spiro-fused imines. *Org. Lett.* **2007,** *9*, 981-983.

8. Levrat, F.; Stoeckli-Evans, H.; Engel, N., Enantiomeric excess determination of α-amino acids by 19F NMR spectroscopy of their N,N-dimethyl-(2,2,2-trifluoro-1-phenylethyl)amine-C,N)palladium complexes. *Tetrahedron: Asymmetry* **2002,** *13*, 2335-2344.

9. Champagne, P. A. D., Justine; Paquin, Jean-Francois, Organic Fluorine as a Hydrogen-Bond Acceptor: Recent Examples and Applications. *Synthesis* **2014,** *47*, 306-322.

10. Guidelines for testing mosquito adulticides for indoor residual spraying and treatment of mosquito nets Available at WHO/CDS/NTD/WHOPES/GCDPP/2006.3 World Health Organization, Geneva. **2006**. (accessed Jan 15)

11. Hartsel, J. A.; Wong, D. M.; Mutunga, J. M.; Ma, M.; Anderson, T. D.; Wysinski, A.; Islam, R.; Wong, E. A.; Paulson, S. L.; Li, J. Y.; Lam, P. C. H.; Totrov, M. M.; Bloomquist, J. R.; Carlier, P. R., Re-engineering aryl methylcarbamates to confer high selectivity for inhibition of *Anopheles gambiae* versus human acetylcholinesterase. *Bioorg. Med. Chem. Lett.* **2012**, 22, 4593-4598.

12. Hagman, W. K. The many roles for fluorine in medicinal chemistry. *J. Med. Chem.* **2008,** *51*, 4359-4369.

13. EPA Toxicity Categories Available at http://www.sporicidin.com/media/literature/spo003_epa%20toxicity%20categories.pdf.

14. Pridgeon, J. W.; Pereira, R. M.; Becnel, J. J.; Allan, S. A.; Clark, G. G.; Linthicum, K. J., Susceptibility of Aedes aegypti, Culex quinquefasciatus say, and Anopheles quadrimaculatus say to 19 pesticides with different modes of action. *J. Med. Entomol.* **2008,** *45*, 82-87.

15. Swale, D. R.; Tong, F.; Temeyer, K. B.; Li, A.; Lam, P. C. H.; Totrov, M. M.; Carlier, P. R.; de Leon, A. A. P.; Bloomquist, J. R., Inhibitor profile of bis(n)-tacrines and N-

methylcarbamates on acetylcholinesterase from *Rhipicephalus (Boophilus) microplus* and *Phlebotomus papatasi*. *Pest. Biochem. Physiol.* **2013,** *106*, 85-92.

16. Kalia, J.; Raines, R. T., Hydrolytic stability of hydrazones and oximes. *Angew. Chem. Int. Ed.* **2008,** *47*, 7523-7526.

17. Modes of Action, available at: http://www.irac-online.org/modes-of-action/. (accessed 3/30/15).

18. Hamaguchi, H.; Kajihara, O.; Katoh, M., Development of a new acaricide, fenpyroximate. *J. Pestic. Sci.* **1995,** *20*, 173-175.

19. Shiraishi, Y.; Murai, M.; Sakiyama, N.; Ifuku, K.; Miyoshi, H., Fenpyroximate binds to the interface between PSST and 49 kDa subunits in mitochondrial NAD*H*-ubiquinone oxidoreductase. *Biochemistry* **2012,** *51*, 1953-1963.

20. Scarponi, L.; Quagliarini, E.; Del Buono, D., Induction of wheat and maize glutathione S-transferase by some herbicide safeners and their effect on enzyme activity against butachlor and terbuthylazine. *Pest Manag. Sci.* **2006,** *62*, 927-932.

21. Grosscurt, A. C.; Terhaar, M.; Jongsma, B.; Stoker, A., P*H*-70-23 - A new acaricide and insecticide interfering with chitin deposition. *Pestic. Sci.* **1988,** *22*, 51-59.

22. Sun, R. F.; Li, Y. Q.; Lu, M. Y.; Xiong, L. X.; Wang, Q. M., Synthesis, larvicidal activity, and SAR studies of new benzoylphenylureas containing oxime ether and oxime ester group. *Bioorg. Med. Chem. Lett.* **2010,** *20*, 4693-4699.

23. Honda, H.; Tomizawa, M.; Casida, J. E., Insect muscarinic acetylcholine receptor: Pharmacological and toxicological profiles of antagonists and agonists. *J. Agric. Food Chem.* **2007,** *55*, 2276-2281.

24. Dick, M. R.; Dripps, J. E.; Orr, N., Muscarinic agonists as insecticides and acaricides. *Pestic. Sci.* **1997,** *49,* 268-276.

25. Benting, J.; Leonhardt, M.; Lindell, S. D.; Tiebes, J., The design, synthesis and screening of a muscarinic acetylcholine receptor targeted compound library. *Comb. Chem. High Throughput Screening* **2005,** *8,* 649-653.

Chapter 4: Experimental

4.1 General

NMR spectra were performed on a Varian Inova-400 (400 MHz) or a JEOL EclipsePlus-500 (500 MHz). ^{13}C NMR spectra were correspondingly recorded at 101 MHz or 126 MHz. ^{19}F NMR spectra were correspondingly recorded at 376 MHz or 471 MHz. Chemical shifts for ^{1}H and ^{13}C are presented in ppm against tetramethylsilane with an internal standard as a reference and ^{19}F NMR used hexafluorobenzene as a reference. Deuterated solvents were purchased from Cambridge Isotope Laboratories. The following abbreviations are used to show coupling in the spectra: s (singlet), d (doublet), t (triplet), q (quartet), p (pentet), h (sextet), hept (heptet), nonet (n), and m (multiplet). High resolution mass spectroscopy (HRMS) was performed on an Agilent 6220 LC/MS time-of-flight mass spectrometer using either electrospray ionization (ESI) or extracted ion chromatogram (EIC). Column chromatography was performed by using flash grade silica gel (SiO_2, 32-63μm). Thin layer chromatography (TLC) was performed on EMD silica gel 60 F_{254} plates. Compounds prepared for enzyme or mosquito bioassay were >95% pure as judged by ^{1}H, ^{13}C and ^{19}F NMR.

Note that TFKs **2-9b-f** and **h**, TFK oximes **3-2b-f** and **h**, TFK methyl oxime ethers **3-5b-h**, and **3-8b-h** do not appear in this section because they have been previously characterized.

4.1.1 General procedures for the synthesis of 4-bromo-*N*-alkylpyrazoles

Method A. Adapted from the procedure by Moslin *et al*. and Chen *et al*.:[1-2] To a solution of sodium hydride (60% dispersion in mineral oil, 1.3 eq) in DMF, a solution of pyrazole (1 eq) in DMF was added drop-wise. The solution was then warmed to room temperature for 2 hours to

which the neat bromoalkane (1.5 eq) was then added drop-wise and stirred for overnight. The resulting mixture was extracted with ether (40-100 mL)and brine (40-50 mL) and dried with $MgSO_4$. The ether layer was concentrated *in vacuo* to furnish the residue. The residue was mixed in water and NBS (1 eq) was added. TLC was used to detect progression of reaction. After 2 hours, the mixture was extracted with DCM and dried with $MgSO_4$, filtered and concentrated *in vacuo*. The residue was purified using flash chromatography on silica gel using a gradient from 5-20% ethyl acetate in hexane, to yield the 4-bromo-N-alkyl pyrazole (**2-7d-f, h**).[1-2]

Method B: Pyrazole was added to a solution of H_2O at room temperature until dissolved. NBS (1 eq) was added slowly to the solution and after 5-15 minutes a white solid began to precipitate. Filtration of the solution afforded 4-bromopyrazole as a yellow solid. To a suspension of NaH (60% dispersion in mineral oil 1.3 eq) in DMF, a solution of 4-bromopyrazole (1 eq) in DMF was added drop-wise at 0 ˚C. The solution was then warmed to room temperature for 2 hours to which the corresponding alkyl bromide (1.5 eq) was then added drop-wise and stirred for overnight. The resulting mixture was extracted with ether (40-100 mL)and brine (40-50 mL) and dried with $MgSO_4$, filtered and concentrated *in vacuo*. The residue was purified using flash chromatography on silica gel using a gradient from 5-20% ethyl acetate in hexane, to yield the 4-bromo-N-alkyl pyrazole (**2-7g, i-r**).

4.1.2 General procedure for the formation of the fluorinated methyl ketones

Method C

A standard literature procedure for TFK synthesis was followed.[3] The 4-bromo-N-alkylpyrazole (1 eq) was dissolved in dry THF at -78 ^{o}C under nitrogen and was stirred for 30 min. *n*-BuLi (1.05 eq) was added drop-wise and the solution was stirred for 2 h at -78 ^{o}C. After two hours, methyl trifluoroacetate (1.2 eq) was added drop-wise and stirred for 30 min at -78 ^{o}C. The solution was then allowed to warm up to room temperature and allowed to stir overnight. The mixture was then quenched with NH_4Cl (10-20 mL) and extracted with ether (40-100 mL), and dried over $MgSO_4$. After concentration *in vacuo* (note: remove shortly after the ether is removed, because the compound is quite volatile), the residue was purified with flash chromatography over silica gel using a gradient of 1-10% ethyl acetate/hexane or 1-10% ether/hexane to yield the TFK (**2-9g-r**).

Method D

A modified literature procedure for DFK synthesis was followed.[3] The 4-bromo-N-alkylpyrazole (1 eq) was dissolved in dry THF at -78 ^{o}C under nitrogen and was stirred for 30 min. *n*-BuLi (1.05 eq) was added drop-wise and the solution was stirred for 2 h at -78 ^{o}C. After two hours, methyl difluoroacetate (1.2 eq) was added drop-wise and stirred for 5 min at -78 ^{o}C. The mixture was then quenched with NH_4Cl (5-10mL) and then allowed to warm up to room temperature and stirred for 30 minutes. The mixture was then extracted with ether (40-100 mL) and dried over $MgSO_4$, filtered, and concentrated *in vacuo*. After concentration *in vacuo* (note: remove shortly after the ether is removed, because the compound is quite volatile), the residue

was purified with flash chromatography over silica gel using a gradient of 1-10% ethyl acetate/hexane or 20-50% DCM/hexane to yield the DFK (**2-10c-r**).

Method E

A modified literature procedure for MFK synthesis was followed.[3] The 4-bromo-N-alkylpyrazole (1 eq) was dissolved in dry THF at -78 ^{o}C under nitrogen and was stirred for 30 min. *n*-BuLi (1.05 eq) was added drop-wise and the solution was stirred for 2 h at -78 ^{o}C. After two hours, ethyl fluoroacetate (1.2 eq) was added drop-wise and stirred for 1 min at -78 ^{o}C. The mixture was then quenched with NH_4Cl (5-10 mL) and then allowed to warm up to room temperature and let stir for 30 minutes. The mixture was then extracted with ether (40-100 mL) and dried over $MgSO_4$, filtered, and concentrated *in vacuo*. After concentration *in vacuo*, the residue was purified with flash chromatography over silica gel using a gradient of 1-10% ethyl acetate/hexane or 20-50% DCM/hexane to yield the DFK (**2-11c-r**).

4.1.3 General procedure for the oxime and oxime ether formation

Method F

Fluorinated methyl ketone (1.0 eq), $NH_2OR{\cdot}HCl$ (1.4 eq), and NaOAc (1.35 eq)were combined in H_2O (2-10 mL). EtOH (2-10 mL) was added to produce a homogenous mixture. The resulting solution was heated to 80 ^{o}C for 14 hours. The solution was allowed to cool to room temperature at which point a solid precipitate began to form. The precipitate was collected by filtration and washed with cold water. The aqueous filtrate was extracted with DCM (40-100 mL), dried with $MgSO_4$, and concentrated *in vacuo* to yield more crystals: If TLC analysis

confirmed the identity of this material with the first crop of crystals, both crops were combined to give the oxime **(3-2g, i-r**).

Method G

A solution of fluorinated methyl ketone (1.0 eq), $NH_2OR{\cdot}HCl$ (1.4-2 eq), and NaOAc (1.35-2 eq), were mixed in EtOH. The resulting solution was heated to reflux overnight. The solution was allowed to cool to room temperature and concentrated in vacuo. The residue was extracted with ethyl acetate (40-100 mL) and dried with $MgSO_4$. The ethyl acetate layer was concentrated *in vacuo* and the residue was purified using column chromatography to furnish the oxime/oxime ether (**3-5d-r, 3-6d-j, 3-7d-g, 3-8d-p, 3-9d-j,** and **3-10d-p**).

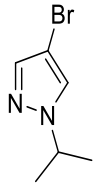

4-bromo-1-isopropyl-1*H*-pyrazole (2-7d): Prepared using the general procedure above (*Method A*) from pyrazole (1.0g, 14.7 mmol), 2-bromopropane (2.1 mL, 22.0 mmol), NaH (60% dispersion in mineral oil, 0.76 g 19.1 mmol), NBS (2.6 g, 17.5 mmol), H_2O (20mL), and DMF (8 mL). Concentration of the reaction mixture *in vacuo* followed by silica gel chromatography (20% ethyl acetate in hexanes) gave the product as a clear liquid (1.34 g, 49%). ^{1}H NMR (500 MHz, $CDCl_3$) δ 8.26 (s, 1H), 8.07 (s, 1H), 4.55 (hept, J = 6.7 Hz, 1H), 1.62 (d, J = 6.7 Hz, 6H); ^{13}C NMR (126 MHz, $CDCl_3$) δ 140.5, 130.4, 119.9, 63.9, 22.8. This compound has been previously reported.[4] (**EXC-I-52**)

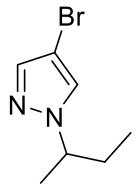

4-bromo-1-(sec-butyl)-1*H*-pyrazole (2-7e): Prepared using the general procedure above (*Method A*) from pyrazole (1.0g, 14.7 mmol), 2-bromobutane (2.1 mL, 22.1 mmol), NaH (60% dispersion in mineral oil, 0.73g 19.1 mmol), NBS (3.12 g, 17.5 mmol), H_2O (20 mL) and DMF (8 mL). Concentration of the reaction mixture *in vacuo* followed by silica gel chromatography (20% ethyl acetate in hexanes) gave the product as a clear liquid (1.6 g, 45%). ^{1}H NMR (500 MHz, $CDCl_3$) δ 8.26 (s, 1H), 8.07 (s, 1H), 4.20 (h, *J* = 6.7 Hz, 1H), 1.94-1.81 (m, 1H), 1.80-1.70 (m, 1H), 1.52 (d, *J* = 6.8 Hz, 3H), 0.84 (t, *J* = 6.9 Hz, 3H); ^{13}C NMR (101 MHz, $CDCl_3$) δ 140.7, 131.4, 113.6, 61.0, 29.5, 20.4, 10.3. This compound has been previously reported.[4] (**EXC-I-50**)

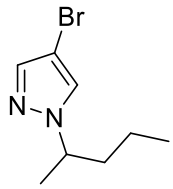

4-bromo-1-(pentan-2-yl)-1*H*-pyrazole (2-7f): Prepared using the general procedure above (*Method A*) from pyrazole (2.0 g, 29.2 mmol), 2-bromopentane (5.5 mL, 44.1 mmol), NaH (60% dispersion in mineral oil, 1.5 g 38.2 mmol), NBS (5.2 g, 29.2 mmol), H_2O (20 mL) and DMF (8 mL). Concentration of the reaction mixture *in vacuo* followed by silica gel chromatography (20% ethyl acetate in hexanes) gave the product as a clear liquid (3.5 g, 55%). ^{1}H NMR (500 MHz, $CDCl_3$) δ 8.27 (s, 1H), 8.07 (s, *1*H), 4.39 (h, *J* = 7.5 Hz, 1H), 1.97-1.90 (m, 1H), 1.79-1.72 (m, 1H), 1.54 (d, *J* = 7.5 Hz, 3H), 1.33 – 1.11 (m, 2H), 0.92 (t, *J* = 7.5 Hz, 3H); ^{13}C NMR (126

MHz, $CDCl_3$) δ 140.5, 139.6, 130.3, 59.0, 38.4, 20.9, 19.2, 13.6. This compound has been previously reported.[5] (**EXC-I-84**)

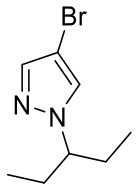

4-bromo-1-(pentan-3-yl)-1*H*-pyrazole (2-7g): Prepared using the general procedure above (*Method B*) from 4-bromopyrazole (1.08 g, 7.35 mmol), 3-bromopentane (1.37 mL, 11.0 mmol), NaH (0.38 mg, 9.55 mmol), and DMF (12 mL). Concentration of the reaction mixture *in vacuo* followed by silica gel chromatography (10% ethyl acetate in hexanes) gave the product as a clear liquid (1.56 g, 97%). ^{1}H NMR (500 MHz, $CDCl_3$) δ 7.47 (s, 1H), 7.38 (s, 1H), 3.87 (tt, *J* = 9.2, 4.9 Hz, 1H), 1.96 – 1.71 (m, 4H), 0.77 (t, *J* = 7.4 Hz, 6H). ^{13}C NMR (101 MHz, $CDCl_3$) δ 139.5, 129.0, 92.5, 70.6, 27.7, 11.2. This compound has been previously reported.[5] (**EXC-II-42**)

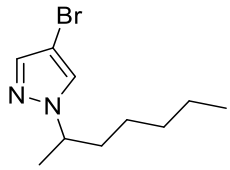

4-bromo-1-(heptan-2-yl)-1*H*-pyrazole (2-7i): Prepared using the general procedure above (*Method B*) from 4-bromopyrazole (1.08 g, 7.35 mmol), 2-bromoheptane (3.5 mL, 11.0 mmol), NaH (0.38 mg, 9.55 mmol), and DMF (12 mL). Concentration of the reaction mixture *in vacuo* followed by silica gel chromatography (10% ethyl acetate in hexanes) gave the product as a clear liquid (1.56 g, 95%). ^{1}H NMR (400 MHz, $CDCl_3$) δ 7.45 (s, 1H), 7.39 (s, 1H), 4.26 (h, *J* = 6.1 Hz, 1H), 1.95 – 1.78 (m, 2H), 1.76 – 1.63 (m, 2H), 1.46 (d, *J* = 6.7 Hz, 3H), 1.35 – 1.19 (m, 4H), 0.92 – 0.80 (m, 3H). ^{13}C NMR (101 MHz, $CDCl_3$) δ 139.0, 127.3, 110.0, 51.9, 41.1, 31.1, 27.4, 26.4, 22.5, 14.0. (**EXC-II-14**)

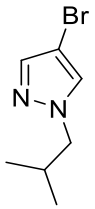

4-**bromo-1-(isobutyl)-1*H*-pyrazole(2-7j):** Prepared using the general procedure above (*Method B*) from 4-bromopyrazole (1.08 g, 7.35 mmol), 1-bromo-2-methylpropane (3.5 mL, 11.0 mmol), NaH (0.38 mg, 9.55 mmol), and DMF (12 mL). Concentration of the reaction mixture *in vacuo* followed by silica gel chromatography (10% ethyl acetate in hexanes) gave the product as a clear liquid (1.56 g, 95%). ^{1}H NMR (400 MHz, $CDCl_3$) δ 7.44 (s, 1H), 7.36 (s, 1H), 3.87 (d, *J* = 7.0 Hz, 2H), 2.24 – 2.10 (n, *J* = 7.0 Hz, 1H), 0.90 (d, *J* = 7.0 Hz, 6H). ^{13}C NMR (101 MHz, $CDCl_3$) δ 139.5, 129.5, 92.5, 60.3, 29.6, 19.8. This compound has been previously reported.[6] (**EXC-II-56**)

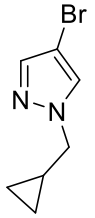

4-bromo-1-(cyclopropylmethyl)-1*H*-pyrazole: Prepared using the general procedure above (*Method B*) from 4-bromopyrazole (500 mg, 3.4 mmol), (bromomethyl)cyclopropane (0.49 mL, 5.1 mmol), NaH (0.18 mg, 4.4 mmol), and DMF (7 mL). Concentration of the reaction mixture *in vacuo* followed by silica gel chromatography (10% ethyl acetate in hexanes) gave the product as a clear liquid (1.56 g, 95%). ^{1}H NMR (400 MHz, $CDCl_3$) δ 7.50 (s, 1H), 7.43 (s, 1H), 3.94 (d, *J* = 7.2 Hz, 2H), 1.34 – 1.16 (m, 1H), 0.65 (q, *J* = 7.0 Hz, 2H), 0.35 (d, *J* = 5.8 Hz, 2H). ^{13}C NMR (101 MHz, $CDCl_3$) δ 140.5, 130.4, 93.4, 60.3, 4.7, 3.8. (**EXC-II-122**)

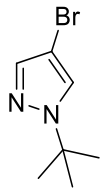

4-bromo-1-(*tert*-butyl)-1*H*-pyrazole (2-7m): A solution of tetramethoxypropane (0.66 mL, 4.00 mmol), *tert*-butylhydrazine hydrochloride (500 mg, 4.00 mmol), concentrated HCl (0.5 mL) and EtOH (8 mL) were refluxed overnight. Upon cooling, the mixture was washed with water and ether. The resulting organic layer was then washed with brine and dried with $MgSO_4$. The residue was mixed in water (10 mL) and NBS (575 mg, 3.23 mmol) was added. TLC was used to detect progression of reaction. After 2 hours, the mixture was extracted with DCM (50 mL) and dried with $MgSO_4$. The residue was purified using flash chromatography on silica gel (5 % ethyl acetate in hexanes) gave the product as a yellow oil (243 mg, 37 %). ^{1}H NMR (400 MHz, $CDCl_3$) δ 7.51 (s, 1H), 7.47 (s, 1H), 1.57 (s, 9H).^{13}C NMR (101 MHz, $CDCl_3$) δ 140.5, 139.1, 119.5, 56.2, 28.1. This compound has been previously reported.[7] (**EXC-II-132**)

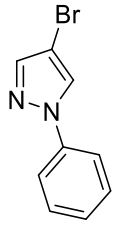

4-bromo-1-phenyl-1*H*-pyrazole (2-7n): A solution of tetramethoxypropane (0.33 mL, 2.00 mmol), phenylhydrazine (0.20 mL, 2.00 mmol), concentrated HCl (0.27 mL) and EtOH (4 mL) were refluxed for overnight. Upon cooling, the mixture was washed with water and ether. The resulting organic layer was then washed with brine and dried with $MgSO_4$. The residue was mixed in water (10 mL) and NBS (357 mg, 2.00 mmol) was added. TLC was used to detect progression of reaction. After 2 hours, the mixture was extracted with DCM (50 mL) and dried

with $MgSO_4$. The residue was purified using flash chromatography on silica gel (5 % ethyl acetate in hexanes) gave the product as a yellow oil (400 mg, 95 %). ^{1}H NMR (400 MHz, $CDCl_3$) δ 7.92 (d, *J* = 0.6 Hz, 1H), 7.66 (s, 1H), 7.63 (dq, *J* = 8.7, 1.2 Hz, 2H), 7.47-7.42 (m, 2H), 7.30 (tt, *J* = 7.7 Hz, 1.2 Hz, 1H). ^{13}C NMR (101 MHz, $CDCl_3$) δ 140.7, 139.8, 129.3, 126.8, 126.2, 119.5, 95.6. This compound has been previously reported.[7] (**EXC-II-132**)

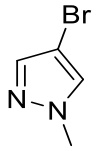

4-bromo-1-methyl-1*H*-pyrazole (2-7o): Prepared using the general procedure above (*Method B*) from 4-bromopyrazole (1 g, 6.8 mmol), methyl iodide (0.63 mL, 10.2 mmol), NaH (0.35 mg, 8.84 mmol), and DMF (12 mL). Concentration of the reaction mixture *in vacuo* followed by silica gel chromatography (15% ethyl acetate in hexanes) gave the product as a clear liquid (681 mg, 65%). ^{1}H NMR (400 MHz, $CDCl_3$) δ 7.40 (s, 1H), 7.34 (s, 1H), 3.85 (s, 3H). ^{13}C NMR (126 MHz, $CDCl_3$) 139.7, 132.8, 92.6, 39.5. This compound has been previously reported.[8]

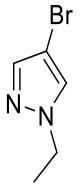

4-bromo-1-ethyl-1*H*-pyrazole (2-7p): Prepared using the general procedure above (*Method B*) from 4-bromopyrazole (1 g, 6.8 mmol), ethyl bromide (0.78 mL, 10.5 mmol), NaH (0.36 mg, 8.9 mmol), and DMF (10 mL). Concentration of the reaction mixture *in vacuo* followed by silica gel chromatography (15% ethyl acetate in hexanes) gave the product as a clear liquid (560 mg, 46%). ^{1}H NMR (400 MHz, $CDCl_3$) δ 8.45 (s, 1H), 7.94 (s, 1H), 4.29 (q, *J* = 7.3 Hz, 2H), 1.48

(t, *J* = 7.3 Hz, 3H). ^{13}C NMR (126 MHz, $CDCl_3$) 134.0, 132.8, 122.6, 47.8, 15.7. This compound has been previously reported.[9] (**EXC-II-94**)

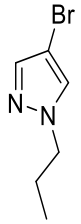

4-bromo-1-propyl-1*H*-pyrazole (2-7q): Prepared using the general procedure above (*Method B*) from 4-bromopyrazole (1.08g, 7.35 mmol), propyl bromide (1.0 mL, 11.01 mmol), NaH (0.38 mg, 9.55 mmol), and DMF (11 mL). Concentration of the reaction mixture *in vacuo* followed by silica gel chromatography (15% ethyl acetate in hexanes) gave the product as a clear liquid (950 mg, 68%). ^{1}H NMR (400 MHz, $CDCl_3$) ^{1}H NMR (400 MHz, $CDCl_3$) δ 8.26 (s, 1H), 8.07 (s, 1H), 4.29 (t, *J* = 7.3 Hz, 2H), 1.74 (h, *J* = 7.3 Hz, 2H), 0.89 (t, *J* = 7.3 Hz, 3H). ^{13}C NMR (126 MHz, $CDCl_3$) 140.0, 132.8, 93.4, 56.2, 23.7, 11.6. This compound has been previously reported.[9](**EXC-II-48**)

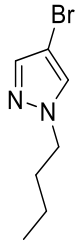

4-bromo-1-butyl-1*H*-pyrazole (2-7r): Prepared using the general procedure above (*Method B*) from 4-bromopyrazole (1.08g, 7.35 mmol), bromobutane (1.18 mL, 11.0 mmol), NaH (0.38 mg, 9.55 mmol), and DMF (12 mL). Concentration of the reaction mixture *in vacuo* followed by silica gel chromatography (15% ethyl acetate in hexanes) gave the product as a clear liquid (1.16 g, 78%). ^{1}H NMR (400 MHz, $CDCl_3$) δ 7.42 (s, 1H), 7.36 (s, 1H), 4.06 (t, *J* = 7.4 Hz, 2H), 1.80

(p, *J* = 7.4 Hz, 2H), 1.27 (h, *J* = 7.4 Hz, 2H), 0.91 (t, *J* = 7.4 Hz, 3H). ^{13}C NMR (101 MHz, $CDCl_3$) δ 139.46, 128.98, 92.52, 52.54, 32.19, 19.66, 13.48. This compound has been previously reported.[6] (**EXC-II-49**)

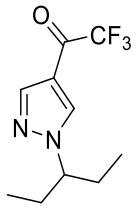

2,2,2-trifluoro-1-(1-(pentan-3-yl)-1*H*-pyrazol-4-yl)ethanone (2-9g): Prepared using the general procedure above (*Method C*) from 4-bromo-1-(pentan-3-yl)-1*H*-pyrazole (**2-7g**) (1.23 g, 5.68 mmol), methyl trifluoroacetate (0.68 mL, 6.81 mmol), *n*-BuLi (2.5 M in hexanes, 2.38 mL, 5.96 mmol), and THF (15 mL). Concentration of the reaction mixture *in vacuo* followed by silica gel flash chromatography (20 % DCM in hexanes) gave the product as a clear oil (897 mg, 67 %). ^{1}H NMR (500 MHz, $CDCl_3$) δ 8.10 (s, 1H), 8.04 (s, 1H), 3.97 (tt, *J* = 9.4, 5.0 Hz, 1H), 1.99 – 1.81 (m, 4H), 0.79 (t, *J* = 7.4 Hz, 6H). ^{13}C NMR (126 MHz, $CDCl_3$) δ 174.7 (q, $^{2}J_{CF}$ = 36.7 Hz), 141.8, 133.7, 116.5 (q, $^{1}J_{CF}$ = 290.1 Hz), 115.6, 67.9, 27.9, 10.5. ^{19}F NMR (471 MHz, $CDCl_3$) δ -74.8. HRMS (ESI) *m/z* calcd for $C_{10}H_{13}F_3N_2O$ $[M+H]^+$ 235.1052, found 235.1059. (**EXC-II-44**)

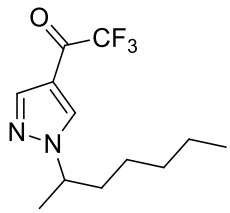

2,2,2-trifluoro-1-(1-(heptan-2-yl)-1*H*-pyrazol-4-yl)ethanone (2-9i): Prepared using the general procedure above (*Method C*) from 4-bromo-1-(heptan-3-yl)-1*H*-pyrazole (**2-7i**) (845 mg, 3.44 mmol), methyl trifluoroacetate (0.41 mL, 4.13 mmol), *n*-BuLi (2.5 M in hexanes, 1.44 mL,

3.62 mmol), and THF (10 mL). Concentration of the reaction mixture *in vacuo* followed by silica gel flash chromatography (50 % DCM in hexanes) gave the product as a clear oil (382 mg, 51 %). ^{1}H NMR (400 MHz, $CDCl_3$) δ 8.06 (s, 1H), 8.04 (s, 1H), 4.34 (h, *J* = 6.7 Hz, 1H), 1.97 – 1.86 (m, 1H), 1.80 – 1.70 (m, 1H), 1.52 (d, *J* = 6.7 Hz, 3H), 1.28 – 1.05 (m, 6H), 0.85 (t, *J* = 6.8 Hz, 3H). ^{13}C NMR (101 MHz, $CDCl_3$) δ 174.8 (q, $^{2}J_{CF}$ = 36.6 Hz), 141.7 (q, $^{3}J_{CF}$ = 2.1 Hz), 132.6 (q, $^{3}J_{CF}$ = 3.0 Hz), 116.7 (q, $^{1}J_{CF}$ = 290.1 Hz), 116.0, 59.9, 36.8, 31.4, 25.8, 22.5, 21.1, 14.0. ^{19}F NMR (471 MHz, $CDCl_3$) δ -75.1. Despite multiple attempts, the molecular ion of this compound was not detected using ESI+, ESI-, and ECI techniques. (**EXC-II-16**)

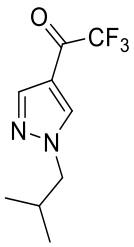

2, 2, 2-trifluoro-1-(1-isobutyl-1*H*-pyrazol-4-yl)ethan-1-one (2-9j): Prepared using the general procedure above (*Method C*) from 4-bromo-1-(isobutyl)-1*H*-pyrazole (**2-7j**) (378 mg, 1.86 mmol), methyl trifluoroacetate (0.22 mL, 2.23 mmol), *n*-BuLi (2.5 M in hexanes, 0.96 mL, 2.4 mmol), and THF (7 mL). Concentration of the reaction mixture *in vacuo* followed by silica gel flash chromatography (20 % DCM in hexane) gave the product as a clear oil (213 mg, 43 %) ^{1}H NMR (400 MHz, $CDCl_3$) δ 8.05 (s, 1H), 8.02 (s, 1H), 3.96 (d, *J* = 6.8 Hz, 2H), 2.25 (n, *J* = 6.8 Hz, 1H), 0.91 (d, *J* = 6.8 Hz, 6H). ^{13}C NMR (101 MHz, $CDCl_3$) δ 174.5 (q, $^{2}J_{CF}$ = 36.7 Hz), 141.8 (q, $^{4}J_{CF}$ = 2.0 Hz), 134.4 (q, $^{4}J_{CF}$ = 2.4 Hz), 116.4 (d, $^{1}J_{CF}$ = 290.3 Hz), 116.1, 603, 29.3, 19.7. ^{19}F NMR (471 MHz, $CDCl_3$) δ -74.2. HRMS (ESI) *m/z* calcd for $C_9H_{11}F_3N_2O$ $[M+H]^+$ 221.0896, found 221.0887. (**EXC-II-66**)

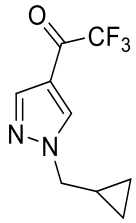

1-(1-(cyclopropylmethyl)-1*H*-pyrazol-4-yl)-2,2,2-trifluoroethan-1-one (2-9k): Prepared using the general procedure above (*Method C*) from 4-bromo-1-(cyclopropylmethyl)-1*H*-pyrazole (**2-7k**) (498 mg, 2.48 mmol), methyl trifluoroacetate (0.30 mL, 2.97 mmol), *n*-BuLi (2.5 M in hexanes, 1.04 mL, 2.4mmol), and THF (7 mL). Concentration of the reaction mixture *in vacuo* followed by silica gel flash chromatography (10 % ethyl acetate in hexanes) gave the product as a clear oil (400 mg, 74 %) ^{1}H NMR (400 MHz, $CDCl_3$) δ 8.20 (s, 1H), 8.08 (s, 1H), 4.05 (d, *J* = 7.3 Hz, 2H), 0.88-0.82 (m, 1H), 0.79 – 0.71 (m, 2H), 0.44 (dd, *J* = 10.7, 5.1 Hz, 2H). ^{13}C NMR (101 MHz, $CDCl_3$) δ 174.5 (q, $^{2}J_{CF}$ = 36.9 Hz), 141.7 (q, $^{4}J_{CF}$ = 2.1 Hz), 133.4 (q, $^{4}J_{CF}$ = 2.7 Hz), 116.4 (q, $^{1}J_{CF}$ = 288 Hz), 116.3, 57.6, 10.5, 4.1. ^{19}F NMR (376 MHz, $CDCl_3$) δ -74.9. HRMS (ESI) *m/z* calcd for $C_9H_9F_3N_2O$ $[M+H]^+$ 219.0739, found 219.0740. (**EXC-II-126**)

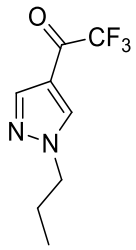

2,2,2-trifluoro-1-(1-(propyl)-1*H*-pyrazol-4-yl)ethanone (2-9q): Prepared using the general procedure above (*Method C*) from 4-bromo-1-(propyl)-1*H*-pyrazole (**2-7q**) (950 mg, 5.02 mmol), methyl trifluoroacetate (0.61 mL, 6.03 mmol), *n*-BuLi (2.5 M in hexanes, 2.1 mL, 5.28 mmol), and THF (15 mL). Concentration of the reaction mixture *in vacuo* followed by silica gel flash chromatography (10 % ethyl acetate in hexanes) gave the product as a clear oil (500 mg, 49 %). ^{1}H NMR (500 MHz, $CDCl_3$) δ 8.02 (s, 1H), 7.99 (s, 1H), 4.09 (t, *J* = 7.1 Hz, 2H), 1.88 (h, *J*

= 7.4 Hz, 2H), 0.88 (t, *J* = 7.4 Hz, 3H). ^{13}C NMR (126 MHz, $CDCl_3$) δ 174.53 (q, $^2J_{CF}$ = 36.7 Hz), 141.87, 134.02, 116.17, 116.48 (q, $^1J_{CF}$ = 278.9 Hz), 54.66, 23.23, 10.95. ^{19}F NMR (471 MHz, $CDCl_3$) δ -74.3. HRMS (ESI) *m/z* calcd for $C_8H_9F_3N_2O$ $[M+H]^+$ 207.0739, found 207.0732. (**EXC-III-50**)

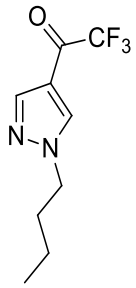

2,2,2-trifluoro-1-(1-(butyl)-1*H*-pyrazol-4-yl)ethanone (2-9r): Prepared using the general procedure above (*Method C*) from 4-bromo-1-(butyl)-1*H*-pyrazole (**2-7r**) (1.16 g, 5.71 mmol), methyl trifluoroacetate (0.69 mL, 6.85 mmol), *n*-BuLi (2.5 M in hexanes, 2.4 mL, 5.99 mmol), and THF (10 mL). Concentration of the reaction mixture *in vacuo* followed by silica gel flash chromatography (10 % ethyl in hexanes) gave the product as a clear oil (760 mg, 61 %). ^{1}H NMR (500 MHz, $CDCl_3$) δ 8.01 (s, 1H), 7.99 (s, 1H), 4.12 (t, *J* = 7.2 Hz, 2H), 1.84 (p, *J* = 7.4 Hz, 2H), 1.28 (h, *J* = 7.4 Hz, 2H), 0.90 (t, *J* = 7.4 Hz, 3H). ^{13}C NMR (126 MHz, $CDCl_3$) δ 174.51 (q, $^2J_{CF}$ = 36.7 Hz), 141.82 (q, $^3J_{CF}$ = 1.8 Hz), 133.96, 116.45 (q, $^1J_{CF}$ = 290.1 Hz), 116.19, 52.81, 31.81, 19.64, 13.44. ^{19}F NMR (471 MHz, $CDCl_3$) δ -74.8. HRMS (ESI) *m/z* calcd for $C_9H_{11}F_3N_2O$ $[M+H]^+$ 221.0896, found 221.0892. (**EXC-III-51**)

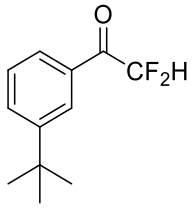

1-(3-(*tert*-butyl)phenyl)-2,2-difluoroethan-1-one (2-10c): Prepared using the general procedure above (*Method D*) from 1-bromo-3-(*tert*-butyl)benzene (**2-8c**) (100 mg, 0.47 mmol), methyl difluoroacetate (0.05 mL, 0.56 mmol), *n*-BuLi (2.5 M in hexanes, 0.2 mL, 0.49 mmol), and THF (4 mL). Concentration of the reaction mixture *in vacuo* followed by silica gel flash chromatography (5 % ethyl acetate in hexanes) gave the product as a clear oil (47 mg, 47 %). ^{1}H NMR (400 MHz, $CDCl_3$) δ 8.09 (t, *J* = 2.1 Hz, 1H), 7.87 (dp, *J* = 7.7, 1.6 Hz, 1H), 7.70 (ddd, *J* = 7.9, 2.1, 1.1 Hz, 1H), 7.44 (t, *J* = 7.8 Hz, 1H), 6.29 (t, $^{2}J_{HF}$ = 53.6 Hz, 1H), 1.35 (s, 9H). ^{13}C NMR (101 MHz, $CDCl_3$) δ 188.0 (t, $^{2}J_{CF}$ = 25.1 Hz), 152.4, 132.3, 131.5 (t, $^{4}J_{CF}$ = 1.7 Hz), 128.8, 127.1 (t, $^{3}J_{CF}$ = 2.8 Hz), 126.5 (t, $^{4}J_{CF}$ = 1.9 Hz), 111.3 (t, $^{1}J_{CF}$ = 253.6 Hz), 35.1, 31.3. ^{19}F NMR (376 MHz, $CDCl_3$) δ -121.9 (d, $^{2}J_{FH}$ = 53.6 Hz). HRMS (ESI) *m/z* calcd for $C_{12}H_{14}F_2O$ $[M+Cl]^-$ 265.0801, found 265.0818. (**EXC-III-3**)

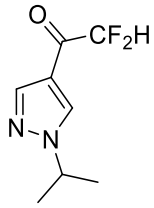

2,2-difluoro-1-(1-isopropyl-1*H*-pyrazol-4-yl)ethan-1-one (2-10d): Prepared using the general procedure above (*Method D*) from 4-bromo-1-(pentan-3-yl)-1*H*-pyrazole (**2-7d**) (200 mg, 1.06 mmol), methyl difluoroacetate (0.11 mL, 1.27 mmol), *n*-BuLi (2.5 M in hexanes, 0.44 mL, 1.11 mmol), and THF (6 mL). Concentration of the reaction mixture *in vacuo* followed by silica gel flash chromatography (100 % DCM) gave the product as a clear oil (96 mg, 48 %). ^{1}H NMR

(400 MHz, $CDCl_3$) δ 8.09 (s, 1H), 8.08 (s, 1H), 5.98 (t, $^2J_{HF}$ = 54.0 Hz, 1H), 4.54 (hept, *J* = 6.7 Hz, 1H), 1.54 (d, *J* = 6.7 Hz, 6H). ^{13}C NMR (101 MHz, $CDCl_3$) δ 182.43 (t, $^2J_{CF}$ = 26.6 Hz), 141.12 (t, $^4J_{CF}$ = 2.5 Hz), 131.08 (t, $^4J_{CF}$ = 3.5 Hz), 116.91, 111.08 (t, $^1J_{CF}$ = 253.4 Hz), 54.75, 22.51. ^{19}F NMR (376 MHz, $CDCl_3$) δ -123.6 (d, $^2J_{FH}$ = 54.0 Hz). HRMS (ESI) *m/z* calcd for $C_8H_{10}F_2N_2O$ $[M+H]^+$ 189.0834, found 189.0838. (**EXC-III-34**)

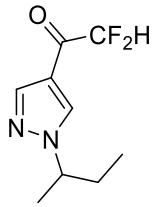

1-(1-(sec-butyl)-1*H*-pyrazol-4-yl)-2,2-difluoroethan-1-one (2-10e): Prepared using the general procedure above (*Method D*) from 4-bromo-1-(sec-butyl)-1*H*-pyrazole (**2-7e**) (268 mg, 1.32 mmol), methyl difluoroacetate (0.14 mL, 1.58 mmol), *n*-BuLi (2.5 M in hexanes, 0.55 mL, 1.39 mmol), and THF (5 mL). Concentration of the reaction mixture *in vacuo* followed by silica gel flash chromatography (60 % DCM in hexanes) gave the product as a clear oil (105 mg, 39 %). ^{1}H NMR (400 MHz, $CDCl_3$) δ 8.04 (t, *J* = 1.0 Hz, 2H), 5.96 (t, *J* = 54.0 Hz, 1H), 4.23 (h, *J* = 6.5 Hz 1H), 2.06 – 1.68 (m, 2H), 1.48 (d, *J* = 6.8 Hz, 3H), 0.78 (t, *J* = 7.4 Hz, 3H). ^{13}C NMR (101 MHz, $CDCl_3$) δ 182.5 (t, $^2J_{CF}$ = 26.6 Hz), 141.2 (t, $^4J_{CF}$ = 2.4 Hz), 132.0 (t, $^4J_{CF}$ = 3.5 Hz), 116.8 (t, $^3J_{CF}$ = 2.3 Hz), 111.1 (t, $^1J_{CF}$ = 252.9 Hz), 60.8, 29.7, 20.5, 10.3. ^{19}F NMR (376 MHz, $CDCl_3$) δ -123.4 (d, $^2J_{FH}$ = 54.0 Hz). HRMS (ESI) *m/z* calcd for $C_9H_{12}F_2N_2O$ $[M+H]^+$ 203.0990, found 203.0988. (**EXC-III-82**)

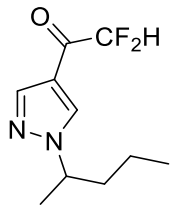

2,2-difluoro-1-(1-(pentan-2-yl)-1*H*-pyrazol-4-yl)ethan-1-one (2-10f): Prepared using the general procedure above (*Method D*) from 4-bromo-1-(pentan-2-yl)-1*H*-pyrazole (**2-7f**) (500 mg, 2.03 mmol), methyl difluoroacetate (0.24 mL, 2.76 mmol), *n*-BuLi (2.5 M in hexanes, 0.96mL, 2.4mmol), and THF (7 mL). Concentration of the reaction mixture *in vacuo* followed by silica gel flash chromatography (50 % DCM in hexane) gave the product as a clear oil (213 mg, 43 %). ^{1}H NMR (400 MHz, $CDCl_3$) δ 8.04 (s, 2H), 5.96 (t, $^{2}J_{HF}$ = 53.9 Hz, 1H), 4.32 (h, J = 6.9 Hz, 1H), 2.08 – 1.58 (m, 2H), 1.48 (d, J = 6.7 Hz, 3H), 1.32 – 1.03 (m, 2H), 0.85 (t, J = 7.4 Hz, 3H). ^{13}C NMR (101 MHz, $CDCl_3$) δ 182.5 (t, $^{2}J_{CF}$ = 26.5 Hz), 141.1 (t, $^{4}J_{CF}$ = 2.6 Hz), 131.9 (t, $^{4}J_{CF}$ = 3.4 Hz), 116.8 (t, $^{3}J_{CF}$ = 2.3 Hz), 111.1 (t, $^{1}J_{CF}$ = 252.9 Hz), 59.2, 38.7, 20.9, 19.1, 13.5. ^{19}F NMR (376 MHz, $CDCl_3$) δ -123.5 (d, $^{2}J_{FH}$ = 53.8 Hz). HRMS (ESI) *m/z* calcd for $C_{10}H_{14}F_2N_2O$ $[M+H]^+$ 217.1146, found 217.1149. (**EXC-III-102**)

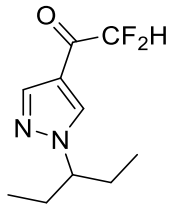

2,2-difluoro-1-(1-(pentan-3-yl)-1*H*-pyrazol-4-yl)ethan-1-one (2-10g): Prepared using the general procedure above (*Method D*) from 4-bromo-1-(pentan-3-yl)-1*H*-pyrazole (**2-7g**) (500 mg, 2.3 mmol), methyl difluoroacetate (0.25 mL, 2.76 mmol), *n*-BuLi (2.5 M in hexanes, 1.03 mL, 2.42 mmol), and THF (7 mL). Concentration of the reaction mixture *in vacuo* followed by silica gel flash chromatography (50 % DCM in hexanes) gave the product as a clear oil (173 mg,

35 %). ^{1}H NMR (400 MHz, $CDCl_3$) δ 8.10 (s, 1H), 8.04 (s, 1H), 5.99 (t, $^{2}J_{HF}$ = 54.0 Hz, 1H), 3.94 (tt, *J* = 9.4, 5.1 Hz, 1H), 2.10 – 1.73 (m, 4H), 0.77 (t, *J* = 7.4 Hz, 6H). ^{13}C NMR (101 MHz, $CDCl_3$) δ 182.6 (t, $^{2}J_{CF}$ = 26.6 Hz), 141.4 (t, $^{4}J_{CF}$ = 2.5 Hz), 133.1 (t, $^{4}J_{CF}$ = 3.5 Hz), 116.6, 111.2 (t, $^{1}J_{CF}$ = 253.1 Hz), 67.6, 28.0, 10.5. ^{19}F NMR (376 MHz, $CDCl_3$) δ -123.4 (d, $^{2}J_{FH}$ = 53.9 Hz). HRMS (ESI) *m/z* calcd for $C_{10}H_{14}F_2N_2O$ $[M+H]^+$ 217.1146, found 217.1150. (**EXC-III-74**)

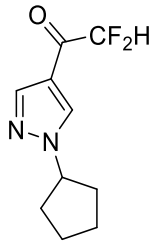

1-(1-cyclopentyl-1*H*-pyrazol-4-yl)-2,2-difluoroethan-1-one (2-10h): Prepared using the general procedure above (*Method D*) from 4-bromo-1-(cyclopentyl)-1*H*-pyrazole (**2-7h**) (300 mg, 1.39 mmol), methyl difluoroacetate (0.18 mL, 1.67 mmol), *n*-BuLi (2.5 M in hexanes, 0.58 mL, 1.46 mmol), and THF (10 mL). Concentration of the reaction mixture *in vacuo* followed by silica gel flash chromatography (100 % DCM) gave the product as a clear oil (99 mg, 27 %). ^{1}H NMR (400 MHz, $CDCl_3$) δ 8.07 (s, 1H), 8.04 (s, 1H), 5.96 (t, $^{2}J_{HF}$ = 53.9 Hz, 1H), 4.56 (p, *J* = 6.8 Hz, 1H), 2.23 – 2.11 (m, 2H), 2.06 – 1.93 (m, 2H), 1.85 (m, 2H), 1.77 – 1.63 (m, 2H). ^{13}C NMR (101 MHz, $CDCl_3$) δ 182.4 (t, $^{2}J_{CF}$ = 26.7 Hz), 141.3 (t, $^{4}J_{CF}$ = 2.5 Hz), 132.1 (t, $^{4}J_{CF}$ = 3.4 Hz), 116.9 (t, $^{3}J_{CF}$ = 2.4 Hz), 111.1 (t, $^{1}J_{CF}$ = 253.0 Hz), 63.8, 32.9, 24.1. ^{19}F NMR (376 MHz, $CDCl_3$) δ -123.5 (d, $^{2}J_{FH}$ = 53.9 Hz). HRMS (ESI) *m/z* calcd for $C_{10}H_{12}F_2N_2O$ $[M+H]^+$ 215.0990, found 215.0996. (**EXC-III-96**)

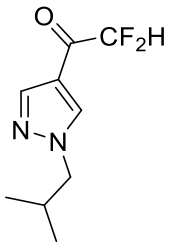

2,2-difluoro-1-(1-isobutyl-1*H*-pyrazol-4-yl)ethan-1-one (2-10j): Prepared using the general procedure above (*Method D*) from 4-bromo-1-(isobutyl)-1*H*-pyrazole (**2-7j**) (260 mg, 1.28 mmol), methyl difluoroacetate (0.14 mL, 1.54 mmol), *n*-BuLi (2.5 M in hexanes, 0.54 mL, 1.34 mmol), and THF (5 mL). Concentration of the reaction mixture *in vacuo* followed by silica gel flash chromatography (60 % DCM in hexanes) gave the product as a clear oil (124 mg, 48 %) ^{1}H NMR (400 MHz, $CDCl_3$) δ 8.06 (s, 1H), 8.02 (s, 1H), 5.97 (t, J = 53.9 Hz, 2H), 3.94 (d, J = 6.8 Hz, 2H), 2.22 (n, J = 6.8 Hz , 1H), 0.90 (d, J = 6.8 Hz, 6H). ^{13}C NMR (101 MHz, $CDCl_3$) δ 182.5 (t, $^{2}J_{CF}$ = 26.6 Hz), 141.5 (t, $^{4}J_{CF}$ = 2.3 Hz), 133.9 (t, $^{4}J_{CF}$ = 3.7 Hz), 117.1, 111.2 ($^{1}J_{CF}$ = 254.3 Hz), 60.2, 29.3, 19.7. ^{19}F NMR (376 MHz, $CDCl_3$) δ -123.5 (d, $^{2}J_{FH}$ = 54.4 Hz). HRMS (ESI) *m/z* calcd for $C_9H_{12}F_2N_2O$ $[M+H]^+$ 203.0990, found 203.0971. (**EXC-III-88**)

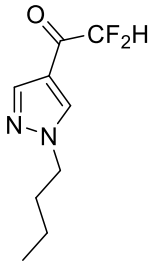

1-(1-butyl-1*H*-pyrazol-4-yl)-2,2-difluoroethan-1-one (2-10r): Prepared using the general procedure above (*Method D*) from 4-bromo-1-(butyl)-1*H*-pyrazole (**2-7r**) (538 mg, 2.84 mmol), methyl difluoroacetate (0.29 mL, 3.41 mmol), *n*-BuLi (2.5 M in hexanes, 1.2 mL, 2.99 mmol), and THF (6 mL). Concentration of the reaction mixture *in vacuo* followed by silica gel flash chromatography (20 % DCM in hexanes) gave the product as a clear oil (288 mg, 50 %). ^{1}H

NMR (400 MHz, $CDCl_3$) δ 8.07 (s, 1H), 8.05 (s, 1H), 5.97 (t, $^2J_{HF}$ = 54.0 Hz, 1H), 4.16 (t, *J* = 7.2 Hz, 2H), 2.01 – 1.75 (p, *J* = 7.5 Hz, 2H), 1.3 (h, *J* = 7.5 Hz, 2H), 0.94 (t, *J* = 7.5 Hz, 3H). ^{13}C NMR (101 MHz, $CDCl_3$) δ 182.56 (t, $^2J_{CF}$ = 26.7 Hz), 141.4 (t, $^4J_{CF}$ = 2.4 Hz), 133.4 (t, $^4J_{CF}$ = 3.6 Hz), 117.2, 111.1 (t, $^1J_{CF}$ = 253.1 Hz), 52.6, 31.8, 19.6, 13.4. ^{19}F NMR (376 MHz, $CDCl_3$) δ -123.4 (d, $^4J_{CF}$ = 54.0 Hz). HRMS (ESI) *m/z* calcd for $C_9H_{12}F_2N_2O$ $[M+H]^+$ 203.0990, found 203.0988. (**EXC-III-7**)

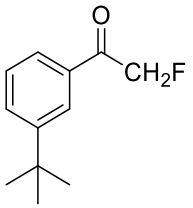

1-(3-(*tert*-butyl)phenyl)-2-fluoroethan-1-one (2-11c): Prepared using the general procedure above (*Method E*) from 1-bromo-3-(*tert*-butyl)benzene (**2-8c**) (300 mg, 1.41 mmol), ethyl fluoroacetate (0.16 mL, 1.69 mmol), *n*-BuLi (2.5 M in hexanes, 0.59 mL, 1.48 mmol), and THF (5 mL). Concentration of the reaction mixture *in vacuo* followed by silica gel flash chromatography (10 % ethyl acetate in hexanes) gave the product as a yellow oil (117 mg, 43 %). ^{1}H NMR (500 MHz, $CDCl_3$) δ 7.88 (t, *J* = 1.8 Hz, 1H), 7.61-7.59 (m, 1H), 7.58-7.56 (m, 1H), 7.35 (t, *J* = 7.8 Hz, 1H), 5.47 (d, $^2J_{HF}$ = 47.0 Hz, 2H), 1.28 (s, 9H). ^{13}C NMR (126 MHz, $CDCl_3$) δ 193.9 (d, $^2J_{CF}$ = 15.4 Hz), 152.4, 133.7, 131.5, 128.8, 125.2 (d, $^4J_{CF}$ = 2.6 Hz), 124.8 (d, $^4J_{CF}$ = 2.5 Hz), 83.7 (d, $^1J_{CF}$ = 182.5 Hz), 31.3. ^{19}F NMR (376 MHz, $CDCl_3$) δ -230.6 (t, $^2J_{FH}$ = 47.0 Hz). HRMS (Mixed EIC) *m/z* calcd for $C_{12}H_{15}FO$ $[2M+Na]^+$ 411.2112, found 411.2134. (**EXC-II-82**)

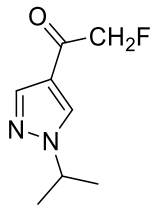

2-fluoro-1-(1-(isopropyl)-1*H*-pyrazol-4-yl)ethan-1-one (2-11d): Prepared using the general procedure above (*Method E*) from 4-bromo-1-(isopropyl)-1*H*-pyrazole (**2-7d**) (551 mg, 2.91 mmol), ethyl fluoroacetate (0.33 mL, 3.49 mmol), *n*-BuLi (2.5 M in hexanes, 1.45 mL, 3.06 mmol), and THF (7 mL). Concentration of the reaction mixture *in vacuo* followed by silica gel flash chromatography (20 % ethyl acetate in hexanes) gave the product as an light-yellow solid (100 mg, 20 %); mp 158.5-159.8 ˚C. ^{1}H NMR (500 MHz, $CDCl_3$) δ 8.06 (s, 1H), 7.98 (s, 1H), 5.07 (d, $^{2}J_{HF}$ = 47.5 Hz, 2H), 4.49 (hept, *J* = 6.7 Hz, 1H), 1.49 (d, *J* = 6.7 Hz, 6H). ^{13}C NMR (126 MHz, $CDCl_3$) δ 189.6 (d, $^{2}J_{CF}$ = 19.6 Hz), 140.4 (d, $^{4}J_{CF}$ = 5.3 Hz), 130.2 (d, $^{4}J_{CF}$ = 9.3 Hz), 119.5 (d, $^{3}J_{CF}$ = 3.1 Hz), 84.8 (d, $^{1}J_{CF}$ = 184.7 Hz), 54.6, 22.7. ^{19}F NMR (471 MHz, $CDCl_3$) δ -226.5 (t, $^{2}J_{FH}$ = 47.5 Hz). HRMS (ESI) *m/z* calcd for $C_8H_{11}FN_2O$ $[M+H]^+$ 171.0928, found 171.0928. (**EXC-II-104**)

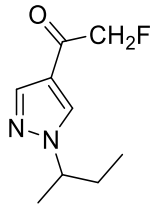

1-(1-(sec-butyl)-1*H*-pyrazol-4-yl)-2-fluoroethan-1-one (2-11e): Prepared using the general procedure above (*Method E*) from 4-bromo-1-(*sec*-butyl)-1*H*-pyrazole (**2-7e**) (500 mg, 2.46 mmol), ethyl fluoroacetate (0.29 mL, 2.95 mmol), *n*-BuLi (2.5 M in hexanes, 1.0 mL, 1.34 mmol), and THF (5 mL). Concentration of the reaction mixture *in vacuo* followed by silica gel flash chromatography (30 % ethyl acetate in hexanes) gave the product as a clear oil (115 mg, 25

%). ^{1}H NMR (400 MHz, $CDCl_3$) δ 8.03 (s, 1H), 8.01 (s, 1H), 5.09 (d, $^{2}J_{HF}$ = 47.5 Hz, 2H), 4.22 (h, *J* = 6.8 Hz, 1H), 2.02 – 1.70 (m, 2H), 1.49 (d, *J* = 6.8 Hz, 3H), 0.79 (t, *J* = 7.4 Hz, 3H). ^{13}C NMR (101 MHz, $CDCl_3$) δ 189.57 (d, $^{2}J_{CF}$ = 19.5 Hz), 140.37 (d, $^{4}J_{CF}$ = 5.3 Hz), 131.12 (d, $^{4}J_{CF}$ = 9.3 Hz), 119.35 (d, $^{3}J_{CF}$ = 3.3 Hz), 84.74 (d, $^{1}J_{CF}$ = 184.6 Hz), 60.64, 29.78, 20.58, 10.37. ^{19}F NMR (376 MHz, $CDCl_3$) δ -226.3 (t, $^{2}J_{HF}$ = 47.5 Hz). HRMS (ESI) *m/z* calcd for $C_9H_{13}FN_2O$ $[M+H]^+$ 185.1084, found 185.1083. (**EXC-III-81**)

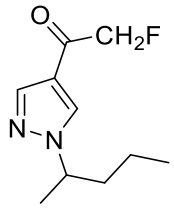

2-fluoro-1-(1-(pentan-2-yl)-1*H*-pyrazol-4-yl)ethan-1-one (2-11f): Prepared using the general procedure above (*Method E*) from 4-bromo-1-(pentan-2-yl)-1*H*-pyrazole (**2-7f**) (504 mg, 2.32 mmol), ethyl fluoroacetate (0.27 mL, 2.78 mmol), *n*-BuLi (2.5 M in hexanes, 0.97 mL, 2.43 mmol), and THF (7 mL). Concentration of the reaction mixture *in vacuo* followed by silica gel flash chromatography (20 % ethyl acetate in hexanes) gave the product as a yellow oil (114 mg, 28 %). ^{1}H NMR (400 MHz, $CDCl_3$) δ 8.04 (s, 1H), 8.03 (s, 1H), 5.11 (d, $^{2}J_{HF}$ = 47.1 Hz, 2H), 4.33 (h, *J* = 6.6 Hz, 1H), 1.90 (m, 1H), 1.71 (m, 1H), 1.50 (d, *J* = 6.8 Hz, 3H), 1.30 – 1.07 (m, 2H), 0.90 (t, *J* = 6.9 Hz, 3H). ^{13}C NMR (101 MHz, $CDCl_3$) δ 189.4 (d, $^{2}J_{CF}$ = 19.5 Hz), 140.2 (d, $^{4}J_{CF}$ = 5.2 Hz), 131.0 (d, $^{4}J_{CF}$ = 9.1 Hz), 119.3 (d, $^{3}J_{CF}$ = 3.1 Hz), 84.7 (d, $^{1}J_{CF}$ = 184.5 Hz), 58.9, 38.7, 21.0, 19.1, 13.5. ^{19}F NMR (376 MHz, $CDCl_3$) δ -226.3 (t, $^{2}J_{HF}$ = 47.1 Hz). HRMS (ESI) *m/z* calcd for $C_{10}H_{15}FN_2O$ $[M+H]^+$ 199.1241, found 199.1241. (**EXC-II-185**)

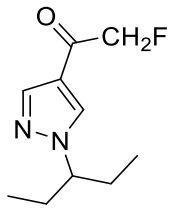

2-fluoro-1-(1-(pentan-3-yl)-1*H*-pyrazol-4-yl)ethan-1-one (2-11g): Prepared using the general procedure above (*Method E*) from 4-bromo-1-(pentan-3-yl)-1*H*-pyrazole (**2-7g**) (525 mg, 2.41 mmol), ethyl fluoroacetate (0.28 mL, 2.89 mmol), *n*-BuLi (2.5 M in hexanes, 1.01 mL, 2.53 mmol), and THF (7 mL). Concentration of the reaction mixture *in vacuo* followed by silica gel flash chromatography (10 % ethyl acetate in DCM) gave the product as a yellow oil (170 mg, 36 %). ^{1}H NMR (500 MHz, $CDCl_3$) δ 8.09 (s, 1H), 8.07 (s, 1H), 5.16 (d, $^{2}J_{HF}$ = 47.6 Hz, 2H), 3.96 (tt, *J* = 9.3, 5.0 Hz, 1H), 2.03 – 1.81 (m, 4H), 0.81 (t, *J* = 7.4 Hz, 6H). ^{13}C NMR (126 MHz, $CDCl_3$) δ 189.6 (d, $^{2}J_{CF}$ = 19.6 Hz), 140.4 (d, $^{4}J_{CF}$ = 5.3 Hz), 130.2 (d, $^{4}J_{CF}$ = 9.3 Hz), 119.5 (d, $^{3}J_{CF}$ = 3.1 Hz), 84.8 (d, $^{1}J_{CF}$ = 184.7 Hz), 54.6, 22.7. ^{19}F NMR (471 MHz, $CDCl_3$) δ -226.3 (t, $^{2}J_{FH}$ = 47.6 Hz). HRMS (ESI) *m/z* calcd for $C_{10}H_{15}FN_2O$ $[M+H]^+$ 199.1241, found 199.1231. (**EXC-II-164**)

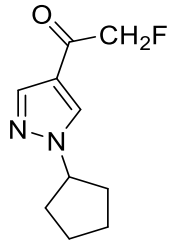

1-(1-cyclopentyl-1*H*-pyrazol-4-yl)-2-fluoroethan-1-one (2-11h): Prepared using the general procedure above (*Method E*) from 4-bromo-1-(cyclopentyl)-1*H*-pyrazole (**2-7h**) (480 mg, 2.23 mmol), ethyl fluoroacetate (0.26 mL, 2.68 mmol), *n*-BuLi (2.5 M in hexanes, 0.94 mL, 2.34 mmol), and THF (7 mL). Concentration of the reaction mixture *in vacuo* followed by silica gel flash chromatography (20 % ethyl acetate in hexanes) gave the product as a yellow oil (132 mg,

30 %) ^{1}H NMR (400 MHz, $CDCl_3$) δ 8.07 (s, 1H), 8.02 (s, 1H), 5.10 (d, $^{2}J_{HF}$ = 47.5 Hz, 2H), 4.66 (p, *J* = 7.0 Hz, 1H), 2.30 – 2.11 (m, 2H), 2.09 – 1.95 (m, 2H), 1.95 – 1.80 (m, 2H), 1.80 – 1.65 (m, 2H). ^{13}C NMR (101 MHz, $CDCl_3$) δ 189.4 (d, $^{2}J_{CF}$ = 19.5 Hz), 140.4 (d, $^{4}J_{CF}$ = 5.1 Hz), 131.2 (d, $^{4}J_{CF}$ = 9.1 Hz), 119.4 (d, $^{3}J_{CF}$ = 3.1 Hz), 84.7 (d, $^{1}J_{CF}$ = 184.4 Hz), 63.6, 32.9, 24.0. ^{19}F NMR (376 MHz, $CDCl_3$) δ -226.2 (t, *J* = 56.1 Hz). HRMS (ESI) *m/z* calcd for $C_{10}H_{13}FN_2O$ $[M+H]^+$ 197.1084, found 197.1087. (**EXC-II-184**)

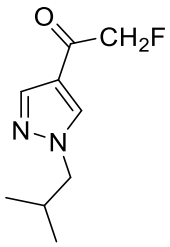

2-fluoro-1-(1-isobutyl-1*H*-pyrazol-4-yl)ethan-1-one (2-11j): Prepared using the general procedure above (*Method E*) from 4-bromo-1-(isobutyl)-1*H*-pyrazole (**2-7j**) (500 mg, 2.46 mmol), ethyl fluoroacetate (0.285 mL, 2.95 mmol), *n*-BuLi (2.5 M in hexanes, 1.03 mL, 2.59 mmol), and THF (7 mL). Concentration of the reaction mixture *in vacuo* followed by silica gel flash chromatography (5 % ethyl acetate in DCM) gave the product as a yellow oil (122 mg, 27 %) ^{1}H NMR (400 MHz, $CDCl_3$) δ 8.02 (s, 2H), 5.10 (d, $^{2}J_{HF}$ = 47.5 Hz, 2H), 3.93 (d, *J* = 7.3 Hz, 2H), 2.36 – 2.10 (n, *J* = 6.7 Hz, 1H), 0.91 (d, *J* = 6.7 Hz, 6H). ^{13}C NMR (101 MHz, $CDCl_3$) δ 189.6 (d, $^{2}J_{CF}$ = 19.8 Hz), 140.7 (d, $^{4}J_{CF}$ = 5.3 Hz), 133.1 (d, $^{4}J_{CF}$ = 10.3 Hz), 110.0, 84.8 (d, $^{1}J_{CF}$ = 184.7 Hz), 60.1, 29.3, 19.8. ^{19}F NMR (376 MHz, $CDCl_3$) δ -226.2 (tt, *J* = 47.6, 1.5 Hz). HRMS (ESI) *m/z* calcd for $C_9H_{13}FN_2O$ $[M+H]^+$ 185.1084, found 185.1095. (**EXC-III-87**)

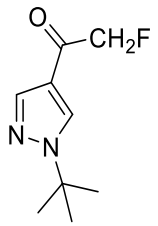

2-fluoro-1-(1-(*tert*-butyl)-1*H*-pyrazol-4-yl)ethan-1-one (2-11m): Prepared using the general procedure above (*Method E*) from 4-bromo-1-(*tert*-butyl)-1*H*-pyrazole (**2-7m**) (500 mg, 2.5 mmol), ethyl fluoroacetate (0.31 mL, 3.20 mmol), *n*-BuLi (2.5 M in hexanes, 1.18 mL, 2.95 mmol), and THF (6 mL). Concentration of the reaction mixture *in vacuo* followed by silica gel flash chromatography (10 % ethyl acetate in hexanes) gave the product as a pale yellow liquid (70 mg, 13 %). ^{1}H NMR (400 MHz, $CDCl_3$) δ 8.14 (s, 1H), 8.02 (s, 1H), 5.10 (d, J = 47.5 Hz, 2H), 1.58 (s, 9H).^{13}C NMR (101 MHz, $CDCl_3$) δ 189.58 (d, $^{2}J_{CF}$ = 19.3 Hz), 140.15 (d, $^{3}J_{CF}$ = 5.5 Hz), 129.48 (d, J = 8.9 Hz), 119.27 (d, $^{3}J_{CF}$ = 3.1 Hz), 84.72 (d, $^{1}J_{CF}$ = 184.6 Hz), 59.64 , 29.50 . ^{19}F NMR (376 MHz, $CDCl_3$) δ -226.5 (t, J = 47.6 Hz). HRMS (ESI) *m/z* calcd for $C_9H_{13}FN_2O$ $[M+H]^+$ 185.1084, found 185.1081. (**EXC-II-171**)

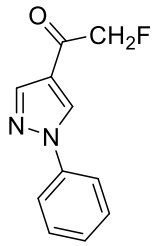

2-fluoro-1-(1-(phenyl)-1*H*-pyrazol-4-yl)ethan-1-one (2-11n): Prepared using the general procedure above (*Method E*) from 4-bromo-1-(phenyl)-1*H*-pyrazole (**2-7n**) (550 mg, 2.50 mmol), ethyl fluoroacetate (0.31 mL, 3.20 mmol), *n*-BuLi (2.5 M in hexanes, 1.18 mL, 2.95 mmol), and THF (7 mL). Concentration of the reaction mixture *in vacuo* followed by silica gel flash chromatography (20 % ethyl acetate in hexanes) gave the product as an light-yellow solid

(130 mg, 25 %); mp 199.1-199.9 ˚C . ^{1}H NMR (400 MHz, $CDCl_3$) δ 8.55 (s, 1H), 8.21 (s, 1H), 7.70 (dq, *J* = 8.2, 1.1 Hz, 2H), 7.47 (t, *J* = 7.6 Hz, 2H), 7.41 – 7.32 (tt, *J* = 7.4, 0.8 Hz, 1H), 5.15 (d, *J* = 47.6 Hz, 2H). ^{13}C NMR (101 MHz, $CDCl_3$) δ 189.7 (d, $^{2}J_{CF}$ = 20.0 Hz), 141.8 (d, $^{2}J_{CF}$ = 5.1 Hz), 139.1, 130.2 (d, $^{3}J_{CF}$ = 10.5 Hz), 129.6, 129.1, 127.9, 125.3, 123.4 (d, $^{4}J_{CF}$ = 3.5 Hz), 119.8, 85.8, 84.0. ^{19}F NMR (376 MHz, $CDCl_3$) δ -226.1 (t, *J* = 47.6 Hz). HRMS (ESI) *m/z* calcd for $C_{11}H_9FN_2O$ $[M+H]^+$ 205.0771, found 205.0763. (**EXC-II-172**)

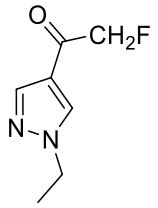

1-(1-ethyl-1*H*-pyrazol-4-yl)-2-fluoroethan-1-one (2-11p): Prepared using the general procedure above (*Method E*) from 4-bromo-1-(ethyl)-1*H*-pyrazole (**2-7p**) (476 mg, 2.72 mmol), ethyl fluoroacetate (0.32 mL, 3.26 mmol), *n*-BuLi (2.5 M in hexanes, 1.14 mL, 2.86 mmol), and THF (7 mL). Concentration of the reaction mixture *in vacuo* followed by silica gel flash chromatography (10 % ethyl acetate in DCM) gave the product as a yellow oil (68 mg, 16 %). ^{1}H NMR (400 MHz, $CDCl_3$) δ 8.03 (s, 1H), 7.98 (s, 1H), 5.07 (d, *J* = 47.4 Hz, 2H), 4.17 (q, *J* = 7.3 Hz, 2H), 1.48 (t, *J* = 7.3 Hz, 3H). ^{13}C NMR (101 MHz, $CDCl_3$) δ 189.46 (d, $^{2}J_{CF}$ = 19.6 Hz), 140.59 (d, $^{4}J_{CF}$ = 5.0 Hz), 131.96 (d, $^{4}J_{CF}$ = 9.7 Hz), 119.77 (d, $^{3}J_{CF}$ = 3.1 Hz), 84.71 (d, $^{1}J_{CF}$ = 184.6 Hz), 47.53, 15.12. ^{19}F NMR (376 MHz, $CDCl_3$) δ -226.3 (t, $^{2}J_{FH}$ = 47.6 Hz). Despite multiple attempts, the molecular ion of this compound was not detected using ESI+, ESI-, and ECI techniques. (**EXC-III-71**)

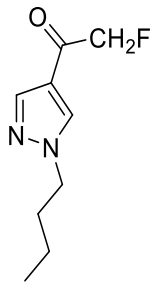

2-fluoro-1-(1-(butyl)-1*H*-pyrazol-4-yl)ethan-1-one (2-11r): Prepared using the general procedure above (*Method E*) from 4-bromo-1-(butyl)-1*H*-pyrazole (**2-7r**) (590 mg, 2.90 mmol), ethyl fluoroacetate (0.34 mL, 3.48 mmol), *n*-BuLi (2.5 M in hexanes, 1.22 mL, 3.05 mmol), and THF (7 mL). Concentration of the reaction mixture *in vacuo* followed by silica gel flash chromatography (20 % ethyl acetate in hexanes) gave the product as a yellow oil (105 mg, 20 %). ^{1}H NMR (400 MHz, $CDCl_3$) δ 8.03 (s, 1H), 8.02 (s, 1H), 5.09 (d, $^{2}J_{HF}$ = 47.5 Hz, 2H), 4.14 (t, *J* = 7.1 Hz, 2H), 1.86 (p, *J* = 7.5 Hz, 2H), 1.31 (h, *J* = 7.5 Hz, 2H), 0.94 (t, *J* = 7.5 Hz, 3H). ^{13}C NMR (101 MHz, $CDCl_3$) δ 189.5 (d, $^{2}J_{CF}$ = 19.5 Hz), 140.6 (d, $^{4}J_{CF}$ = 5.2 Hz), 132.6 (d, $^{4}J_{CF}$ = 9.8 Hz), 119.8, 84.8 (d, $^{1}J_{CF}$ = 184.7 Hz), 52.5, 31.9, 19.6, 13.4. ^{19}F NMR (376 MHz, $CDCl_3$) δ -226.2 (t, $^{2}J_{CF}$ = 48.3 Hz). HRMS (ESI) *m/z* calcd for $C_9H_{13}FN_2O$ $[M+H]^+$ 185.1084, found 185.1090. (**EXC-II-117**)

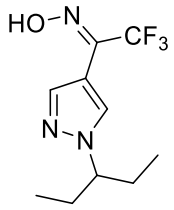

***(E)*-2,2,2-trifluoro-1-(1-pentan-3-yl-1*H*-pyrazol-4-yl)ethan-1-one oxime(3-2g):** Prepared using the modified general procedure above (*Method G*) from 1-(1-(pentan-3-yl)-1*H*-pyrazol-4-yl)-2,2,2-trifluoroethan-1-one (**2-9g**) (200 mg, 0.85 mmol), hydroxylamine hydrochloride (178 mg, 2.56 mmol), sodium hydroxide (102 mg, 2.56 mmol), and EtOH (10 mL). Concentration of

the reaction mixture *in vacuo* followed by silica gel flash chromatography (20 % ethyl acetate in hexanes) gave the product as a white solid (38 mg, 18 %); mp 132.5-133.8 ˚C. ^{1}H NMR (500 MHz, Acetone-d_6) δ 8.07 (d, J = 28.8 Hz, 2H), 3.97 (tt, J = 9.4, 5.0 Hz, 1H), 1.99 – 1.81 (m, 4H), 0.79 (t, J = 7.4 Hz, 6H), OH peak not detected. ^{13}C NMR (126 MHz, Acetone-d_6) δ 139.2 (d, $^{3}J_{CF}$ = 2.6 Hz), 139.1 (q, $^{2}J_{CF}$ = 31.5 Hz), 132.5, 121.7 (q, $^{1}J_{CF}$ = 273.5 Hz), 106.8, 66.4, 27.9, 10.0. ^{19}F NMR (471 MHz, $CDCl_3$) δ -66.6. HRMS (ESI) *m/z* calcd for $C_{10}H_{14}F_3N_3O$ $[M+H]^+$ 250.1161, found 250.1156. (**EXC-II-46**)

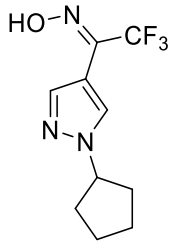

***(E)*-1-(1-cyclopentyl-1*H*-pyrazol-4-yl)-2,2,2-trifluoroethan-1-one oxime (3-2h):** Prepared using the modified general procedure above (*Method G*) from 1-(1-(cyclopentyl)-1*H*-pyrazol-4-yl)-2,2,2-trifluoroethan-1-one (**2-9h**) (200 mg, 0.86 mmol), hydroxylamine hydrochloride (179 mg, 2.58 mmol), sodium hydroxide (103 mg, 2.58 mmol), and EtOH (10 mL). Concentration of the reaction mixture *in vacuo* followed by silica gel flash chromatography (20 % ethyl acetate in hexanes) gave the product as a white solid (50 mg, 24 %); mp 147.1-148.4 ˚C. ^{1}H NMR (400 MHz, Acetone-d_6) δ 11.80 (s, 1H), 8.43 (s, 1H), 7.94 (s, 1H), 4.85 (p, J = 7.1 Hz, 1H), 2.22 – 2.12 (m, 2H), 2.10 – 1.99 (m, 2H), 1.94 – 1.82 (m, 2H), 1.77 – 1.66 (m, 2H). ^{13}C NMR (126 MHz, Acetone-d_6) δ 139.11 (d, $^{2}J_{CF}$ = 31.3 Hz), 138.97 (q, $^{3}J_{CF}$ = 2.1 Hz), 131.34, 121.69 (q, $^{3}J_{CF}$ = 273.5 Hz), 107.15, 62.98, 32.69, 24.04. ^{19}F NMR (376 MHz, Acetone-d_6) δ -66.6. HRMS (ESI) *m/z* calcd for $C_{10}H_{12}F_3N_3O$ $[M+H]^+$ 248.1005, found 248.1011. (**EXC-II-45**)

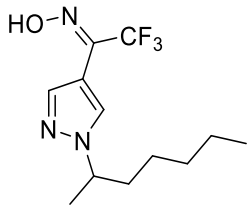

***(E)*-1-(1-heptan-2-yl-1*H*-pyrazol-4-yl)-2,2,2-trifluoroethan-1-one oxime (3-2i):** Prepared using the modified general procedure above (*Method G*) from 1-(1-(heptan-2-yl)-1*H*-pyrazol-4-yl)-2,2,2-trifluoroethan-1-one (**2-9i**) (100 mg, 0.38 mmol), hydroxylamine hydrochloride (79 mg, 1.14 mmol), sodium hydroxide (45 mg, 1.14 mmol), and EtOH (7 mL). Concentration of the reaction mixture *in vacuo* followed by silica gel flash chromatography (10 % ethyl acetate and 10% DCM in hexanes) gave the product as an off-white solid (34 mg, 32 %); 89.4-90.8 ˚C. ^{1}H NMR (400 MHz, $CDCl_3$) δ 10.06 (s, 1H), 8.21 (s, 1H), 8.02 (s, 1H), 4.37 (h, *J* = 6.6 Hz, 1H), 1.99 – 1.87 (m, 1H), 1.81 – 1.69 (m, 1H), 1.52 (d, *J* = 6.8 Hz, 3H), 1.30 – 1.08 (m, 6H), 0.81 (t, *J* = 6.8 Hz, 3H). ^{13}C NMR (101 MHz, $CDCl_3$) δ 140.1 (q, $^{2}J_{CF}$ = 32.4 Hz), 139.6 (q, $^{3}J_{CF}$ = 2.1 Hz), 130.9 , 121.1 (q, $^{1}J_{CF}$ = 274.7 Hz), 107.1, 59.1, 36.8, 31.3, 25.6, 22.4, 21.1, 13.9. ^{19}F NMR (376 MHz, $CDCl_3$) δ -66.6. HRMS (ESI) *m/z* calcd for $C_{12}H_{18}F_3N_3O$ $[M+H]^+$ 278.1474, found 278.1476. (**EXC-II-18**)

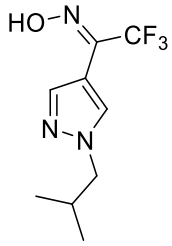

***(E)*-2,2,2-trifluoro-1-(1-isobutyl-1*H*-pyrazol-4-yl)ethan-1-one oxime (3-2j):** Prepared using the general procedure above (*Method F*) from 1-(1-(isobutyl)-1*H*-pyrazol-4-yl)-2,2,2-trifluoroethan-1-one (**2-9j**) (160 mg, 0.73 mmol), hydroxylamine hydrochloride (68 mg, 0.98 mmol), sodium acetate (84 mg, 1.02 mmol), H_2O (5 mL) and EtOH (5 mL). Concentration of the

reaction mixture *in vacuo* gave the product as a white solid (136 mg, 74 %); mp 133.2-134.7 ˚C. ^{1}H NMR (400 MHz, Acetone-d_6) δ 11.81 (s, 1H), 8.41 (s, 1H), 7.93 (s, 1H), 4.05 (d, J = 6.8 Hz, 2H), 2.22 (n, J = 6.8 Hz, 1H), 0.89 (d, J = 6.8 Hz, 6H). ^{13}C NMR (126 MHz, Acetone-d_6) δ 139.1 (q, $^{2}J_{CF}$ = 30.4 Hz), 139.0 (q, $^{4}J_{CF}$ = 2.4 Hz), 132., 121.7 (q, $^{1}J_{CF}$ = 273.5 Hz), 107.3, 59.1, 29.3, 19.1. ^{19}F NMR (376 MHz, Acetone-d_6) δ -66.6. HRMS (ESI) *m/z* calcd for $C_9H_{12}F_3N_3O$ $[M+H]^+$ 236.1005, found 236.1006. (**EXC-II-69**)

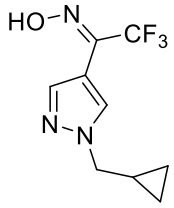

***(E)*and*(Z)*-1-(1-(cyclopropylmethyl)-1*H*-pyrazol-4-yl)-2,2,2-trifluoroethan-1-one oxime (3-2k):** Prepared using the general procedure above (*Method F*) from 1-(1-(cyclopropylmethyl)-1*H*-pyrazol-4-yl)-2,2,2-trifluoroethan-1-one (**2-9k**) (200 mg, 0.92 mmol), hydroxylamine hydrochloride (86 mg, 1.24 mmol), sodium acetate (105 mg, 1.28 mmol), H_2O (5mL) and EtOH (5 mL). Concentration of the reaction mixture *in vacuo* gave the product as a white solid (80 mg, 38 %); mp 116.2-117.5 ˚C. ^{1}H NMR (400 MHz, Acetone-d_6) δ 11.82 (s, 1H), 8.48 (s, 0.75H), 7.98 (s, 0.25H), 7.93 (s, 0.75H), 7.67 (s, 0.25H), 4.10 (d, J = 7.2 Hz, 1.5H), 4.02 (d, J = 7.2 Hz, 0.5H), 1.42 – 1.24 (m, 1H), 0.64 – 0.32 (m, 4H). ^{13}C NMR (101 MHz, Acetone-d_6) δ 139.3 (q, $^{2}J_{CF}$ = 31.8 Hz), 138.9 (q, $^{4}J_{CF}$ = 2.2 Hz), 137.4 (q, $^{4}J_{CF}$ = 1.8 Hz), 132.1, 128.8 (q, $^{4}J_{CF}$ = 2.9 Hz), 121.7 (q, $^{1}J_{CF}$ = 273.5 Hz), 107.5, 56.4, 11.1, 11.1, 3.2, 3.2, doubling of numerous resonances suggests an *E/Z* isomer mixture. ^{19}F NMR (376 MHz, Acetone-d_6) δ -64.7, -66.6, Z/E isomers in a 1:3 ratio. HRMS (ESI) *m/z* calcd for $C_9H_{10}F_3N_3O$ $[M+H]^+$ 238.0848, found 238.0852. (**EXC-II-130**)

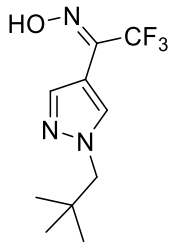

***(E)*-2,2,2-trifluoro-1-(1-neopentyl-1*H*-pyrazol-4-yl)ethan-1-one oxime (3-2l):** Prepared using the general procedure above (*Method C*) from 4-bromo-1-(neopentyl)-1*H*-pyrazole (**2-7l**) (592 mg, 2.92 mmol), methyl trifluoroacetate (0.35 mL, 3.50 mmol), *n*-BuLi (2.5 M in hexanes, 1.45 mL, 3.06 mmol), and THF (8 mL). Concentration of the reaction mixture *in vacuo* followed by silica gel flash chromatography (10 % ethyl acetate in hexanes) gave the desired trifluoromethyl ketoneas a crude oil that was converted to the oxime using the general procedure above (*Method F*). 1-(1-(Neopentyl)-1*H*-pyrazol-4-yl)-2,2,2-trifluoroethan-1-one (**2-9l**) (282 mg, 1.20 mmol), hydroxylamine hydrochloride (113 mg, 1.63 mmol), sodium acetate (139 mg, 1.69 mmol), H_2O (5mL) and EtOH (5 mL). Concentration of the reaction mixture *in vacuo* gave the product as a white solid (131 mg, 44 %); mp 176.4-177.5 ˚C. ^{1}H NMR (400 MHz, Acetone-d_6) δ 11.86 (s, 1H), 8.39 (s, 1H), 8.16 – 7.76 (m, 1H), 4.05 (s, 2H), 0.96 (s, 9H). ^{13}C NMR (101 MHz, Acetone-d_6) δ 139.0 (d, $^{2}J_{CF}$ = 31.5 Hz), 138.7 (q, $^{4}J_{CF}$ = 2.2 Hz), 133.7 (q, $^{4}J_{CF}$ = 1.1 Hz), 123.0 (q, $^{1}J_{CF}$ = 274.1 Hz), 107.2, 62.9, 32.5, 26.9. ^{19}F NMR (376 MHz, Acetone-d_6) δ -66.6. HRMS (ESI) *m/z* calcd for $C_{10}H_{14}F_3N_3O$ $[M+H]^+$ 250.1161, found 250.1164. (**EXC-II-110**)

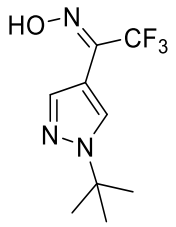

***(E)*and*(Z)*-1-(1-(tert-butyl)-1*H*-pyrazol-4-yl)-2,2,2-trifluoroethan-1-one oxime (3-2m):**

Prepared using the general procedure above (*Method C*) from 4-bromo-1-(*tert*-butyl)-1*H*-pyrazole (**2-7m**) (243 mg, 1.20 mmol), methyl trifluoroacetate (0.14 mL, 1.44 mmol), *n*-BuLi (2.5 M in hexanes, 0.50 mL, 1.26 mmol), and THF (5 mL). Concentration of the reaction mixture *in vacuo* followed by silica gel flash chromatography (5 % ethyl acetate in hexanes) gave the product as an impure pale yellow liquid taken to the next reaction using the general procedure above (*Method F*). 1-(1-(*tert*-butyl)-1*H*-pyrazol-4-yl)-2,2,2-trifluoroethan-1-one (**2-9m**) (83 mg, 0.38 mmol), hydroxylamine hydrochloride (53 mg, 0.77 mmol), and sodium acetate (65 mg, 0.80 mmol) were combined in H_2O (5mL) and EtOH (5 mL). Concentration of the reaction mixture *in vacuo* gave the product as a white solid (70 mg, 80 %); mp 199.5-200.6 ˚C. ^{1}H NMR (400 MHz, Acetone-d_6) δ 11.78 (s, 0.75H), 11.47 (s, 0.25H), 8.34 (s, 0.75H), 7.84 (s, 0.25H), 7.81 (s, 0.75H), 7.56 (s, 0.25H), 1.50 (s, 6.75H), 1.47 (s, 2.25H). ^{13}C NMR (101 MHz, Acetone-d_6) δ 138.6 (q, $^{4}J_{CF}$ = 2.3 Hz), 137.1 (q, $^{4}J_{CF}$ = 2.1 Hz), 130.9, 121.7 (q, $^{1}J_{CF}$ = 272.5 Hz), 59.1, 28.8, 28.8, doubling of numerous resonances suggests an *E/Z* isomer mixture. ^{19}F NMR (376 MHz, Acetone-d_6) δ -64.7, -66.5, Z/E isomers in a 1:3 ratio. HRMS (ESI) *m/z* calcd for $C_9H_{12}F_3N_3O$ $[M+H]^+$ 236.1005, found 236.0991. (**EXC-II-135**)

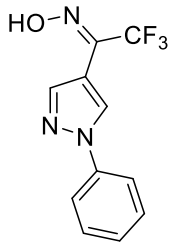

***(E)*and*(Z)*-2,2,2-trifluoro-1-(1-phenyl-1*H*-pyrazol-4-yl)ethan-1-one oxime (3-2n):** The required trifluoromethyl ketone was prepared using the general procedure above (*Method C*) from 4-bromo-1-(phenyl)-1*H*-pyrazole (**2-7n**) (400 mg, 1.79 mmol), methyl trifluoroacetate (0.22 mL, 2.15 mmol), *n*-BuLi (2.5 M in hexanes, 0.75 mL, 1.88 mmol), and THF (7 mL). Concentration of the reaction mixture *in vacuo* followed by silica gel flash chromatography (5 % ethyl acetate in hexanes) gave the product as an impure pale yellow liquid taken to the next reaction using the general procedure above (*Method F*) from 1-(1-(phenyl)-1*H*-pyrazol-4-yl)-2,2,2-trifluoroethan-1-one (**2-9n**) (386 mg crude, 1.61 mmol), hydroxylamine hydrochloride (150 mg, 2.17 mmol), sodium acetate (185 mg, 2.25 mmol) were combined in H_2O (5mL) and EtOH (5 mL). Concentration of the reaction mixture *in vacuo* gave the product as a white solid (120 mg, 29 % over two reactions); mp 213.0-213.9 ˚C. ^{1}H NMR (500 MHz, Acetone-d_6) δ 12.00 (s, 1H), 8.91 (s, 1H), 8.51-6.18 (m, 6H). ^{13}C NMR (126 MHz, Acetone-d_6) δ 141.3, 141.1, 140.9 – 140.5 (m), 139.7 , 139.6, 139.5, 139.5, 138.6 (q, $^{2}J_{CF}$ = 31.9 Hz), 129.7, 129.7, 129.5, 129.5, 129.4, 129.4, 128.4, 128.3, 127.7, 127.6, 127.3, 127.0, 126.9, 126.8, 126.7, 126.6, 122.7, 120.5, 112.0, 119.4, 119.0, 118.6, 109.6, 107.5, doubling of numerous resonances suggests an *E/Z* isomer mixture. ^{19}F NMR (376 MHz, Acetone-d_6) δ -64.7, -66.6, Z/E isomers in a 1:5 ratio. HRMS (ESI) *m/z* calcd for $C_{11}H_8F_3N_3O$ $[M+H]^+$ 256.0692, found 256.0681. (**EXC-II-143**)

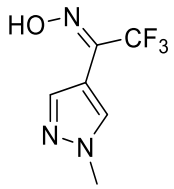

***(E)*-2,2,2-trifluoro-1-(1-methyl-1*H*-pyrazol-4-yl)ethan-1-one oxime (3-2o):** Prepared using the general procedure above (*Method C*) from 4-bromo-1-(methyl)-1*H*-pyrazole (**2-7o**) (681 mg, 4.23 mmol), methyl trifluoroacetate (0.51 mL, 5.08 mmol), *n*-BuLi (2.11 M in hexanes, 2.1 mL, 4.44 mmol), and THF (7 mL). Concentration of the reaction mixture *in vacuo* followed by silica gel flash chromatography (30 % ethyl acetate in hexanes) gave the product as an impure oil. The crude was taken to the next reaction using the general procedure above (*Method F*) from 1-(1-(methyl)-1*H*-pyrazol-4-yl)-2,2,2-trifluoroethan-1-one (**2-9o**) (238 mg crude, 1.34 mmol), hydroxylamine hydrochloride (125 mg, 1.80 mmol), and sodium acetate (154 mg, 1.88 mmol) were combined in H_2O (5mL) and EtOH (5 mL). Concentration of the reaction mixture *in vacuo* gave the product as a white solid (97 mg, 38 % after two reactions); mp 164.8-165.7 ˚C. ^{1}H NMR (400 MHz, Acetone-d_6) δ 11.81 (s, 1H), 8.39 (s, 1H), 7.90 (s, 1H), 3.97 (s, 3H). ^{13}C NMR (126 MHz, Acetone-d_6) δ 139.9 (q, $^{4}J_{CF}$ = 1.8 Hz), 139.7 (q, $^{2}J_{CF}$ = 33.2 Hz), 134.1, 122.6 (q, $^{1}J_{CF}$ = 273.4 Hz), 108.5, 39.2. ^{19}F NMR (376 MHz, Acetone-d_6) δ -66.7. HRMS (ESI) *m/z* calcd for $C_6H_6F_3N_3O$ $[M+H]^+$ 194.0535, found 194.0529. (**EXC-II-111**)

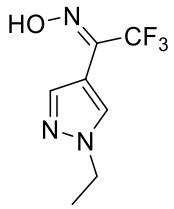

***(E)*-1-(1-ethyl-1*H*-pyrazol-4-yl)-2,2,2-trifluoroethanone oxime (3-2p):** The required trifluoromethyl ketone was prepared using the general procedure above (*Method C*) from 4-

bromo-1-(ethyl)-1*H*-pyrazole (**2-7p**) (676 mg, 3.86 mmol), methyl trifluoroacetate (0.47 mL, 4.05 mmol), *n*-BuLi (2.5 M in hexanes, 1.62 mL, 4.05 mmol), and THF (10 mL). Concentration of the reaction mixture *in vacuo* followed by silica gel flash chromatography (25 % ether in hexanes) gave the product as an impure oil. The crude was taken to the next reaction using the modified general procedure above (*Method G*) from 1-(1-(Ethyl)-1*H*-pyrazol-4-yl)-2,2,2-trifluoroethan-1-one (**2-9p**) (135 mg, 0.70 mmol), hydroxylamine hydrochloride (146 mg, 2.11 mmol), and sodium hydroxide (84 mg, 2.1 mmol) were combined in EtOH (7 mL). Concentration of the reaction mixture *in vacuo* followed by silica gel flash chromatography (20 % ethyl acetate in hexanes) gave the product as an off-white solid (28 mg, 19 %); mp 163.9-164.9 ˚C. ^{1}H NMR (500 MHz, Acetone-d_6) δ 11.83 (s, 1H), 8.45 (s, 1H), 7.94 (s, 1H), 4.29 (q, J = 7.3 Hz, 2H), 1.48 (t, J = 7.3 Hz, 3H). ^{13}C NMR (126 MHz, Acetone-d_6) δ 140.0 (q, $^{2}J_{CF}$ = 31.5 Hz), 139.9 (q, $^{3}J_{CF}$ = 1.8 Hz), 132.8, 122.6 (q, $^{1}J_{CF}$ = 273.5 Hz), 108.3, 47.8, 15.7. ^{19}F NMR (376 MHz, Acetone-d_6) δ -66.6. Despite multiple attempts, the molecular ion of this compound was not detected using ESI+, ESI-, and ECI techniques.. (**EXC-II-36**)

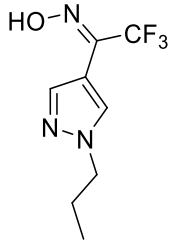

***(E)*-2,2,2-trifluoro-1-(1-propyl-1*H*-pyrazol-4-yl)ethan-1-one oxime (3-2q):** Prepared using the general procedure above (*Method F*) from 1-(1-(propyl)-1*H*-pyrazol-4-yl)-2,2,2-trifluoroethan-1-one (**2-9q**) (200 mg, 0.97 mmol), hydroxylamine hydrochloride (91 mg, 1.31 mmol), sodium acetate (111 mg, 1.36 mmol), H_2O (5mL) and EtOH (5 mL). Concentration of the reaction mixture *in vacuo* gave the product as a white solid (48 mg, 21 %); mp 140.4-141.3

˚C. ^{1}H NMR (400 MHz, Acetone-d_6) δ 11.84 (s, 1H), 8.44 (s, 1H), 7.94 (s, 1H), 4.21 (t, J = 7.0 Hz, 2H), 1.91 (h, J = 7.4 Hz, 2H), 0.90 (t, J = 7.4 Hz, 3H). ^{13}C NMR (101 MHz, Acetone-d_6) δ 140.1 (q, $^{2}J_{CF}$ = 31.3 Hz), 140.0 (q, $^{4}J_{CF}$ = 2.2 Hz), 133.4, 122.6 (q, $^{1}J_{CF}$ = 275.0 Hz), 108.2, 54.4, 24.2, 11.2. ^{19}F NMR (376 MHz, Acetone-d_6) δ -66.6. HRMS (ESI) *m/z* calcd for $C_8H_{10}F_3N_3O$ $[M+H]^+$ 222.0848, found 222.0855. (**EXC-II-59**)

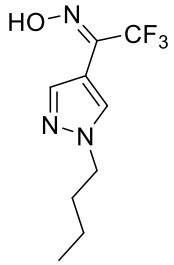

***(E)*-2,2,2-trifluoro-1-(1-butyl-1*H*-pyrazol-4-yl)ethan-1-one oxime (3-2r):** Prepared using the general procedure above (*Method F*) from 1-(1-(butyl)-1*H*-pyrazol-4-yl)-2,2,2-trifluoroethan-1-one (**2-9r**) (200 mg, 0.91 mmol), hydroxylamine hydrochloride (88 mg, 1.23 mmol), sodium acetate (104 mg, 1.27 mmol), H_2O (5 mL) and EtOH (5 mL). Concentration of the reaction mixture *in vacuo* gave the product as a white solid (148 mg, 71 %); mp 96.1-97.4 ˚C. ^{1}H NMR (400 MHz, Acetone-d_6) δ 11.88 (s, 1H), 8.45 (s, 1H), 7.95 (s, 1H), 4.25 (t, J = 7.1 Hz, 2H), 1.94 – 1.8 (p, J = 7.4 Hz 2H), 1.29 (h, J = 7.4 Hz, 2H), 0.93 (t, J = 7.4 Hz, 3H). ^{13}C NMR (101 MHz, Acetone-d_6) δ 139.0 (q, $^{2}J_{CF}$ = 31.5 Hz), 139.0 (q, $^{3}J_{CF}$ = 2.2 Hz), 132.4, 121.7 (q, $^{1}J_{CF}$ = 273.5 Hz), 107.3, 51.6, 32.0, 19.4, 12.8. ^{19}F NMR (376 MHz, Acetone-d_6) δ -66.6. HRMS (ESI) *m/z* calcd for $C_9H_{12}F_3N_3O$ $[M+H]^+$ 236.1005, found 236.1008. (**EXC-II-58**)

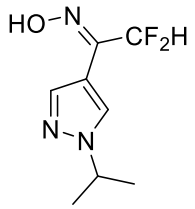

***(E)*-2,2-difluoro-1-(1-isopropyl-1*H*-pyrazol-4-yl)ethan-1-one oxime (3-3d):** Prepared using the general procedure above (*Method G*) from 2,2-difluoro-1-(1-(isopropyl)-1*H*-pyrazol-4-yl)ethan-1-one (**2-10d**) (88 mg, 0.47 mmol), hydroxylamine hydrochloride (61 mg, 0.94 mmol), sodium acetate (77 mg, 0.94 mmol), and EtOH (7 mL). Concentration of the reaction mixture *in vacuo* followed by silica gel flash chromatography (20 % ethyl acetate in hexanes) gave the product as a white solid (85 mg, 90 %); mp 160.1-161.5 ˚C. ^{1}H NMR (400 MHz, Acetone-d_6) δ 11.40 (s, 1H), 8.36 (s, 1H), 8.01 (s, 1H), 6.34 (t, $^{2}J_{HF}$ = 54.2 Hz, 1H), 4.62 (hept, J = 6.7 Hz, 1H), 1.50 (d, J = 6.7 Hz, 6H). ^{13}C NMR (101 MHz, Acetone-d_6) δ 143.59 (t, $^{2}J_{CF}$ = 27.9 Hz), 139.18 (t, $^{4}J_{CF}$ = 2.3 Hz), 129.97, 116.09 (t, $^{1}J_{CF}$ = 237.6 Hz), 107.33 (t, $^{3}J_{CF}$ = 1.7 Hz), 53.83, 22.08. ^{19}F NMR (376 MHz, Acetone-d_6) δ -116.1 (d, $^{2}J_{FH}$ = 54.2 Hz). HRMS (ESI) *m/z* calcd for $C_8H_{11}F_2N_3O$ $[M+H]^+$ 204.0942, found 204.0942. (**EXC-3-17**)

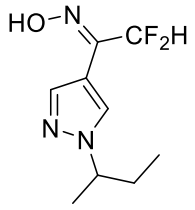

***(E)*-1-(1-(sec-butyl)-1*H*-pyrazol-4-yl)-2,2-difluoroethan-1-one oxime (3-3e):** Prepared using the general procedure above (*Method G*) from 2,2-difluoro-1-(1-(*sec*-butyl)-1*H*-pyrazol-4-yl)ethan-1-one (**2-10e**) (35 mg, 0.17 mmol), hydroxylamine hydrochloride (24 mg, 0.35 mmol), sodium acetate (28 mg, 0.35 mmol), and EtOH (5 mL). Concentration of the reaction mixture *in vacuo* gave the product as an off-white solid (24 mg, 64 %); mp 171.1-172.0 ˚C. ^{1}H NMR (400

MHz, Acetone-d_6) δ 11.38 (s, 1H), 8.37 (s, 1H), 8.02 (s, 1H), 6.37 (t, $^2J_{HF}$ = 54.3 Hz, 1H), 4.38 (h, J = 6.5 Hz 1H), 2.00 – 1.73 (m, 2H), 1.48 (d, J = 6.7 Hz, 3H), 0.76 (t, J = 7.4 Hz, 3H). ^{13}C NMR (101 MHz, Acetone-d_6) δ 143.6 (t, $^2J_{CF}$ = 27.8 Hz), 139.3 (t, $^4J_{CF}$ = 2.3 Hz), 131.0, 116.1 (t, $^1J_{CF}$ = 237.4 Hz), 107.1, 59.7, 29.5, 20.2, 9.9. ^{19}F NMR (376 MHz, Acetone-d_6) δ -116.2 (d, $^2J_{FH}$ = 54.3 Hz). HRMS (ESI) *m/z* calcd for $C_9H_{13}F_2N_3O$ $[M+H]^+$ 218.1099, found 218.1099. (**EXC-III-35**)

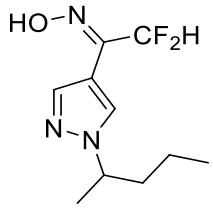

***(E)*-2,2-difluoro-1-(1-(pentan-2-yl)-1*H*-pyrazol-4-yl)ethan-1-one oxime (3-3f):** Prepared using the general procedure above (*Method G*) from 2,2-difluoro-1-(1-(pentan-2-yl)-1*H*-pyrazol-4-yl)ethan-1-one (**2-10f**) (52 mg, 1.15 mmol), hydroxylamine hydrochloride (103 mg, 1.49 mmol), sodium acetate (130 mg, 1.59 mmol), and EtOH (5 mL). Concentration of the reaction mixture *in vacuo* followed by recrystallization with hexane/DCM gave the product as a slight yellow solid (52 mg, 68 %); mp 102.0-103.0 ˚C. ^{1}H NMR (400 MHz, Acetone-d_6) δ 11.37 (s, 1H), 8.38 (s, 1H), 8.00 (s, 1H), 6.37 (t, $^2J_{HF}$ = 54.0 Hz, 1H), 4.48 (h, J = 7.0 Hz, 1H), 1.97-1.68 (m, 2H), 1.48 (d, 2H, J= 6.8 Hz), 1.26-1.11 (m, 2H), 0.86 (t, 3H, J = 8.0 Hz). ^{13}C NMR (101 MHz, Acetone-d_6) δ 143.7, 139.2, 131.0, 116.5 (t, $^1J_{CF}$ = 238.4 Hz), 107.1, 58.0, 38.6, 20.6, 19.0, 13.0. ^{19}F NMR (376 MHz, Acetone-d_6) δ -116.3 (d, $^2J_{FH}$ = 54.0 Hz). HRMS (ESI) *m/z* calcd for $C_{10}H_{15}F_2N_3O$ $[M+H]^+$ 232.1255, found 232.1246. (**KOF-I-010**)

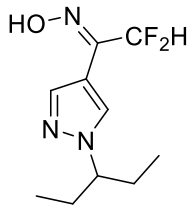

***(E)*-2,2-difluoro-1-(1-(pentan-3-yl)-1*H*-pyrazol-4-yl)ethan-1-one oxime (3-3g):** Prepared using the general procedure above (*Method G*) from 2,2-difluoro-1-(1-(pentan-3-yl)-1*H*-pyrazol-4-yl)ethan-1-one (**2-10g**) (83 mg, 0.38 mmol), hydroxylamine hydrochloride (53 mg, 0.77 mmol), sodium acetate (63 mg, 0.30 mmol), and EtOH (6 mL). Concentration of the reaction mixture *in vacuo* followed by silica gel flash chromatography (5 % ethyl acetate in DCM) gave the product as an off-white solid (65 mg, 73 %); mp 126.8-128.2 ˚C. ^{1}H NMR (400 MHz, Acetone-d_6) δ 11.44 (s, 1H), 8.39 (s, 1H), 8.06 (s, 1H), 6.38 (t, $^{2}J_{HF}$ = 54.2 Hz, 1H), 4.11 (tt, J = 9.5, 4.7 Hz, 1H), 2.00 – 1.76 (m, 4H), 0.73 (t, J = 7.4 Hz, 6H). ^{13}C NMR (101 MHz, Acetone-d_6) δ 143.7 (t, $^{2}J_{CF}$ = 27.7 Hz), 139.5 (t, $^{2}J_{CF}$ = 2.3 Hz), 132.3, 116.2 (t, $^{1}J_{CF}$ = 237.4 Hz), 106.9 (t, $^{3}J_{CF}$ = 1.7 Hz), 27.9, 10.0. ^{19}F NMR (376 MHz, Acetone-d_6) δ -116.2 (d, $^{2}J_{FH}$ = 54.2 Hz). HRMS (ESI) *m/z* calcd for $C_{10}H_{15}F_2N_3O$ $[M+H]^+$ 232.1255, found 232.1255. (**EXC-III-76**)

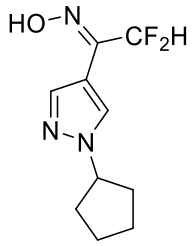

***(E)*-2,2-difluoro-1-(1-(cyclopentyl)-1*H*-pyrazol-4-yl)ethan-1-one oxime (3-3h):** Prepared using the general procedure above (*Method G*) from 2,2-difluoro-1-(1-(cyclopentyl)-1*H*-pyrazol-4-yl)ethan-1-one (**2-10h**) (100 mg, 0.47mmol), hydroxylamine hydrochloride (52 mg, 0.61 mmol), sodium acetate (57 mg, 0.66 mmol), and EtOH (5 mL). Concentration of the reaction

mixture *in vacuo* followed by recrystallization with hexane/DCM gave the product as an off-white solid (52 mg, 56 %); mp 159.0-160.4 ˚C. ^{1}H NMR (400 MHz, Acetone-d_6) δ 11.39 (s, 1H), 8.39 (s, 1H), 8.00 (s, 1H), 6.38 (t, $^{2}J_{HF}$ = 54.0 Hz, 1H), 4.82 (p, J = 7.0 Hz, 1H), 2.19 – 2.11 (m, 2H), 2.06-1.98 (m, 2H), 1.90-1.82 (m, 2H), 1.74-1.68 (m, 2H). ^{13}C NMR (101 MHz, Acetone-d_6) δ 143.7 (t, $^{2}J_{CF}$ = 27.7 Hz), 139.3 (t, $^{2}J_{CF}$ = 2.3 Hz), 131.1, 116.2 (t, $^{1}J_{CF}$ = 236.2 Hz), 107.3, 62.8, 32.7, 24.0. ^{19}F NMR (376 MHz, Acetone-d_6) δ -116.2 (d, $^{2}J_{FH}$ = 56.1 Hz). HRMS (ESI) *m/z* calcd for $C_{10}H_{15}F_2N_3O$ $[M+H]^+$ 230.1093, found 230.1094. (**KOF-I-013**)

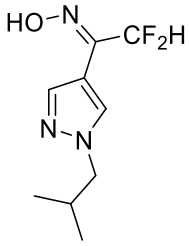

***(E)*-2,2-difluoro-1-(1-isobutyl-1*H*-pyrazol-4-yl)ethan-1-one oxime (3-3j):** Prepared using the general procedure above (*Method G*) from 2,2-difluoro-1-(1-isobutyl-1*H*-pyrazol-4-yl)ethan-1-one (**2-10j**) (30 mg, 0.148 mmol), O-methyl hydroxylamine hydrochloride (21 mg, 0.30 mmol), sodium acetate (24 mg, 0.30 mmol), and EtOH (4 mL). Concentration of the reaction mixture *in vacuo* followed by silica gel flash chromatography (5 % ethyl acetate in DCM) gave the product as an off-white solid (24 mg, 75 %); mp 122.0-123.2 ˚C. ^{1}H NMR (400 MHz, Acetone-d_6) δ 11.43 (s, 1H), 8.37 (s, 1H), 8.01 (s, 1H), 6.38 (t, $^{2}J_{HF}$ = 54.2 Hz, 1H), 4.03 (d, J = 6.6 Hz, 2H), 2.23 (n, J = 6.6 Hz, 1H), 0.89 (d, J = 6.6 Hz, 6H). ^{13}C NMR (101 MHz, Acetone-d_6) δ 143.6 (t, $^{2}J_{CF}$ = 27.7 Hz), 139.4 (t, $^{4}J_{CF}$ = 2.3 Hz), 132.7, 116.1 (t, $^{1}J_{CF}$ = 237.3 Hz), 107.4, 59.0, 29.3, 19.1. ^{19}F NMR (376 MHz, Acetone-d_6) δ -116.2 (d, $^{1}J_{FH}$ = 54.0 Hz). HRMS (ESI) *m/z* calcd for $C_9H_{13}F_2N_3O$ $[M+H]^+$ 218.1099, found 218.1080. (**EXC-III-90**)

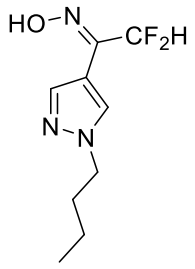

***(E)*-1-(1-butyl-1*H*-pyrazol-4-yl)-2,2-difluoroethan-1-one oxime (3-3r):** Prepared using the general procedure above (*Method G*) from 2,2-difluoro-1-(1-(butyl)-1*H*-pyrazol-4-yl)ethan-1-one (**2-10r**) (100 mg, 0.53 mmol), hydroxylamine hydrochloride (50 mg, 0.72 mmol), sodium acetate (61 mg, 0.74 mmol), and EtOH (5 mL). Concentration of the reaction mixture *in vacuo* followed by silica gel flash chromatography (20 % ethyl acetate in hexanes) gave the product as a white solid (74 mg, 64 %); mp 172.0-173.2 ˚C . ^{1}H NMR (400 MHz, $CDCl_3$) δ 11.07 (s, 1H), 8.22 (s, 1H), 8.19 (s, 1H), 6.27 (t, $^{2}J_{HF}$ = 54.1 Hz, 1H), 4.19 (t, *J* = 7.2 Hz, 2H), 1.87 (p, t, *J* = 7.2 Hz, 2H), 1.32 (h, *J* = 7.2 Hz, 2H), 0.92 (t, *J* = 7.2 Hz, 3H). ^{13}C NMR (101 MHz, $CDCl_3$) δ 144.0 (t, $^{4}J_{CF}$ = 28.1 Hz), 140.5 (t, $^{4}J_{CF}$ = 2.0 Hz), 132.5, 115.6 (t, $^{1}J_{CF}$ = 239.3 Hz), 108.0, 52.3, 32.3, 19.8, 13.6. ^{19}F NMR (376 MHz, $CDCl_3$) δ -115.4 (d, $^{2}J_{FH}$ = 54.2 Hz). Despite multiple attempts, the molecular ion of this compound was not detected using ESI+, ESI-, and ECI techniques.

(**EXC-III-8**)

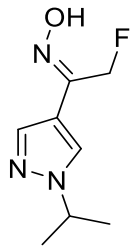

***(Z)*-2-fluoro-1-(1-isopropyl-1*H*-pyrazol-4-yl)ethan-1-one oxime (3-4d):** Prepared using the general procedure above (*Method F*) from 2-fluoro-1-(1-(isopropyl)-1*H*-pyrazol-4-yl)ethan-1-one (**2-11d**) (crude, 2.64 mmol), hydroxylamine hydrochloride (247 mg, 3.56 mmol), sodium

acetate (304 mg, 3.70 mmol), water (5 mL) and EtOH (5 mL). Concentration of the reaction mixture *in vacuo* followed by silica gel flash chromatography (20 % acetone in hexane) gave the product as an light-yellow solid (40 mg, 16 %); mp 134.9-136.4 ˚C. ^{1}H NMR (400 MHz, Acetone-d_6) δ 10.79 (s, 1H), 8.35 (s, 1H), 7.96 (s, 1H), 5.19 (d, $^{2}J_{HF}$ = 47.8 Hz, 2H), 4.60 (hept, *J* = 6.7 Hz, 1H), 1.49 (d, *J* = 6.7 Hz, 6H). ^{13}C NMR (101 MHz, Acetone-d_6) δ 144.8 (d, $^{2}J_{CF}$ = 18.3 Hz), 139.3 (d, $^{4}J_{CF}$ = 1.7 Hz), 129.7, 111.7, 83.3 (d, $^{1}J_{CF}$ = 165.2 Hz), 53.7, 22.1. ^{19}F NMR (376 MHz, Acetone-d_6) δ -215.4 (t, $^{2}J_{FH}$ = 47.8 Hz). HRMS (ESI) *m/z* calcd for $C_8H_{12}FN_3O$ $[M+H]^+$ 186.1037, found 186.1036. (**EXC-II-154**)

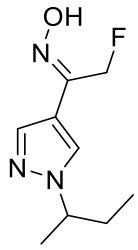

***(Z)*-1-(1-(sec-butyl)-1*H*-pyrazol-4-yl)-2-fluoroethan-1-one oxime (3-4e):** Prepared using the general procedure above (*Method G*) from 2-fluoro-1-(1-(*sec*-butyl)-1*H*-pyrazol-4-yl)ethan-1-one (**2-11e**) (crude, 2.5 mmol), hydroxylamine hydrochloride (218 mg, 3.88 mmol), sodium acetate (287 mg, 3.5 mmol), and EtOH (5 mL). Concentration of the reaction mixture *in vacuo* followed by silica gel flash chromatography (30 % ethyl acetate in hexane) gave the product as an light-yellow solid (75 mg, 15 % over two reactions); mp 145.9-147.4 ˚C. ^{1}H NMR (500 MHz, Acetone-d_6) δ 10.86 (s, 1H), 8.38 (s, 1H), 8.01 (s, 1H), 5.22 (d, $^{2}J_{HF}$ = 47.8 Hz, 2H), 4.38 (h, *J* = 6.7 Hz, 1H), 2.02 – 1.88 (m, 1H), 1.88 – 1.76 (m, 1H), 1.50 (d, *J* = 6.7 Hz, 3H), 0.79 (t, *J* = 6.7 Hz, 3H). ^{13}C NMR (126 MHz, Acetone-d_6) δ 144.9 (d, $^{2}J_{CF}$ = 18.3 Hz), 139.4 (d, $^{4}J_{CF}$ = 1.5 Hz), 130.8, 111.5, 83.3 (d, $^{1}J_{CF}$ = 165.2 Hz), 59.7, 29.6, 20.3, 9.9. ^{19}F NMR (471 MHz, Acetone-d_6) δ -215.3 (t, $^{2}J_{FH}$ = 47.8 Hz). HRMS (ESI) *m/z* calcd for $C_9H_{14}FN_3O$ $[M+H]^+$ 200.1193, found 200.1194. (**EXC-II-163**)

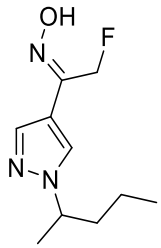

***(Z)*-2-fluoro-1-(1-(pentan-2-yl)-1*H*-pyrazol-4-yl)ethan-1-one oxime (3-4f):** Prepared using the general procedure above (*Method F*) from 2-fluoro-1-(1-(pentan-2-yl)-1*H*-pyrazol-4-yl)ethan-1-one (**2-11f**) (crude, 2.35 mmol), hydroxylamine hydrochloride (220 mg, 3.2 mmol), sodium acetate (269 mg, 3.3 mmol), water (5 mL) and EtOH (5 mL). Concentration of the reaction mixture *in vacuo* followed by silica gel flash chromatography (20 % ethyl acetate in hexane) gave the product as an light-yellow solid (54 mg, 11 % over two reactions); mp 100.5-101.6 ˚C. ^{1}H NMR (500 MHz, Acetone-d_6) δ 10.88 (s, 1H), 8.39 (s, 1H), 8.01 (s, 1H), 5.22 (d, $^{2}J_{HF}$ = 47.8 Hz, 2H), 4.51 (h, J = 6.7 Hz, 1H), 2.00 – 1.90 (m, 1H), 1.81 – 1.69 (m, 1H), 1.50 (d, J = 6.7 Hz, 3H), 1.31 – 1.19 (m, 1H), 1.18 – 1.06 (m, 1H), 0.89 (t, J = 7.4 Hz, 3H). ^{13}C NMR (126 MHz, Acetone-d_6) δ 144.8 (d, $^{2}J_{CF}$ = 18.3 Hz), 139.4 (d, $^{4}J_{CF}$ = 1.5 Hz), 130.7, 111.6, 83.3 (d, $^{1}J_{CF}$ = 165.2 Hz), 58.0, 38.7, 20.7, 19.1, 13.0. ^{19}F NMR (471 MHz, Acetone-d_6) δ -215.2 (t, $^{2}J_{FH}$ = 47.8 Hz). HRMS (ESI) *m/z* calcd for $C_{10}H_{16}FN_3O$ $[M+H]^+$ 214.1352, found 214.1346. (**EXC-II-160**)

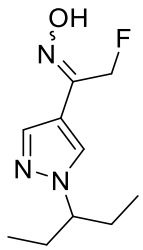

***(E)*and*(Z)*-2-fluoro-1-(1-(pentan-3-yl)-1*H*-pyrazol-4-yl)ethan-1-one oxime (3-4g):** Prepared using the general procedure above (*Method F*) from 2-fluoro-1-(1-(pentan-3-yl)-1*H*-pyrazol-4-yl)ethan-1-one (**2-11g**) (69 mg, 0.35 mmol), hydroxylamine hydrochloride (33 mg, 0.47 mmol),

sodium acetate (40 mg, 0.49 mmol), water (3 mL) and EtOH (3 mL). Concentration of the reaction mixture *in vacuo* followed by silica gel flash chromatography (35 % ethyl acetate in hexane) gave the product as a white solid (61 mg, 82 %); mp 128.9-130.1 ˚C. ^{1}H NMR (500 MHz, Acetone-d_6) δ 10.90 (s, 0.95H), 10.70 (s, 0.05H), 8.49 (s, 0.05H), 8.36 (s, 0.95H), 8.02 (s, 0.95H), 7.83 (s, 0.05H), 5.53 (d, $^{2}J_{HF}$ = 48.0 Hz, 0.1H), 5.22 (d, $^{2}J_{HF}$ = 48.0 Hz, 1.9H), 4.07 (tt, *J* = 8.2, 4.7 Hz, 1H), 1.99 – 1.76 (m, 4H), 0.74 (t, *J* = 7.4 Hz, 5.7H), 0.72 (t, *J* = 7.4 Hz, 0.3H). ^{13}C NMR (126 MHz, Acetone-d_6) δ 149.5, 147.1, 145.7, 141.8, 141.0, 140.5 (d, $^{4}J_{CF}$ = 1.3 Hz), 138.5, 137.8, 133.4, 132.8, 112.3, 110.2, 84.2 (d, $^{1}J_{CF}$ = 165.3 Hz), 77.2 (d, $^{1}J_{CF}$ = 164.8 Hz), 71.7, 67.1, 65.6, 28.9, 10.9, doubling of numerous resonances suggests an *E/Z* isomer mixture. ^{19}F NMR (471 MHz, Acetone-d_6) δ -215.19 (t, *J* = 48.0 Hz), -231.6 (t, *J* = 48.0 Hz), E/Z isomers in a 24:1 ratio. HRMS (ESI) *m/z* calcd for $C_{10}H_{16}FN_3O$ $[M+H]^+$ 214.1350, found 214.1351. (**EXC-II-123**)

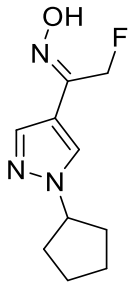

***(Z)*-1-(1-cyclopentyl-1*H*-pyrazol-4-yl)-2-fluoroethan-1-one oxime (3-4h):** Prepared using the general procedure above (*Method F*) from 2-fluoro-1-(1-(cyclopentyl)-1*H*-pyrazol-4-yl)ethan-1-one (**2-11h**) (crude, 2.45 mmol), hydroxylamine hydrochloride (229 mg, 3.3 mmol), sodium acetate (281 mg, 3.43 mmol), water (5 mL) and EtOH (5 mL). Concentration of the reaction mixture *in vacuo* followed by silica gel flash chromatography (20 % ethyl acetate in hexane) gave the product as a light-yellow solid (100 mg, 19 % over two reactions); mp 129.9-130.8 ˚C.

^{1}H NMR (400 MHz, Acetone-d_6) δ 10.82 (s, 1H), 8.35 (s, 1H), 7.97 (s, 1H), 5.19 (d, $^{2}J_{HF}$ = 47.8 Hz, 2H), 4.94 – 4.66 (p, J = 7.1 Hz, 1H), 2.20 – 2.08 (m, 2H), 2.08 – 1.96 (m, 2H), 1.93 – 1.79 (m, 2H), 1.76 – 1.62 (m, 2H). ^{13}C NMR (101 MHz, Acetone-d_6) δ 144.8 (d, $^{2}J_{HF}$ = 18.3 Hz), 139.5 (d, $^{4}J_{HF}$ = 1.7 Hz), 130.8, 111.8, 83.2 (d, $^{1}J_{CF}$ = 165.3 Hz), 62.8, 32.7, 24.0. ^{19}F NMR (376 MHz, Acetone-d_6) δ -215.3 (t, $^{2}J_{FH}$ = 47.8 Hz). HRMS (ESI) *m/z* calcd for $C_{10}H_{14}FN_3O$ $[M+H]^+$ 212.1193, found 212.1189. (**EXC-II-158**)

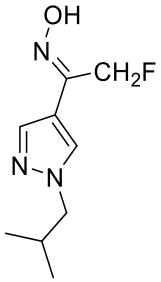

***(Z)*-2-fluoro-1-(1-isobutyl-1*H*-pyrazol-4-yl)ethan-1-one oxime (3-4j):** Prepared using the general procedure above (*Method G*) from 2-fluoro-1-(1-isobutyl-1*H*-pyrazol-4-yl)ethan-1-one (**2-11j**) (30 mg, 0.16 mmol), hydroxylamine hydrochloride (23 mg, 0.31 mmol), sodium acetate (26 mg, 0.31 mmol), and EtOH (4 mL). Concentration of the reaction mixture *in vacuo* followed by silica gel flash chromatography (100 % DCM) gave the product as a yellow solid (26 mg, 81 %); mp 129.0-130.1 ˚C. ^{1}H NMR (400 MHz, Acetone-d_6) δ 10.83 (s, 1H), 8.33 (s, 1H), 7.96 (s, 1H), 5.19 (d, $^{2}J_{HF}$ = 47.7 Hz, 2H), 4.00 (d, J = 7.2 Hz, 2H), 2.28 – 2.15 (n, J = 7.2 Hz, 1H), 0.89 (d, J = 6.7 Hz, 6H). ^{13}C NMR (101 MHz, Acetone-d_6) δ 144.8 (d, $^{2}J_{CF}$ = 18.4 Hz), 139.5 (d, $^{3}J_{CF}$ = 1.8 Hz), 132.5, 111.8, 83.3 (d, $^{1}J_{CF}$ = 165.2 Hz), 59.0, 29.4, 19.1. ^{19}F NMR (376 MHz, Acetone-d_6) δ -215.4 (t, $^{2}J_{FH}$ = 47.7 Hz). HRMS (ESI) *m/z* calcd for $C_9H_{14}FN_3O$ $[M+H]^+$ 200.1193, found 200.1197. (**EXC-III-89**)

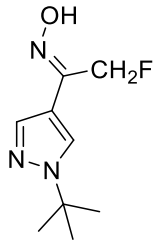

***(Z)*-1-(1-(tert-butyl)-1*H*-pyrazol-4-yl)-2-fluoroethan-1-one oxime (3-4m):** Prepared using the general procedure above (*Method G*) from 2-fluoro-1-(1-(tert-butyl)-1*H*-pyrazol-4-yl)ethan-1-one (**2-11m**) (38 mg, 0.21 mmol), hydroxylamine hydrochloride (20 mg, 0.28 mmol), sodium acetate (24 mg, 0.29 mmol), and EtOH (5 mL). Concentration of the reaction mixture *in vacuo* followed by silica gel flash chromatography (20 % ethyl acetate in hexane) gave the product as a white solid (14 mg, 34 %); mp 169.0-170.6 ˚C. ^{1}H NMR (400 MHz, Acetone-d_6) δ 10.74 (s, 1H), 8.37 (s, 1H), 7.99 (s, 1H), 5.19 (d, $^{2}J_{HF}$ = 47.8 Hz, 2H), 1.59 (s, 9H). ^{13}C NMR (101 MHz, acetone) δ 144.9 (d, $^{2}J_{CF}$ = 18 Hz) 139.2 (d, $^{3}J_{CF}$ = 1 Hz), 128.4, 111.7, 83.3 (d, $^{1}J_{CF}$ = 166 Hz), 58.6, 28.9. ^{19}F NMR (376 MHz, Acetone-d_6) δ -215.7 (t, J = 47.8 Hz). HRMS (ESI) *m/z* calcd for $C_9H_{14}FN_3O$ $[M+H]^+$ 200.1192, found 200.1191. (**EXC-II-173**)

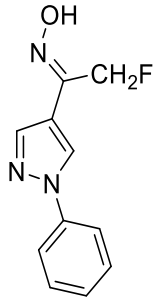

***(Z)*-2-fluoro-1-(1-phenyl-1*H*-pyrazol-4-yl)ethan-1-one oxime (3-4n)**: Prepared using the general procedure above (*Method F*) from 2-fluoro-1-(1-(phenyl)-1*H*-pyrazol-4-yl)ethan-1-one (**2-11n**) (36 mg, 0.18 mmol), hydroxylamine hydrochloride (17 mg, 0.24 mmol), sodium acetate (21 mg, 0.25 mmol), water (3 mL) and EtOH (3 mL). Concentration of the reaction mixture *in*

vacuo followed by silica gel flash chromatography (20 % ethyl acetate in hexane) gave the product as a white solid (18 mg, 47 %); mp 92.1-94.0 ˚C. ^{1}H NMR (400 MHz, Acetone-d_6) δ 11.05 (s, 1H), 8.96 (q, J = 0.6 Hz, 1H), 8.25 (d, J = 0.6 Hz, 1H), 7.90 (dd, J = 8.7, 1.1 Hz, 2H), 7.52 (t, J = 7.3, 2H), 7.35 (tt, J = 7.3, 1.1 Hz, 1H), 5.37 (d, $^{2}J_{HF}$ = 47.7 Hz, 2H). ^{13}C NMR (101 MHz, acetone) δ 144.3 (d, $^{2}J_{CF}$ = 19 Hz), 141.5, 141.5, 139.8, 129.5, 129.4, 129.1, 126.8, 126.5, 119.1, 118.7, 114.2, 83.1 (d, $^{1}J_{CF}$ = 166 Hz). ^{19}F NMR (376 MHz, Acetone-d_6) δ -215.7 (t, J = 47.7 Hz). HRMS (ESI) *m/z* calcd for $C_{11}H_{10}FN_3O$ $[M+H]^+$ 220.0880, found 220.0882. (**EXC-II-174**)

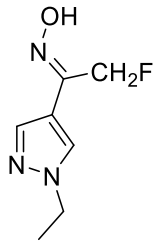

***(Z)*-1-(1-ethyl-1*H*-pyrazol-4-yl)-2-fluoroethan-1-one oxime (3-4p):** Prepared using the general procedure above (*Method G*) from 2-fluoro-1-(1-(ethyl)-1*H*-pyrazol-4-yl)ethan-1-one (**2-11p**) (40 mg, 0.26 mmol), hydroxylamine hydrochloride (35 mg, 0.51 mmol), sodium acetate (42 mg, 0.51 mmol), and EtOH (5 mL). Concentration of the reaction mixture *in vacuo* followed by silica gel flash chromatography (20 % ethyl acetate in DCM) gave the product as an light-yellow solid (30 mg, 70 %); mp 99.2-101.5 ˚C. ^{1}H NMR (400 MHz, Acetone-d_6) δ 10.81 (s, 1H), 8.34 (s, 1H), 7.95 (s, 1H), 5.18 (d, $^{2}J_{HF}$ = 47.8 Hz, 2H), 4.25 (q, J = 7.3 Hz, 2H), 1.44 (t, J = 7.3 Hz, 3H). ^{13}C NMR (101 MHz, Acetone-d_6) δ 144.7 (d, $^{2}J_{CF}$ = 18.0 Hz), 139.5 (d, $^{3}J_{CF}$ = 1.8 Hz), 131.4, 112.0, 83.3 (d, $^{1}J_{CF}$ = 165.1 Hz), 46.7, 14.9. ^{19}F NMR (376 MHz, Acetone-d_6) δ -215.4 (t, J = 47.8 Hz). Despite multiple attempts, the molecular ion of this compound was not detected using ESI+, ESI-, and ECI techniques.. (**EXC-III-79**)

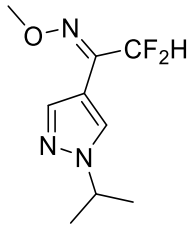

***(E)*-2,2-difluoro-1-(1-(isopropyl)-1*H*-pyrazol-4-yl)ethan-1-one O-methyl oxime (3-6d):** Prepared using the general procedure above (*Method G*) from 2,2-difluoro-1-(1-(isopropyl)-1*H*-pyrazol-4-yl)ethan-1-one (**2-10d**) (50 mg, 0.31 mmol), *O*-methyl hydroxylamine hydrochloride (57 mg, 0.40mmol), sodium acetate (67 mg, 0.43 mmol), and EtOH (5 mL). Concentration of the reaction mixture *in vacuo* followed by silica gel flash chromatography (100 % DCM) gave the product as a clear oil (49 mg, 75 %). ^{1}H NMR (400 MHz, $CDCl_3$) δ 8.08 (s, 1H), 8.04 (s, 1H), 6.33-6.05 (t, 1H, $^{2}J_{FH}$ = 52.6 Hz), 4.56-4.46 (hept, 1H, *J* = 7.4 Hz), 4.04 (s, 3H), 1.52-1.50 (d, 6H, *J* = 7.4 Hz). ^{13}C NMR (101 MHz, $CDCl_3$) δ 143.2 (t, $^{2}J_{CF}$ = 24.5 Hz), 140.1, 129.7, 115.5 (t, $^{1}J_{CF}$ = 241 Hz), 107.4, 63.1, 54.2, 22.7. ^{19}F NMR (376 MHz, $CDCl_3$) δ -115.0 (d, *J* = 52.6 Hz). HRMS (ESI) *m/z* calcd for $C_9H_{13}F_2N_3O$ $[M+H]^+$ 218.1099, found 218.1098. (**KOF-I-014**)

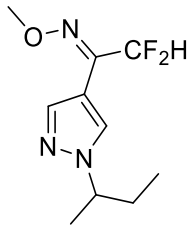

***(E)*-2,2-difluoro-1-(1-(sec-butyl)-1*H*-pyrazol-4-yl)ethan-1-one O-methyl oxime (3-6e):** Prepared using the general procedure above (*Method G*) from 2,2-difluoro-1-(1-(sec-butyl)-1*H*-pyrazol-4-yl)ethan-1-one (**2-10e**) (100 mg, 0.50 mmol), *O*-methyl hydroxylamine hydrochloride (54 mg, 0.64mmol), sodium acetate (57 mg, 0.69 mmol), and EtOH (5 mL). Concentration of the reaction mixture *in vacuo* followed by silica gel flash chromatography (20% ethyl acetate in DCM)

gave the product as a clear oil (81 mg, 73 %). ^{1}H NMR(400 MHz, $CDCl_3$): δ(ppm) = 8.06 (s, 1H), 8.04 (s, 1H), 6.17 (t, $^{2}J_{FH}$ = 52.6 Hz, 1H), 4.19 (h, J = 6.7 Hz, 1H), 4.06 (s, 3H), 1.98-1.73 (m, 2H), 1.50 (d, 3H, *J* = 4.0 Hz), 0.82 (t, 1H, *J* = 6.0 Hz). ^{13}CNMR (100 MHz, $CDCl_3$): δ(ppm) = 143.2, 140.2, 130.4, 115.3 ($^{1}J_{CF}$ = 241.2 Hz), 107.3, 63.1, 60.3, 29.9, 20.7, 10.5. ^{19}FNMR (376 MHz, $CDCl_3$): δ(ppm) = -115.0 (d, $^{2}J_{HF}$ = 52.6 Hz). HRMS (ESI) *m/z* calcd for $C_{10}H_{15}F_2N_3O$ $[M+H]^+$ 232.1255, found 232.1252. (**KOF-I-015**)

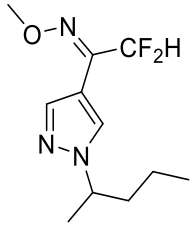

***(E)*-2,2-difluoro-1-(1-(pentan-2-yl)-1*H*-pyrazol-4-yl)ethan-1-one O-methyl oxime (3-6f):** Prepared using the general procedure above (*Method G*) from 2,2-difluoro-1-(1-(pentan-2-yl)-1*H*-pyrazol-4-yl)ethan-1-one (**2-10f**) (120 mg, 0.55 mmol), *O*-methyl hydroxylamine hydrochloride (77 mg, 0.72 mmol), sodium acetate (75 mg, 0.77 mmol), and EtOH (5 mL). Concentration of the reaction mixture *in vacuo* followed by silica gel flash chromatography (20% ethyl acetate in DCM) gave the product as a clear oil (95 mg, 77 %). ^{1}H NMR (400 MHz,$CDCl_3$): δ(ppm) = 8.05 (s, 1H), 8.03 (s, 1H), 6.17 (t, $^{2}J_{HF}$ = 52.6 Hz, 1H), 4.29 (h, *J* = 6.7 Hz, 1H), 4.06 (s, 3H), 1.95-1.65 (m, 2H), 1.48 (d, 3H, J = 8.0 Hz), 1.27-1.09 (m, 2H), 0.89 (t, 1H, *J* = 6.5 Hz). ^{13}C NMR (100MHz, $CDCl_3$): δ(ppm) = 143.2, 140.1, 130.3, 115.3 ($^{1}J_{CF}$ = 241 Hz), 107.3, 63.1, 58.6, 39.0, 21.1, 19.3, 13.6. ^{19}F NMR (376MHz, $CDCl_3$): δ(ppm) = -115.0 (d, $^{2}J_{HF}$ = 52.6 Hz). HRMS (ESI) *m/z* calcd for $C_{11}H_{17}F_2N_3O$ $[M+H]^+$ 246.1417, found 246.1411. (**KOF-I-16**)

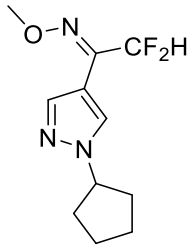

***(E)*-2,2-difluoro-1-(1-(cyclopentyl)-1*H*-pyrazol-4-yl)ethan-1-one O-methyl oxime (3-6h):** Prepared using the general procedure above (*Method G*) from 2,2-difluoro-1-(1-(cyclopentyl)-1*H*-pyrazol-4-yl)ethan-1-one (**2-10f**) (150 mg, 0.70 mmol), *O*-methyl hydroxylamine hydrochloride (100 mg, 0.91 mmol), sodium acetate (102 mg, 0.98 mmol), and EtOH (5 mL). Concentration of the reaction mixture *in vacuo* followed by silica gel flash chromatography (20% ethyl acetate in DCM) gave the product as a clear oil (100 mg, 63 %). ^{1}H NMR (400MHz,$CDCl_3$): δ(ppm) = 8.08 (s, 1H), 8.03 (s, 1H), 6.32-6.06 (t, 1H, $^{2}J_{FH}$ = 54 Hz), 4.65 (p, 1H, *J* = 7.3 Hz), 4.04 (s, 3H), 2.18-2.12 (m, 2H), 2.04-1.96 (m, 2H), 1.90-1.81 (m, 2H), 1.74-1.66 (m, 2H). ^{13}C NMR (100 MHz, $CDCl_3$): δ(ppm) = 143.2, 140.3, 130.5, 115.5 ($^{1}J_{CF}$ = 241 Hz), 110.9, 62.8, 33.0, 24.1. ^{19}F NMR (376MHz, $CDCl_3$): δ(ppm) = -115.1 (d, $^{2}J_{HF}$ = 52.6 Hz). HRMS (ESI) *m/z* calcd for $C_{11}H_{15}F_2N_3O$ $[M+H]^+$ 244.1255, found 244.1252. (**KOF-I-017**)

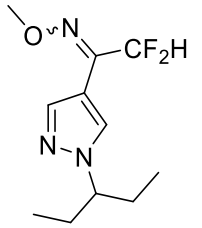

***(E)*and*(Z)*-2,2-difluoro-1-(1-(pentan-3-yl)-1*H*-pyrazol-4-yl)ethan-1-one O-methyl oxime (3-6g):** Prepared using the general procedure above (*Method G*) from 2,2-difluoro-1-(1-(pentan-3-yl)-1*H*-pyrazol-4-yl)ethan-1-one (**2-10g**) (100 mg, 0.46 mmol), *O*-methyl hydroxylamine hydrochloride (77 mg, 0.93 mmol), sodium acetate (76 mg, 0.93 mmol), and EtOH (7 mL). Concentration of the reaction mixture *in vacuo* followed by silica gel flash chromatography (50

% DCM in hexanes) gave the product as a clear oil (55 mg, 49 %). ^{1}H NMR (400 MHz, $CDCl_3$) δ 8.05 (s, 0.22H), 8.03 (s, 1H), 7.82 (s, 0.77H), 7.68 (s, 0.77H), 7.00 (t, $^{2}J_{HF}$ = 54.0 Hz, 1.4H), 6.19 (t, $^{2}J_{HF}$ = 54.0 Hz, 0.6H), 4.05 (s, 0.9 H),3.95 (s, 2.1H), 3.87 (tt, *J* = 8.2, 4.7 Hz, 1H), 2.02 – 1.62 (m, 4H), 0.75 (t, *J* = 7.4 Hz, 6H). ^{13}C NMR (101 MHz, $CDCl_3$) δ 145.9 (t, $^{2}J_{CF}$ = 24.5 Hz), 140.3, 137.9 (t, $^{4}J_{CF}$ = 1.5 Hz), 131.5, 128.1, 110.6, 106.4 (t, $^{1}J_{CF}$ = 239.7 Hz), 66.9, 66.9, 63.0, 62.8, 28.3, 28.2, 10.6, doubling of numerous resonances suggests an *E/Z* isomer mixture. ^{19}F NMR (376 MHz, $CDCl_3$) δ -115.1 (d, *J* = 54.6 Hz), -124.1 (d, *J* = 53.5 Hz) *E/Z* isomers in a 7:2 ratio. HRMS (ESI) *m/z* calcd for $C_{11}H_{17}F_2N_3O$ $[M+H]^+$ 246.1418, found 246.1425. (**EXC-III-77**)

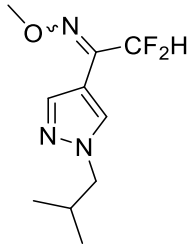

***(E)*and*(Z)*-2,2-difluoro-1-(1-isobutyl-1*H*-pyrazol-4-yl)ethan-1-one O-methyl oxime (3-6j):** Prepared using the general procedure above (*Method G*) from 2,2-difluoro-1-(1-isobutyl-1*H*-pyrazol-4-yl)ethan-1-one (**2-10j**) (30 mg, 0.148 mmol), *O*-methyl hydroxylamine hydrochloride (0.025 mg, 0.30 mmol), sodium acetate (24 mg, 0.30 mmol), and EtOH (4 mL). Concentration of the reaction mixture *in vacuo* followed by silica gel flash chromatography (100 % DCM) gave the product as an light-yellow oil (17 mg, 51 %). ^{1}H NMR (400 MHz, $CDCl_3$) δ 8.04 (s, 0.6H), 7.81 (s, 0.7H), 7.67 (s, 0.7H), 7.00 (t, $^{2}J_{HF}$ = 54.0 Hz, 0.6H), 6.19 (t, $^{2}J_{HF}$ = 54.0 Hz, 0.4H), 4.05 (s, 0.9H), 3.96 (s, 2.1H), 3.91 (d, *J* = 7.3 Hz, 0.6H), 3.89 (d, *J* = 7.3 Hz, 1.4H), 2.42 – 2.06 (n, *J* = 7.2 Hz, 1H), 0.90 (d, *J* = 6.7, 6H). ^{13}C NMR (101 MHz, $CDCl_3$) δ 145.7 (t, $^{2}J_{CF}$ = 24.6 Hz), 140.4, 138.0, 132.4, 129.2, 115.2 (t, $^{1}J_{CF}$ = 239.7 Hz), 106.4 (t, $^{1}J_{CF}$ = 239.7 Hz), 63.1, 62.8,

59.89 59.8, 29.5, 29.5, 19.8, the doubling of numerous resonances suggests an *E/Z* isomer mixture. ^{19}F NMR (376 MHz, $CDCl_3$) δ -115.2 (d, $^2J_{FH}$ = 54.0 Hz), -124.2 (d, $^2J_{FH}$ = 54.0 Hz), *E/Z* isomers in a 5:2 ratio. HRMS (ESI) *m/z* calcd for $C_{10}H_{15}F_2N_3O$ $[M+H]^+$ 232.1255, found 232.1246. (**EXC-III-92**)

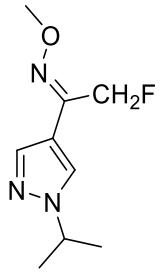

***(E)*-2-fluoro-1-(1-isopropyl-1*H*-pyrazol-4-yl)ethan-1-one *O*-methyl oxime (3-7d):** Prepared using the general procedure above (*Method G*) from 2-fluoro-1-(1-(isopropyl)-1*H*-pyrazol-4-yl)ethan-1-one (**2-11d**) (crude from previous reaction, 1.32 mmol), *O*-methyl hydroxylamine hydrochloride (221 mg, 2.64 mmol), sodium acetate (216 mg, 2.64 mmol), and EtOH (10 mL). Concentration of the reaction mixture *in vacuo* followed by silica gel flash chromatography (20 % ethyl acetate in hexanes) gave the product as an light-yellow oil (40 mg, 15 % after two reactions). ^{1}H NMR (400 MHz, $CDCl_3$) δ 8.07 (s, 1H), 7.91 (s, 1H), 5.13 (d, *J* = 47.5 Hz, 2H), 4.49 (hept, *J* = 6.7 Hz, 1H), 4.00 (s, 3H), 1.49 (d, *J* = 6.7 Hz, 6H). ^{13}C NMR (101 MHz, $CDCl_3$) δ 144.4 (d, $^2J_{CF}$ = 18.7 Hz), 139.8 (d, $^4J_{CF}$ = 2.4 Hz), 129.5, 111.5, 82.9 (d, $^1J_{CF}$ = 168.8 Hz), 62.4, 54.1, 22.7. ^{19}F NMR (376 MHz, $CDCl_3$) δ -215.3 (t, $^2J_{FH}$ = 47.6 Hz). HRMS (ESI) *m/z* calcd for $C_9H_{14}FN_3O$ $[M+H]^+$ 200.1199, found 200.1200. (**EXC-III-67**)

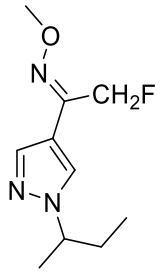

***(Z)*-1-(1-(sec-butyl)-1*H*-pyrazol-4-yl)-2-fluoroethan-1-one O-methyl oxime (3-7e):** Prepared using the general procedure above (*Method G*) from 2-fluoro-1-(1-(sec-butyl)-1*H*-pyrazol-4-yl)ethan-1-one (**2-11e**) (35 mg, 0.19 mmol), *O*-methyl hydroxylamine hydrochloride (32 mg, 0.38 mmol), sodium acetate (32 mg, 0.32 mmol), and EtOH (4 mL). Concentration of the reaction mixture *in vacuo* followed by silica gel flash chromatography (20 % ethyl acetate in hexanes) gave the product as an light-yellow oil (37 mg, 90 %). ^{1}H NMR (400 MHz, $CDCl_3$) δ 8.02 (s, 0.3H), 7.79 (s, 0.7H), 7.69 (s, 0.7H), 7.45 (s, 0.3H), 5.68 (d, $^{2}J_{HF}$ = 47.6 Hz, 0.6H), 5.42 (d, $^{2}J_{HF}$ = 47.6 Hz, 1.4H), 4.25 (h, *J* = 7.4 Hz, 0.6H), 4.01 (s, 0.9H), 3.95 (s, 2.1H), 2.08 – 1.65 (m, 2H), 0.78 (d, *J* = 7.4 Hz, 3H). ^{13}C NMR (101 MHz, $CDCl_3$) δ 149.5 (d, $^{2}J_{CF}$ = 19.3 Hz), 144.5 (d, $^{2}J_{CF}$ = 18.7 Hz), 139.8 (d, $^{4}J_{CF}$ = 2.5 Hz), 137.6 (d, $^{4}J_{CF}$ = 4.3 Hz), 130.4, 127.0 (d, $^{3}J_{CF}$ = 8.1 Hz), 113.5, 111.4, 83.0 (d, $^{1}J_{CF}$ = 168.9 Hz), 77.6 (d, $^{1}J_{CF}$ = 167.3 Hz) , 62.4, 62.3, 60.2, 60.1, 30.0, 30.0, 20.8, 10.5, 10.5, the doubling of numerous resonances suggests an *E/Z* isomer mixture. ^{19}F NMR (376 MHz, $CDCl_3$) δ -215.3 (t, $^{2}J_{FH}$ = 47.6 Hz), -231.4 (t, $^{2}J_{FH}$ = 47.6 Hz), *E/Z* isomers in a 2:5 ratio. HRMS (ESI) *m/z* calcd for $C_{10}H_{16}FN_3O$ $[M+H]^+$ 214.1350, found 214.1357. (**EXC-III-82**)

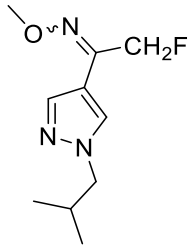

***(E)*and*(Z)*-2-fluoro-1-(1-isobutyl-1*H*-pyrazol-4-yl)ethan-1-one O-methyl oxime (3-7j):**

Prepared using the general procedure above (*Method G*) from 2-fluoro-1-(1-isobutyl-1*H*-pyrazol-4-yl)ethan-1-one (**2-11j**) (30 mg, 0.16 mmol), *O*-methyl hydroxylamine hydrochloride (27 mg, 0.32 mmol), sodium acetate (26 mg, 0.32 mmol), and EtOH (4 mL). Concentration of the reaction mixture *in vacuo* followed by silica gel flash chromatography (20 % ethyl acetate in hexanes) gave the product as an light-yellow oil (19 mg, 54 %). ^{1}H NMR (400 MHz, $CDCl_3$) δ 8.05 (s, 0.6H), 7.91 (s, 0.4H), 7.80 (s, 0.6H), 7.65 (s, 0.4H), 5.42 (d, $^{2}J_{HF}$ = 47.8 Hz, 1.2H), 5.15 (d, $^{2}J_{HF}$ = 47.8 Hz, 0.8H) 3.95 (s, 1.2H), 3.89 (s, 1.8H), 3.91 (d, *J* = 7.2 Hz, 0.8H), 3.88 (d, *J* = 7.2 Hz, 1.2H), 2.24 (n, *J* = 7.2 Hz, 1H), 0.90 (d, *J* = 7.2 Hz, 2.4H), 0.89 (d, *J* = 7.2 Hz, 3.6H). ^{13}C NMR (101 MHz, $CDCl_3$) δ 149.4 (d, $^{2}J_{CF}$ = 19.4 Hz), 144.4 (d, $^{2}J_{CF}$ = 18.8 Hz), 140.1 (d, $^{4}J_{CF}$ = 2.4 Hz), 137.9 (d, $^{4}J_{CF}$ = 3.9 Hz), 132.4, 129.2 (d, $^{3}J_{CF}$ = 7.1 Hz), 113.9, 111.7, 82.9 (d, $^{1}J_{CF}$ = 169.0 Hz), 77.5 (d, $^{1}J_{CF}$ = 162.4 Hz), 62.5, 62.3, 59.8, 59.8, 29.5, 29.5, 19.8, the doubling of numerous resonances suggests an *E/Z* isomer mixture. ^{19}F NMR (376 MHz, $CDCl_3$) δ -215.3 (t, $^{2}J_{FH}$ = 47.7 Hz), -231.6 (tq, $^{2}J_{FH}$ = 47.7, 1.7 Hz), *E/Z* isomers in a 2:3 ratio. HRMS (ESI) *m/z* calcd for $C_{10}H_{16}FN_3O$ $[M+H]^+$ 214.1350, found 214.1347. (**EXC-III-91**)

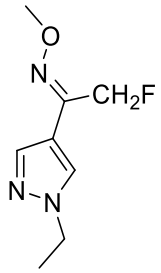

***(Z)*-1-(1-ethyl-1*H*-pyrazol-4-yl)-2-fluoroethan-1-one O-methyl oxime (3-7p):** Prepared using the general procedure above (*Method G*) from 2-fluoro-1-(1-(ethyl)-1*H*-pyrazol-4-yl)ethan-1-one (**2-11p**) (crude from previous reaction, 1.43 mmol), *O*-methyl hydroxylamine hydrochloride (238 mg, 2.86 mmol), sodium acetate (236 mg, 2.86 mmol), and EtOH (10 mL). Concentration of the reaction mixture *in vacuo* followed by silica gel flash chromatography (20 % ethyl acetate in hexanes) gave the product as an light-yellow oil (25 mg, 10 % after two reactions). ^{1}H NMR (400 MHz, $CDCl_3$) δ 8.08 (s, 1H), 7.92 (s, 1H), 5.14 (d, $^{2}J_{HF}$ = 47.6 Hz, 2H), 4.19 (q, J = 7.3 Hz, 2H), 4.02 (s, 3H), 1.49 (t, J = 7.3 Hz, 3H). ^{13}C NMR (101 MHz, $CDCl_3$) δ 144.36 (d, $^{2}J_{CF}$ = 18.9 Hz), 140.08 (d, $^{4}J_{CF}$ = 2.4 Hz), 131.3, 111.9, 82.9 (d, $^{1}J_{CF}$ = 168.8 Hz), 62.4, 47.2, 15.4. ^{19}F NMR (376 MHz, $CDCl_3$) δ -215.4 (t, $^{2}J_{FH}$ = 47.5 Hz). HRMS (ESI) *m/z* calcd for $C_8H_{12}FN_3O$ $[M+H]^+$ 186.1043, found 186.1044. (**EXC-III-65**)

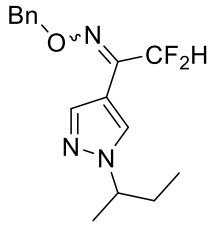

***(E)*and*(Z)*-1-(1-(sec-butyl)-1*H*-pyrazol-4-yl)-2,2-difluoroethan-1-one O-benzyl oxime (3-9e):** Prepared using the general procedure above (*Method G*) from 2,2-difluoro-1-(1 (sec-butyl)-1*H*-pyrazol-4-yl)ethan-1-one (**2-10e**) (35 mg, 0.17 mmol), *O*-benzyl hydroxylamine hydrochloride (55 mg, 0.35 mmol), sodium acetate (29 mg, 0.35 mmol), and EtOH (4 mL). Concentration of

the reaction mixture *in vacuo* followed by silica gel flash chromatography (100 % DCM) gave the product as an light-yellow oil (40 mg, 76 %). ^{1}H NMR (400 MHz, $CDCl_3$) δ 8.09 (s, 0.6H), 8.05 (s, 0.6H), 7.83 (s, 0.4H), 7.71 (s, 0.4H), 7.45 – 7.29 (m, 5H), 7.05 (t, $^{2}J_{HF}$ = 54.3 Hz, 0.4H), 6.22 (t, $^{2}J_{HF}$ = 54.3 Hz, 0.6H), 5.29 (s, 1.2H), 5.20 (s, 0.8H), 4.20 (h, *J* = 7.1 Hz, 1H), 2.04 – 1.67 (m, 2H), 1.49 (d, *J* = 7.1 Hz, 0.9H), 1.47 (d, *J* = 7.1 Hz, 2.1H), 0.79 (t, *J* = 7.1 Hz, 3H). ^{13}C NMR (101 MHz, $CDCl_3$) δ 143.7 (t, $^{2}J_{CF}$ = 28.2 Hz), 140.5 (t, $^{4}J_{CF}$ = 2.0 Hz), 137.8, 136.7 (t, $^{4}J_{CF}$ = 4.4 Hz), 136.7, 130.4, 128.5, 128.5, 128.3, 128.2, 128.0, 127.2, 115.3 (t, $^{1}J_{CF}$ = 240.0 Hz), 107.4, 106.5 (t, $^{1}J_{CF}$ = 235.1 Hz), 77.5, 77.2, 60.2, 30.0, 29.9, 20.7, 20.7, 10.5, 10.5, the doubling of numerous resonances suggests an *E/Z* isomer mixture. ^{19}F NMR (376 MHz, $CDCl_3$) δ -115.1 (d, *J* = 54.3 Hz), -124.1 (d, *J* = 54.3 Hz), *E/Z* isomers in a 2:3 ratio. HRMS (ESI) *m/z* calcd for $C_{16}H_{19}F_2N_3O$ $[M+H]^+$ 308.1568, found 308.1555. (**EXC-III-85**)

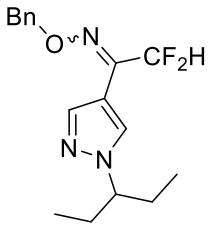

***(E)* and *(Z)*-2,2-difluoro-1-(1-(pentan-3-yl)-1*H*-pyrazol-4-yl)ethan-1-one O-benzyl oxime (3-9g):** Prepared using the general procedure above (*Method G*) from 2,2-difluoro-1-(1-(pentan-3-yl)-1*H*-pyrazol-4-yl)ethan-1-one (**2-10g**) (100 mg, 0.46 mmol), *O*-benzyl hydroxylamine hydrochloride (148 mg, 0.93 mmol), sodium acetate (76 mg, 0.93 mmol), and EtOH (5 mL). Concentration of the reaction mixture *in vacuo* followed by silica gel flash chromatography (100 % DCM) gave the product as a clear oil (98 mg, 66 %). ^{1}H NMR (400 MHz, $CDCl_3$) δ 8.11 (s, 0.4H), 8.02 (s, 0.4H), 7.83 (s, 0.6H), 7.68 (s, 0.6H), 7.42 – 7.29 (m, 5H), 7.05 (t, $^{2}J_{HF}$ = 54.0 Hz, 0.4H), 6.21 (t, $^{2}J_{HF}$ = 54.0 Hz, 0.4H), 5.19 (s, 2H), 3.88 (tt, *J* = 8.2, 4.7 Hz, 1H), 2.01 – 1.72 (m,

4H), 0.76 (t, J = 7.4 Hz, 3.6H), 0.74 (t, J = 7.4 Hz, 2.4H). ^{13}C NMR (101 MHz, $CDCl_3$) δ 146.3 (t, $^2J_{CF}$ = 24.6 Hz), 143.7 (t, $^2J_{CF}$ = 28.1 Hz), 140.7 (t, $^4J_{CF}$ = 2.0 Hz), 138.0 (t, $^4J_{CF}$ = 1.5 Hz), 136.8, 136.7, 131.5, 128.5, 128.5, 128.3, 128.2, 128.2, 128.2, 128.0, 115.3 (t, $^1J_{CF}$ = 240.1 Hz), 110.6, 109.0, 107.2, 106.6, 104.2, 77.5, 77.2, 66.9, 66.9, 28.3, 28.1, 10.6, 10.6, the doubling of numerous resonances suggests an *E/Z* isomer mixture. ^{19}F NMR (376 MHz, $CDCl_3$) δ -115.1 (d, J = 54.0 Hz), -124.1 (d, J = 54.0 Hz), *E/Z* isomers in a 3:2 ratio. HRMS (ESI) *m/z* calcd for $C_{17}H_{21}F_2N_3O$ $[M+H]^+$ 322.1731, found 322.1740. (**EXC-III-80**)

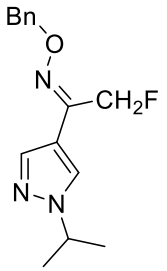

***(Z)*-2-fluoro-1-(1-isopropyl-1*H*-pyrazol-4-yl)ethan-1-one O-benzyl oxime (3-10d):** Prepared using the general procedure above (*Method G*) from 2-fluoro-1-(1-(isopropyl)-1*H*-pyrazol-4-yl)ethan-1-one (**2-11d**) (crude from previous reaction, 1.32 mmol), *O*-benzyl hydroxylamine hydrochloride (421 mg, 2.64 mmol), sodium acetate (216 mg, 2.64 mmol), and EtOH (10 mL). Concentration of the reaction mixture *in vacuo* followed by silica gel flash chromatography (20 % ethyl acetate in hexanes) gave the product as an light-yellow oil (35 mg, 10 % after two reactions). ^{1}H NMR (400 MHz, $CDCl_3$) δ 8.07 (s, 1H), 7.98 (s, 1H), 7.42 – 7.28 (m, 5H), 5.26 (s, 2H), 5.16 (d, J = 47.6 Hz, 2H), 4.48 (hept, J = 6.7 Hz, 1H), 1.48 (d, J = 6.7 Hz, 6H). ^{13}C NMR (101 MHz, $CDCl_3$) δ 144.9 (d, $^2J_{CF}$= 19.0 Hz), 140.0 (d, $^4J_{CF}$ = 2.3 Hz), 137.3, 129.6 (d, $^4J_{CF}$ = 1.0 Hz), 128.5, 128.0, 127.9, 111.6, 83.0 (d, $^1J_{CF}$ = 168.9 Hz), 76.8, 54.1, 22.7. ^{19}F NMR

(376 MHz, $CDCl_3$) δ -215.3 (t, $^2J_{FH}$ = 47.6 Hz). HRMS (ESI) *m/z* calcd for $C_{15}H_{18}FN_3O$ $[M+H]^+$ 276.1512, found 276.1523. (**EXC-III-68**)

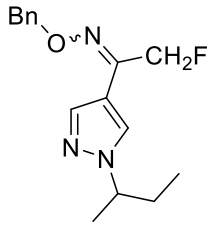

***(E)*and*(Z)*-1-(1-(sec-butyl)-1*H*-pyrazol-4-yl)-2-fluoroethan-1-one O-benzyl oxime (3-10e):**

Prepared using the general procedure above (*Method G*) from 2-fluoro-1-(1-(sec-butyl)-1*H*-pyrazol-4-yl)ethan-1-one (**2-11e**) (35 mg, 0.19 mmol), *O*-benzyl hydroxylamine hydrochloride (61 mg, 0.38 mmol), sodium acetate (32 mg, 0.38 mmol), and EtOH (4 mL). Concentration of the reaction mixture *in vacuo* followed by silica gel flash chromatography (20 % ethyl acetate in hexanes) gave the product as a yellow oil (26 mg, 81 %). ^{1}H NMR (400 MHz, $CDCl_3$) δ 8.05 (s, 0.6H), 7.98 (s, 0.6H), 7.81 (s, 0.4H), 7.70 (s, 0.4H), 7.42 – 7.27 (m, 5H), 5.47 (d, $^2J_{HF}$ = 47.5 Hz, 1.2H), , 5.26 (s, 0.8H), 5.17 (d, $^2J_{HF}$ = 47.5 Hz, 0.8H), 5.14 (s, 1.2H), 4.29 – 4.12 (h, J = 6.7 Hz, 1H), 2.05 – 1.67 (m, 2H), 1.48 (d, *J* = 6.8 Hz, 1.8H), 1.46 (d, *J* = 6.8 Hz, 1.2H), 0.81 (d, *J* = 7.4 Hz, 1.8H), 0.79 (d, *J* = 7.4 Hz, 1.2H). ^{13}C NMR (101 MHz, $CDCl_3$) δ 150.0 (d, $^2J_{CF}$ = 19.5 Hz), 145.0 (d, $^2J_{CF}$ = 19.1 Hz), 140.1 (d, $^4J_{CF}$ = 2.2 Hz), 137.7 (d, $^4J_{CF}$ = 4.2 Hz), 137.4, 137.3, 130.5, 128.4, 128.4, 128.1, 128.0, 127.9, 127.1 (d, $^3J_{CF}$ = 8.2 Hz), 113.5, 111.5, 83.0 (d, $^1J_{CF}$ = 169.0 Hz), 78.7, 77.2, 77.0, 76.8, 76.7, 60.2, 60.1, 30.0, 29.9, 20.8, 20.7, 10.2, 10.5, the doubling of numerous resonances suggests an *E/Z* isomer mixture. ^{19}F NMR (376 MHz, $CDCl_3$) δ -215.31 (t, $^2J_{FH}$ = 47.5 Hz), -231.2 (t, $^2J_{FH}$ = 47.5 Hz), *E/Z* isomers in a 1:1 ratio. HRMS (ESI) *m/z* calcd for $C_{16}H_{20}FN_3O$ $[M+H]^+$ 290.1669, found 290.1673. (**EXC-III-84**)

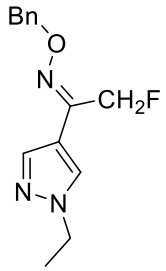

***(Z)*-1-(1-ethyl-1*H*-pyrazol-4-yl)-2-fluoroethan-1-one O-benzyl oxime (3-10p):** Prepared using the general procedure above (*Method G*) from 2-fluoro-1-(1-(ethyl)-1*H*-pyrazol-4-yl)ethan-1-one (**2-11p**) (crude from previous reaction, 1.43 mmol), *O*-benzyl hydroxylamine hydrochloride (456 mg, 2.86 mmol), sodium acetate (234 mg, 2.86 mmol), and EtOH (10 mL). Concentration of the reaction mixture *in vacuo* followed by silica gel flash chromatography (100 % DCM) gave the product as an light-yellow oil (30 mg, 8 % after two reactions). ^{1}H NMR (400 MHz, $CDCl_3$) δ 8.07 (s, 1H), 7.96 (s, 1H), 7.42 – 7.27 (m, 5H), 5.26 (s, 2H), 5.16 (d, *J* = 47.6 Hz, 2H), 4.16 (q, *J* = 7.3 Hz, 2H), 1.47 (t, *J* = 7.3 Hz, 3H). ^{13}C NMR (101 MHz, $CDCl_3$) δ 144.8 (d, $^{2}J_{CF}$ = 18.8 Hz), 140.3 (d, $^{4}J_{CF}$ = 2.3 Hz), 137.3, 131.4, 128.5, 128.0, 126.9, 112.0, 83.0 (d, $^{1}J_{CF}$ = 168.8 Hz), 76.9, 47.2, 15.3. ^{19}F NMR (376 MHz, $CDCl_3$) δ -215.4 (t, $^{2}J_{FH}$ = 47.6 Hz). HRMS (ESI) *m/z* calcd for $C_{14}H_{16}FN_3O$ $[M+H]^+$ 262.1350, found 262.1347. (**EXC-III-66**)

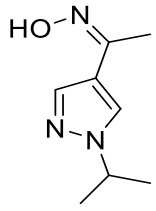

***(E)*-1-(1-isopropyl-1*H*-pyrazol-4-yl)ethan-1-one oxime (3-11)**: (E)- or (Z)- configuration unknown. Prepared using the modified general procedure above (*Method C*) from 4-bromo-1-(isopropyl)-1*H*-pyrazole (**2-7d**) (500 mg, 2.64 mmol), *N*,*N*'-dimethylacetamide (0.29 mL, 2.78 mmol), *n*-BuLi (2.5 M in hexanes, 1.1 mL, 2.78 mmol), and THF (10 mL). Concentration of the

reaction mixture *in vacuo* followed by silica gel flash chromatography (30 % ethyl acetate in hexanes) gave the product as a crude oil that was taken to the next reaction. Using the modified general procedure above (*Method G*) from 1-(1-isopropyl-1*H*-pyrazol-4-yl)ethan-1-one (crude, 1.70 mmol), hydroxylamine hydrochloride (356 mg, 5.13 mmol), sodium hydroxide (205 mg, 5.13 mmol), and EtOH (9 mL). Concentration of the reaction mixture *in vacuo* followed by silica gel flash chromatography (10 % ethyl acetate in hexanes) gave the product as an off- white solid (68 mg, 24 %); mp 155.8-157.0 ˚C. ^{1}H NMR (400 MHz, $CDCl_3$) δ 9.83 (s, 1H), 8.26 (s, 1H), 7.85 (s, 1H), 4.50 (hept, 1H, *J* = 6.7 Hz), 2.19 (s, 3H), 1.49 (d, *J* = 6.7, Hz, 6H). ^{13}C NMR (101 MHz, $CDCl_3$) δ 150.2, 146.3, 139.7, 137.0, 129.8, 124.7, 119.2, 114.1, 22.9, 19.1. HRMS (ESI) *m/z* calcd for $C_8H_{13}N_3O$ $[M+H]^+$ 168.1131, found 168.1131. (**EXC-II-15**)

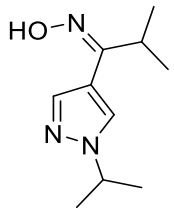

***(E)*-1-(1-isopropyl-1*H*-pyrazol-4-yl)-2-methylpropan-1-one oxime (3-12):** This compound is assumed to be (E)-configured to minimize steric interactions of the oxime an *i*-Pr group. Prepared using the modified general procedure above (*Method C*) from 4-bromo-1-(isopropyl)-1*H*-pyrazole (**2-7d**) (200 mg, 1.06 mmol), *N*-methoxy-*N*-methylisobutyramide (166 mg, 1.27 mmol), *n*-BuLi (2.5 M in hexanes, 0.44 mL, 1.11 mmol), and THF (6 mL). Concentration of the reaction mixture *in vacuo* followed by silica gel flash chromatography (20 % ethyl acetate in hexanes) gave the product as a crude oil that was taken to the next reaction. Using the general procedure above (*Method G*) from 1-(1-isopropyl-1*H*-pyrazol-4-yl)-2-methylpropan-1-one (crude, 0.36 mmol), hydroxylamine hydrochloride (50 mg, 0.72 mmol), sodium acetate (59 mg, 0.72 mmol), and EtOH (4 mL). Concentration of the reaction mixture *in vacuo* followed by silica

gel flash chromatography (20 % ethyl acetate in DCM) followed by recrystallization gave the product as a white solid (28 mg, 40 %); mp 138.0-139.1 ˚C. ^{1}H NMR (400 MHz, Acetone-d_6) δ 9.91 (s, 1H), 8.31 (s, 1H), 7.87 (s, 1H), 4.56 (hept, J = 6.7 Hz, 1H), 2.96 (hept, J = 6.8 Hz, 1H), 1.47 (d, J = 6.7 Hz, 6H), 1.16 (d, J = 6.8 Hz, 6H). ^{13}C NMR (101 MHz, Acetone-d_6) δ 152.9, 139.9, 130.5, 114.2, 54.4, 32.6, 23.0, 21.8. HRMS (ESI) *m/z* calcd for $C_{10}H_{17}N_3O$ $[M+H]^+$ 196.1444, found 196.1439. (**EXC-III-27**)

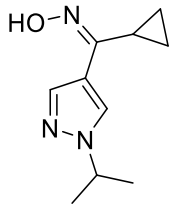

***(E)*-cyclopropyl(1-isopropyl-1*H*-pyrazol-4-yl)methanone oxime (3-13):** This compound is assumed to be (E)-configured to minimize steric interactions of the oxime an *c*-Pr group. Prepared using the modified general procedure above (*Method C*) from 4-bromo-1-(isopropyl)-1*H*-pyrazole (**2-7d**) (200 mg, 1.06 mmol), N-methoxy-N-methylcyclopropanecarboxamide (164 mg, 1.27 mmol), *n*-BuLi (2.5 M in hexanes, 0.44 mL, 1.11 mmol), and THF (6 mL). Concentration of the reaction mixture *in vacuo* followed by silica gel flash chromatography (30 % ethyl acetate in hexanes) gave the product as a crude oil that was taken to the next reaction. Using the general procedure above (*Method G*) from cyclopropyl(1-isopropyl-1*H*-pyrazol-4-yl)methanone (crude, 0.33 mmol), hydroxylamine hydrochloride (42 mg, 0.65 mmol), sodium acetate (53 mg, 0.65 mmol), and EtOH (5 mL). Concentration of the reaction mixture *in vacuo* followed by silica gel flash chromatography (20 % ethyl acetate in DCM) gave the product as a white solid (25 mg, 71 %); mp 149.3-150.2 ˚C. ^{1}H NMR (400 MHz, Acetone-d_6) δ 9.84 (s, 1H), 8.33 (s, 1H), 7.99 (s, 1H), 4.56 (hept, J = 6.7 Hz, 1H), 1.89 – 1.76 (m, 1H), 1.48 (d, J = 6.7 Hz, 4H), 0.83 – 0.67 (m, 6H). ^{13}C NMR (101 MHz, Acetone-d_6) δ 147.9, 139.2, 129.2, 114.8, 53.5,

22.1, 12.8, 4.9. HRMS (ESI) *m/z* calcd for $C_{10}H_{15}N_3O$ $[M+H]^+$ 194.1293, found 194.1293. (**EXC-III-16**)

4.2 Enzyme assay and determination of IC_{50} Values

Enzyme assays were performed by Dr. Dawn Wong (Carlier group). The Ellman reagent (5,5′-dithiobis-(2-nitrobenzoic acid) (DTNB), ≥98%), acetylthiocholine iodide (ATCh, ≥98%), bovine serum albumin (BSA, heat shock fractionated, A7030, lyophilized powder, ≥98%), dimethyl sulfoxide (DMSO, ≥99.9%) and recombinant *h*AChE (C1682) were purchased from Sigma-Aldrich (St. Louis, MO, USA). Recombinant WT and G119S *Ag*AChE were prepared as previously described.[10] Propoxur (technical grade) was purchased from Mobay Chemical Corporation, Pittsburgh, PA, USA. Standard clear polystyrene 96-well microplates (flat bottom wells, MPG-655101) and SealPlate adhesive films (LMT-SEAL-EX) were purchased from Phenix Research Products (Candler, NC, USA). Non-sealing polystyrene Costar corner notch lid covers (No. 3931 or 3099) for 96-well microplates were obtained from Corning Incorporated (Corning, NY, USA). Other chemicals and materials were purchased from Fisher Scientific Company LLC (Suwanee, GA, USA) or Sigma-Aldrich (St. Louis, MO, USA). Unless otherwise stated, the following buffers were used in this work: 1) buffer A is 0.1 M sodium phosphate buffer containing 0.02% NaN_3 (w/v), pH 7.7 at room temperature (23 ± 1°C), while 2) buffer B is buffer A containing 0.3% (v/v) Triton X-100, and 1 mg/mL bovine serum albumin (BSA), pH 7.7 at room temperature (23 ± 1°C). It is important to note that all stock solutions of fluorinated methyl ketones were prepared and stored in a well ventilated fumehood.

Wild-type AChE enzymes (r*Ag*AChE-WT and *h*AChE) were diluted in ice-cold buffer B and observed using a modified Ellman assay[10] (described below) to give an approximate reaction

rate of 40.0 mO.D./min (or ~0.0049 U/ml) at room temperature (23 ± 1°C), as previously reported.[9] Resistant enzyme (r*Ag*AChE-G119S) were diluted similarly and observed at a reaction rate of approximately 28.0 mO.D./min (or 0.0034 U/ml). All diluted enzymes were kept over ice prior to use. Aliquots of the diluted enzymes (10 μL) thus prepared were separately incubated, in duplicate, in a 96-well microplate with buffer A (150 μL), following the addition of an inhibitor solution (20 μL). The inhibitor solutions were prepared in buffer A with a DMSO concentration of 1% (v/v); the final assay concentration of DMSO was thus 0.1% (v/v). Note that inhibitor-free solvent controls substituted the inhibitor solution with 1% (v/v) DMSO in buffer A (20 μL). After waiting for the desired incubation time *t* at room temperature (23 ± 1°C), a freshly prepared solution of ATCh and DTNB (4 and 3 mM respectively, in buffer A, 20 μL), was added and mixed manually to start the enzymatic reaction. Thus, a total volume of 200 μL and optical pathlength of 0.60 cm was achieved in each well, with the following final concentrations: 0.015% (v/v) Triton X-100, 0.05 mg/mL BSA, 0.4 mM ATCh, 0.3 mM DTNB. Enzyme activity, in the absence and presence of inhibitor (v_0 and v, respectively), was monitored continuously at 405 nm at room temperature (23 ± 1°C) for up to 2.3 min on a DYNEX Triad microplate reader (DYNEX Technologies, Chantilly, VA, USA), analyzed using the Concert TRIAD Series Analysis Software (version 2.1.0.17), and corrected for spontaneous substrate hydrolysis.

Inhibition potency of the fluoromethylketone inhibitors was typically assessed by measuring the IC_{50} values (nM) following 10 and 60 min incubations of the enzymes. A dose-response experiment was carried out with a series of inhibitor concentrations [I] ranging from 10^{-5} to 10^{-11} M in buffer A, starting with a 0.01 M inhibitor stock solution in DMSO, and two sets of inhibitor-free controls. At least ten inhibitor concentrations (in duplicate) were used, with one set of inhibitor-free solvent control placed next to the highest [I] wells, and the other inhibitor-free

solvent control set close to the lowest [I] wells. The enzyme residual activity (v/v_0) were determined and used to construct dose-response curves (Prism 5.0, GraphPad Software Inc., La Jolla, CA, USA). Inhibitors assayed contained 0.1% DMSO (v/v) constant solvent in buffer A. For inhibitors that showed high volatility (see below), only the enzyme activity v_0 from the unaffected inhibitor–free solvent control was used. These were typically obtained from the inhibitor-free solvent controls that were distal from the highest [I] used on the microplate (next to the lowest [I] wells), and showed high enzyme activity compared to the other set of inhibitor-free solvent controls that were next to the highest [I] wells. The IC_{50} values (nM) were determined from at least two repeat experiments, using all the dose-response data collected. Standard error (SE) of the IC_{50} values are calculated from the 95% confidence interval according to the standard error formula SE = (upper limit – lower limit)/(2x1.96).[11]

4.3 Mosquito toxicity assay

Mosquito toxicity determinations were carried out by the Bloomquist group (University of Florida. *Anopheles gambiae* eggs (G3 (MRA-112) and Akron (MRA-913) were obtained from MR4, and reared in tap water with fish food for larval sustenance (Tetra Fish, Blacksburg, VA, USA). Adult female non-blood fed *An. gambiae* (both G3 and Akron strains) 3-5 days old, were used for filter paper assay of tarsal contact toxicity, which were performed in exposure tubes according to the 2006 World Health Organization recommendations[12] with slight modifications. In brief, filter papers (15 x 12 cm) were treated with 2.0 mL of various concentrations of the fluorinated ketone in ethanol, are allowed to dry overnight. For the G3 strain, batches of 20-25 mosquitos (in triplicate) were transferred to a holding tube and allowed to adapt for one hour. Due to lower colony numbers, toxicity assays with the Akron strain used

batches of 10-15 mosquitoes in duplicate. Mosquitoes were then transferred to the exposure tube (held horizontally) that contained a treated filter paper. Knockdown was noted after 1 h, and all mosquitoes were transferred back to the holding tube (held upright) and given free access to 10% (w/v) sugar water. Mortality was recorded at 24 h. Both during exposure and the 23 h period, mosquito tubes were kept in an environmental chamber at 24 ± 1˚ and 75 percent RH. To determine LC_{50} values typically 5-8 concentrations were examined and mortality data were used to probit analysis using Poloplus or SAS probit.[13]

4.4 References

1. Moslin, R. M. W., David S.; Wrobleski, Stephen T.; Tokarski, John, S; Kuman, Amit Amide substituted heterocyclic compounds useful as modulators of IL-12-23 and/or IFN alpha responses WO 2014074661 A1, May 15, 2014.

2. Chen, L. D., M. P.; Feng, L.-C.; Hawley, R. C.;Yang, M.-M. Pyrazole-substituted arylamide derivatives and their use as P2X3 and/or P2X23 purinergic receptor antagonists and their preparation and use in the treatment of disease. WO 2009077367 A1, June 25, **2009**.

3. Nair, H. K.; Lee, K.; Quinn, D. M., *m*-(N,N,N-Trimethylammonio)trifluoroacetophenone - a femtomolar inhibitor of acetylcholinesterase. *J. Am. Chem. Soc.* **1993,** *115*, 9939-9941.

4. Zak, M.; Liederer, B. M.; Sampath, D.; Yuen, P. W.; Bair, K. W.; Baumeister, T.; Buckmelter, A. J.; Clodfelter, K. H.; Cheng, E.; Crocker, L.; Fu, B.; Han, B. S.; Li, G. K.; Ho, Y. C.; Lin, J.; Liu, X. C.; Ly, J.; O'Brien, T.; Reynolds, D. J.; Skelton, N.; Smith, C. C.; Tay, S.; Wang, W. R.; Wang, Z. G.; Xiao, Y.; Zhang, L.; Zhao, G. L.; Zheng, X. Z.; Dragovich, P. S., Identification of nicotinamide phosphoribosyltransferase (NAMPT) inhibitors with no evidence of CYP3A4 time-dependent inhibition and improved aqueous solubility. *Bioorg. Med. Chem. Lett.* **2015,** *25*, 529-541.

5. Yarmoliuk, D. V.; Arkhipov, V. V.; Stambirskyi, M. V.; Dmytriv, Y. V.; Shishkin, O. V.; Tolmachev, A. A.; Mykhailiuk, P. K., Direct Noncatalytic Electrophilic Trifluoroacetylation of Electron-Rich Pyrazoles. *Synthesis* **2014,** *46*, 1254-1260.

6. Albrecht, B. K. B., David; Bellon, Steven; Bode, Christiane M.; Booker, Shon; Boezio, Alessandro; Choquette, Deborah; D'Amico, Derin; Harmange, Jean-Christophe; Hirai, Satoko Fused heterocyclic derivatives as HGF modulators and their preparation and *Method*s of use US 20090318436, March 18, **2009**.

7. Mullens, P. R., An improved synthesis of 1-methyl-1H-pyrazole-4-boronic acid pinacol ester and its corresponding lithium hydroxy ate complex: application in Suzuki couplings. *Tetrahedron Lett.* **2009,** *50*, 6783-6786.

8. Chang, K. C.; Grimmett, M. R.; Ward, D. D.; Weavers, R. T., Nitration of brominated pyrazoles in aqueous sulfuric-acid. *Aust. J. Chem.* **1979,** *32*, 1727-1734.

9. Wong, D. M.; Li, J.; Chen, Q.-H.; Han, Q.; Mutunga, J. M.; Wysinski, A.; Anderson, T. D.; Ding, H.; Carpenetti, T. L.; Verma, A.; Islam, R.; Paulson, S. L.; Lam, P. C. H.; Totrov, M.; Bloomquist, J. R.; Carlier, P. R., Select small core structure carbamates exhibit high contact toxicity to "carbamate-resistant" strain malaria mosquitoes, *Anopheles gambiae* (Akron). *PLoS One* **2012,** *7*, e46712.

10. Ellman, G., A new and rapid colorimetric determination of acetylcholinesterase activity. *Biochem. Pharmacol.* **1961,** *7*, 88-95.

11. Altman, D. G.; Bland, J. M., How to obtain the P value from a confidence interval. *BMJ (Clinical research ed.)* **2011,** *343*, d2304.

12. Guidelines for testing mosquito adulticides for indoor residual spraying and treatment of mosquito nets Available at WHO/CDS/NTD/WHOPES/GCDPP/2006.3 World Health Organization, Geneva. **2006**. (accessed Jan 15).

13. Robertson, J. L. P., H. K.; Russell, R. M. PoloPlus Probit and Logit Analysis; LeOra Software, 2002.